NOVEL REGENERATION METHODOLOGY FOR PROLONGATION OF REFORMING CATALYST LIFETIME;

by

NGOMO   HORACE   MANGA

B.Sc.(Hons) M.Sc. (University of Lagos)

A Thesis presented to the School of Postgraduate Studies,

University of Lagos,

in partial fulfilment of the requirements for the degree of

Doctor of Philosophy in Chemical Engineering.

University of Lagos,

November (1990)

SCHOOL OF POSTGRADUATE STUDIES
UNIVERSITY OF LAGOS

<u>CERTIFICATION</u>

THIS IS TO CERTIFY THAT THE THESIS -
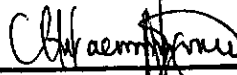
NOVEL REGENERATION FOR PROLONGATION

OF REFORMING CATALYST LIFETIME

SUBMITTED TO THE SCHOOL OF POSTGRADUATE STUDIES

UNIVERSITY OF LAGOS FOR THE AWARD OF THE DEGREE OF

DOCTOR OF PHILOSOPHY

IS A RECORD OF ORIGINAL RESEARCH CARRIED OUT BY

NGOMO HORACE MANGA

IN THE DEPARTMENT OF

CHEMICAL ENGINEERING

Ngomo Horace Manga	_(signature)_	21 02 199
AUTHOR'S NAME	SIGNATURE	DATE
PROF. A. A. SUSU	_(signature)_	21/2/91
SUPERVISOR'S NAME	SIGNATURE	DATE
DR. D. S. ARIBIKE	_(signature)_	21/2/91
INTERNAL EXAMINER'S NAME	SIGNATURE	DATE
PROF. A. A. SUSU	_(signature)_	21/2/91
INTERNAL EXAMINER'S NAME	SIGNATURE	DATE
DR. S. K. LAYOKUN	_(signature)_	21/2/91
EXTERNAL EXAMINER'S NAME	SIGNATURE	DATE

SUPERVISORS APPROVAL

I have read this thesis and found it to be of satisfactory quality for a Doctorate Degree.

Date_____   Professor A. A. Susu_____

ii

ABSTRACT

The deactivation of $Pt - Al_2O_3$ reforming catalyst by coking was investigated by the performance of several sets of deactivation-regeneration experiments in a Berty CSTR. The overall objective was the prevention of catalyst mortality. Catalyst regeneration after deactivation was by a novel methodology, introduced with a view to improving the life-time of the catalyst. The methodology, formulated from the results of a systematic study of the nature and types of coke deposited during reforming of $Pt - Al_2O_3$ catalyst, hinged on the prolonged removal of toxic coke on the catalyst surface in order to delay its accumulation to a lethal level. Toxic coke had been identified to be responsible for the mortality of the catalyst. The prolongation of the catalyst lifetime by this methodology and the response of the catalyst in terms of coking were evaluated by comparing the results obtained in this study with previous works. Hence several sets of multiple deactivation-regeneration experiments were performed in which the oxidizable and toxic coke deposited after each run were quantified. The model reaction, the dehydrogenation of cyclohexane on $0.3\% Pt - Al_2O_3$, was performed at a reactor temperature of $430°C$, reactant vapour pressure of 0.234 atm. and carrier gas flowrate of 100ml/min. Catalyst regeneration consisted of oxidation at $430°C$ with 2-3% O_2 in N_2 carrier at a flowrate of 120ml/min followed by prolonged reduction of coke at $500°C$ in H_2 at a flowrate of 40ml/min. Results showed that the catalyst remained

iii

1. The prolonged toxic coke removal in the highest possible quantity is responsible for the prolongation of catalyst lifetime. An improvement of more than 2 fold (22 cycles in a previous work(6) and 52 here) clearly indicated the toxicity of secondary coke and the efficiency of this regeneration methodology.

2. The secondary coke is deposited in layers in confirmation of previous results (9) and consists of several types. The number of reducible cokes formed may be dependent on the coking propensity of the reactant used.

3. A total of three types of coke are deposited on the catalyst surface: primary coke, secondary coke and tertiary coke. The tertiary coke is graphitic in nature and cannot be removed even after very prolonged reduction.

4. The level of oxidizable and toxic coke with each cycle are generally characterized by oscillations in between some fairly stable values. The catalyst surface is very unstable as shown by the occurence of redispersion. This instability partly explains the occurence of the oscillations in the amount of oxidizable and toxic coke with cycle number.

5. No clear correlations exist between catalyst surface parameters. Where they do exist, they are dependent on too many conditions. Hence the results from a reactive surface are an interplay of a lot of factors many of which may not be easily understood.

6. Specifically, no correlation exist between activity and dispersion. Toxic coke is more crucial in determining catalyst lifetime than the level of dispersion.

7. During multiple deactivation-regeneration cycles, the catalyst sinters during reduction and redisperses during oxidation.

active even at the 52nd cycle when it was terminated whereas catalyst mortality had been shown to have occured at the 22nd cycle in a previous experiment in which prolonged reduction was not used. The improvement observed here was a clear manifestation of the success of this regeneration methodology.

The oxidizable and toxic coke values versus cycle numbers also showed oscillations in between some fairly constant values. The oscillations suggested the occurence of some reversible surface changes. To probe the changes, the catalyst surface was characterized by the performance of titration experiments cycle by cycle at $430^{o}C$ after oxidation and after prolonged reduction. The dispersion of metal sites on the support, which is the surface parameter generally used as a measure of potential catalyst activity, was the parameter of interest in the surface characterization study. Results showed the usually observed trend- that the dispersions after oxidation are higher than those after reduction and the average decline of dispersion from oxidation to reduction was calculated to be 39.25%. Whereas the dispersion after oxidation stayed constant for almost 6 runs before declining, the dispersion after reduction declined continuously from one run to another. Unexpectedly, it was observed that the cycles with low dispersions were characterized by high toxic coke removal and high deactivation times.

Two theoretical models of the reaction-deactivation process were developed and the model parameters estimated in a straight forward manner without decoupling the coking reaction from the main reaction. The two models were found to adequately describe the the deactivation run data. The modelling of the deposition of coke in multilayers on real surface was presented and the results showed good agreement with the experimental results. Furthermore, a theoretical model of the effect of diffusion in the catalyst regeneration process was developed using Langmuir-Hinshelwood kinetics.

From the discussion of the results the following conclusions were drawn

8. The multilayer coking model on real surface adequately describes the data of residual activity and coke content.

9. The methodology for the straight-forward simultaneous determination of both reaction kinetics and decay rates without decoupling the main reaction from the decay, used by Forzatti and Ferraris for an integral reactor data is also applicable for mixed flow data generated in a CSTR.

10. Catalyst regeneration is adequately modelled by Langmuir-Hinshelwood kinetics. The coke and the gas consumption profiles increase and reduce respectively towards the center of the catalyst due to diffusional resistances.

AKNOWLEDGEMENTS

studies. Finally my thanks to almighty God for my good health despite the strains.

DEDICATION

To grand auntie.

Poured the bit into the pool,

like the greats before me.

Ngomo Horace,

November, 1990

Contents

xvi

Chapter 1

INTRODUCTION

A catalyst is a substance which increases the rate of attainment of equilibrium of a rection system without causing any great alteration in the free energy changes involved. A catalyst accelerates reaction by providing alternative mechanism for accomplishing the reaction and this alternate path is a more rapid one. As far back as 1836, Berzelius(1) had evidence of a 'catalytic' force in operation. In the reactions he studied, he realised the substance was virtualy unchanged by the reaction. Although the concept of a catalytic force as proposed by Berzelius(1) has now been discarded, the term catalysis is retained to describe all the processes in which the rate of reaction is influenced by a substance that remains chemically unaffected.

The use of catalysis is of paramount importance to mordern chemistry since more than 80% of all new industrial reactions involve catalysts in one way or the another. Catalysis is divided into three distinct fields(2).

1. **heterogenous catalysis,** in which the catalytically active substance is present in another phase than the products and the reactants. The chemical reactions take place at the interface of these phases. Typically, the reactants and products are

1

gases or liquids and the catalyst is solid.

2. **homogenous catalysis,** in which the the catalytic substance, the products and the reactants are all in the same phase: usually the liquid phase.

3. **biological catalysis,** in which the catalytic active substance is a very large and complex organic molecule called an enzyme. These catalysts are closely related to living nature and its chemical processes. Their state is usually colloidal.

For industrial applications it is very important to separate reactants, products and catalyts after completion of the reaction . Because of the ease with which this can often be done with heterogenous catalysts, industrial (and thus also scientific) attention has been directed mostly towards this type of catalysis(3). Heteregenous catalysis is commonly subdivided into the following groups of reactions:

1. **Catalysis by metals**

2. **Catalysis by non-metallic compounds,** e.g. oxides, sulphides and solid acids

3. **Bifunctional** (group 1 and 2)

The first step in a catalytic reaction is physical adsorption followed by chemisorption. A necessary precursor to reaction is the adsorption of the reactant on the surface of the catalyst. If we suppose that the surface atoms of the catalyst are capable of forming the same number of chemical bonds as an atom in the bulk, the surface will therefore have a degree of unsaturation which is manifested by free energy. The process of saturating free valencies is termed adsorption. In physical adsorption, the strength and nature of the adsorption bonds can vary with type of catalyst, adsorbates, temperature etc. Physical adsorption can in principle occur between all gases and all solids. Chemisorption is a

necessary condition for catalysis to take place. A chemically adsorbed specie interacts with the metal-adsorbate chemical bond in such a way that a metal-adsorbate chemical bond is formed, i.e electrons are transfered between the adsorbent and the adsorbate or they are shared. Because of this new chemical bond formation, molecules exhibit a stronger specificity in their preference for certain adsorption sites, orientation, dissociation etc. On purely arbitrary grounds one often divides chemisorption into different categories-weak when the metal-adsorbate bond, at low pressures and temperatures below ambient can be broken readily. If the bond is broken only upon heating above room temperature then the adsoption is called strong.

The study of the structure of the catalysts largely belongs to the realm of solid state physics, whereas preparation is a task for inorganic chemistry. In recent years, from the tools of physics, a very large number of techniques have become available that permit the investigation of surface phenomena on the atomic scale. Most of these involve scattering of electrons, atoms, ions or photons. Electrons that are emmited from the valence shells or from the inner shells of surface atoms as a result of bombardment by electrons or photons of higher energy are the probes of ultraviolet photoelectron spectroscopy, Auger electron, X-ray spectroscopy. These techniques are employed to determine the chemical composition of the surface and the oxidation states of surface atoms. The multidisciplinary complexity of catalysis is the main origin of the fact that inspite practical application, many of the fundamental problems have remained so far unresolved. The importance of these problems are demonstrated by the continuing research dealing with them(4).

One of the most important industrial catalytic process is reforming reactions in the petroleum refinery. The main purpose of reforming is the improvement of fuel quality. This improvement is achieved by an increase in the octane rating of the fuel, to a value

sufficiently high enough to satisfy the demands of high compression ratio engines(5). Early petrol suffered from the phenomenon of pre-ignition leading to knocking. The octane number of the fuel is increased not only by the products of catalytic naphtha reforming but also by the addition of lead compounds. The catalyts applied in reforming reactions have to show a high seletivity in the formation of aromatics and branched alkanes above unbranched alkanes since the former have a higher octane rating.

Most widely used reforming catalysts are one of the following-a precious metal, a precious metal on a support, or an alloy of two precious metals on a support. A catalyst of just a precious metal alone is a monometallic catalyst while a catalyst of two metals on a support is a bimetallic. Currently,the most used reforming catalyst are the bimetallics, such as Pt-Re and Pt-Ir, which after sulphiding show good stability and seletivity. The bimetallics are prefered to the monometallics because of their better resistance towards deactivation by coking and sulphur poisoning. This thesis will be entirely dedicated specifically to the study of the behaviour of $0.3\% Pt - Al_2O_3$ catalysts in reforming reactions as model for understanding reforming catalyst behaviour in general.

Reforming catalysts in a flow of reactant fluid undergo a gradual loss of activity due to sintering, poisonous impurities in the feed, and deposition of carbonaceous materials-coke. Sintering is the agglomeration of active sites made possible by the mobility of the metal atoms caused by very high run-away temperatures. Agglomeration leads to loss of metal surface area and hence a reduction in sites available for reaction. Poisoning can be eliminated by elaborate purification of the feed before use and sintering can be avoided by adequate temperature control. Whereas sintering and poisoning can be controlled, coking cannot. Coke is the general denomination given to the formation of carbonaceous materials on a catalyst surface. Coke is the end product of carbon disproportionation, condensation, and hydrogen abstraction reactions of adsorbed carbon-containing species.

4

Coke formation generally occurs via a sequence of elementary reactions which in turn depend on the type of main reaction under study, feed composition, type of catalyst used and reactor environment(3,5).

The eventual irreversible loss of catalyst activity (mortal state) is a result of coking and not even the introduction of the more coke-resistant bimetallic catalysts have been able to prevent catalyst mortality due to coking(3,6).

Restoring catalyst activity after deactivation is necessary if the catalyst is to be of further use. Regeneration would entail the removal of the coke deposits on the catalyst surface. The regeneration method being used in industry (7) involves burning off the coke deposits in an air stream-a process known as oxidation. This process removes only one type of coke-oxidizable coke - research has established the existence of more than one type of coke. The non-oxidizable type of coke (toxic coke) accumulates on the surface and eventually leads to the mortal state of the catalyst (6,7).

OBJECTIVE OF STUDIES

Prolongation of catalyst lifetime by the development of more accurate methods of coke removal requires a detailed understanding of the step by step coking mechanism, the nature of the coke forms deposited on the catalyst and the operating conditions that favour a higher selectivity for the desirable reaction. Understanding the coking mechanism requires the simulation of catalyst mortality in the laboratory and monitoring of the nature and quantity of the coke formed as the catalyst progresses to mortality. In industry, the reforming reactions are performed in hydrogen atmosphere(7,8). Hydrogen converts potential coke precursor molecules into harmless compounds thus reducing coking (8). Deactivations times in hydrogen are, therefore, desirably long. Nitrogen can also serve as a reforming medium but cannot be used in industry. Owing to its inertness it has no action on coke precursors. Hence, deactivation times in nitrogen are short,

5

aging of the catalyst as well as catalyst deterioration to mortality is rapid.

Though deactivation times in industry are desirably long, for laboratory investigations, however, the deactivation times have to be reduced drastically if several process variables are to be investigated and catalyst mortality achieved. Nitrogen, therefore, for reasons given above is prefered to hydrogen for laboratory simulation of catalyst mortality. The uncertainty here had been whether the catalyst mortal state that would be simulated in the laboratory can be extrapolated to the industrial catalyst where hydrogen is used. Laboratory reforming reactions had been carried out in nitrogen till catalyst mortality occured(6,7) and the results were found to simulate the industrial catalyst. In that work, use was made of multiple deactivation-regeneration schemes to achieve a catalyst mortal state in both the monometallic $Pt - Al_2O_3$ and bimetallic $Pt - Re - Al_2O_3$ catalysts using cyclohexane dehydrogenation to benzene in nitrogen. Three types of coke were identified to have been deposited on the catalyst surface(7) and were labelled as oxidizable(primary) coke, secondary(reduceable)coke and tertiary(non-oxidisable and non-reduceable) coke. The accumulation of secondary and tertiary coke on the catalyst surface were found to have been responsible for the mortality of the two catalysts investigated. It was also observed that the prolongation of the catalyst life may be dependent on the slow down of the transformation process from the non-toxic oxidizable coke to the more toxic secondary and tertiary coke.

The above findings could not be said to be conclusive for two reasons. Firstly, they were drawn from an investigation carried out only in nitrogen. Secondly, the reaction investigated-the dehydrogenation of cyclohexane required just the metallic sites of the $Pt - Al_2O_3$ catalyst. Hence further work was done(9) whereby the reaction studied-the deactivation of Methylcyclopentane (MCP) on $Pt - Al_2O_3$ catalyst required both the metallic sites and the acidic sites on the catalyst surface. Hydrogen and nitrogen atmo-

6

spheres were used. The nature and levels of coke forms deposited on the catalyst using both atmospheres were compared for several deactivation-regeneration cycles (11 in all). The results were found to be a realistic simulation of the industrial catalyst for the period under investigation and thus confirmed the findings of the previous investigation(7) in which cyclohexane was used.

In view of the suggested linkage of toxic coke to the mortality of the catalyst, the regeneration method used involved the prolonged removal of the toxic coke and quantification of the coke (toxic and oxidizable coke)(9). However, the effect of the regeneration method on catalyst life prolongation was not demonstrated as vital variables were not changed and no work with similar experimental design existed in literature for comparison.

The problem with the use of MCP to investigate catalyst mortality is the rapidity with which it reacts and coke on the catalyst surface. Results using MCP have abundantly demonstrated that observation(8,9). Rapid coking leads to loss of vital details as it is difficult to monitor all the changes effectively. Cyclohexane is a slower coking reagent. Hence the recourse to use of cyclohexane in this thesis to investigate its deactivation of of $Pt - Al_2O_3$ catalyst. Both oxidizable (primary) and the toxic coke forms are quantified for several deactivation- regeneration cycles. The coke monitoring should determine the extent of involvement of the coke type(s), in deactivation and mortality while kinetic studies would determine the optimal process conditions that would maximize yield and minimize coking. Coke monitoring could also suggest the location of the coke.

If accumulation of toxic coke causes the mortality of catalyst as had been experimentally determined(7) it stands to reason that the toxic coke must be inflicting irreversible harmfull changes on the catalyst's surface morphology. One way of monitoring such surface structural changes is through a cycle by cycle catalyst surface characterization

7

as the catalyst ages to obtain the 'catalyst surface structure profile.' A possible correlation between coking and surface character should be able to explain observed changes in reforming reactions and the effects of implemented changes during reactions on the state of the catalyst.

Thus, in line with our stated objectives the following have been done:

1. We have determined the mixing charateristics of the available reactor, a Berty CSTR, so as to asses its suitability for the procurement of reliable data.

2. We have strived to achieve catalyst mortality in the laboratory by the performance of a long series of deactivation-regeneration experiments on $Pt - Al_2O_3$ reforming catalyst in the course of which we have quantified the primary and secondary coke deposited cycle by cycle. Catalyst regeneration was carried out by a method that hinges on the prolonged removal of secondary coke to the maximum at the appropriate conditions. The efficiency of this regeneration method has been evaluated by comparism with data from previous work(7).

3. We have carried out titration experiments by which we would characterize the catalyst suface structure.

4. To theoretically analyze the coke structure, a multilayer coking model on real surface has been proposed and data from the titration experiments used for the model parameter estimation.

5. In addition, a generalised, theoretical model for the effect of diffusion during catalyst regeneration has been presented to evaluate the significance of diffusion during the regeneration process. From the experimental and theoretical analysis, we have obtained information which should rationalize the success of our new methodology

8

and explain the state of a deactivating reforming catalyst. This information is desirable for the development of an effective method for the prolongation of catalyst lifetime with predictable effects.

Chapter 2

LITERATURE SURVEY

2.1 COKING OF REFORMING CATALYST

The oil-processing industry started to use metal based catalysts almost immediately after the pioneering patents appeared in 1949(8). These catalysts consisted of very finely dispersed platinum on its support: $\gamma - alumina\ Al_2O_3$. The moderately acidic alumina not only prevents sintering of Pt particles, but also has a catalytic activity of its own. The original idea was to combine the outstanding hydrogenation/ dehydrogenation activity of Pt with a catalyst, which can isomerize and promote dehydrocyclization, next to some cracking(10). The reactions on alumina are supposed to run via the carbenium ion mechanisms, whereby the initial carbenium ions are formed by addition of protons to olefins and to a lesser extent, by abstraction of hydride anions(11).

Later it appeared that Pt could do more than just hydrogenate and dehydrogenate (12,13). At low temperature, before it becomes covered by carbonaceous layers it can catalyse hydrogenolysis, isomerization and dehydrocyclization at a high rate. When industrial conditions are applied, the most important (remaining) function of Pt covered

by carbonaceous layers is, indeed, to catalyse dehydrogenation and other reactions derived from it, such as aromatization (an essential part of aromatization takes place on Pt) (13).

After 1968, the reactors for naphta reforming were refilled by one of the (or the combination of) new generation catalysts: the bimetallics (14). The combination Pt-Re appeared to be the most widely used, but also Pt-Sn and Pt-Ir catalysts were important. The second metallic component has, most likely, more than one function. The focus of this review is, however, limited to catalysis on $Pt - Al_2O_3$. Most studies have been carried out using a $Pt - Al_2O_3$ reforming catalyst.

Under practical industrial conditions, adsorption of hydrocarbons always takes place in the presence of (external) hydrogen(4,7,8,9). The presence of hydrogen supresses, of course, all steps in which hydrogen is split off from the hydrocarbon molecules or their fragments. At reaction temperature a certain fraction of adsorbed species is dehydrogenated too deeply, and is unreactive at that temperature. This fraction eliminates part of the metal surface from the reaction, causing the active surface to be always smaller than the total metal surface. The dehydrogenated species (coke) lose more and more hydrogen on increasing the temperature. The thermodynamics of reforming reactions are such that it is desirable to work at high temperatures and pressures but these are the conditions that favour coking(8). In the absence of hydrogen, ethene can dehydrogenate at temperatures of about 300K so fast that the adsorbed layer contain graphitic structures(14).

2.1.1 COKE FORMATION AND STRUCTURE OF COKE.

As already mentioned a series of fragmentation reactions and successive dehydrogenation reactions leads to the formation of unreactive, highly dehydrogenated species and

these molecules may combine to form more toxic coke deposits. Further removal of this hydrogen by successive fragmentation (hydrogenolysis) and dehydrogenation leads to a more graphitic form of coke (this also involves migration to a nucleation site where the irreversible deposits grow).

2.1.2 Coke Location and Structure

Graphitic coke is very resistant to removal by hydrogen. Other mechanisms suggested in the literature for metal site coking also indicate there are different types of coke on surface(7,9). The routes for these coke formations are based on polymerization reactions occuring on the metal surface(14,15). J. Biswas deduced(16) that coke from long term reformer operation is on the alumina support of the $Pt - Al_2O_3$ and that coke on the Pt sites was limited to the early stages of deactivation. He distinguished between two types of coke deposits on the metal sites after oxidation of the deactivated catalyst; one of the coke easily removable with hydrogen and the other less readily so. He suggested that the less readily removable type must be graphitic in nature.

Omoleye(7) and Osaheni et al.(9) had clearly distinguished between three types of coke deposits on $Pt - Al_2O_3$ during reforming with methylcyclopentane. They distinguished the cokes on the basis of their reactivity with oxygen and hydrogen. On oxidation of a deactivated catalyst, one coke type was removed as carbon dioxide was given off, on reduction with hydrogen a second coke type was identified in the formation of methane. Osaheni et al.(9) reasoned that since the coke reduction profile did not level off to zero in the amount of methane formed, a third type of coke, resistant to both oxidation and reduction must be retained on the surface. The three identified coke were thus labelled oxidizable coke(primary coke) reduceable coke(secondary coke) and non-oxidizable and non-reduceable (tertiary) coke. They further suggested(9) that the cokes are not formed

12

indepedently but by a transformation of one coke form to the other and postulated the following sequence : *Oxidizable coke→Toxic coke→graphitic coke.* Osaheni et al. also observed that the reduceable coke (secondary coke) occurs in layers and that the layers represented reduceable coke of varying resistance to reduction with the most resistant occuring on the catalyst-coke interface. The most resistant coke was suggested to be graphitic in nature. J. Barbier(17) carried out a temperature-programmable oxidation of coked $Pt - Al_2O_3$ catalyst and revealed the existence of two oxidation states represented by two peaks; one at around $300°C$ and the other at$400°C$. Many materials are known to catalyse the gasification of coke and this includes several metals. He explained, on the strength of evidence from previous work(18), that the low temperature combustion was due to the presence of coke on the metallic sites and the high temperature combustion was due to coke on the alumina sites. He further explained the existence of two oxidation states by suggesting that either platinum catalyses the oxidation of carbon, or that coke deposited on the metal is *different* from that deposited on the alumina.

2.1.3   Nature of catalyst and amount of Coke

Much of what is known of metal crystallite structure is due to the pioneering work from the laboratory of G. Somorjai(19). The activity of platinum-based catalysts is dependent on the surface crystallite configuration(16,19,20). Hence, the influence which carbonaceous layers have on the hydrocarbon reaction is also dependent on structural factors. The metal catalyst is normally dispersed on the support as small crystallites, usually in the size range of $8 - 100Å$ units in diameter(16,20). Crystallite corner atoms have a coordination number of 4, edge atoms 6 or 7 and atoms on the face of the plane 8 or 9. Corner atoms predominate on the surface of extremely small crystallites while large crystallites consist entirely of face atoms. The electron deficient character of corner

13

atoms makes these atoms more active for certain reactions.

It is known that the carbonaceous deposites are most easily formed on sites with the highest coordination number on metal atoms, such as those at the foot of steps and flat surfaces.(16,19,20). In contrast the atoms on edges, corners and other exposed low coordinated sites are less covered by carbonaeceous layers. This is because of higher coke cleaning rates there as well as steric influences. The lesser susceptibility of small particles to self-poisoning than large ones has been studied in more details with Pt (21). With Pt, in almost all experiments with n-Hexane in the feed, a higher activity for small particles is observed(21). A. Sarkany(22) also confirmed the structure sensitivity of the formation of carbonaeceous deposits over a group of monofunctional $Pt - SiO_2$ catalysts of varying dispersions.

Somorjai(19,20) had demonstrated the structure sensitivity of cyclohexane dehydrogenation by providing data showing that the dehydrogenation of cyclohexane to benzene occurs only on stepped platinum surfaces at an appreciable rate at low pressures and that the rate is constant as long as there are steps on the surface. Literature has been reviewed showing that metal particles of varying size certainly differ in their propensity to form metal-to-single-carbon atom multiple bonds(8). The smaller particles of various metals show a lower activity in multiple bond formation, than the large particles.

M. Boudart(23) suggested that all reactions might not be equally sensitive to the geometric arrangements in various metal surfaces or to the differencees in the electronic structure of sites with different coordination. Boudart divided the reactions into structure-sensitive and structure insensitive. The operational criteria for structure sensitivity, according to him is the specific activity (the rate per unit surface area) or the TON(turn over numbers (rate per site). TON's should differ by more than a factor of 5-10 when the dispersion, D, varied sufficiently.

14

2.2 THEORETICAL DEVELOPMENT

It should have been possible to use a catalyst continuously for a long time as long as the catalyst's mechanical properties remained intact were it not for coking. With the formidable difficulties in physically following the progress and nature of coke accumulation on-stream, modelling becomes an attractive alternative for the prediction of the state of the deactivating catalyst from knowledge of the chemistry of the coking reactions. This section on theoretical development will discuss efforts by various researchers to model coking and the progress so far. This part will be discussed under the following truncations:

1. **Dehydrogenation of Cyclohexane**

2. **Voorhies model**

3. **Levenspiels' model**

4. **Model of Fromet**

5. **Corella and Asua**

6. **Cooper and Trimms model**

7. **Klingmann and Lee**

It should be clarified that the enumerated authors are not the only ones in the literature with models associated with their names. Mention is made or discussion of other relevant models is done under the enumerated ones. They have, however, been enumerated for the wide reviews and applications their models have attracted in the literature.

DEACTIVATION AND ACTIVITY MODELLING.

Even though there are examples of catalyst deactivation resulting purely from the physical coverage of the active metal sites by coke molecules, there are still doubts as to whether electronic factors affect coking or deactivating catalyst. Agrawal et al.(24) stated that, if deactivation is due to reduction in the number of active sites then the kinetic behaviour should remain unchanged with deactivation and the reduction in the rate constant will then be attributed to the fractional reduction in the number of the active sites. However, if the deactivation is due to electronic factors, the value of the kinetic parameters would be expected to change on deactivation and this will provide a new insight into deactivation mechanism.

As early as 1945, Voorhie(25) succeeded in obtaining an empirical relationship between the activity of a catalyst and the time of reaction. Ever since then, quite a number of researchers have come up with one form of a model or another. Wojiechowski(26) related activity of a catalyst to both time and temperature of reaction. Babier et al.(27) found that the overall activity of $Pt - Al_2O_3$ catalyst decreased as the coke deposit per unit mass of platinum increased. They also reported that the activity of unpoisoned metal in the midst of poisoned ones is the same as that of an uncoked and unpoisoned metal. The effect of the coke deposit level on the activity of the catalyst form the basis of the empirical equation derived by various authors like Froment and Bischoff (28) and Dumez and Froment (29). They have shown the need to relate activity of a coked catalyst through an empirical equation to the coke content and to relate the coke content to the properties of the catalyst (composition of reaction mixture, temperature and time) through a continuity equation. The significance or not of the chlorine content of the catalyst with regards to its effect on catalyst activity has been a matter of contention. Nora Figoli et al.(30) studied the influence of the chlorine content on the behaviour of catalysts for n-heptane reforming and showed that after 24 hours of continuous operation

16

or about 1000ml of n-heptane processed, the initial chlorine content of the catalyst did not change and so it was not necessary to add chlorine to maintain its concentration on the catalyst. The same conclusion was noted to have been reached by Svajgl(31). The activity and selectivity tests by Nora Figoli et al.(30) showed that 0.8-0.9% Cl on the catalyst was convinient for the catalyst stability for the conditions under which they worked. Parmaliana et al.(32) in their contribution, noted that the chlorine content influences, not the formation of coke, but the nature and mechanism of the formation of carbonaceous residues contributing to coking and that even without the chlorine content, the catalyst will still coke. They, however, in their analysis, show the chlorine content as the determining factor controlling catalyst regenerability, which *ipso facto*, the catalyst lifetime.

Cooper and Trimm(33) also gave a model relating activity to the coke content of the catalyst. Other researchers like Szepe and Levenspiel(34), Levenspiel(35), Wolf and Peterson(36) and Corella and Asua(37) Omoleye and Susu(7) gave models that relate the activity of the catalyst directly to the reaction conditions.

2.2.1 Dehydrogenation of Cyclohexane

The dehyrogenation of cyclohexane to benzene has been chosen as the reaction of study. The mechanism of the reaction on Pt-Re was studied by Susu, Enoh and Ogunye(38). They postulated the following reaction scheme:

$$C_6H_{12(gas)} \qquad\qquad\qquad C_6H_{6(gas)}$$
$$k_1 \downarrow\uparrow k_{-1} \qquad\qquad\qquad k_4 \downarrow\uparrow k_{-4}$$
$$C_6H_{12(ads)} \xrightarrow{k_2(step2)} C_6H_{10(acids)} \xrightarrow{k_3(step3)} C_6H_{6(ads)}$$
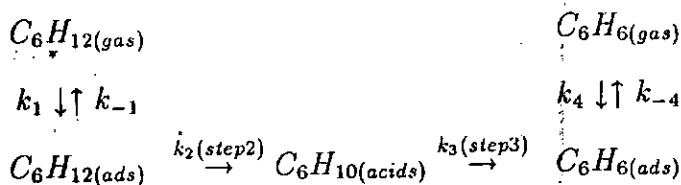
1. Step 1 is the adsorption of cyclohexane on to the catalyst surface:

2. Step 2 is the surface conversion of adsorbed cyclohexane to adsorbed cyclohexene

3. Step 3 is the conversion of adsorbed cyclohexene to adsorbed benzene while

4. Step 4 is the desorption of adsorbed benzene to free gas molecules.

The rate expression for each step represented by Langmuir-Hinshelwood rate equation is shown below for four separate rate determining steps:

Step 1:

$$r_{(C_6H_{12})} = \frac{k_1(C_6H_{12})}{\left(1 + \left(\frac{C_6H_6}{K_4}\right)\right)\left(\frac{H_2^3}{K_3K_4} + \frac{H_2^2}{K_3} + 1\right)} \tag{2.1}$$

Step2: Surface conversion of adsorbed cyclohexane to adsorbed cyclohexane

$$r_{(C_6H_{12})} = \frac{k_2K_1(C_6H_{12})}{1 + K_1(C_6H_{12}) + \frac{(C_6H_{12})}{K_4}H_2^2/(K_3 + 1)} \tag{2.2}$$

Step 3: Conversion of adsorbed cyclohexane to adsorbed benzene

$$r_{(C_6H_{12})} = \frac{\frac{k_3K_1K_2C_6H_{12}}{H_2}}{1 + K_1(C_6H_{12}) + \frac{K_1K_2(C_6H_{12})}{H_2} + (C_6H_6)/K_4} \tag{2.3}$$

Step 4: Desorption of adsorbed benzene

$$r_{(C_6H_{12})} = \frac{\frac{K_4K_1K_2K_3(C_6H_{12})}{(H_2^3)}}{(1 + K_1(C_6H_{12})(1 + K_2/H_2 + \frac{K_2K_3}{H_2^3}))} \tag{2.4}$$

They proposed that the second step is rate controlling in hydrogen carrier and hence the overall rate expression for the disappearance of cyclohexane is given by:

$$-r_{(C_6H_{12})} = \frac{k_2K_1C_6H_{12}}{(1 + K_1C_6H_{12} + \frac{(C_6H_6)}{K_4}(H_2^2/K_3 + 1))} \tag{2.5}$$

In hydrogen carrier the activation energies were found to be 87.9 and 121.3KJ-mole for $T \leq 553K$ and $> 553K$ respectively. The order of reaction with respect to cyclohexane was first order.

Echiyoga and Toyota(39) also proposed a Langmuir-Hinshelwood equation for a single site reaction without any terms in the denominator for benzene and hydrogen. They

18

explained that the terms for benzene and hydrogen are negligible compared to the other terms in the denominator. Hence the rate equation was reduced to:

$$- r_{C_6H_{12}} = \frac{K_1 K_2 (C_6H_{12})}{(1 + K_1(C_6H_{12}))} \tag{2.6}$$

In agreement with the above results of Susu et al.(38), Somorjai et al.(40) identified cyclohexene as an intermediate in the dehydrogenation of cyclohexane to benzene and found the conversion of cyclohexane to adsorbed cyclohexane to be the rate determining step.

Various authors have developed models in the area of catalyst deactivation and others have have carried out experiments on the basis of which they have developed models to explain their results. These models will be reviewed and compared to put in focus the need for the model(s) that would be developed by this author in the next chapter. The experiments done will be reviewed separately so as to distinguish clearly the various methodologies that have been employed by different researchers to study catalyst deactivation, and the effect of the various process variables on activity.

ACTIVITY MODELLING

The usual framework within which activity modelling is done is based on the principle of separability in which the effect of activity can be factored out(41,42,43). Thus, kinetic dependencies, which are time- independent, and activity dependencies, which are not, are separable (Butt(43), Szepe and Levenspiel(35)). Modelling based on separability has been severely criticized particularly because of a feature that is unique to coking-the formation of multilayers(41). There is also theoretical and experimental evidence to show that assumption of separable kinetics is questionable(43). Most models describing the deactivation of the catalyst by coking are based on either of these principles. Below is a review of these models.

2.2.2 Voorhies Model

Voorhies (25) is credited with the first and the most commonly used correlation in catalyst deactivation. The overall coke concentration C_c, was related to the time, t, by the equation:

$$C_c = At^n \qquad (2.7)$$

where n and A are constants. This correlation has very limited predictive value as the constants A and n vary not only with the reaction scheme but also with the space velocity employed in the reactor. When used to model the coke deactivation in the hydroisomerisation and the cracking of normal paraffins using modernite bifunctional catalyst, Eberly et al.(44) found that the constants depended on the reaction conditions- n varied from 0.29 to 0.049. Even though the model can predict the coke content with respect to the time of deactivation, it is not a rate law from which mechanism of coke formation can be derived and cannot be used to study the kinetics of deactivation.

2.2.3 Levenspiels Model

For the conversion of reactant A to product R, Levenspiel(35) proposed the following reaction paths for the deactivation based on the separability approach :

$$A \rightarrow R + P \qquad (2.8)$$

$$A \searrow_P \rightarrow R \; parallel \; reactions \qquad (2.9)$$

$$A \rightarrow R \rightarrow P \; series \; reaction \qquad (2.10)$$

$$A \quad \rightarrow \quad R \qquad (2.11)$$

$$A \quad \rightarrow \quad P(side \; by \; side \; reaction) \qquad (2.12)$$

20
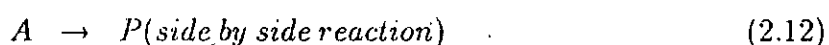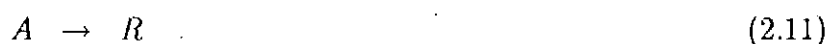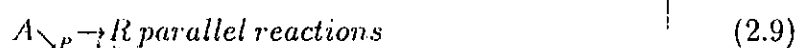
where P is coke. The rate equations for the main and the coking reactions are given by

$$\text{Reaction rate} = F_1(\text{main stream temp}) \times F_3(\text{main stream concentration})$$

$$\times F_5(\text{activity of the catalyst})$$

$$-R_A = kC_A^n \tag{2.13}$$

$$-R_A = k_o \exp\left(\frac{-E}{RT}\right)C_A^n \tag{2.14}$$

$$\text{Deactivation rate} = F_2(\text{main stream temp}) \times F_4(\text{main stream conc})$$

$$\times F_6 \,(\text{present state of catalyst})$$

$$\frac{-da}{dt} = k_d C_i a^d \tag{2.15}$$

Therefore

$$\frac{-da}{dt} = k_{do}(\exp\frac{E_{do}}{RT})C_i^{n'} a^d \tag{2.16}$$

For parallel and consecutive reactions.

$$A\searrow_{P_1} \rightarrow R \rightarrow P\downarrow \tag{2.17}$$

$$\frac{-da}{dt} = k_d(C_A + C_R)^n a^d \tag{2.18}$$

Since $C_A + C_R$ is a constant for specific concentration

$$\frac{-da}{dt} = k_d a^d \;(\text{independent rate of deactivation}) \tag{2.19}$$

Conditions;

1. Activity independent concentration $n' = 0$

2. 1st order reaction $n = 1$

21

3. 1st order of deactivation $d = 1$

1. For reactions performed with **batch solids and batch fluids**

$$a = a_o \exp\left(-k_d t\right) \tag{2.20}$$

$$In\frac{C_{Ao}}{C_A} = \frac{K_w}{K_d V}(1 - \exp\left(-k_d t\right)) \tag{2.21}$$

2. For reactions performed with **batch solids, mixed constant flow of fluid**

$$a = a_o \exp\left(-k_d t\right) \tag{2.22}$$

$$In\left(\frac{C_{Ao}}{C_A}\right) - 1 = In k\tau - k_d t \tag{2.23}$$

where;

$$\tau' = \frac{WC_{Ao}}{F_{Ao}}$$

3. For reactions performed with **batch solid, plug constant flow of fluid**

$$a = a_o \exp\left(-k_d t\right) \tag{2.24}$$

$$In\, In(C_{Ao}/C_A) = In\tau' k - k_d t \tag{2.25}$$

4. For reactions performed with **batch solids changing fluid flow** and keeping C_A fixed.

$$In\tau' = k_d t + In\frac{(C_{AO} - C_A)}{kC_A} \tag{2.26}$$

where the feed flow rate is varied to keep the final concentration of reactant constant.

5. For reactions performed with **batch solid, plug flow changing flow of fluid** keeping $\bar{C}_A$,out fixed

$$In\tau^1 = k_d t + In\frac{1}{K}In\frac{C_{Ao}}{C_A}$$ (2.27)

The above methods for the predictions of the activity of the catalyst with respect to the time of deactivation can be extended to any reaction order n and deactivation order d if activity is concentration independent, i.e $n^1 = 0$

Conditions

1. Activity made independent of concentration by keeping concentration of the reactant C_a constant.

2. n^{th} order of reaction

3. d^{th} order of deactivation

For parallel deactivation in a mixed reactor,

$$A\searrow_{P_1}\rightarrow R$$ (2.28)

$$-r_A = kC_A^n a = k_d' a$$ (2.29)

$$\frac{-da}{dt} = k_d' C_A^{n'} a^d = k_d' a^d$$ (2.30)

where C_A is kept constant. From the equation above,

$$\tau'^{d-1} = C_1 + C_2 t$$ (2.31)

where:

$$C_1 = \frac{(C_{Ao} - C_A)^{d-1}}{k'}$$ (2.32)

$$C_2 = \frac{(C_{Ao} - C_A)^{d-1}}{k'}(d-1)k_d'$$ (2.33)

$$\tau' = W\frac{C_{Ao}}{F_{Ao}}$$ (2.34)

For the zeroth order of deactivation:

$$\frac{1}{\tau'} = \frac{-k'k_d t}{C_{Ao} - C_A} + \frac{k'}{C_{Ao} - C_A} \qquad (2.35)$$

1st order of deactivation:

$$In\tau' = In\frac{(C_{Ao} - C_A)}{k} + k_d t \qquad (2.36)$$

2nd order of deactivation:

$$\tau' = \frac{C_{AO} - C_A}{k} + \frac{(C_{Ao} - C_A)}{k'}k_d' t \qquad (2.37)$$

3rd order of deactivation:

$$\tau'^2 = \frac{C_{Ao} - C_A}{k'} + 2\frac{(C_{Ao} - C_A)^2}{k'}k'dt \qquad (2.38)$$

With the right order of deactivation d, a plot of τ'^{d-1} vs t will be linear in accordance with equation 2.31. While Levenspiel's model is based on sound theoretical principles, it cannot be used in this work due to the following reasons;

1. The rate equation is based on a simple reaction system while the rate of dehydrogenation of cyclohexane on $Pt - Al_2O_3$ is best described by the Langmuir-Hinshelwood equation.

2. In most cases, the activity of deactivating catalyst is dependent on the concentration of the reactant. Levenspiel's method of keeping the reactant concentration constant during deactivation, for such cases, is difficult to attain in reality. A time consuming experimental scheme is necessary to attain this condition in the laboratory. A series of experiments are performed at various space times τ with each experiment serving as a data point at a given reactant concentration, C_a, in order to obtain a single model of the set conditions.

24

3. While Levenspiel's model will give information about the orders of deactivation and reaction, it will not provide any information about the number of active sites involved in the main and the coking reactions.

4. Furthermore, the model does not take into consideration, the mechanism leading to deactivation. Hence, all information in the types of coking that have been observed in catalyst deactivation is lost.

2.2.4 The model of Froment

Froment (28) developed two models for catalyst deactivation by coking, one describing catalyst deactivation by purely site coverage and another describing the deactivation by both active site coverage and pore blockage by coke.

Site coverage

For a single site: If the conversion of A to B is rate controlling for the reaction:

$$A \rightleftharpoons B \tag{2.39}$$

The rate equation is given by:

$$r_A = k_r k_A C_S (C_A - \frac{C_B}{K}) \tag{2.40}$$

The irreversible adsorption of the coke precursor C is represented by:

$$C + S \rightarrow CS \tag{2.41}$$

The total number of sites is given by:

$$C_t = C_S + C_{AS} + C_{BS} + C_{CS} \tag{2.42}$$

25

but $C_{AS} = C_A K_A C_S$ and $C_{BS} = K_B C_B C_S$ Hence:

$$C_t = C_S(1 + K_A C_A + K_B C_B + \frac{C_{CS}}{C_S})$$ (2.43)

Substituting 2.43 into 2.40 and rearranging

$$-r_A = \frac{k_r C_t K_A (C_A - C_B/K)}{1 + K_A C_A + K_B C_B + C_{CS}/C_S}$$ (2.44)

$$-r_A = \frac{C_t - C_{CS}}{C_t} k_r C_t K_A \frac{C_A - C_B/K}{(1 + K_A C_A + K_B C_B)}$$ (2.45)

Equation 2.44 is non-separable while 2.45 is separable with

$$\frac{C_t - C_{CS}}{C_t}$$ (2.46)

being the fraction of the active sites, for the main reaction. For an m_A sites of the main reaction the activity of the catalyst is given by:

$$\phi_A = \frac{(C_t - C_{CS})^{m_A}}{C_t}$$ (2.47)

$0 \leq \phi_A \leq 1$. If the coke precursor is formed by a reaction parallel to the main reaction i.e

$$AS \rightarrow CS$$
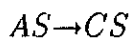
the rate equation for the coking reaction is given by:

$$r_c = \frac{k_C C_t K_A \phi_c C_A}{1 + K_A C_A + K_B C_B}$$ (2.48)

or

$$r_c = r_C^o \phi_c$$ (2.49)

and if the precursor is formed by the reaction in series with the main reaction, i.e

$$BS \rightarrow CS$$

26
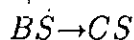
$$r_c = \frac{k_C C_t K_b \phi_c C_B}{1 + K_A C_A + K_B C_B} \tag{2.50}$$

or

$$r_c = r_C^o \phi_c \tag{2.51}$$

Following the same procedure as in the main reaction and for m_c^{th} site of the coking reaction reaction the coking activity is given by:

$$\phi_c = \frac{(C_t - C_{CS})^{m_c}}{C_t} \tag{2.52}$$

$0 \le \phi_c \le 1$. The rate of coke formation r_C and the rate of fractional site coverage, r_s^o, is given by:

$$r_s^o = \frac{r_c^o}{C_t M_c} \phi_c \tag{2.53}$$

Froment(1980) related the activity, ϕ, to the rate of fractional site coverage r_S by the equation:

$$\phi_A = \phi_C \tag{2.54}$$

and

$$\phi_C = \exp\left(\int_0^t r_s^o dt\right) \tag{2.55}$$

and for differential operation:

$$\phi_A = \phi_C \tag{2.56}$$

and

$$\phi_A = \exp\left(-r_s^o t\right) \tag{2.57}$$

2.2.5   The Model of Corella and Asua

The model of Corella and Asua(37) is based on a parallel coking reaction system which, for a non simple reaction, they represented by:

$$A + B \quad \rightarrow \quad R + V \tag{2.58}$$

27

$$A + B \rightarrow S + V \tag{2.59}$$

$$A + 6B \rightarrow 4U + 4V \tag{2.60}$$

$$(n + h)A \rightarrow P \tag{2.61}$$
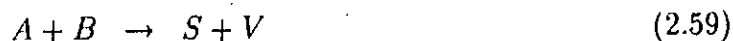
or for simple reactions represented by Froment equation:

$$A \rightarrow R + S \tag{2.62}$$

$$M \rightarrow P \tag{2.63}$$

Reactions 2.59 to 2.61 and 2.63 are the main reactions while 2.61 and 2.63 are the coking reactions. M is the substrate causing deactivation and it is adsorbed on the catalyst surface. Corella and Asua (37) represented the rate of activity decay by:

$$\frac{da}{dt} = \frac{(kinetic\ term)(Pressure\ term)^{n+h}}{(chemisorption\ term)^{h}} a^{d} \tag{2.64}$$

with the order of deactivation d, given by:

$$d = (m + h - 1)/m \tag{2.65}$$

In this study, the coke precursor M is the same as A, the cyclohexane molecule. The different mechanisms of the model of Corella and Asua(37) are given by: **Mechanism d-1**:

M is adsorbed in the coking reaction the same way it is adsorbed in the main reaction.

$$M + S \stackrel{adsorption\ step}{\rightleftharpoons} MS \tag{2.66}$$

$$nM_g + hM \stackrel{coke\ precursor\ formation\ step}{\rightleftharpoons} P_1 S_h \tag{2.67}$$

$$P_1 S_h \rightleftharpoons P_2 S_h \rightleftharpoons P_3 S_h (coking\ sequence\ step) \tag{2.68}$$
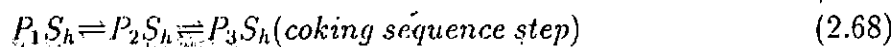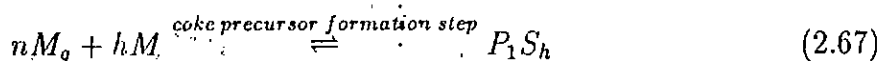
When coke precursor formation step is rate controlling:

For $h = 1$

$$a^{1/m} = \exp\left(-\int_0^t \frac{k_d K_M P_M^{n+1}}{(1 + K_A P_A + K_R P_R + (M-1)K_S P_S)} dt\right) \qquad (2.69)$$

For $h \neq 1$

$$\frac{-da}{dt} = \frac{mh L^{(h-1)} k_d K_M^h P_M^{n+h}}{(1 + K_A P_A + K_R P_R + (M-1)K_S P_S)^h} a^{(m+h-1)/m} \qquad (2.70)$$

The order of deactivation, $d = (m + h - 1)/m$

Mechanism d-2:

M is adsorbed in a different way in the main reaction as MS, and adsorbed in the coking reaction as $M * S$. This indicates a different energy of adsorption.

$$M + S \quad \overset{K_M^* (adsorption\,step)}{\rightleftharpoons} \quad M * S \qquad (2.71)$$

$$n M_g + h M * S \quad \overset{k_s}{\rightleftharpoons} \quad P_1 S_h (coke\,precursor\,formation\,step) \qquad (2.72)$$
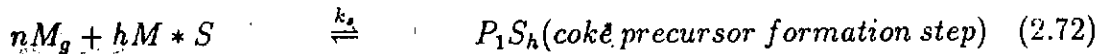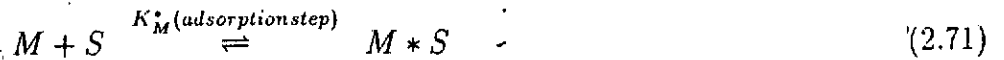
where:

$$K_M = \frac{C_{M*S}}{C_S P_M} \qquad (2.73)$$

$$k_d = \frac{C_{p_1}}{C_{M*S} P_M^2} \qquad (2.74)$$

$$P_1 S_h \rightleftharpoons P_2 S_h \rightleftharpoons P_3 S_h (coking\,sequence\,step) \qquad (2.75)$$
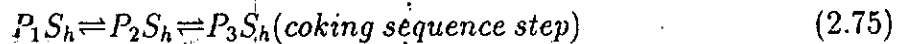
When the coke precursor formation step is the rate controlling for the $h \neq 1$

$$a^{(1-h)/m} = \frac{-h(1-h)}{L^{1-h}} \int_0^t \frac{k_d K_{M*}^h P_M^{n+h}}{(1 + K_A P_A + K_R P_R + (M-1)K_S P_S + K_{M*} P_M)} dt + 1 \qquad (2.76)$$

A summary of the different mechanisms and the corresponding deactivation functions are tabulated. The models of Corella and Asua (37) are very comprehensive and informative. A lot of deactivation parameters useful in analyzing the specific mechanism of catalyst deactivation can be obtained from them. However, some of the mechanism will be difficult to use due to insufficient information on some of the constants, like K_{M*} necessary

to model the catalyst deactivation. The assumption that h is both the number of active sites involved in the controlling step of the deactivation reaction as well as the number of adsorbed reactant molecules involved in the rate controlling step of the deactivation reaction presupposes that one adsorbed reactant molecule occupies only one active site. This asssumption may not hold for molecules that are adsorbed in the dissociated forms. An example is methane which is adsorbed in the forms: $CH_2 - CH_3$ and $\dot{H}_2$. Hence, one methane can be adsorbed on 1,2 or even 3 active sites. Owing to the complexity of the mechanism, Corella and Asua limited the test of their model to the d-1 and d-2 in their work on isobutene. The d-1 and d-2 mechanisms are likely to be adequate for the description of the deactivation of $Pt - Al_2O_3$.

The different mechanism and deactivation functions are found on Table(7).

2.2.6 Model of Cooper and Trimm

Following Froments general analysis of kinetics of coking, Cooper and Trimm (33) derived a deactivation model where the deactivation function was related to the number of coked sites on the catalyst. From Froment(28) the main reaction is represented by:

$$A + * \quad \rightleftharpoons \quad A* \tag{2.77}$$

$$A* \quad \xrightarrow{rate\ controlling\ step} \quad B* \tag{2.78}$$

$$B* \quad \rightleftharpoons \quad B + * \tag{2.79}$$

The coking side reaction may involve either $A*$ or $B*$ and will result in the total number of active sites C_t being reduced by the number of coked sites, C_k. For the coking mechanism of the type:

$$hA* \xrightarrow{r.d.s} C + nA \rightarrow Coke \tag{2.80}$$

Cooper and Trimm (33) represented the rate of loss of active sites with respect to increase in the number of coked sites formed by:

$$\frac{-dC*}{dC_K} = \alpha C_*^n \tag{2.81}$$

and the rate of coke formation with respect to time for the hth site mechanism by:

$$\frac{dC_k}{dt} = \frac{k(K_A C_A)^h C_t^h \phi^h}{(1 + K_j C_j)^h} \tag{2.82}$$

Therefore K_j is the adsorption coefficient and C_j is the conc of species j.

Cooper and Trimm(33) gave a table of deactivation function for various orders as shown in Table 2.1. They, however, did not specifically define the exponent n but it is clear from the coking rate controlling step equation that it is the number of free reactant molecules reacting with the coke precursor to form a molecule of coke. The same n was referred to as the order of coking reaction in the table of deactivation above.

31

$\frac{-dC_*}{dC_k}$	single site	Dual Site
α	$(1 - \alpha_1 C_k) = \phi_1$	$(1 - \alpha_4 C_4)^2 = \phi_4$
αC_*	$\exp(-\alpha_2 C_k) = \phi_2$	$exp(-2\alpha_5 C_k) = \phi_5$
αC_*^2	$(1 + \alpha_3 C_k)^{-1} = \phi_3$	$(1 + \alpha_6 C_k)^{-2} = \phi_6$

Table 2.1: Deactivation functions by Cooper and Trimm(33)

The above models in the table cannot be used in the above form as the required variable-the number of coked sites C_k, cannot be monitored.

2.2.7 Model of Butt(43)

The main reaction type:

$$A + S \rightleftharpoons B + S \qquad (2.83)$$

and the poisoning reaction type, where:

$$L + S \rightleftharpoons L.S \qquad (2.84)$$

where L is the poison on site, S. Butt described the following diffusion and reaction equations:

$$D_A \nabla^2 - \xi \frac{\partial C_A}{\partial t} - \rho K_A C_A S = 0 \qquad (2.85)$$

$$D_L \nabla^2 - \xi \frac{\partial C_L}{\partial t} - \rho K_L C_L S = 0 \qquad (2.86)$$

with the following initial and boundary conditions:

$$S = 1 \qquad\qquad t = 0 \qquad all\ r$$

$$C_A = C_{AO} \qquad\qquad C_L = C_L \quad t > 0 \quad r = R$$

$$\frac{\partial C_A}{\partial r} = \frac{\partial C_L}{\partial r} = 0 \qquad t > 0 \qquad r = 0 \tag{2.87}$$

$$D_A \nabla^2 C_A - \rho K_A C_A = 0 \qquad t = 0 \qquad all\ r$$

$$D_L \nabla^2 C_L - \rho K_L C_L = 0 \qquad t = 0 \qquad all\ r$$

The rate of activity loss is given by:

$$\frac{ds}{dt} = -K_{L,d} C_L S \tag{2.88}$$

With the use of Wheeler-Robells(45) analysis based on the fixed bed ion-exchange (adsorption) theory of Bohart and Adams(46) and the parallel poisoning reaction controlling, Butt obtained:

$$S = 1 - \frac{C_p}{C_{p_s}} \tag{2.89}$$

and:

$$\frac{C_p/C_{p\infty}}{=} \frac{1 - \exp\frac{-N_T\theta}{\theta_\infty}}{1 + \exp\frac{-N_T\theta}{\theta_\infty} \exp\frac{(N_T Z)}{L} - 1} \tag{2.90}$$

where

$$N_T = \frac{K_p L}{V}$$

. For the first order reactions, conversions obtained from concentration gradient equation: $\frac{1}{L}\frac{\partial C}{\partial Z}\Big| = KC$ was given by;

$$In\frac{C_L}{C_o} = -(1/L)\int_0^L k_o S dz \tag{2.91}$$

Substituting for both S and $\frac{C_p}{C_{p_s}}$ using equation 2.89 and 2.90 for parallel poisoning and intergrating yields:

$$In\frac{C_L}{C_o} = \frac{K_o}{K_p} In\left(1 - \exp\left(-\frac{N_T\theta}{\theta_\infty}\right)\right) + \exp\left(N_T - \left(\frac{1-\theta}{\theta_\infty}\right)\right) \tag{2.92}$$

33

2.2.8 Klingman and Lees' Multilayer Coking Model

Klingman and Lee developed a model that took into acount the multilayer deposition of coke on the catalyst surface. The justification for this was founded in the knowledge that coke deposited on the catalyst surface exceeds multilayer coverage(43). They represented multilayer coke by a series of irreversible elementary surface reactions (adsorption steps) thus:

$$P + S \quad \rightarrow \quad P.S \, Monolayer \, coke \tag{2.93}$$

$$P + P.S \quad \rightarrow \quad (2P).S \tag{2.94}$$

$$P + P.S \quad \rightarrow \quad (3P).S \tag{2.95}$$

$$P + (nP).S \quad \rightarrow \quad [(n+1)P].S \tag{2.96}$$
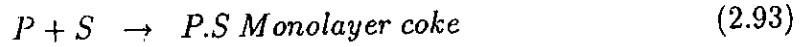
The first step is for monolayer coking, since one molecule of coke precursor adsorbs onto a vacant site S to form monolayer coke. Multilayer coke forms, as shown, when the precursors deposits onto a mono or multilayer coke. The net rate for the coking steps were obtained as:

$$R_{ps} \quad = \quad k_{p_c} C_p C_v - k_{p_1} C_{ps} C_p \tag{2.97}$$

$$R_{2ps} \quad = \quad k_{p_1} C_{ps} C_p - k_{p_2} C_{2ps} C_p \tag{2.98}$$

$$R_{3ps} \quad = \quad k_{2p} C_{2ps} C_p - k_{p_3} C_{3ps} C_p \tag{2.99}$$

and in the general case:

$$R_{nps} = k_{p(n-1)} C_{(n-1)ps} C_p - k_{p_n} C_{nps} C_p \tag{2.100}$$

where C_p is the concentration of coke precursor, C_v is the surface concentration of vacant sites, and C_{nps} ($n = 1, 2, 3, ... N$) is the surface concentration of active sites occupied by monolayer $n = 1$ and multilayer $n > 1$ coke. N is the total number of coke layers. The

authors assumed the rate constants for the formation of all multilayer coke to be the same:

$$k_{p_1} = k_{p_2} = k_{p_n} = k_p \tag{2.101}$$

This assumption involves the hypothesis that the affinity of coke to precursor is the same regardless of the number of coke layers. Total number of catalysts sites:

$$C_t = C_v + \sum_{n=1}^{N} C_{np.s} + \sum_{i} C_{i.s} \tag{2.102}$$

For the main and coking reaction occuring on the same sites

$$C_t \gamma = \sum_{n=1}^{N} C_{np.s} \tag{2.103}$$

where γ is the fraction of catalyst deactivated. Thus, we have

$$C_t(1 - \gamma) = C_v + \sum_{i} C_{i.s} \tag{2.104}$$

From knowledge of the multilayer coke distribution the following relationship between coke content and the fraction of catalyst deactivated was obtained:

$$C_c = q \sum_{n=1}^{N} n C_{np.s} \tag{2.105}$$

$$= qCp.s \left[\frac{f(1 - f^n) - N f^N (1 - f)}{(1 - f)^2} + \frac{1 - f^N}{1 - f} \right] \tag{2.106}$$

where:

$$C_c = \text{is the coke content in weight per unit surface area} \tag{2.107}$$

$$q = \text{the monolayer coke weight per site} \tag{2.108}$$

$$N = \text{the total number of coke layers} \tag{2.109}$$

$$f = \text{the coke distribution factor} \tag{2.110}$$

The following relationship was also obtained:

$$\frac{C_c}{Q} = \gamma \left[\frac{1}{1 - f} - \frac{N f^N}{1 - f^N} \right] \tag{2.111}$$

35

where $Q = C_t q$ is the weight of coke required to cover all active sites with one layer of coke. For infinite layer the equation reduces to:

$$\frac{C_c}{Q} = \frac{\gamma}{1-f} \qquad (2.112)$$

From above we have:

$$\frac{C_c}{Q} = \gamma \left[1 + \frac{\gamma}{\overline{K_p}(1-\gamma)} \right] \qquad (2.113)$$

where

$$\overline{K_p} = \frac{K_p}{(1+G)^n} \qquad (2.114)$$

where $\overline{K_p} = lumped\ multilayer\ parameter$. Now the residual activity remaining after deactivation, A, is given as:

$$A = 1 - \gamma \qquad (2.115)$$

Hence the fractional activity is related to the coke content as follows:

$$\frac{C_c}{Q} = (1 - A)\left[1 + \frac{1-A}{\overline{K_p}A} \right] \qquad (2.116)$$

For a finite number of layers the relationship between coke content and the fraction of catalyst deactivated is given by:

$$\frac{1-f}{f(1-f^N)} = \frac{\overline{K_p}(1-\gamma)}{\gamma} \qquad (2.117)$$

The distribution factor f,for infinite layer is essentially the same as for finite layer. The results obtained by considering infinite layer can describe the initial stages of coking when the fraction of catalyst deactivated γ, is relatively small. Hence rewritting equation 2.116

$$\frac{C_c}{1-A} = Q + \left(\frac{Q}{\overline{K_p}} \right)\left(\frac{1-A}{A} \right) \qquad (2.118)$$

assuming, of course, that $A = 1 - \gamma$. Klingman and Lee evaluated the model parameters using the activity data of Dumez and Froment(29). The model 2.118 predictes a straight

line, where Q is the monolayer coke coverage and $\overline{K_p}$ lumped parameter. The model adequately predicted the experimental coke content data in the earlier part of deactivation after which it was obvious that it required the more realistic finite layer result to describe the relationship over the entire activity of interest.

Klingman and Lee's assumption of surface homogeneity is an idealisation, as most solid catalysts contain cracks, and non-uniform pores within which the major fraction of the surface area resides(47). It is this heterogeneity that gives the catalyst surface varying energies of adsorption. It would then be interesting to evaluate the effect of ignoring the assumption of surface homogeneity on multilayer coking i.e 2.101. This will be developed in the next chapter.

2.3   EXPERIMENTAL DEACTIVATION STUDIES

2.3.1   Effect of Coke Accumulation on the dehydrogenation Activtity of Pd-Sn-Silica

It is usually known that the active sites of metallic catalyst would be covered by coke gradually from stonger to weaker sites. Accordingly, with the increase in coverage by coke, the activation energy of the reaction might be expected to increase and the pre-exponential factor might be expected to decrease. To examine the above hypothesis Masai(48) measured the activation energy and the pre-exponential factor during the course of deactivation over several Pd-Sn-Silica catalyst. They(48) studied the dehydrogenation of cyclohexane to benzene using a conventional fixed bed reactor at normal pressure. The activity of the fresh catalyst was stabilized by successive reaction and regeneration until the conversion was reproducible. Kinetic measurements were carried

37

out at low conversion to minimize the effect of deactivation. For the measurement of activation energy, coke was accumulated at the same temperature. They found that the rate equation was of zero order with respect to cyclohexane on all the catalysts.

Although the amount of coke on other catalysts was below measureable levels, the activity of these catalysts was recovered by the usual regeneration method. Calcination in the flow of air diluted by nitrogen and subsequent reduction in the flow of hydrogen(32). The authors concluded that the decrease of the pre-exponential factor with increasing process time is most likely the result of the increasing coverage of active sites by coke. The desorption of benzene was considered to be the rate determining step of the dehydrogenation of cyclohexane over Ni and Pd.

2.3.2   On the Dehydrogenation Reaction of n-Butane deactivation of Alumina-Chromia catalyst

An experimental study on the dehydogenation reaction of n-butane to n-butene with alumina-chromia catalyst was performed using a differential reactor(49). N-butene produced, and coke deposit on the catalyst were continuosly measured and the mechanism of the reaction of dehydrogenation of n-butene and coke deposition investigated. Accordingly, they found that there are two types of active sites effective for dehydrogenation reaction- Lewis acid sites and Brønsted acid sites, and that the coke deposition takes place only at the Lewis acid sites. The rate equation of these reactions were obtained. Otake et al.(50) also studied the same dehydrogenation reaction and concluded that the reaction scheme for coke formation is:

$$n-butane \xrightarrow{r_1} butene \xrightarrow{r_c} coke$$
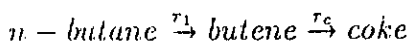
and obtained the rate equation for n-butene production and coke formation as:

$$r_1 = k_1 \phi P_{C_4 H_{10}} \tag{2.119}$$

where $\phi = 1 - \frac{C_c}{C_{c\infty}}$

$$r_c = k_c P_{C_4 H_8} \tag{2.120}$$

According to their results the rate of coke formation is not affected by the coke deposit on the catalyst while the rate of n-butene production is lowered by it. Otake et al.(50) defined the overall effectiveness factor which contains both the effect of pore diffusion and that of the deactivation of the catalyst. It is given as $E_f = E_{f_o}$. Toel et. al(51) performed a similar experiment for the dehydrogenation reaction of n-butane and obtained different results from those of Otake et. al. Otake, for example, reported that the effective diffusivity decrease with coke deposit while Toel et al.(52) obtained different results. The following points are raised.

1. If the dehydrogenation of n-butene and coke formation take place at the same sites in the catalyst, it is questionable that the coke deposit affects only the dehydrogenation reaction.

2. If both reactions take place at different active sites, the deposited coke should affect only the coke formation.

The purpose of the work were to elucidate the mechanisms of the reactions of dehydrogenation for n-butane and coke deposition with the deactivation of alumina-chromia catalyst and to obtain the reaction rate equations. Toei et al. used a microbalance which enabled them to measure the increase in coke weight with time on-stream.

39

Order of deactivation	Single site(h)	Dual Site(h)
0	$r_t = r_0(1 - \alpha_1 C_k)$	$r_t = r_0(1 - \alpha_4 C_4)^2$
1	$r_t = r_0(\exp(-\alpha_2 C_k))$	$r_t = r_0(\exp(-2\alpha_5 C_5))$
2	$r_t = r_0(1 + \alpha_3 C_k)^{-1}$	$r_t = r_0(1 + \alpha_6 C_k)^{-2}$

Table 2.2: Deactivation functions by Cooper and Mechanisms by Cooper and Trimm

2.3.3 The coking of Pt-alumina Reforming Catalyst.

Cooper and Trimm(33) studied the kinetics of coking of a $Pt - Al_2O_3$ catalyst by the dehydrocylization, dehydrogenation, dehydroisomerization, and isomerisation of C_6 hydrocarbons between the temperatures of $450^\circ C$ and $550^\circ C$ under 10 bar pressure. The reactions were carried out in a tubular reactor suspended from one arm of a microbalance. The results were analyzed using the general coking scheme.

$$A + * \rightleftharpoons A* \qquad (2.121)$$

$$A* \overset{r.d.s}{\rightarrow} B* \qquad (2.122)$$

$$B* \rightleftharpoons B + * \qquad (2.123)$$

Cooper and Trimm(33) obtained the modelling equations shown in the Table 2.2. Generally,

$$r_t = r_0 \phi \qquad (2.124)$$

where ϕ is the activity of the coking reaction since the variable used in this modelling is the number of coked sites. The quantity of coke in mg deposited on the catalyst with respect to the time on-stream was monitored for each hydrocarbon reaction at various temperatures. The quantity of coke deposited per gram of catalyst was plotted against the time on-stream for each reaction. At various coke levels, the slope $\frac{dC_k}{dt}$ was determined

40

Temperature	Reaction Controlling step
$450^\circ C$	$A* \rightarrow C \rightarrow Coke$
$500^\circ C$	$A* \rightarrow C + 2A \rightarrow Coke$
$550^\circ C$	$A* \rightarrow C + 4A \rightarrow Coke$

Table 2.3: Effect of temperature on Rate controlling Step

and a table of rate of coking versus coke content was obtained. The modelling equations of the table were tested with each set of data and the modelling equation that best fits the data was determined for each reaction.

From the results, Cooper and Trimm(33) found that one molecule of cyclohexane reacted with one adsorbed coke precursor molecule during the reaction of benzene and cyclohexane. Hence, they concluded that the mechanism of reaction of benzene on $Pt - Al_2O_3$ catalyst was by molecular condensation on the metal function of the catalyst. This implies that a simple site exponential form activity decay can best describe the coke formation due to the dehydrogenation of cyclohexane and hydrogenation of benzene on $Pt - Al_2O_3$ catalyst. The deactivation function was given by

$$\phi = \exp\left(-\alpha C_k\right) \tag{2.125}$$

where C_k is the number of coked sites. The rate controlling step was represented as:

$$A* \rightarrow C + A \rightarrow Coke \tag{2.126}$$

Cooper and Trimm showed that temperature has a significant effect on the mechanism of coking and the deactivation function of the catalyst. The rate controlling steps varied with temperature as demonstrated in Table 2.3 for the deactivation of $Pt - Al_2O_3$ for the n-hexane reaction. Since Cooper and Trimm used the direct quantity of primary

coke deposited on the catalyst to model the deactivation of the catalyst, the deactivation function obtained is applicable to the primary coke formation reaction. The presentation of only six modelling equations and the failure to show the procedure of development of such equations limit the models applicability. Cooper and Trimm(33) did not only fail to mention this relationship in their paper but also assumed exponent m (number of active sites involved in the rate controlling step of the main reaction) to be unity in their model development. Hence, the six modelling equations presented are applicable to a single mechanism of the main reaction .

2.3.4 Isobutene Oxidation on Active Charcoal by a Parallel Reaction

Model Development

Corella and Asua(37) showed that a method of studying the deactivation of catalyst when the distributioin of the product changes with time. The study was carried out on the oxidation of isobutene to methylacrolein on a $5\% HgCl_2 - active\ charcoal$ catalyst at 0.95 atmosphere in an isothermal and differential fixed bed reactor at $220^\circ C$, $200^\circ C$, and $180^\circ C$. The model proposed for main reaction was represented by:

$$A + B \rightarrow R + V \tag{2.127}$$

$$A + B \rightarrow S + V \tag{2.128}$$

$$A + 6B \rightarrow 4U + 4V \tag{2.129}$$

where:

$$A = Isobutene \tag{2.130}$$

$$B = Oxygen \tag{2.131}$$
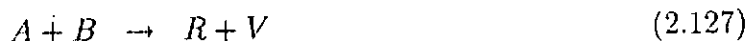
$$R = Mehtylacrolein \tag{2.132}$$

$$U = Carbondioxide \tag{2.133}$$

$$V = Water \tag{2.134}$$

The mechanism of Catalyst deactivation by coking was represented by

$$(n + h)A \rightarrow P \tag{2.135}$$

where n can be 0,1,2, and h can be 1,2 due to the improbability of three body collision. For the parallel main network, the kinetics of deactivation was represented for each of the products by :

$$r_{Ro} = (r_{Ro})_o a_1 \tag{2.136}$$

$$\frac{-da_1}{dt} = \psi_1(P_i, T)a_1^{d_1} \tag{2.137}$$

$$r_{So} = (r_{So})_o a_2 \tag{2.138}$$

$$\frac{-da_2}{dt} = \psi_{o2}(P_i, T)a_2^{d_2} \tag{2.139}$$

$$r_{Uo} = (r_{Uo})_o a_3^{d_3} \tag{2.140}$$

Generally, for reaction j:

$$r_j = (r_j)_o a_j \tag{2.141}$$

$$\frac{da_j}{dt} = \psi_{oj}(P_i, T)a_j^{d_j} \tag{2.142}$$

.there is the possibility that $a_1 \neq a_2 \neq a_3$ Defining yield of product R as:

$$Y_{\frac{R}{A}} = Y_R = \frac{moles \, of \, R \, obtained}{moles \, of \, A \, fed} \tag{2.143}$$

The activity, was given by :

$$a_1 = \frac{r_{Ro}}{(r_{Ro})_o} = Y_R/Y_{Ro} \tag{2.144}$$

43

For the differential reactor system and $d_j = 1$

$$a_j = a_{jo} \exp\left(-\int_o^t \psi_{oj}(P_i, T)dt\right) \tag{2.145}$$

$$a_j = a_{jo} \exp\left(-\psi_{oj}(P_i, T)t\right) \tag{2.146}$$

$$a_{jo} = 1 (initial\ activity) \tag{2.147}$$

$$Ina_j = -\psi_o(P_i, T) \tag{2.148}$$

If $d_j \neq 1$:

$$(a_j^{1-d_j} - 1) = (1 - d_j)\psi_{oj}(P_i, T)t \tag{2.149}$$

To determine the value of d_j, the data of the activity versus time, t, is required.

For the main product R, consideration has been given to the four different kinetic equations from two out of the six different mechanisms depicted in Table(7). The tests were limited to the d-1 and the d-2 mechanism. The same approach was used for the second product S. For the third product U, its deactivation equation was represented by the empirical equation of the type:

$$\frac{-da}{dt} = \psi_{o3}(P_i, T)a_3^{d_3} \tag{2.150}$$

For the differential operation, when $d_3 = 1$, after intergration of the above equation the following was obtained:

$$Ina_3 = -\psi_{o3}(P_i, T)t = k_{d_3} P_A^{n_1} t \tag{2.151}$$

when $d_3 \neq 1$:

$$a_3^{1-d_3} - 1 = (d_3 - 1)k_{d_3} P_A^{n_1} t \tag{2.152}$$

Data Collection

In order to identify the influence of each reactant in the deactivation order d_j, two separate sets of experiments were done keeping the pressure of one of the reactants

44

constant and varying the pressure of the other reactant.

Sample Data Analysis for the product R.

A table of the yield of R, Y_r and the time on stream t, was obtained at each temperature. Y_r was plotted against t, and the activity $\frac{Y_r}{Y_{ro}}$ was obtained at various times on stream. $In\, a = In\frac{Y_r}{Y_{ro}}$ was then plotted against t as in equation 2.149 to verify the value of d or h. At $220°C$ with the assumption that $d = 1$ a graph of $In\, a\, vs\, t$ was linear indicating that $d = h = 1$. This was confirmed also at $180°C\, and\, 200°C$. The same result was obtained regardless of which of the two reactants was held constant. In an earlier work, Corella and Asua had found that $m = 1$. Hence, the four equations to be tested for n with $m = 1$ and $h = 1$ from table after linearisation were reduced to: $d - 1$ mechanism 2nd step:

$$\frac{P_A^{n+1}}{\psi_{o1}(P_i, T)} = \frac{1}{K_{d_1} K_{A_1}} P_A + \frac{K_{B_1}}{K_{d_1} K_{A_1}} P_B \qquad (2.153)$$

$d - 1$ mechanism, 3rd step:

$$\frac{P_A^{n+1}}{\psi_{o1}(P_i, T)} = \frac{1}{K_{d_1} K'_{A_1}} + \frac{K_{A_1}}{K_{d_1} K'_{A_1}} P_A + \frac{K_{B_1}}{K_{d_1} K'_{A_1}} P_B + \frac{K''_{A_1}}{K_{d_1} K'_{A_1}} P_A^{n+1} \qquad (2.154)$$

$d - 2$ mechanism 2nd step:

$$\frac{P_A^{n+1}}{\psi_{o1}(P_i, T)} = \frac{1}{K_{d_1} K^*_{A_1}} + \frac{K_{A_1} + K^*_{A_1}}{K_{d_1} K^*_{A_1}} P_A + \frac{K_{B_1}}{K_{d_1} K^*_{A_1}} P_B \qquad (2.155)$$

$d - 2$ mechanism, 3rd step:

$$\frac{P_A^{n+1}}{\psi_{o1}(P_i, T)} = \frac{1}{K_{d_1} K^{*'}_{A_1}} + \frac{K_{A_1}}{K_{d_1} K^{*'}_{A_1}} P_A + \frac{K_{B_1}}{K_{d_1} K^{*'}_{A_1}} P_B + \frac{K^{*'}_{A_1}}{K_{d_1} K^{*'}_{A_1}} P_A^{n+1} \qquad (2.156)$$

where:

$$\psi_{o1} = (1/t) In\, a_1 \qquad (2.157)$$

To determine which of the four equations would give the corect mechanism of reaction:

- the values of the deactivation parameters $K_{d_1}, K^*_{a_1}, K'_{a_1}$ must be positive.

- the values of K_{A_1} and K_{B_1} obtained from the equation must agree with those obtained from the kinetic study of the fresh catalyst without deactivation.

Using data of (P_i, T) at different P_A and P_B at each temperature and adjusting the linearised equation by the least square method, Corrella and Asua(37) found that equation 2.155 gave the best fit with $n = 1$. Hence, the main reaction and the rate of activity decay of the catalyst in the formation of wetting acrolein are given by:

$$r_R = (r_{R_o})a_1 \tag{2.158}$$

$$\frac{-da}{dt} = \frac{K_{d_1} K^*_{A_1} P_A^2}{1 + (K_{A_1} + K^*_{A_1} P_A + K_{B_1} P_B}a_1 \tag{2.159}$$

The same procedure was followed for the modelling of the reaction of the second product, and the same set of deactivation. Kinetic parameters were obtained for m, n and h. The value of d_3 was found to be 1 and that of n found to be zero with respect to the third product CO_2. Its rate of activity decay was therefore given by:

$$\frac{-da_3}{dt} = K_{d_3} a_3 \tag{2.160}$$

while the deactivation kinetic parameters m, n, h were found to be independent of temperature, the kinetic constants K_d and K_{A_1} vary with temperature in accordance with Arrhenius relationship. The model of Corella and Asua has demonstrated a method of modelling the activity decay of the catalyst with respect to each product of a non-simple reaction. The approach of solving the equation of deactivation makes it possible to determine both the deactivation kinetic parameters m, n, h as well as the fresh catalyst kinetic constants K_d and K_A. It was observed that the deactivation equation was already determined from a previous experiment. Previous determination of m made the solution of the equation less rigorous.

46

2.3.5 The Model of Omoleye and Susu

Omoleye and Susu(7) simulated the deactivation of an industrial catalyst $0.3\% Pt - Al_2O_3$ to the mortal state in the laboratory by use of multiple deactivation-regeneration scheme in a $CSTR$. The aging of the catalyst was accelerated by use of N_2 gas. In addition to this remarkable achievement, they observed a hitherto unreported phenomenon-the existence of stability states with respect to catalyst lifetime. They developed a model for activity loss during reaction and tested its accuracy with their data. The acclaimed general applicability of their model was demonstrated when it was successfully used in modelling the deactivation of MCP on $Pt - Al_2O_3$ catalyst(9). Omoleye and Susu (6), based on a critical study of the coking models of Froment (28), Corella and Asua (37) and that of Cooper and Trimm, presented a model that eliminated the short commings of the studied models. The foregoing is the detailed development of the model.

Following the general analysis of coking kinetics by Froment (28) and Corella and Asua (37), we have

$$A \rightleftharpoons A*$$

$$nA + hA* \xrightarrow{k_c} P_1*_h \tag{2.161}$$

$$P_1*_h \rightleftharpoons P_2*_h \rightleftharpoons P_3*_h \ P_{n'}*_h \rightarrow P_{n'}h_*$$
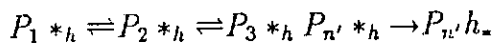
$n = 1, 2, 3$. Generally from the modelling of Cooper and Trimm:

$$\frac{-dC_*}{dC_k} = \alpha C_*^n \tag{2.162}$$

and from Froment(1980):

$$\frac{C_*}{C_t} = \phi_A^{1/m} \tag{2.163}$$

The rate of coke formation is given by:

$$\frac{dC_k}{dt} = k_c A^n A*^h \tag{2.164}$$

$$\frac{dC_k}{dt} = K_c K_A^h \frac{C_A^{n+h} C_*^h}{(1 + K_A C_A)^h} \tag{2.165}$$

47

- When $n = 1$, that is when the number of free gas molecules involved in the coking reaction is one, from 2.162

$$\int_{C_t}^{C_*} \frac{dC_*}{C_*} = -\alpha \int_0^{C_k} dC_k \qquad (2.166)$$

$$In\frac{C_*}{C_t} = -\alpha C_k \qquad (2.167)$$

where:

$$C_* = C_t \exp\left(-\alpha C_k\right) \qquad (2.168)$$

substitute 2.168 into 2.163

$$\phi_A^{1/m} = \exp\left(-\alpha C_k\right)$$

$$\phi_A = \exp\left(-\alpha C_k\right)^m \qquad (2.169)$$

$$\frac{dC_k}{dt} = \frac{kK_A^h C_A^{1+h}}{\left(1 + K_A C_A\right)^h} C_t^h \exp\left(-\alpha C_k\right)^h \qquad (2.170)$$

Intergrating with respect to C_k we have:

$$C_k = \frac{1}{\alpha h} In\left(\alpha h K_c K_A^h C_t^h \int_o^t \frac{C_A^{1+h}}{\left(1 + K_A C_A\right)^h} dt + 1\right) \qquad (2.171)$$

substituting in 2.169 and rearranging we have:

$$\phi_A = \left(\alpha h k_c K_A^h C_t^h \int_o^t \frac{C_A^{1+h}}{\left(1 + K_A C_A\right)^h} dt + 1\right)^{-m/h} \qquad (2.172)$$

Therefore, for $n = 1$

$$\phi_A = \left(\alpha h k_c K_A^h C_t \int_o^t \frac{C_A^{1+h}}{\left(1 + K_A C_A\right)^h} dt + 1\right)^{-m/h} \qquad (2.173)$$

or

$$\phi_A^{-h/m} = \alpha h k_c K_A^h C_t^h \int_o^t \frac{C_A^{1+h}}{\left(1 + K_A C_A\right)^h} dt + 1 \qquad (2.174)$$

hence:

$$\frac{d\phi_A}{dt} = -\alpha m k_c K_A^h C_t^h \frac{C_A^{1+h}}{\left(1 + K_A C_A\right)^h} \phi_A^{(m+n)/m} \qquad (2.175)$$

48

the order of deactivation if $n = 1$ is given by:

$$d = (m + h)/m \qquad (2.176)$$

- When $n \neq 1$, i.e. when the number of free gas molecules involved in the rate controlling step of the coking reaction is not 1; from 2.162

$$\int_{C_t}^{C_*} \frac{dC_*}{C_*^n} = -\alpha \int_o^{C_k} dC_k \qquad (2.177)$$

$$C_* = (C_t^{1-n} - (1-n)\alpha C_k \alpha)^{1/(1-n)} \qquad (2.178)$$

substitute in 2.163:

$$\psi_A^{1/m} = (C_t^{1-n} - (1-n)C_k\alpha)^{1/(1-n)} \qquad (2.179)$$

$$\frac{dC_k}{dt} = \frac{k_c K_A^h C_A^{h+n}}{(1 + K_A C_A)^h}(C_t^{1-n} - (1-n)\alpha C_k)^{h/(1-n)} \qquad (2.180)$$

Intergrating with respect to C_k we have:

$$\frac{1-n}{(1-n)(1-n)\alpha(h-n+1)}(C_t^{1-n} - (1-n)\alpha C_k)^{(\frac{-h+n-1}{n-1})}$$
$$-(C_t^{1-n})^{(\frac{-h+n-1}{n-1})}$$
$$= k_c K_A^h \int_o^t \frac{C_A^{n+h}}{(1 + K_A C_A)^h}dt \qquad (2.181)$$

Substituting $C_t^{1-n} - (1-n)\alpha C_k = (\phi_A C_t^m)^{(1-n)/m}$ into above equation we have:

$$\frac{1-n}{(1-n)\alpha(h-n+1)}(\phi_A C_t^m)^{(n-h-1)/m} - C_t^{n-h-1} = k_c K_A^h \int_o^t \frac{C_A^{n+h}}{(1 + K_A C_A)^h} \qquad (2.182)$$

Rearranging we have:

$$\phi_A^{(n-h-1)/m} = \frac{\alpha(h-n+1)k_c K_A^h}{C_t^{n-h-1}} \int_o^t \frac{C_A^{n+h}}{(1 + K_A C_A)^h}dt + 1 \qquad (2.183)$$

This is the Omoleye and Susu modelling Equation. Differentiating 2.183 we have;

$$\frac{d\phi_A}{dt} = \frac{-m\alpha k_c K_A^h}{C_t^{n-h-1}} \cdot \frac{C_A^{n+h}}{(1 + K_A C_A)^h}\phi_A^{(m+h+1-n)/m} \qquad (2.184)$$

49

Hence the order of deactivation is $d = (m + h + 1 - n)/m$. The concentration C_A is given by:

$$C_A = \frac{C_{A_o}(1 - X_A)}{1 + \varepsilon X_A} \qquad (2.185)$$

The Omoleye and Susu model above was developed for the deactivation of the main reaction for all the models using the concentration of the reactants or products in the modelling equation, the deactivation constant, K_A and the rate constant k_c were assumed constant and uninfluenced by deactivation. They have, however, been found to vary with stages of deactivation. The average value is hence employed in the modelling equation since the change in their values with deactivation cannot be simultaneously monitored with the change in the concentration of the reactant or products. For an intergral reaction system, and with the correct number of molecules n, the number of adsorbed reactant h, and the number of active sites, m, a linear plot with an intercept of unity will be obtained when $\phi_A^{(n-h-1)/m}$ is plotted against $\int_o^t \frac{C_A^{n+h}}{1+K_A C_A^h} dt$ according to equation 2.183.

The advantage of this model over the others discussed earlier is its flexibility of use. The model can use the concentration of the reactants versus time of reaction data as well as the number of coked sites, C_k with time of reaction.

2.3.6 Osaheni and Susu:Estimation of Toxic Coke

An estimation of the quantity of toxic coke deposited on $Pt - Al_2O_3$ catalyst during reforming operations was studied by the authors using methylcyclopentane as the model reforming reaction(9). The reaction was carried out in the same reactor used by Omoleye and Susu(34) but at 390^oC with a reactant partial pressure of 0.092 atmospheres (70 torr), in H_2 and N_2 carriers (total pressure of 1 atmosphere).

The oxidizable coke level was measured as grams of carbon oxidized at 430°C with air while toxic coke level was monitored as moles of methane (also in grams carbon) removed at 500°C during reduction with hydrogen. The reduction continued till the toxic coke profile was found to be fairly stable. Since the toxic coke profiles never reduced to zero it meant that some of the toxic coke was retained on the catalyst surface. This coke was suggested to be graphitic in structure. Prior to this work(9) no attempt had been made to estimate the coking level of the toxic forms of coke which actually led to the mortal state of the catalyst(6,7). Hence this was the first time known to this author that toxic coke would be quantified. This tallied with the objectives of their work(9) which was to find suitable conditions for the removal and quantification of toxic coke forms (secondary and tertiary) which had been identified to cause catalyst mortality.

In their work(9), done in a $CSTR$, three cycles were carried out in hydrogen before switching over to accelerated ageing in O_2-free N_2. After each cycle, the quantity of oxidizable coke was measured and the toxic coke level was monitored with time during reduction in order to estimate its quantity. The major finding of this work(9), unreported before, at the time, was the occurence of toxic coke in layers and that these layers represented toxic coke of varying resistance to reduction and with the most resistant occuring at the catalyst-coke interface. These conclusions on the structure of the coke were graphically illustrated by the coke reduction profiles. The reaction temperature, W/F ratio and the partial pressure of MCP were maintained at constant values of $390°C$, $0.11 gmincm^{-1}$ and 092 atm. respectively. The modelling of the deactivation of $Pt - Al_2O_3$ catalyst by methylcyclopentane was done following the model Omoleye and Susu.

The experimental design to achieve the objectives of this thesis and particularly the emphasis on removal of toxic coke derives from the results of the work of Omoleye and Susu(6,7), Osaheni and Susu(9) and of course the numerous pace-setters in catalytic

deactivation studies.

2.4 CATALYST REGENERATION MODELLING

Given the cost of reforming catalyst, the catalyst has to be regenerated after deactivation and this has to continue till the catalyst can no longer respond to regeneration or when the regenerated activity is no longer economically viable.

Regeneration of coke-induced deactivation is industrially achieved by burning off the coke in an air stream(6,8). If air is passed through a coked catalyst bed, hot enough to get ignition, burning starts as the air hits the catalyst and forms a hot spot or hot layer(52). The hot spot formation is caused by the exothermic oxidation reaction when the coke is converted into CO_2 and CO. This can cause thermal sintering of the catalyst. A common technique is to reduce the oxygen concentration of air to about 2-3% (7,52).

Regeneration is a gas-solid reaction. The essential feature in most gas-solid reaction is that the conditions inside the particle change with time since the solid itself is involved in the reaction. When reaction occurs simultanously with mass transfer within porous structure, a concentration gradient is established and the interior surfaces are exposed to lower reactant concentrations than surfaces near the exterior. The effect of mass transfer within a porous structure on observed reaction characteristics were first analyzed quantitatively by Thiele(53). This was further developed by A. Wheeler(54) and P.B Weisz and Goodwin(55,56). Several investigators have studied the rates of combustion of carbonaceous deposits in porous catalysts under diffusion controlled conditions. The rates reported are usually (although not always) based on the amount of carbon gasified (Weisz and Goodwin(55,56), Haggerbaumer and Lee(57), Pansing W.F.(58)).

The important results of these investigations have been the estimation of the intrinsic

activation energies. The observed activation energies all fall between 35 and 40kcal/g-mole, but the adsorption of oxygen and desorption of products affect the kinetics in a way which varied substantialy with temperature, pressure, and nature of the carbon(59). The intrinsic rate of reaction of reaction is strongly affected by the form of the of the form of the carbon and the nature of the, nature of the impurities present. This makes the agreements of the burning rates as reported by the various investigators markedly good(59).

Effron and Hoelsher(60) studied oxidation rates of four types of graphites at temperatures of $420 - 533^oC$, mostly in 1 atm. of pure oxygen. The rates of reaction per unit area varied by a factor of about 5 between the most active and least active graphites, but the activation energy was 35.5kcal/gmol in each case.

The physical situation in regeneration is that of a gas reacting with a solid of low porosity to yield a porous reacted layer often called the ash layer(Weisz and Goodwin(55), Sohn and Svekely(61), Froment and Bischoff(62), Wen C.Y.(63)). The reaction takes place in a narrow zone that moves progressively from the outer to the centre of the particle. Such a situation is described by the much familiar heterogenous shrinking core model (55,61,63). Heterogenous because there exists two distinct layers inside the particle, with clearly distinct properties.

P.B. Weisz and R.D. Goodwin(55,56) studied the combustion of carbonaceous deposits within porous catalysts particles. Their studies dealt with the kinetic processes of combustion, with oxygen, of carbonaceous deposits contained in the pores and granules of a porous refractory solid. An understanding of the mechanism involved in this type of rate processes is not only of technological interest, but it involves kinetic models which are instructive of a broader scope of rate processes. Weisz and Goodwin obtained combustion rate data on individual catalyst granules. The data were evaluated in terms

53

of fractional amount of carbon burned (or remaining) vs time.

On the basis of information obtained, two distinct limiting models for burn-off mechanism were recognised. The intrinsic region of chemical kinetics, with combustion rate at any one time substantially equal at all points on the bead radius, and the totally mass transport controlled region characterised by shell-progressive burn-off.

2.4.1 Shell Progressive Region of Kinetics.

Oxygen diffusing into the structure is totally consumed upon initial contact with carbonaceous fuel. For the sphere the following equations were derived:

$$\frac{d^2C_{ox}}{dr^2} + 2\frac{dC_{ox}}{r\,dr} = 0 \tag{2.186}$$

$$r\frac{dC_{ox}}{dr} = R_o \tag{2.187}$$

$$\frac{dN_{ox}}{dt} = D4\pi R_o^2 \left(\frac{dC_{ox}}{dr}\right)_{r=R_o} \tag{2.188}$$

where $D = porous\ granule\ diffusivity\ for\ oxygen$

$$\frac{dN_c}{dt} = carbon\ removal\ rate \tag{2.189}$$

$$\frac{dN_c}{dt} = n\frac{dN_{ox}}{dt} \tag{2.190}$$

Introducing

$$y = \frac{N_c}{N_{c,o}} = \frac{R_b}{R_o{}^3} \tag{2.191}$$

where y = fraction of initial carbon remaining and $N_{c,o}$ the initial amount of carbon on the solid. From above:

$$1/2 1 - Y^{2/3} - 1/3(1 - Y) = Kt \tag{2.192}$$

$$K = n\frac{DC_{ox}}{R_o^2 C_c} \tag{2.193}$$

One major draw back of the physical model of Weisz and Goodwins' shell progressive model is that the shell progressive reaction is significantly insensitive to many phenomena which may otherwise be critical. Since the rate is controlled by diffusion process, details of chemical or physical texture and intrusive reactivity are of no consequence as long as it remains sufficiently reactive.

The grain model accounting explicitly for the structure of the solid was developed by Sohn and Szekely(61). In the model, the particle is considered to consist of a matrix of very small grains between which the fluid has easy access through the pores.

The fluid reactant concentration in the particle of any geometry is obtained from:

$$\varepsilon \frac{\partial C_{As}}{\partial t} = D_{ep} \frac{\partial^2 C_{As}}{\partial r^2} - De \frac{\partial C_{Ag}}{\partial y} \times (1 - \varepsilon_s a_g) \tag{2.194}$$

To obtain the concentration profile in the grain the general model equation is used:

$$\varepsilon_g \frac{\partial C_{Ag}}{\partial t} = D_{eg} \frac{\partial^2 C_{As}}{\partial y^2} - r_A \rho_{sg} \tag{2.195}$$

$$\frac{\partial C_{sg}}{\partial t} = -r_s \rho_{sg} \tag{2.196}$$

with the following initial and boundary conditions:

$$t = 0 \quad C_{ag} = C_{ago} \quad C_{sg} = C_{sgo}$$

$$y = 0 \quad \frac{\partial C_{Ag}}{\partial y} = 0 \tag{2.197}$$

$$y = Y \quad C_{Ag} = C_{As}r$$

From the various considerations we have the approximate solution and analytical solution the same as that developed by Weisz and Goodwin(55):

$$Y = \frac{t}{t_\infty} = 1 - 31 - x^{2/3} + 2(1 - x) \tag{2.198}$$

2.4.2 Model with interfacial and Intraparticle Gradients

. Froment and Bischoff(62) present a theoretical treatment of the simultaneous diffusion and reaction of a spherical, isothermal coked catalyst in a flow of reactant gas. A simple

first order was assumed for the reaction of the gas and the solid fuel. When the particle is assumed to be isothermal, only differential material balances have to be written. Diffusion of species within the porous structure can be represented by Ficks first law and an overall invariant effective diffusion coefficient,

$$Flux = -D_{eff}\left(\frac{dc}{dr}\right)$$

The differential balance on the reacting gaseous component A-the continuity equation for A contains an accumulation term accounting for the transient nature of the process, a term arising from the transport by effective diffusion and a reaction term (62):

$$\frac{\partial}{\partial t}\varepsilon C_{As} = (1/r^2)\frac{\partial}{\partial r}\left(D_e r^2 \frac{\partial C_{As}}{\partial r}\right) - r_A \rho_s \tag{2.199}$$

while the continuity equation for the reacting component of the solid is:

$$\frac{\partial C_s}{\partial t} = -r_s \rho_s \tag{2.200}$$

The initial and boundary conditions at $t = 0$ are as follows:

$$C_{As} = C_{As} \tag{2.201}$$

$$C_s = C_{so} \tag{2.202}$$

In the center of the sphere, $r = 0$ we have as follows:

$$-\frac{\partial C_{As}}{\partial t} = 0 \tag{2.203}$$

for reasons of symmetry at the surface, $r = R$, we have as follows:

$$D_e\left(\frac{\partial C_{As}}{\partial r}\right)_{r=R} = k_g(C_A - C_{As}^s) \tag{2.204}$$

where C_{As}^s is the concentration of A at the particle surface. In general the equations cannot be intergrated analytically (62). Wen(63),intergrated the general equation numerically for the following rate equations:

$$r_A \rho_s = akC_{As}^n C_s^m \tag{2.205}$$

56

where a is the number of moles of A reacting with one mole of S.

$$r_s \rho_s = k C_{As}^n C_s^m \tag{2.206}$$

The results obtained for values of $n = 2$ and $m = 1$ in the absence of interfacial gradients gave gas consumption profiles and coke consumption profiles for the reaction at various reduced times. The profiles were presented for the case of high and low Thiele Modulus(53).

While the general model as proposed models the general regeneration problem, it has not been widely applied for gas-solid reactions following the Langmuir-Hinshelwood kinetics. This is because most gas-solid reactions are generally considered to be non-catalytic reactions (53,60,61,62,63). However, there is evidence strongly suggesting that coke regeneration, particularly the oxidation process, may be a catalyzed process (17,18,59). In the next chapter, a general model will be presented to evaluate effect of diffusional resistances during catalyst regeneration for gas-solid reactions following Langmuir-Hinshelwood kinetics.

2.5 CATALYST CHARACTERIZATION BY GAS CHEMISORPTION

In 1938, Brunnauer, Emmet and Teller(64) put forth a generalised theory of physical adsorption in some detail. The main highlight of the development was a clear specification of the volume of gas adsorbed on monolayer coverage. The means then became available, for the first time, of computing the total surface area of a porous body. e.g catalyst from physical adsorption data. Before the BET theory, proposed equilibrium models failed to yield an unequivocal means for determining monolayer coverage.

The BET development was motivated more by concern for catalyst surface area determination than for an adsorption-process rationale. Earlier Emmet and Brunauer(47) had described the use of adsorption isotherms for the determination of surface area of various iron catalysts in ammonia synthesis. The success of the BET theory of physical adsorption in determining surface coverage influenced a similar argument for the determination of the number of metal sites associated with the adsorption of a given amount of gas if the mechanism of the adsorption is fully understood. This technique, therefore, requires the formation of a chemical monolayer of the gas and that a simple relationship exists between the surface atoms and absorbed molecules.

A number of gases are capable of being chemisorbed by various metals (65). In practice, hydrogen, oxygen and carbon monoxide are the most frequently used gases in the determination of catalyst metal area. There is considerable difficulty in the interpretation of the results of carbon monoxide adsorption on metal surfaces since CO can adsorb in two different forms; linear and a bridged configuration (65). Since it is hard to define the relative amounts of CO in the linear or bridged form, it is very difficult to determine the number of surface metal atoms from the amount of CO adsorbed. How-

ever, modified methods with use of Electron Microscopy (EM) made simpler the use and interpretation of data using CO. The experimental design to bypass the drawiback in use of CO by employing EM is very elaborate(4). The problem associated with the use of oxygen is the formation of a surface oxide that can be more than one layer thick and of undefined stoichiometry (66). Oxygen is also reported to chemisorb to a large extent on alumina (67) thus making it less suitable for the determination of the metal area on alumina-supported metal catalysts.

Two methods have been extensively used in gas chemisorption experiments:- the static method and the continuous flow methods. Early workers used the static method to determine the gas uptake by various catalysts (65). In this method a known quantity of sorbable gas is allowed to contact the catalyst for a specified length of time and then evacuated. The gas uptake is then determined by the change in volume or weight of feed. Gas flow methods offer a simpler means for measuring chemisorbed volumes (68,69). The catalyst is contacted with a flow of inert gas containing a small amount of adsorbate. The concentration of adsorbate in exit stream is monitored continuously and the volume chemisorbed is measured from the time required for breakthrough of the adsorbate relative to a blank. The pulse method was first reported by Gruber(70). In Grubers method, a pulse of adsorbate is injected into the flow of inert gas and passed over the catalyst. The volume of adsorbate is measured before and after contact with the catalyst, and the volume adsorbed given by difference. A modification of this method (71) involves the injection of pulses appreciably less, rather than more than the anticipated uptake. The pulses are fully adsorbed until the monolayer is complete. Benerisi et al. (72) proposed a method of rapid measurement of hydrogen chemisorption on supported catalyst metals. This method involves equilibration of the sample at $0^{\circ}C$ with a stream of argon containing low concentration of hydrogen, and subsequently heating the sample in the same

argon-hydrogen stream to drive off the adsorbed hydrogen. The hydrogen driven off is measured by means of a thermal conductivity detector. Several workers (68,69,70) have compared the results from these methods with some disagreements in their conclusions. J. Beenhaker(4) first carried out an in-situ reduction of the catalyst with hydrogen flow and cooling down to $O^{\circ}C$. The extent of hydrogen adsorption was then determined by injecting 100μ pulses of absorbing gas into hydrogen or nitrogen (argon) flow. The pulses were detected by a thermal conductivity detector (TCD) coupled to an intergrator. The injection of the pulses continued until saturation of the metal surface had been achieved.

A comparison of data obtained by static and flow methods for the determination of hydrogen chemisorption on $Pt - Al_2O_3$ catalyst showed variation with temperature. At ambient temparature there was agreement of the data while at elevated temperature there was no agreement due to reversible chemisorption of hydrogen in the static method- a phenomenon not observed in the flow method. Boudart and Spenade (73) working at low temperature, showed that 90% of the hydrogen in a static system was adsorbed instantaneously while the remaining gas uptake proceeded slowly. Gases have been observed to be adsorbed at different states. Gruber (66) reported the existence of two kinds of adsorbed hydrogen with coverages 1×10^{12} to 4×10^{12} atoms when $\eta - alumina$ was exposed at high temperatures to molecular hydrogen. Amenomiya (74) found altogether five different states of chemisorbed hydrogen on γ alumina but only two predominated above room temperature with a number of sites for either of two types. The findings of Stephen et al (75) was crucial. They measured the adsorption of hydrogen on serveral $Pt - Al_2O_3$ catalysts and concluded that the adsorption of hydrogen on aluminia was negligible.

It has been demonstrated that by a number of workers that while alumina may have little activity for dissociative hydrogen adsorption, a substantial amount of hydrogen

atoms may migrate from a supported metal to the alumina support. This phenomenon, termed spill over effect, has also been observed with Pt-silica system (76). Kramer and Andre(77) showed that the rate of spill over increases with hydrogen pressure, adsorption temperature and metal dispersion. The amount of spill over hydrogen is proportional to the square root of adsorption time at low coverages and reaches a limiting value at high temperature and long adsorption time. A mechanism involving fast adsorption of hydrogen and the metal and fast spill over of atomic hydrogen over the face boundary to the alumina was proposed. It is suggested that the spill over of hydrogen may be arrested by blocking the surface sites on alumina for adsorption of atomic hydrogen. Sodium Acetate has been found to do this effectively.

The much familiar hydrogen titration of oxygen on alumina supported platinum metal is due to Benson and Bourdart (67).

$$PtO_{surface} + (3/2)H_{2(gas)} \rightarrow Pt - H_{surface} + H_2O_{(gas)} \qquad (2.207)$$
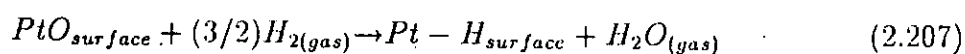
They opined that the residual water generated by the above equation is removed by the alumina support, It is therefore possible to measure the loss of three atoms of hydrogen from the gas phase for every platinum atom. They pointed out the fact that there was no need to leave out oxygen from the sample and the catalyst need not be reduced prior to measurement since the sample is deliberately exposed to oxygen. Furthermore, the adsorption of hydrogen in the oxidized alumina contributes a very small amount to the uptake of hydrogen . From the reaction, chemisorbed hydrogen: chemisorbed oxygen: and hydrogen: and hydrogen titre are in a ratio of 1:1:3. Benson and Boudart obtained the same ratio using the static method.

A review of the Benson and Boudart(67) stoichiometry by Mears and Hansford (78)

for the $H_2 - O_2$ titration by the flow technique led to the following reaction scheme

$$Pt_{(surface)} + H_{2(gas)} \rightarrow Pt - H_{2(surface)} \qquad (2.208)$$

$$Pt_{(surface)} + (1/2)O_{2(gas)} \rightarrow Pt - O_{(surface)} \qquad (2.209)$$

$$Pt_{(surface)} + 2H_{2(gas)} \rightarrow Pt - H_{2(surface)} + 2H_2O_{(support)} \qquad (2.210)$$
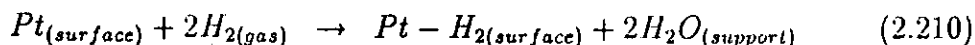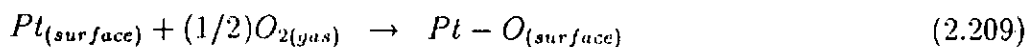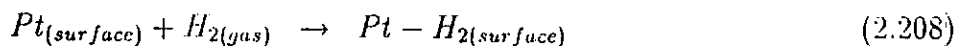
This corresponds to a ratio of 2:1:4 for chemisorbed hydrogen, chemsorbed oxygen and Hydrogen titre respectively. Mears and Hansford argued that the stoichiometry of Benson and Boudart(67) could have arisen from the lower outgassing time adopted by Benson and Boudart in which case the catalyst could be expected to contain some residual hydrogen and hence an apparently lower chemisorption of it would be observed. Wison and Hall(79) reported the ratio could vary from 2:1:4 to 1:1:3 on increasing the temperature of pre-treatment in hydrogen at condition which would produce sintering.

Kobayashi et al.(80) found the uptake of hydrogen on a freshly reduced Pt-alumina catalyst decreased with increased temperature of reaction. They also reported that all oxygen adsorbed on a low dispersed catalyst reacted in hydrogen pure injected at $25^{\circ}C$. However, on well dispersed catalysts some of the adsorbed oxygen did not take part in the $H_2 - O_2$ reaction on injection of hydrogen pulses at room temperature. To account for all the variations so far discussed with regard to chemisorbed volume and stoichiommetry, John Freel (67) proposed the generalized equations for $H_2 - O_2$ tritration.

$$\frac{(2x+y)}{2}H_2 + XO_* \rightarrow yH_* + XH_2O \qquad (2.211)$$

$$\frac{(2x+y)}{4}O_2 + yH_* \rightarrow xO_* + (y/2)H_2O \qquad (2.212)$$
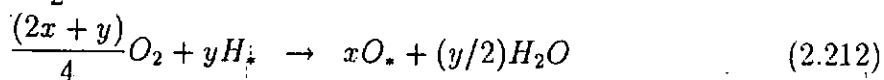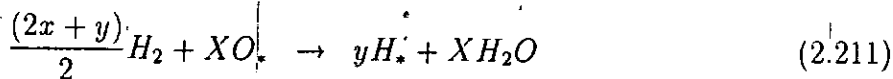
where H_* and O_* represent adsorbed atoms, H_2 and O_2 gas phase, molecules. The equations do not imply any stoichiommetry to either adsorbed species. They merely require that one adsorbate is removed quantitatively and replaced by the other in an amount equal to its own adsorption on the bare surface.

Inspite of some of the advantages mentioned above, $H_2 - O_2$ titration method for determining the Pt surface is not without criticism(81), the primary one being the dubious oxygen to surface Pt ratio. Wilson and Hall(79) noted changes in O(ads):Pt(s) stoichiometry as a function of particle size reporting that 1:1 stoichiometry occurs on particles greater than $20\mathring{A}$, while 1:2 prevails for smaller particles. Mears and Hansford(78) indicated two mechanisms for the titration reaction to be operative depending on the nature of the support. For Pt on Al_2O_3 or SiO_2 the water produced during the titration at $25°C$ is adsorbed by the hydrophylic support according to the scheme

$$PtO + 2H_{2(g)} \rightarrow PtH_{2(surface)} + H_2O_{(support)} \qquad (2.213)$$
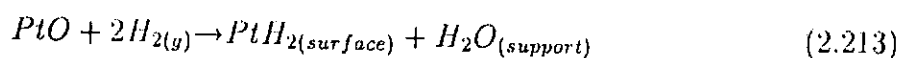
The water is held by the Pt when the latter is either unsupported or on a hydrophobic support.

$$Pt - O + (3/2)H_2 \rightarrow Pt \overset{h}{-} H_2O \qquad (2.214)$$
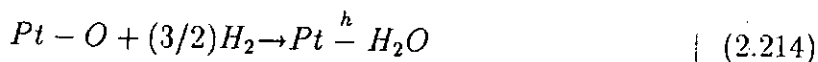
The $H_2 - O_2$ titration suffers from doubtful $\frac{O_{ads}}{Pt(s)}$ ratios and, therefore, cannot be recommended as a standard technique. It does have value for specific studies in that no drastic pretreatments need be used, thus minimizing possible catalyst alterations during the measurements.

Chapter 3

THEORETICAL MODELS

Introduction

Since all design methods assume some description or model, however crude, of the process ocurring, it is necessary to express these processes in mathetical terms. If the model is to be of any practical use it must be reliable. Clearly, the final design can be no better than the assumption made in deriving the model. If a model depends on parameters which have been been obtained by curve fitting experimental data then the values obtained will have little generality beyond the specific system for which they were determined since they are certainly of little value in the design. In fact, the answer is known i.e the plant is operating.

Not all important parameters necessary for plant design are measurable. Because theoretical models are mathematical representations of physical processes, they provide a means of approximating the effects of experimentally immeasurable parameters and phenomena without recourse to wasteful experiments. Perhaps the greatest obstacle to the development of more detailled models has been the computational effort involved in solving the resulting equations. Even though digital computers have alleviated the

problems, the use of efficient numerical analysis has assumed considerable importance, especially in view of the highly non-linear forms of the equations.

This chapter shall feature the formulation of the following models

1. Catalyst deactivation by multilayer coking model on real surface

2. Effect of diffusional resistance on catalyst regeneration

3. Deactivation-kinetics of the reaction of cyclohexane on $Pt - Al_2O_3$

3.1 MULTILAYER COKING MODEL ON REAL SURFACE

Multilayer coking on real catalyst surface is a modification of the multilayer coking model presented by Klingman and Lee(41). As with the model of Klingman and Lee, the main concept in the formulation of the multilayer coking model on real surface presented here is that coke deposits on the catalyst in successive layers with each layer covering a fraction of the one immediately below it. The model assumes that at any given time, the coke distribution can consist of any number of layers; from one layer to N layers. The layer build up results from a series of elementary irreversible surface reactions that lead directly to a relationship between coke content and fraction of catalyst deactivated. The coke content at monolayer coverage can also be deduced. An infinite number of layers is considered by the model although only a finite number of layers should exist. Consideration of an infinite layer reveals all the features of coking.

The Langmuir postulate on which the multilayer coking is based assumes that the solid surface upon which adsorption occurs is homogenous i.e the surface is energitically uniform so that the free energy change accompanying the adsorption of the first molecule

65

or atom is identical to the change associated with subsequent adsorption of that molecular or atomic species. Few gas-solid catalysts systems, however, conform to the homogenous surface postulates(47). Hence, unlike in the model of Klingman and Lee, the multilayer coking model will be extended to real, heterogenous surfaces.

3.1.1 Theory

Consider a scheme in which the main and the coking reactions occur on the same sites. It is also supposed that all the sites remain accessible to the reactant. If coke precursor P can form upon deposition whether the sites S, are vacant or occupied by coke, then the multilayer coke builds up from the series of elementary surface reactions thus

$$P + S \xrightarrow{k_{p_c}} P.S \downarrow monolayer\ coke \tag{3.1}$$

$$P + P.S \xrightarrow{k_{p_1}} (2P).S \downarrow \tag{3.2}$$

$$P + (2P).S \xrightarrow{k_{p_2}} (3P).S \downarrow \tag{3.3}$$

$$P + (nP).S \xrightarrow{k_{p_n}} [(n+1)].S \downarrow \tag{3.4}$$
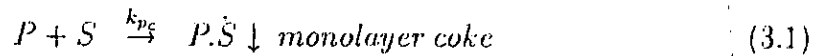
The net rates for the coking steps are;

$$R_{p.s} = k_{p_c} C_p C_v - k_{p_1} C_{p.s} C_p \tag{3.5}$$

$$R_{2p.s} = k_{p_n} C_p - k_{p_2} C_{2p.s} C_p \tag{3.6}$$

$$R_{3p.s} = k_{p_2} C_{2p.s} C_p - k_{p_3} C_{3p.s} C_p \tag{3.7}$$

$$R_{np.s} = k_{p_{(n-1)p.s}} C_{np.s} C_p - k_{p_n} C_p C_{np.s} \tag{3.8}$$

where

$$C_v = \text{surface concentration of vacant sites} \tag{3.9}$$

$$C_p = \text{Concentration of coke precursor} \tag{3.10}$$

66

$C_{np.s}$ = Surface concentration of active sites occupiedby mono($n = 1$) and multilayer ($n > 1$) co

and N = *total number of coke layers*. Generally the above equations can be represented as:

$$R np.s = k_{p_{n(n-1)}} C_{(n-1)p.s} C_p - k_{p_n} C_{np.s} C_p \tag{3.11}$$

For real surface coking;

$$k_{p_1} \neq k_{p_2} \neq \cdots \neq k_{p_n} \tag{3.12}$$

This assumption involves the hypothesis that the affinity of coke precursor, unlike in the model of Klingman and Lee, is different regardless of the number of coke layers. Hence this consideration constitutes the major difference between this development and the multilayer coking model as presented by Klingman are Lee(41). The implications of this development will be obvious in the course of the derivation. For real surfaces, the activation energy is assumed to have a linear relationship with surface coverage.

$$E_{ads} = E_{ads}^o + \gamma\theta \quad \theta = \text{coverage}$$

$$E_{des} = E_{des}^o - \beta\theta \quad q = q_o - \alpha\theta$$

where

$$E_{asd} = \text{energy of adsorption} \tag{3.13}$$

$$E_{des} = \text{energy of desorption} \tag{3.14}$$

$$K_{ad} = A\exp\left[-\left(\frac{E_{ads} + \gamma\theta}{KT}\right)\right] \tag{3.15}$$

$$\theta = \text{Coverage} \tag{3.16}$$

$$q = q_o - \alpha\theta \tag{3.17}$$

Since $k's$ are not equal the following is true for the energies of adsorption of the layers

$$E_1 \neq E_2 \neq E_3 \neq + \cdots \neq E_n$$

67

Considering the distribution of multilayer coke at any time:

$$\frac{R_{(n-1)p.s}}{R_{np.s}} = \frac{dC_{(n-1)p.s}}{dC_{np.s}} = \frac{C_{(n-2)p.s} - C_{(n-1)p.s}}{C_{(n-1)} - C_{np.s}} \tag{3.18}$$

and

$$\frac{C_{np.s}}{C(n-1)p.s} = f \tag{3.19}$$

where f is a constant that describes the distribution of layers at anytime: If 3.19 holds between mono and dilayer, we have

$$fC_{p.s} = C_{2p.s} \tag{3.20}$$

$$\frac{dC_{p.s}}{dC_{2p.s}} = \frac{K_p C_p C_v - k_{p_1} C_p C_{p.s}}{k_{p_1} C_{p.s} C_p - k_{p_2} C_p C_{2p.s}} \tag{3.21}$$

From 3.19 we have

$$(1/f) = \frac{dC_{p.s}}{dC_{2p.s}} \tag{3.22}$$

Hence 3.21 becomes

$$\frac{k_{p_c} C_p C_v - k_{p_1} C_p C_{p.s}}{k_{p_1} C_p C_{p.s} - k_{p_2} C_p C_{2p.s}} = 1/f \tag{3.23}$$

$$\frac{k_p C_v}{C_{p.s}} - k_{p_1} = (1/f)k_{p_1} - k_{p_2} \tag{3.24}$$

$$\frac{1}{k_{p_1}}\left[\frac{k_{p_c} C_v}{C_{p.s}} + k_{p_2} - k_{p_1}\right] = \frac{1}{f} \tag{3.25}$$

$$\frac{k_{p_c} C_v}{k_{p_1} C_{p.s}} + \frac{k_{p_2}}{k_{p_1}} - 1 = \frac{1}{f} \tag{3.26}$$

We then relate C_v and $C_{p.s}$ to determine the distribution of vacant sites. The distribution factor, f, should also be known From the total site balance:

$$C_t = C_v + \sum_{n=1}^{N} C_{np.s} + \sum_i C_{i.s} \tag{3.27}$$

$$C_t \gamma = \sum_{n=1}^{N} C_{np.s} \tag{3.28}$$

where γ is the fraction of catalyst deactivated.

$$C_t(1 - \gamma) = C_v + \sum C_{i.s} \qquad (3.29)$$

$$C_{i.s} = \text{Concentration of surface intermediate} \qquad (3.30)$$

With the concentration of surface intermediates expressed in terms of the concentration of reactants, product and vacant sites, we have

$$C_v + \sum_i C_{i.s} = C_v[1 + \sum_i (K_i C_{i.s})^{m_i}]^n \qquad (3.31)$$

$$C_t(1 - \gamma) = C_v(1 + G)^n \qquad (3.32)$$

where $G = \sum (K_i C_i)^{m_i}$ combining equation 3.28 and 3.32 yields

$$\frac{C_v}{C_{p.s}} = \frac{C_t}{C_{p.s}} \left[\frac{1 - \gamma}{(1 + G)^n} \right] \qquad (3.33)$$

The fraction of catalyst deactivated can be related to the distribution factor, f, through 3.19, 3.20, 3.32 as follows: Recall

$$C_t \gamma = \sum_{n=1}^{N} C_{np.s} \qquad (3.34)$$

Expanding $C_{np.s}$ we have

$$C_t \gamma = C_{p.s} + C_{2p.s} + C_{3p.s} + \cdots + C_{Np.s} \qquad (3.35)$$

Sustituting 3.20, 3.35 becomes

$$C_t \gamma = C_{p.s} + f C_{p.s} + f^2 C_{p.s} + f^3 C_{p.s} + \cdots + f^{(N-1)} C_{p.s} \qquad (3.36)$$

Sum of a geometric progression in f.

$$f C_t \gamma = f C_{p.s} + f^2 C_{p.s} + f^3 C_{p.s} + \cdots + f^N C_{p.s} \qquad (3.37)$$

69

Subtrtacting 3.36 from 3.35, we have:

$$C_t\gamma - fC_t\gamma = C_{p.s} - C_{p.s}f^N \tag{3.38}$$

$$C_t\gamma = C_{p.s}\left[\frac{(1-f^N)}{(1-f)}\right] \tag{3.39}$$

for infinite layer $N \to \infty$

$$\frac{C_t}{C_{p.s}} = \frac{1}{\gamma(1-f)} \tag{3.40}$$

To get the distribution factor f, we combine equations 3.23, 3.33 and 3.40

$$\frac{k_{p_c}C_t}{k_{p_1}C_{p.s}} \cdot \frac{(1-\gamma)}{(1+G)^n} + \frac{k_{p_2}}{k_{p_1}} - 1 = f \tag{3.41}$$

Substituting 3.40 into 3.41, we have

$$\frac{k_{p_c}}{k_{p_1}\gamma(1-f)}\frac{1-\gamma}{(1+G)^n} + \frac{k_{p_1}}{k_{p_1}} - 1 = f \tag{3.42}$$

$$\frac{\beta G'(1-\gamma)}{\gamma(1-f)} + \alpha - 1 = \frac{1}{f} \tag{3.43}$$

where:

$$\alpha = \frac{k_{p_2}}{k_{p_1}} \tag{3.44}$$

$$\beta = \frac{k_{p_c}}{k_{p_1}} \tag{3.45}$$

$$G' = \frac{1}{(1+G)^n} \tag{3.46}$$

Rearranging (21) we have

$$\beta\frac{G'(1-\gamma)}{\gamma} + \alpha(1-f) - (1-f) = \frac{(1-f)}{f} \tag{3.47}$$

$$f^2(\alpha - 1) - f(\beta G'\frac{(1-\gamma)}{\gamma} + \alpha) + 1 = 0 \tag{3.48}$$

Equation 3.48 is a quadratic in f, where the roots are given by:

$$f = \frac{(\beta G'\frac{(1-\gamma)}{\gamma} + \alpha) \pm \sqrt{\left(\beta G'\frac{(1-\gamma)}{\gamma} + \alpha\right)^2 - 4(\alpha - 1)}}{2(\alpha - 1)} \tag{3.49}$$

70

Making further simplifying assumptions by assuming that the roots are real and equal

$$\left(\beta G'' \frac{(1-\gamma)}{\gamma} + \dot{\alpha}\right)^2 - 4(\alpha - 1) = 0 \tag{3.50}$$

Hence this 3.49 reduces to

$$f = \frac{\beta G''(1-\gamma)}{2(\alpha-1)\gamma} + \frac{\alpha}{2(\alpha-1)} \tag{3.51}$$

For positive roots $\alpha > 1$

Considering the case of severe surface heterogeneity where $\alpha >> 1$ i.e when the differences in energy of adsorption between succcesive layers is high.

$$f = \beta G'' \frac{(1-\gamma)}{2\gamma} + \frac{1}{2} \tag{3.52}$$

$$f = \frac{\beta'(1-\gamma)+\gamma}{2\gamma} \tag{3.53}$$

where

$$\beta' = \frac{(\beta G')}{\alpha} \tag{3.54}$$

With the distribution known, we can obtain the relationship between coke content and the fraction of catalyst deactivated. Let q be the monolayer coke weight per site:

$$C_c = q \sum_{n=1}^{N} n C_{np.s} \tag{3.55}$$

$$= qC_{p.s}(C_{p.s} + 2C_{2p.s} + 3C_{3p.s} + \cdots + NC_{Np.s}) \tag{3.56}$$

$$= q(C_{p.s} + 2fC_{p.s} + 3f^2 C_{p.s} + \cdots + Nf^{N-1}C_{p.s}) \tag{3.57}$$

Substituting 3.19 into 3.57 and arranging we have

$$C_c = qC_{p.s}[(1 + f + f^2 + \cdots + f^{n-1}) + (f + 2f^2 + 3f^3) + (N-1)f^{N-1}] \tag{3.58}$$

Now multiplying 3.58 by f and then subtracting the resulting equation from 3.58 and rearranging we have:

$$(1-f)C_c = qC_{p.s}[(1-f^N) + f(1 + f + f^2 + \ldots + f^{N-2} + Nf^N] \tag{3.59}$$

$$f(1-f)C_c = qC_{p.s}[f(1-f^N) + f(f + f^2 + f^3 + \ldots + f^N) - Nf^{N+1}] \tag{3.60}$$

71

subtracting 3.60 from 3.60 and rearranging we have:

$$C_c = q C_{p.s} \left[\frac{f(1-f^N)}{(1-f)(1-f)} - \frac{f(1-f^N)}{(1-f)(1-f)} + \frac{N f^N (1-f)}{(1-f)(1-f)} \right] \qquad (3.61)$$

Substituting 3.39 into 3.61 we have

$$\frac{C_c}{Q} = \gamma \left[\frac{1}{1-f} - \frac{N f^N}{1-f^N} \right] \qquad (3.62)$$

where $Q = q C_t$, the amount of coke required to cover all active sites with one coke layer.

For infinite layer, ie $N \to \infty$, 3.62 reduces to

$$\frac{C_c}{Q} = \frac{\gamma}{(1-f)} \qquad (3.63)$$

Substituting 3.53 into 3.63 we have

$$\frac{C_c}{Q} = \frac{2\gamma}{\gamma + \beta'(1-\gamma)} \qquad (3.64)$$

and noting that the residual activity is related to the fraction of catalyst deactivated by $A = 1 - \gamma$, we obtain

$$\frac{C_c}{Q} = \frac{(1-A)^2}{(1-A) + \beta' A} \qquad (3.65)$$

and

$$\frac{1-A}{C_c} = \frac{1}{2Q} + \frac{\beta' A}{2Q(1-A)} \qquad (3.66)$$

where A plot of $\frac{(1-A)}{C_c}$ against $\frac{A}{(1-A)}$ should yield a straight line with intercept $1/2Q$ and slope $\frac{\beta'}{2Q}$. It should be noted that at the initial stage when the fraction of catalyst deactivated is small, γ, the distribution of finite and infinite layers is the same hence equation above also holds for the finite layer.

Data for residual activity was obtained from hydrogen chemisorption experiments in a CSTR for $0.3\% Pt - Al_2O_3$. The initial activity was obtained by determining the number of accessible Pt atoms on the fresh catalyst before cyclohexane dehydrogenation

reactions at $430°C$ at reactant vapour pressure of 0.0763 atm.($14°C$). After each reaction the number of accessible Pt atoms on the coked catalyst was determined. The determination was done after each reaction.

The number of Pt sites on the fresh catalyst was determined and then the fractional residual activity after each determination was then calculated from

$$\text{Fractional Residual Activity} = \frac{\text{Pt sites}}{\text{Pt sites on fresh catalyst}}$$

After the determination, the coke was oxidized for the quantification of the oxidizable coke.

A summary of the results of residual activity determination from hydrogen chemisorption experiments is shown in Table 12 in chapter 5

3.1.2 Parameter Estimation

A plot of Fractional Residual Activity versus oxidizable coke content was made. The plot showed a decaying curve with little scatter. The plot was extrapolated to the initial fractional activity. From the plot, the range of fractional activity versus coke content data was widened by extrapolation. The data values were then used to plot the model equation. From the plot the parameters were computed. The plot and its discussion follow in the next chapter.

3.2 Effect of Diffusional Resistance on Catalytic Regeneration of Catalyst

Regeneration of a catalyst after deactivation due to coking entails the removal of the coke deposits on the catalyst surface before further reaction. If air is passed through a coked catalyst bed, hot enough to get ignition, burning starts as the air hits the catalyst (52). The coke is then converted to gaseous products. The coke removed by this process is known as oxidizable coke. This oxidation process does not remove all the coke as some of it remain more tightly adsorbed on the catalyst surface (6,8,9,16,17). On reduction with H_2, a second type of coke, reduceable coke, is removed(6,9,16). The unreduceable coke is graphitic in nature and can only be removed by chemical means(17).

Intraparticle diffusion effect is one of the most important problems in heterogenous catalytic reactions as it causes many interesting phenomena. Wheeler(54) studied the effect of intraparticle diffusion on catalyst poisoning and showed that the overall activity decreased by about 10% of the initial value. Weisz and Goodwin(55,56) studied the regeneration of fouled catalyst by the combustion of coke with oxygen and showed that the rate determining step was the diffusion of O_2 through the porous ash layer.

In this section, the retardation in the catalyst regeneration due to diffusion has been solved for the case of a general model with interfacial diffusion gradients. The regeneration process is generally assumed to be a gas-solid non catalytic process. Hence most researchers on catalyst regeneration have presented solutions of the rate equations based on assumption of an interger power law, usually first order with respect to the solid reactant and first order with respect to the gaseous reactant (Hagerbaumer and Lee (57), Sohn and Svekely(61), Froment and Bischoff(62), Pansing(58), Goodwin and Weisz(55)). Wen provided a numerical solution of the general model for interfacial and

74

intrapaticle diffusion with n^{th} order to the concentration of the solid reactant.

Experimental investigations by several authors suggest that regeneration of coked catalyst may be a catalyzed process(17,55,56,97). Experimental results of Weisz and Goodwin(56) showed that a chromia-alumina catalyst shows rates two to three orders of magnitude greater than that observed on silica alumina, although the activation energies remain the same. They attributed the difference in rates to the catalytic properties of the chromium. Nora Figoli et al.(97) and Barbier et al.(17) provided evidence strongly suggesting that Pt catalyzed oxidation of coke at low temperature 300°.

In view of the above, the model presented here assumes the regeneration process to be a catalyzed one. As is usual with catalytic processes, this model formulation therefore assumes that the regenerating gas first adsorbs on a site before reaction. A Langmuir-Hinshelwood type kinetic expression is therefore suggested to be appropriate in modelling the rate of gasification of coke. Methods of simplifying the expected partial differential modelling equations have been provided by various authors: Akehata et al.(82), Prater and Lago(83). The specific case of the cracking of cumene to benzene and propylene has been analyzed by Prater and Lago(83) using a numerical technique.

Attempts at modelling the regeneration process as a catalyzed reaction had been made by Effron and Hoelscher in their study of the oxidation of graphite(60). They assumed the reaction to proceed via the formation of an oxygen-surface complex as a first step before reaction with the carbonaceous material.

The emphasis of the preceding works(55,56,57,58) except for those of Wen(63), Sohn and Szekeley(61) lay on the kinetics of the gasification process. Where the effect of diffusion process has been studied, so much emphasis has been on the identification of the conditions (particularly temperature) at which the intraparticle diffusion becomes rate limiting(55,56,57) with the neglect of external mass transfer limitations.

75

For the regeneration process to be effective, the gas present in the ambient fluid must be transported to the surface of the coked pellet and the reaction product has to be transported from the surface. Hence for a complete description of the diffusional limitations in regeneration, the diffusional process has to be divided into two parts; bulk fluid to the outer surface of the pellet and the diffusion to the reaction site. At the outer surface of the particle the gas has to diffuse through the stagnant gas film. Hence, the presentation here is a generalised treatment of the effect of the diffusional processes on the regeneration, at constant temperature, of a catalyst coked under non-diffusion-limiting conditions.

Model Formulation

To get to the catalyst surface the regenerating gas has to first diffuse through the stagnant gas film existing at the external surface of the hot solid catalyst. Inside the porous pellet, the reactant gas has to overcome the interfacial resistance between the fluid and solid phase and also the resistance due to countercurrent diffusion of products. Against these resistances, the reactant gas will adsorb on the active sites. This reaction is considered fast, hence there will be a concentration gradient for the gas, decreasing towards the center where it is being consumed and the reaction rate will be slower.

To calculate this lowering of rate expressed by the effect of the diffusion parameter, the simultaneous diffusion and reaction on the pellet have to be modelled.

Assumptions

- Isothermal pellet, no radial temperature gradients in the pellet.

- Uniformly coked catalyst pellet.

Taking material balance on a spherical isothermal pellet, located in a gas stream, A,

with which the coke reacts; hence taking material balance on a spherical isothermal pellet, located in a gas stream, A, with which the coke reacts; taking material balance for reactant gas A, we have

$$\frac{D_A}{RT}\left(\frac{\partial^2 P_A}{\partial r^2} + \frac{2}{r}\frac{\partial P_A}{\partial r}\right) = \frac{\partial P_A}{\partial t} + reaction \tag{3.67}$$

For the solid reactant (coke) C_c, depletion we have,

$$\frac{\partial C_c}{\partial t} = reaction \tag{3.68}$$

3.2.1 Reaction

The regenerating gas first chemisorbs on an active site then reacts with the solid reactant, thus exposing more sites. Considering a simple chemisorption scheme with surface controlling, the reactant gas first adsorbs on an active site, S. Recall that though the catalyst is assumed deactivated there are still residual sites which account for residual activity.

$$A_{2(gas)} + S \underset{}{\overset{k}{\rightleftharpoons}} A_2.S \tag{3.69}$$

$$C_{c(s)} + A_2.S \overset{k_r}{\rightarrow} Products \tag{3.70}$$
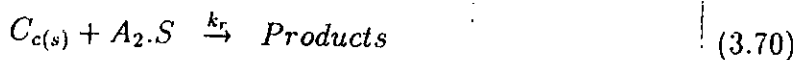
$$K_A = \frac{C_{A.S}}{P_A.C_s}$$

$$r_{products} = k_r C_c K_A P_A C_s \tag{3.71}$$

Assuming weakly adsorbed products, we then have the following balance for the total sites at any time.

$$C_t \doteq C_s + K_A P_A C_s \tag{3.72}$$

$$= C_s(1 + K_A P_A)$$

$$C_s = \frac{C_t}{(1 + K_A P_A)} \tag{3.73}$$

77

$$Reaction = \frac{k_r C_t C_c K_A P_A}{(1 + K_A P_A)} \quad (3.74)$$

Substituting 3.74 into 3.67 and 3.68

$$\frac{\partial C_c}{\partial t} = \frac{k_r C_t C_c K_A P_A}{(1 + K_A P_A)} \quad (3.75)$$

Intergrating:

$$C_c = C_{co} exp\left(-\int_0^t \frac{k_r C_t K_A P_A}{(1 + K_A P_A)} dt\right) \quad (3.76)$$

$$C_c = C_{co} exp\left(-\left[\frac{k_r C_t K_A P_A}{(1 + K_A P_A)}\right]_{av} t\right) \quad (3.77)$$

where

$$\left[\frac{k_r C_t K_A P_A}{(1 + K_A P_A)}\right]_{av} = \frac{1}{t}\int_0^t \frac{k_r C_t K_A P_A}{(1 + K_A P A)} dt$$

The rate at which the reaction layer moves is very slow with respect to the rate of transport of material. The transient term in equation 3.67 $\frac{\partial P_A}{\partial t} = 0$. This is the pseudo-steady-state assumption. Hence rewriting 3.67 with the substitution of equation 3.74 we have:

$$\frac{D_A}{RT}\left(\frac{\partial^2}{\partial r^2} + \frac{2}{r}\frac{\partial P_A}{\partial r}\right) = \frac{k_r C_t C_c K_A P_A}{(1 + K_A P_A)} \quad (3.78)$$

Boundary Conditions

At the center of the sphere i.e. at

$$r = 0$$

$$\frac{\partial P_A}{\partial r} = 0 \text{ for all } t \quad (3.79)$$

By equating the surface flux to the rate of bulk mass transport, we have the following boundary conditions at the external surface of the pellet at $r = a$

$$\frac{D_A}{RT}\left(\frac{\partial P_{A.s}}{\partial r}\right)\Bigg|_{r=a} = k_g(P_A^b - P_A^s) \quad (3.80)$$

It is assumed that P_A^b, the gas partial pressure in the bulk is constant. k_g is the mass transfer coefficient in the gas film surrounding the catalyst surface and P_A^s is the partial pressure of A at the surface. Making the following definitions;

$$\text{Dimensionless gas conc. } \phi_A = P_{As}/P_{Ao} \tag{3.81}$$

$$\text{Dimensionless radius } x = \frac{r}{a} \tag{3.82}$$

$$\text{Dimensionless coke conc. } \phi_c = \frac{C_c}{C_{co}} \tag{3.83}$$

$$K_A' = K_A P_{Ao} \tag{3.84}$$

$$\theta = k_r t C_t \tag{3.85}$$

$$\xi = \frac{a^2 R T C_{co} C_t}{P_{Ao} D_A} \tag{3.86}$$

$$\tag{3.87}$$

Substituting the variables in equations we have, for 3.67

$$\frac{\partial^2 \phi_A}{\partial x^2} + \frac{2}{x}\frac{\partial \phi_A}{\partial x} = \frac{a^2 R T}{P_{Ao} D_A}\left[\frac{C_t \phi_c C_{co} k_r K_A P_{Ao} \phi_A}{(1 + K_A \phi_A P_{Ao})}\right] \tag{3.88}$$

Hence

$$\frac{\partial^2 \phi_A}{\partial x^2} + \frac{2}{x}\frac{\partial \phi_A}{\partial x} = \xi\left[\frac{\phi_C K_A' \phi_A}{(1 + K_A' \phi_A)}\right] \tag{3.89}$$

and from 3.77, we have;

$$\phi_c = \exp\left(-\left[\frac{k_r C_t K_A P_A}{(1 + K_A P_A)}\right]_{av} t\right)$$

or

$$\phi_c = \exp\left(-\left[\frac{K_A' \phi_A}{(1 + K_A' \phi_A)}\right]_{av} \theta\right) \tag{3.90}$$

Boundary Conditions

At the center of the sphere

$$x = 0$$

79

$$\frac{\partial \phi_A}{\partial x} = 0 \tag{3.91}$$

At the external surface of the catalyst, the boundary condition is the dimensionless form of 3.80 i.e at

$$x = a$$

$$\frac{D_A P_{Ao}}{RTa}\left(\frac{\partial \phi_A}{\partial x}\right)_{x=a} = k_g\left((P_{Ao}\phi_A)^b - (P_{Ao}\phi_A)^s\right) \tag{3.92}$$

where the superscripts, b and s, denote conditions at the bulk and at the surface respectively.

Now $\phi_A^b = 1$ since the concentration at the bulk is assumed approximately equal to the initial concentration, and of course, $P_{Ao} = constant$. Hence from 3.92, we have

$$2\frac{\partial \phi_A}{\partial x} = \frac{2RTk_g}{D_A}(1 - \phi_A^s) \tag{3.93}$$

Hence;

$$\left(\frac{\partial \phi_A}{\partial x}\right)_{x=a} = \frac{RTN_b}{2}(1 - \phi_A^s) \tag{3.94}$$

Where Biot number,

$$N_b = \frac{(2ak_g)}{D_A}$$

or

$$\left(\frac{\partial \phi_A}{\partial x}\right)_{x=a} = \frac{N_b'}{2}(1 - \phi_A^s) \tag{3.95}$$

where N_b', modified Biot number, $N_b' = RTN_b$. Hence equation 3.89 and 3.90 can be solved together with boundary conditions 3.91 and 3.95 to give coke consumption profiles at different dimensionless times as well as reactant gas profiles within the pellet.

80

3.2.2 Method of solution

The reaction term in equation 3.89 was linearized by Taylor series expansion in terms of the ϕ_A and the first two terms collected

$$\frac{\phi_c K'_A \phi_A}{(1 + K'_A \phi_A)} = \frac{\phi_c K'_A \phi_{Ao}}{1 + K'_A \phi_{Ao}} + (\phi_A - \phi_{Ao}) \left[\frac{(1 + K_A \phi_{Ao} \phi_c K'_A - \phi_c K'_A \phi_{Ao} K'_A)}{(1 + K'_A)^2} \right] \quad (3.96)$$

$$\frac{\phi_c K'_A \phi_A}{(1 + K'_A \phi_A)} = \frac{\phi_c K'_A \phi_{Ao}}{1 + K'_A \phi_{Ao}} + \frac{(\phi_A - \phi_{Ao}) \phi_c K'_A}{(1 + K'_A \phi_{Ao})^2} \quad (3.97)$$

$$\frac{\phi_c K'_A \phi_A}{1 + K'_A \phi_A} = \phi_c [P + \phi_A P_1 - P_2] \quad (3.98)$$

where:

$$P = \frac{K'_A \phi_{Ao}}{1 + K'_A \phi_{Ao}} \quad (3.99)$$

$$P_1 = \frac{K'_A}{(1 + K'_A \phi_{Ao})^2} \quad (3.100)$$

$$P_2 = \frac{K'_A \phi_{Ao}}{(1 + K'_A \phi_{Ao})^2} \quad (3.101)$$

The exponential terms in equations 3.90 was also expanded in an exponential series.

$$\exp x = 1 + x + \frac{x^2}{2}! + \cdots + \frac{x^n}{n}! \quad (3.102)$$

Hence expanding equation 3.90 we have

$$\phi_c = 1 - \left[\frac{K'_A \phi_A}{(1 + K'_A \phi_A)} \right]_{av} \theta - \left(\left[\frac{K'_A \phi_A}{(1 + K'_A \phi_A)} \right]_{av} \theta \right)^2 \quad (3.103)$$

Collecting the first two terms of the expansion we have that

$$\phi_c = 1 - \left[\frac{K'_A \phi_A}{1 + K'_A \phi_A} \right]_{av} \theta \quad (3.104)$$

From linearization of equation 3.89, we have 3.104 as

$$\phi_c = 1 - \theta [P + \phi_A P_1 - P_2]_{av} \quad (3.105)$$

81

Hence with the above linearizations equations 3.89 and 3.90 can be rewritten as:

$$\frac{\partial^2 \phi_A}{\partial x^2} + \frac{2}{x}\frac{\partial \phi_A}{\partial x} = \xi \phi_c [P + \phi_A P_1 - P_2]_{av} \qquad (3.106)$$

and

$$\phi_c = 1 - \theta[P + \phi_A P_1 - P_2]_{av} \qquad (3.107)$$

Finite Differences were now used to discretize the above equations 3.106 and 3.107 and boundary conditions 3.91 and 3.95. For 3.95, the finite difference representation is as follows

$$\frac{\partial^2 \phi_A}{\partial x^2} + \frac{2}{x}\frac{\partial \phi_A}{\partial x} = \frac{1}{i(\delta x)^2}[(i+1)\phi_{A(i+1,j)} - 2i\phi_{A(i,j)} + (i-1)\phi_{A(i-1,j)}]\, i \neq 0$$

$$= \frac{6}{(\delta x)^2}[\phi_{A(1,j)} - \phi_{A(o,j)}]\, i = 0 \qquad (3.108)$$

From 3.107 we have

$$\frac{1}{(\delta x)^2}[(i+1)\phi_{A(i+1,j)} - 2i\phi_{A(i,j)} + (i-1)\phi_{A(i-1,j)}] =$$

$$\xi \phi_{c(i,j)}[P + \phi_{A(i,j)}P_1 - P_2] \qquad (3.109)$$

at the boundary at $x = 1$, i.e at $i = 10$ 3.95

$$\frac{\phi_{A(11,j)} - \phi_{A(9,j)}}{2(\delta x)} = \frac{N_b'}{2(1 - \phi_A^s)} \qquad (3.110)$$

Hence

$$\phi_{A(11,j)} = \phi_{A(9,j)} + N_b'(1 - \phi_A^s) \qquad (3.111)$$

Hence 3.109 then becomes

$$\frac{1}{10}(\delta x^2[11\phi_{A(11,j)} - 20\phi_{A(10,j)} + 9\phi_{A(9,j)}] =$$

$$\xi \phi_{c(10,j)}[P + \phi_{A(10,j)}P_1 - P_2] \qquad (3.112)$$

82

Now the fictitious point $\phi_{A(11,j)}$ is eliminated between 3.111 and 3.112

$$\frac{1}{10(\delta x)^2}[11[\phi_{A(9,j)} + N_b'(\delta x)(1 - \phi_{A(10,j)})]$$
$$-20\phi_{A(10,j)} + 9\phi_{A(9,j)}] = \xi\phi_{c(10,j)}[P + \phi_{A(10,j)}P_1 - P_2] \qquad (3.113)$$

and when $\delta x = 0.1$, we have at the conditions where $x = 1$, or $i = 10$,

$$10[20\phi_{A(9,j)} - \phi_{A(10,j)}(N_b' + 20)] = \xi\phi_{c(10,j)}[P + \phi_{A(10,j)}P_1 - P_2] \qquad (3.114)$$

and at $i = 0$, at the center of the particle, we have

$$600(\phi_{A(1,j)} - \phi_{A(0,j)}) = \xi\phi_{c(0,j)}[P + \phi_{A(0,j)}P_2 - P_2] \qquad (3.115)$$

Equation 3.107 is represented as:

$$\phi_{c(i,j)} = 1 - \theta[P + \phi_{A(i,j)}P_1 - P_2] \qquad (3.116)$$

3.2.3 Computational Technique

Equations 3.114 and 3.115 represent the boundary conditions while equations 3.109 is the general equation. A set of linear equations for all the radial points were written from 3.109. At each time step for a given θ (dimensionless time) the gas profile ϕ_A was first guessed for the first time step, for the computation of values of coke consumption profiles from the set of equations generated from 3.116 at all the radial positions. Then the computed coke consumption profile was used to recompute the gas profile using the set of linear equations generated from 3.109. The recomputed gas profile now replaced the guessed values in 3.116.

This procedure continued till convergence was achieved for all values. The effect of diffusion on the process was accessed by variation of the modified Biot number and *sigma* which were the parameters with a diffusion term.

83

The results from these computations will be shown and discussed in the results section.

3.3 MODELLING THE DEACTIVATION KINETICS OF THE REACTION OF CYCLOHEXANE

The major fraction of large tonnage production in the chemical industry is based on reactions catalysed by solids. Kinetic studies of these reactions are the basis for more accurate reactor design and for progress in the understanding of the phenomenon of catalysis. In the experimental investigation, many precautions have to be taken, some of which may be contradictory, to measure the true chemical reaction rate. If it is obscured by physical phenomena, the kinetic analysis becomes too cumbersome and involves too many parameters to lead to reliable results.

The formulation of a reliable model adequate for the description of reaction deactivation data represents quite a difficult task. Apart from the simplifying assumptions usually made in normal kinetic analysis, e.g existence of rate determining step or of most abundant surface intermediates, the assumptions of correlating deactivation kinetics in terms of separable rate form is universally made (43). Separability involves factoring out the activity term. The approach is to determine the kinetics in the absence of coking and to account for the deactivation afterwards. One way is to extrapolate the measured conversions to zero coke content or zero time. Modelling by inseparability involves the coupling of the coking equation to that or those for the main reaction(s) and to account for the decline in rates. This will account for effect of coke on the rate(s) of the main reaction.

Theory can be applied to the derivation of reaction deactivation kinetics but it may happen that the same set of experimental data is well described by completely different

equations. Furthermore, an interaction may arise between chemical kinetics and catalyst deactivation so that the same reactant conversion data are mathematically described by different combination of kinetics and deactivation model. Hence, although the parameters calculated from such models may be adequate for describing the experimental data, they may have no physical meaning(42). All these point to the need for a chemical and mechanistic investigation of the reaction-deactivation phenomenon as a basis in the derivation of a reliable raction deactivation rate equation.

A chemical investigation had been carried out to explain the deactivation mechanism of methanol oxidation on $Fe_2O_3 - MoO_3$ catalyst(42). The kinetics for the fresh and the deactivated catalysts were derived in the light of a chemical investigation carried out by Carbucicchio(84). In the study of the deactivation of $Pt - Al_2O_3$ in a CSTR, it was shown that after deactivation was assumed completed, the catalyst still maintained a residual activity. Since this author is unaware of any chemical investigation of the fresh and deactivated $Pt - Al_2O_3$ catalyst, the existence of residual activity will be ascribed to the incomplete uniform coverage of the catalyst surface due to coking.

In this section, a reaction - deactivation kinetic model for the deactivation of cydo-hexane over Pt catalyst will be presented based on the coking mechanisms of Corella and Asua on the dehydrogenation reaction mechanism proposed by Susu et al. (38).

3.3.1 Derivation of Reaction-Deactivation Kinetic Model

. A reaction-deactivation kinetic model for cyclohexane reaction on $Pt - Al_2O_3$ catalyst. Susu et al.(38) studied the mechanism of the dehydrogenation of cyclohexane on

$Pt - Al_2O_3$ and postulated the following reaction scheme.

$$C_6H_{12} \qquad\qquad\qquad C_6H_6$$

$$k_1 \downarrow\uparrow k_{-1} \qquad\qquad\qquad k_4 \uparrow\downarrow k_{-4}$$

$$C_6H_{12(ads)} \xrightarrow{k_2 step\, 2} C_6H_{10} \xrightarrow{k_3 (step\, 3)} C_6H_{6(ads)}$$
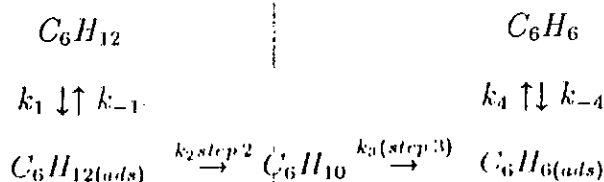
Assuming a single site mechanism of the main reaction and weak adsorption of products, the following equation for the rate of reaction was derived by Susu et al.(38) and corroborated by Somorjai et al.(40). After simplifying assumptions the following equation was derived.

$$r_A = \frac{k_r C_t K_A C_A}{(1 + K_A C_A)} \tag{3.117}$$

where A is the cyclohexane molecule.

The following is the highly simplified scheme leading to the equation as proposed by Susu et al.(38). The cyclohexane, A adsorbed on a site S, before reaction; i.e

$$A + S \underset{}{\overset{k}{\rightleftharpoons}} A.S \tag{3.118}$$

$$A.S \;\rightarrow\; Products \tag{3.119}$$

For weak adsorption of the products, and for the surface reaction controlling, we have

$$r_A = k_r C_{A.s} \tag{3.120}$$

In the presence of coking, the total sites will be

$$C_t = C_s + K_A C_A C_s + C_c \tag{3.121}$$

where C_c is the adsorbed coke

$$C_s = \frac{C_t - C_c}{(1 + K_A C_A)} \tag{3.122}$$

Now the substituting 3.122 into 3.120, we have

$$-r_A = \frac{k_r K_A (C_t - C_c)}{(1 + K_A C_A)} \tag{3.123}$$

87

or

$$r_A = \frac{k_r K'_A C_A C_t (1 - \gamma)}{(1 + K_A C_A)}$$ (3.124)

where

$$\gamma = C_c / C_t$$

γ is the fraction of catalyst deactivated for a single main reaction. The term $(1 - \gamma)$ expresses the decay of the catalyst. For an adequate expression of this decay term, it is necessary to develope a reliable mechanism for catalyst deactivation.

In the absence of literature on the chemical investigation on fresh and deactivated $Pt - Al_2O_3$, the specification of deactivation term will be limited to a mechanistic investigation. The arguments in the development of the coking mechanisms of Corella and Asua(37) will be adopted here and limited to the d-1 mechanism.

For the simple reaction represented by Froment(28) as

$$A \rightarrow R + S$$ (3.125)

$$M \rightarrow P$$ (3.126)

where M is coke precursor or the substance causing deactivation and it is adsorbed on the surface. In this analysis, the coke precursors M is the same as A.

Elementary Steps of the Coking (Corella and Asua)

M the coke precursor adsorbs on a site S

$$M + S \overset{k_m}{\rightleftharpoons} MS$$ (3.127)

where

$$K_m = \frac{C_m}{P_m C_s}$$ (3.128)

1. **The coke precursor formation step**

d-1 Mechanism

By this mechanism, M the coke precursor is adsorbed in the main reaction as follows

$$nM_g + hMS \rightleftharpoons P_1S_h \tag{3.129}$$

$$P_1S_h = coke\ precursor \tag{3.130}$$

$$n = 0, 1, 2 \tag{3.131}$$

$$h = 1, 2 \tag{3.132}$$

Coking Sequence

$$P_1S_h \rightleftharpoons P_2S_h \rightleftharpoons P_3S_h\ \text{Step 2 is the rate controlling step} \tag{3.133}$$

$$nM_g + hMS \rightleftharpoons P_1S_h \rightleftharpoons P_2S_h \rightleftharpoons P_3S_h \tag{3.134}$$
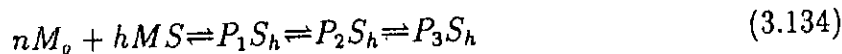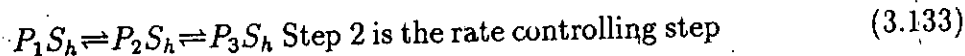
$$\frac{dC_{P_1S_h}}{dt} = k_d P_m^n C_{ms}^h \tag{3.135}$$

$$C_{ms} = K_m P_m C_s \tag{3.136}$$

Hence

$$\frac{dC_{P_1S_h}}{dt} = k_d P_m^{n+m} K_m^h C_s^h \tag{3.137}$$

For weakly adsorbed products, we have

$$C_t = C_s + K_A C_A C_s + h C_{P_1S_h} \tag{3.138}$$

Factorizing, we have

$$C_s = \frac{C_t - h C_{P_1S_h}}{(1 + K_A C_A)} \tag{3.139}$$

Substituting 3.139 into 3.137, we have

$$\frac{dC_{P_1S_h}}{dt} = \frac{k_d P_m^{n+h} K_m^h (C_t - h C_{P_1S_h})^h}{(1 + K_A C_A)^h}. \tag{3.140}$$

89

In this analysis, as earlier mentioned the coke precusor M is the same as em A, hence, we can replace A for M above Rewritting above equation,

$$\frac{dC_{P_1 S_h}}{dt} = \frac{k_d C_A^{m+h} K_A^h (C_t - hC_{P_1 S_h})^h}{(1 + K_A C_A)^h}$$
(3.141)

Now intergrating 3.141

$$\int_0^{C_{P_1 S_h}} \frac{dC_{P_1 S_h}}{(C_t - hC_{P_1 S_h})} = \int_0^t \frac{k_d C_A^{m+h} K_A^h}{(1 + K_A C_A)^h} dt$$
(3.142)

or

$$In \, C_t \frac{(C_t - C_A)}{C_t} = \int_0^t \frac{k_d C_A^{m+h} K_A^h}{(1 + K_A C_A)^h}$$
(3.143)

and for $h = 1$

$$\ln C_t (1 - \gamma) = \int_0^t \frac{K_d C_A^{n+h} K_A^h}{(1 + K_A C_A^{n+h} C_A)^h} dt \tag{3.144}$$

hence

$$\gamma = 1 - \exp \left(\int_0^t \frac{K_d C_A^{n+h} K_A^h}{(1 + K_A C_A)^h} dt \right) \tag{3.145}$$

Substituting 3.145 into 3.124 we have

$$r_A = \frac{k_r (C_A K_A)^m C_t^m}{(1 + K_A C_A)^m} \left[1 - f \left(1 - \exp \left(- \int_0^t \frac{k_d K_A C_A^{n+1}}{(1 + K_A C_A)} dt \right) \right) \right]^m \tag{3.146}$$

Where f is the constant and $f < 1$. f accounts for the incomplete deactivation, or residual activity.

and for $h \neq 1$

Intergrating 3.141 we have

$$\frac{C_t}{h(1 - h)} \left[\left(\frac{C_t - h C_{P_1 S_h}}{C_t} \right)^{1-h} - 1 \right] = \int_0^t \frac{k_d K_A^h C_A^{n+h}}{(1 + K_A C_A)^h} dt \tag{3.147}$$

$$\left[(1 - \gamma)^{1-h} - 1 \right] = \frac{-h(1 - h)}{C_t} \int_0^t \frac{k_d K_A^h C_A^{n+h}}{(1 + K_A C_A)^h} dt \tag{3.148}$$

Hence

$$\gamma = 1 - \left[-\frac{h(1 - h)}{C_t} \int_0^t \frac{k_d K_A^h C_A^{n+h}}{(1 + K_A C_A)^h} dt + 1 \right]^{1/(1-h)} \tag{3.149}$$

Substituting 3.149 into 3.124 we have

$$r_A = \frac{k_r (K_A C_A)^m C_t^m}{(1 + K_A C_A)^m} \left[1 - f \left(1 - \left[-\frac{h(1 - h)}{C_t} \int_0^t \frac{k_d K_A^h C_A^{n+h}}{(1 + K_A C_A)^h} dt + 1 \right] \right) \right]^m \tag{3.150}$$

For an mth site of the main reaction.

3.3.2 Computational Method

From three reaction-deactivation kinetic runs, the procedure was to first calculate values of the parameters K_A, f, C_t, k_r, and k_d in the main reaction from the experimental

data at the lowest and highest times on stream from each of the runs. The catalyst was considered either fresh or completely deactivated but still active so that intergration with respect to time, t, was not required. Then, temptative values for the parameters were then secured from the experimental data at different times. Finally the parameter estimates were then used as start values in the general analysis when all the parameters were estimated together in the models. Since m is the number of sites involved in the main reaction, m was fixed to between 1 and 2 as 3 site mechanism of the main reaction is highly improbable. On fixing m, that left the equation with K_A, f, C_t, k_r and k_d to be determined. Limitation of m to 1 and 2 was informed by the need to reduce the complexity of the highly non linear search routine of the programme.

The estimated values were used to compute decline in conversion with time for a number of runs. Alternatively, a more realistic method but full of oscillations and supersensitive to step changes was to guess a value for m, like was done for the other parameters and letting the computer program work out an m. The standard deviation of the models from the experimental was calculated.

The model parameters in Equations 3.146 and 3.150 were estimated by minimizing y, the residuals (objective function), which is the set of deviations between the experimental and predicted values of the rate for $i = 1$ to N observations.

$$y = \sum_{i=1}^{N} \left(r_{Ai} - \hat{r}_{Ai} \right)^2 .$$

where $\hat{r}_{Ai}$ is the predicted rate represented by rate expression equation 3.146 or 3.150 and r_{Ai} is the rate for the expression for reaction in a mixed flow reactor. This author deliberately constrained all the parameters to be greater than zero, while $f < 1$ had been defined as such. The idea of imposing constraints is due to arguments on physical grounds which lead to the conclusion that K_A, k_d, k_r, C_t, must be non-negative. Consequently,

fitting the model without restricting the region of search for the parameters estimates to $K_A \geq 0$, $k_r \geq 0$, $k_d > 0$ $and\, C_t > 0$ would have led to unreasonable estimates, sometimes negative numbers.

3.3.3 Model Parameter Estimation

A non linear least square technique, Flexible Polyhedron Simplex Method for constrained optimization (85,86) was used to estimate the model parameters by minimization of the non linear objective function. This technique, is an improvement of the regular Simplex technique and is known to be very effecient and easily implementable on computer. It is better than the direct search method because it takes less computer time even though the convergence to termination is slow.

A computer programme written for the implementation of the flexible polyhedron technique to minimize the objective function took 38 minutes to run on the compaq deskpro 286 micro computer. Results shall be shown in the chapter 5 on Results.

Chapter 4

EXPERIMENTAL

INTRODUCTION

The experimental investigation consisted of the performance of long series of deactivation-regeneration experiments at different operating conditions, quantification of coke on the catalyst and hydrogen chemisorption experiments for the characterization of the catalyst surface. As much as possible, it is desirable to provide experimental evidence in support of the conclusions reached from modelling equations. For example, titration experiments could provide direct explanation for the existence of residual activity and quantification of such residual activity.

For experimental data to be reliable, the apparatus had to be appropriate, apart from the need for a good experimental design. For example, it was desirable to eliminate temperature gradients and diffusional limitations as those factors are capable of falsifying the real rate of reaction(87). The CSTR, particularly the Berty type was, fortunately, suited for this investigation. Hence, the Berty CSTR was employed here. Its' temperature controller maintained the furnace temperature to an accuracy of $\pm 1^{\circ}C$ while its high speed magnetic stirrer provided sufficient gas turbulence to minimize dif-

fusional resistances. Any required reactant vapour pressure was kept constant by the use of thermostatic heater immersed in a water bath or a cooling bath with a 50-50 mixture of ethylene glycol/water. Metallic conduites connected the various units along which were valves that controlled flowrate.

4.1 APPARATUS

The apparatus consisted of a water bath and saturator, CSTR and temperature controller, fluidised sand bath, F.I.D. gas chromatograph industrial gas cylinders and regulators, on-line sampling valve, and flow control valves. The following is a description of the apparatus used for the entire investigation. The general experimental set-up of the system is shown in Figure 1 and is self explanatory. A brief description of each unit is given below:

4.1.1 Cooling Bath and Saturator

This unit was used to prepare the feed to the reactor The bath model FRIO Frigid flow bath circulator of the New Brunswick qScientific Co. Inc. consists essentially of a trough containing an anti-freeze (a 50/50 mixture of ethylene-glycol and water). The liquid reactant was placed inside the saturator equipped with inlet and outlet stream connections. A stream of gas was passed through the saturator which partially vapourized the reactant depending on the temperature maintained in the bath. The gas flowrate was adjusted to avoid entrainment and the liquid reactant level in the saturator was kept low for the same purpose.

4.1.2 Reactor

The CSTR used in the experimental set up was of the Berty type, purchased from Autoclave Engineers. It consisted of a catalytic reactor, a differential pressure transmitter, a temperature controller and a magnetic stirrer for high speed rotary agitation. The bolted enclosure unit consists of a body, cover, closure gasket and capscrews. A confined stainless steel gasket is used for high temperature application. There are facilities for linking the reactor through thermocouples to the temperature controller. An inlet pipe bearing the reactant was connected to the base of the reactor while an outlet pipe connected to the upper section of the reactor carried the product stream. A jacket type, three zone furnace is furnished as standard equipment with the reactor. This furnace has resistance windings and insulation enclosed in the heating jacket which slides over the body and covers of the reactor. The furnace is provided with flexible armour leads with male and female twist lock connectors for connection to a control console.

4.1.3 Temperature Controller

The Barber Colman temperature controller was connected to the reactor by means of thermocouples and was capable of monitoring the temperature of five different systems, simultaneously. The temperature controller regulated the temperature to within $\pm 1°C$ of the set point.

4.1.4 Fluidized Sand Bath

In order to achieve an O_2-free carrier gas stream, cuprous oxide put in a U-tube which is immersed in a fluidized bath was used to remove any trace of oxygen from the gas stream before it entered the reactor system. The fluidized bath ensured uniform heating.

Column temp.	$75^{\circ}C$
Carrier gas	Nitrogen
Carrier gas flow rate	20m/min
Attenuation	64
Range	10^2
Chart speed	5mm/min.

Table 4.1: GC conditions for Benzene Conversions

The cuprous oxide in the U-tube was activated by reducing the oxide at $330^{\circ}C$ with H_2 until the black oxide just began to turn red. The reduction process took three hours. It was used in the temperature range of $330 - 350^{\circ}C$

4.1.5   F.I.D Gas Chromatograph

The Hitachi gas chromatograph was connected on line and used for the analysis of the products. A Bentor 34-diisodecylphathalate column was used for the separation of the products. The chromatograph was equipped with an amplifier and a wide range of reacting conditions could be employed to give a good resolution depending on the product being analysed.

Typical operating conditions for deactivation studies and for monitoring methane are shown in Tables 4.1 and 4.2. And for monitoring methane during reduction procedure:

4.1.6   Gas Cylinders and Regulators

Three (3) gas cylinders containing air, N_2 and hydrogen were connected on line with each cylinder equiped with double stage regulators for controlling the outlet pressure.

97

Column temperature	$75^\circ C$
Carrier gas flowrate	20ml/min
Attenuation	8
Chart	5

Table 4.2: GC conditions for Coke Monitoring

Nitrogen, hydrogen and air were purchased from Industrial Gases, Lagos. The air was used to burn off polymerous carbon compounds (coke) deposited on the catalyst surface during reaction.

4.1.7 On-line Sampling Valve

The exit stream from the reactor enters the sampling valve which has two outlets - one leading to the gas chromatograph and the other to the atmosphere.

The sampling valve enables a fixed and known volume of sample to be injected into the gas chromatograph each time.

4.1.8 TCD(Thermal Conductivity Detector)

The Thermal Conductivity Detector (Carle GC 8700) was used for gas analysis and it is particularly suitable for separating a mixture of light gases into their various components. The conductivity dectector makes use of the differences in the thermal conductivity of the gases as the basis for separating them. Some gases are known to have a very high thermal conductivity and hence act as references or as carriers during analysis. Hydrogen and helium fall into this category and are therefore widely used as carriers in analytical work with TCD. Hydrogen was therefore used as carrier in the TCD for this work.

The Carle TCD used in this investigation had two columns placed side by side. The first column was an 8ft ×1/8*in* packed with mixed poropak (80% PPN,20% PPQ) and the second column was a 6ft ×1/8 packed with molecular sieve 5A. Depending on the gases being analyzed, the Carle had facilities to place the two columns in series or bypass one of the columns. By an appropriate manipulation of the series/bypass controlling valve, the separated components of a gas mixture were observed.

Assay	99.5% minimum
Specific gravity 20°C	0.777 to 0.7799
Molecular weight	84.16
Retractive Index	1.426 to 1.427

Table 4.3: Cyclohexane Properties(Phillips Petroleum)

4.2 MATERIALS

4.2.1 GASES

Pure methane gas was purchased from AIR Products and was used for calibration. N_2, O_2 and H_2 were purchased from Industrial Gases, Lagos. In use, nitrogen was first passed through reduced cuprous oxide bed(Figure 1) at 330°C to remove traces of oxygen during deactivation studies. After 8 hours of operation, the oxygen trap was reactivated by reducing in hydrogen.

4.2.2 Barium Hydroxide

Barium hydroxide with a molarity of 0.15 was prepared and was appropriately standardized and used as the trapping agent for carbon dioxide. Carbon dioxide together with water vapour are the products obtained during oxidation of the coke deposits of deactivated catalysts.

$$C + O_2 \rightarrow CO_2$$

$$Ba(OH)_2 + CO_2 \rightarrow BaCO_3 + H_2O$$
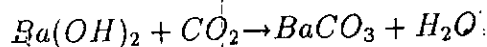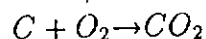
Metallic content	0.3% Pt (w/w)
Surface Area	$180 m^2 g^{-1}$
Pour volume	$0.50 cm^3 g^{-1}$
Size of pellet	12 - 16mm
Compacted	density 0.62kg/l
Chloride content	0.6%

Table 4.4: Commercial Platinum Properties

The excess barium hydroxide was titrated against a standard solution of hydrochloric acid to estimate the level of oxidizable coke deposited on the catalyst.

4.2.3 Hydrochloric acid

0.166MHCl acid was prepared and standardized with a solution of Na_2CO_3. Phenolpthalein dissolved in alcohol was used as indicator (1gm Phenolpthalein dissolved in 100ml Methanol).

4.2.4 Catalyst

A commercial $Pt - Al_2O_3$ with the properties listed in table 4.4 was used:

4.3 EXPERIMENTAL PROCEDURES

As earlier stated, metallic conduites along which were fitted gate values, connected the various units. By closing and shutting them, gases were directed to bypass or connect units which were not involved in certain procedures. The main experimental set-up is

shown in Figure 1.

The entire experimental work consisted of several sets of of experiments done at different conditions to achieve the stated objectives. Fortunately, because many previous works on $0.3\% Pt - Al_2O_3$had been done in this laboratory using the same equipment outlined above (6,7,9), the recommendations from the reports of those workers provided the start-off point, the precautions taken, the best operating conditions, the variables which had to be predetermined and those not to worry about. For example, it had been previously determined that nitrogen from Industrial Gases, Lagos, had an oxygen contamination of about 0.66% of its volume, hence prepurification of N_2 was necessary before use. Also, using the available CSTR, it was known that fresh catalyst had to be first dried at $100°C$ in nitrogen flowing at 40ml/min for one hour followed by reduction at $500°C$ with H_2 flowing at 40ml/min for 2 hours to ensure a clean and stable catalyst surface necessary for reproducible results. This catalyst pretreatment was done on *all* fresh catalyst before any deactivation run.

4.3.1 Mixing Experiments

The two known ideal flow patterns are plug flow and mixed flow. Though real reactors never fully follow these flow patterns a large number of designs approximate these ideals with negligible error. Deviation from ideal flow can be caused by chanelling of fluid, recycling of fluid, or by creation of stagnant regions in the vessel(89).

If precise rate laws or models are to be derived from raw data, precise analytical methods, free of non-ideality, are then required. The problems of non ideal flow are intimately tied to those of scale-up. Often, the uncontrollable factor in scale up is the magnitude of the non ideality of the flow which often differs between small and large units. This factor may lead to gross errors in design. Hence the need for investigation

of the extent of non-ideality of flow in reactors. If we have a complete distribution map of the fluid, i.e. the residence time distribution of the flowing fluid, then we are able to predict the behaviour of a vessel as a reactor(89,90). Residence time of fluids is determined easily by the stimulus response experiment. In such experiments, a disturbance is introduced into a non reacting system and how the system responds to this stimulus, is observed. Analysis of the response gives the desired information about the system.

The mixing characteristic of the reactor (Berty CSTR) was determined by measuring the response of the non-reacting system to a pulse input of H_2 injected into a steadily flowing stream of N_2 at various agitation speeds. The interest was to determine the operating region (range of agitator speed) in which apparent perfect mixing prevailed as judged by obedience of the effluent pulse concentration to the theoretical response predictable for a single CSTR.

Procedure

Nitrogen was used as carrier gas while hydrogen was used as tracer(pulse). The system was connected such that the hydrogen pulse could go through or bypass the reactor and into the TCD. The TCD had two in built columns. The first column was removed and replaced with an unpacked one. The flow control devise on the TCD consisted of two valves labelled ('fill/inject' and 'series/bypass'). Material was sampled into the columns using the 'fill/inject' valve while with the 'series/bypass' valve the two columns could be placed in series or the second one can be bypassed. I would abbreviate the labels F/I and S/B respectively. The experimental arrangment is shown in Figure 2. The TCDs' sampling valve stayed at position 'fill' while the S/B valve stayed at position 'bypass' all through the analysis. Pulsing was done through the main sampling valve in the main experimental arrangement (Figure 1).

When the necessary equipment arrangment was complete the carrier gas was allowed

to flow through the the TCD at 40ml/min. This flowrate was measured at the exit of the TCD. The TCD was operated at $70°C$. Pulsing was then done through the main sampling valve in the arrangment. The effect of the degree of mixing on residence time was determined by pulsing at different agitator speeds.

4.3.2 Deactivation-Regeneration Runs

For this study, five grams of catalysts were arranged on the stainless steel wire basket of the reactor (Figure 1). The catalyst was then pretreated as described above. The purified nitrogen gas was bubbled through a cyclohexane saturator immersed in a water bath and maintained at the desired temperature. For this study, the reactant-gas mixture at flowrate of 100ml/min or 200ml was maintained through the reactor whose temperature was $430°C$. Transfer resistances between the fluid and solid may be eliminated by sufficient turbulence from high agitation at the appropriate agitation speed determined from the mixing experiment. Samples of product stream from the reactor were injected at intervals by means of an on-line sampling valve of known volume to the gas chromatograph. As soon as the catalyst activity was observed to be very low, about 0.05%, the reactant-gas mixture was switched to bypass the saturator. The inert nitrogen carrier was passed through the reactor to flush out unreacted cyclohexane.

Coke burn off was achieved by passing air or air diluted with N_2 to about 2-3% O_2 at a flowrate of 120ml/min and at a reactor temperature of $430°C$. The burn off lasted for a minimum of 3 hours. No CO was produced in the combustion of coke as determined by the TCD. The CO_2 produced from the reaction was trapped by bubbling the exit gas through a saturator containing $Ba(OH)_2$. A white precipitate was formed and the excess $Ba(OH)_2$ was titrated against 0.166MHCL using phenolpthalein as indicator. The quantity of oxidizable coke was estimated from the titration results. After coke burn off,

104

the surface of the catalyst was in an oxidized state and had to be reduced in hydrogen to the active metal state. Also, not all the coke was removed by the burn-off as some of the coke was irreversibly adsorbed on the catalyst surface and constituted toxic coke.

Restoring the reduced state of the catalyst by passing through H_2 at the appropriate gas flowrate and temperature also served in the removal of the toxic type of coke through the formation of methane. Hence, the reduction time was extended to last far beyond the two hours normally required for restoration of the reduced catalyst state. This was to ensure the maximum possible removal of toxic coke and the restoration of the clean catalyst surface. How successfully this was done, was acessed by the number of successive deactivation and regeneration cycles the catalyst was able to withstand before mortality occured. The reduction was determined by monitoring the formation of methane at intervals by injecting the product stream at the selected intervals into the gas chromatograph. The reduction (regeneration) was deemed complete and hence stopped only when the peak of the chromatograms remained relatively constant with time. The effect of this procedure, unused before, on the catalyst lifetime was evaluated by comparison with previous work where the above methodology of prolonged coke removal with time at the appropriate thermodynamic conditions was not applied. The amount of toxic coke deposited was quantified.

The procedure of deactivation-regeneration and reduction is termed a cycle. After the reduction the catalyst was ready for another deactivation. Before another run, the cuprous oxide trap was normally reduced again at about $330°C$ for about 2 hours to ensure efficient removal of O_2 from N_2 or H_2. The period of effectiveness of the cuprous oxide trap was previously determined in a preliminary experiment. During the reduction, the water vapour formed was let off the system into the atmosphere. Several cycles were carrried out and the response of the catalyst in terms of conversions, coke deposits

and residual activity were quantified for the various process conditions. The catalyst remained active through all the cycles carried out in each set of deactivation runs. A summary of all the deactivation runs performed and their operating conditions are shown in Table 5.

4.3.3 Oxidizable Coke Structure Determination

Oxidizable coke is the most familiar of all coke types and for workers who do not distinguish between coke types, any reference of quantified coke is usually oxidizable coke. Despite the frequent reference to oxidizable coke in the literature, information on its structure is rare and not much is known of its mode of occurence on the catalyst surface. What is obvious, due to its ease of combustion, is that it is amorphous carbon. By passing the combustion gas mixture from the reactor via the TCD before absorption in the $Ba(OH)_2$, the structure of oxidizable coke as it occured on the catalyst surface was graphically observed. This was observed from the profile of carbondioxide composition of the gas mixture with time at constant temperature. The TCD also revealed the gases present in the combustion mixture. For this work, the TCD was operated as follows. The carrier gas H_2, was connected to flow through the TCD at a flow rate of 40ml/min. When flow was verified, the TCD power supply was then switched on and its temperature maintained at $70^\circ C$. The product gas mixture flowing at 120ml/min was connected from the metallic outlet of the reactor into the sample inlet on the TCD. The experimental arrangement is shown in Figure 3. To get the required result - chromatograph of CO_2 - the following valve manipulations were adopted on the TCD.

Prior to sampling, the F/I valve was at position fill, while the S/R valve was at position series. To monitor, the F/I valve was switched to inject. This directed flow through the first column. When the first peak for CO_2 eluted, the series/bypass value

was switched quickly to 'bypass' for the other products to elute in the following succession CO_2, O_2 and N_2.

4.3.4 Catalyst Characterization Experiments

From deactivation-regeneration runs we obtained data on the conversions and the amount of coke(oxidizable and toxic coke) deposited. It was also desirable to monitor the accompanying structural changes (metal dispersion,particle size) occuring on the catalyst surface as a result of continuous reuse as such changes could account for the observations. For example, it was reviewed in the literature that graphitic coke stayed on the catalyst surface. Hence, some fraction of the active surface was obliterated irreversibly. It was, therefore, necessary to quantify the amount of available 'working' surface before a deactivation run. In the same vein, it was necessary to quantify the original 'working' surface that was recovered from every regeneration. This would provide a measure of the effectiveness of the adopted regeneration methodology. Characterization of the catalyst surface was done by hydrogen titration of the adsorbed oxygen- $H_2 - O_2$ titration.

Metal platinum atoms are very prone to oxidation even at room temperature. Hence on exposure to air, and during oxidation, the accessible Pt metal atoms easily pick up oxygen. From the titration of the surface oxygen atoms with hydrogen,the number of accessible surface Pt atoms, as well as their size and dispersion, can be calculated from the stoichiometry of the titration reaction. Since the dehydrogenation of cyclohexane uses just the metallic sites, these parameters determine the effectiveness of the catalyst for this reaction.

Procedure

The catalyst characterization was accomplished by pulsing H_2 into a flowing stream of N_2 over the catalyst. Pulse detection was by the TCD. The unreacted hydrogen

was measured from the resulting peak. Initially there were several accessible sites with attached oxygen and the full amount of hydrogen was taken up by such sites to replace the O_2 and water was given off according to the stoichiometry. The water is deposited on the alumina support. Hence, the size of the H_2 peak was expected to be small initially, when the sites were numerous and then increase rapidly to a stable value as the few unoccupied sites took up little H_2 and the full amount of H_2 pulsed, eluted. The experimental set-up and operational conditions were the same as in the mixing experiments (Figure 2). However, the reactor agitator speed, all through the titrations, was not changed. Titration was continued with time for as long as the successive pulse size changed.

The following set of titrations were done in the following sequence:

- In the course of a set of deactivation-regeneration experiments, titration experiments were done after deactivation. That was for the determination of the residual activity left after deactivation. Reactor temperature was maintained constant at $430°C$.

In the course of another set of deactivation-regeneration runs (see Table 5) starting with a fresh catalyst, the following sequence of titrations were done:

1. The fresh catalyst was titrated at room temperature to determine the fresh catalyst surface followed by this sequence of operations:reduction of the fresh catalyst at $500°$ for 2 hours; reduction of the temperature to $430°C$ and titration.

2. Titration after deactivation for the determination of the site coverage and consequently the residual activity.

3. Titration after each coke burn-off for the determination of effectiveness of coke burn-off under the given conditions-at $430°C$.

108

4. Titration at 430°C after each prolonged reduction at at 500°C to determine the effect of reduction at the given conditions-particularly with regards to sintering.

Chapter 5

RESULTS

Introduction

Following the objectives of this investigation as stated in the introduction, the experiments to accomplish the objectives were carried out in the order in which they were presented in chapter 3 viz mixing experiments, deactivation-regeneration runs, oxidizable coke structure determination, and titration experiments. Thus, the results shall be presented in the following sequence.

(A) EXPERIMENTAL RESULTS

1. Mixing Experiments

2. Deactivation Regeneration Runs

3. Oxidizable Coke Structure

4. Titration Experiments

(B) THEORETICAL MODELLING RESULTS

1. Multilayer Coking Model

110

2. Effect of Interfacial Diffusion Resistance on Catalyst regeneration

3. Reaction-Deactivation Kinetic Model

5.1   EXPERIMENTAL RESULTS

5.1.1   Mixing Experimental Results

A major contributor to the precision of kinetic data obtained in the catalytic reactor is the manner of flow in the reactor. One way of determining the flow characteristics and hence the suitability of the reactor for data collection is by measuring the response of the reactor to a tracer injected into a carrier at different agitator speeds. Hence in this section the results of the response of the inert carrier, N_2, to a pulse input of hydrogen at various agitator speeds on the CSTR are presented. It was assumed that the reactor was well stirred at all agitator speeds.

First order reaction in the concentration of the tracer was assumed for the non reacting system. From the material balance on a CSTR, we have, for a first order system(90);

$$C/C_o = \exp{(-t/\theta)} \qquad (5.1)$$

$$In\, C/C_o = -t/\theta \qquad (5.2)$$

where $\frac{C}{C_o}$ is the ratio of the tracer concentration to the initial tracer concentration at any dimensionless time t/θ.

Hence for perfect mixing at all agitator speeds, a straight line is predicted, from a plot of $In\, C/C_o$ vs t/θ with a slope of -1.

The linear plot in agreement to the first order model occured at agitator speeds of 900, 1200, and 1325 RPM (Figure 4). Hence opereating within those speeds will

111

provide perfect mixing. The others were close approximations to linear plots except for an inexplicable poor agreement at the agitator speed of 750 RPM. From the combined plot in Figure 4, however, the data points jointly approximate to a linear plot and hence predict averagely good mixing. Poor prediction of linearity, apart from indicating poor mixing may also indicate the existence of interfacial resistances.

5.1.2 Deactivation-Regeneration Runs

It is pertinent to recall here that after a deactivation run, the catalyst was regenerated by oxidation with pure or diluted air $2 - 3\% O_2$ in N_2 and then reduced with hydrogen before another run and the complete process of deactivation to regeneration is referred to as a cycle. This is necesary because it gives a measure of the usefull life of the catalyst. It is also usefull here to reiterate that the objective of this experiment was to profile the behaviour of the catalyst and so identify and suggest how to prevent those factors that cause activity decline of the catalyst to mortality. The overall objective also involves application of methods directed at retarding mortality.

Table 5 shows the number of deactivation-regeneration runs. These numerous runs were done to attain specific objectives as tabulated in the table. Irrespective of the objectives, all the experiments involved a deactivation-regeneration. Such objectives could be to determine the effect of flowrate (experiment number 6 and 7), achieving catalyst mortality (experiment number 1), determination of surface coverage for the quantification of residual activity, determination of surface coverage for the cycle by cycle (experiments set 9 and 11), respectively.

The deactivation-regeneration results will be discussed under the following headings:

1. Mortality Studies

112

2. Effect of Flowrate

3. Effect of catalyst weight

- **Mortality Studies**

New methods, intended to retard catalyst progress to mortality were applied and the quantities of oxidizable (primary) and reduceable (secondary) coke deposits were determined after each cycle.

The product of cyclohexane reforming on $Pt - Al_2O_3$ at 703K ($430^{\circ}C$) is benzene. Figure 5 shows the conversion profiles for benzene with time on fresh $Pt - Al_2O_3$ catalyst. The initial conversion of benzene on the first catalyst was 0.88. The high benzene conversion remained relatively stable for about 130 minutes before a sharp decline to about 5% after 155 minutes. Figure 5 also shows benzene profiles on the regenerated catalyst for cycles 2, 3, 4, 5, 7. The benzene conversion did not drop significantly on the regenerated catalyst, cycle 2. The conversion to benzene in cycle 2 was almost the same as on the fresh catalyst although for cycle 2 the deactivation time was 180 minutes, up from 160 minutes on the fresh catalyst. Figures 6 and 7 show conversion profiles for some of the cycles while Figures 8 to 16 show toxic coke removal profiles. A common feature of the deactivation profiles is that after remaining fairly stable for a long time, the conversion drops steeply showing profiles that are almost parallel to one another. This pattern is exhibited by all the deactivation profiles for all the 52 cycles investigated. The stability of the deactivation curves for some time was an indication of uniform coking of the catalyst surface. At the start of deactivation, there are several active sites and conversion stays high. As the number of active sites reduces due to the coke deposition, the effect of blocking successive sites becomes significant on the conversion. Hence the sharp drop as seen in the deactivation profiles.

113

2. Effect of Flowrate

3. Effect of catalyst weight

● Mortality Studies

New methods, intended to retard catalyst progress to mortality were applied and the quantities of oxidizable (primary) and reduceable (secondary) coke deposits were determined after each cycle.

The product of cyclohexane reforming on $Pt - Al_2O_3$ at 703K (430°C) is benzene. Figure 5 shows the conversion profiles for benzene with time on fresh $Pt - Al_2O_3$ catalyst. The initial conversion of benzene on the first catalyst was 0.88. The high benzene conversion remained relatively stable for about 130 minutes before a sharp decline to about 5% after 155 minutes. Figure 5 also shows benzene profiles on the regenerated catalyst for cycles 2, 3, 4, 5, 7. The benzene conversion did not drop significantly on the regenerated catalyst, cycle 2. The conversion to benzene in cycle 2 was almost the same as on the fresh catalyst although for cycle 2 the deactivation time was 180 minutes, up from 160 minutes on the fresh catalyst. Figures 6 and 7 show conversion profiles for some of the cycles while Figures 8 to 16 show toxic coke removal profiles. A common feature of the deactivation profiles is that after remaining fairly stable for a long time, the conversion drops steeply showing profiles that are almost parallel to one another. This pattern is exhibited by all the deactivation profiles for all the 52 cycles investigated. The stability of the deactivation curves for some time was an indication of uniform coking of the catalyst surface. At the start of deactivation, there are several active sites and conversion stays high. As the number of active sites reduces due to the coke deposition, the effect of blocking successive sites becomes significant on the conversion. Hence the sharp drop as seen in the deactivation profiles.

113

The conversion to benzene was not correlated with the overall oxidizable coke deposited for each cycle. However, the general observation from Figure 17a and 17b is that the deactivation times for a cycle that follows another with a high oxidizable coke content is relatively high - in some cases higher than that for the preceding cycle e.g cycle 7 with a deactivation time of 240 minutes is after cycle 6 with a deactivation time of 920 and a high oxidazable coke of 0.1359 g carbon; cycle 15 with a deactivation time of 180 minutes comes after 14, which has a deactivation time of 110 minutes and oxidizable coke of 0.0768g carbon. Cycle 29 with a deactivation time of 415 minutes comes after cycle 28 which has a deactivation time of 75 minutes and oxidizable coke of 0.098g carbon. Cycle 36 with a high deactivation time of 370 mins comes after 35 which has a high oxidizable coke of 0.100g carbon. Cycle 48 with a deactivation time of 795 minutes comes after cycle 47 which has a deactivation time of 605 minutes and oxidizable coke level of 0.0837g deposits.

In general, the oxidizable coke showed oscillations in between some fairly stable values.

Toxic Coke Deposits.

Figure 8 shows the profiles for secondary (toxic) coke removal with time after regeneration of the $Pt - Al_2O_3$ catalyst. The secondary coke profile after the first regeneration showed an initial toxic coke removal that was stable; 3 maxima were exhibited and the locations varied between 5-30 minutes for the first peak, 120-130 minutes for the second peak, and 160-170 minutes for the third. Two maxima were also exibited after the second regeneration and times of appearance of the two maxima coincided with the second and third which occured during the first regeneration. They occured between 120-130 minutes and 160-170 minutes, respectively. In cycle one, the initial rate of secondary coke removal stayed low for most of the time with oscillations that produced the max-

114

ima. The maxima have been explained to suggest the deposition of toxic coke in layers on the catalyst surface(9). Each maximum represents a reduceable coke form. Fig. 9 and 10, show some plots of toxic coke profiles. The amount of toxic coke deposited is determined by integrating the area under the toxic coke profile. Typical profiles that exhibited maxima are shown in Figures 11, 12, and 13.

It was observed that the very first maximum in the toxic coke profiles occuring between 5 to 30 minites was very high. Figure 14 showing cycles 42, 46, 47, 48, 49 typify this observation. The values were 354×10^{-9}, 238×10^{-9}, 184×10^{-9}, and 253.31×10^{-9} moles CH_4 for cycles 42, 46, 47, 48, 49 respectively. Of course the high maximum indicates coke with a very high reactivity in hydrogen, evidence of low bonding strength to the bulk toxic coke constituent. Lying closest to the oxidizable coke layer, this layer represented by this high maximum could have been oxidized under modified conditions.

The toxic coke profile generally showed a progressive decline in toxic coke reactivity in hydrogen with the least reactive lying closest to the catalyst coke interface thus confirming the postulation that the slow transformation of oxidizable coke occurs at the catalyst coke interface(9). After prolonged removal, not all the coke could be removed. Figure 16 shows removal for more than 750 minutes, showing that a third type of coke, resistant to both oxidation and reduction is retained on the catalyst surface and must be graphitic in nature(1,2,3).

Massive accumulation of toxic coke is observed between the 16-26 cycles and between 32-52 cycles. It was expected that the build up of toxic coke would be an indication of approach to mortality and therefore expectation of correspondingly low deactivation times should be high. On the contrary, deactivation times within this period were high. The huge amount of toxic coke removed could be viewed as (a) a reflection of the amount accumulated on the catalyst surface and /or (b) an indication of the nature of the coke

in terms of reactivity with hydrogen. This may mean that some of the accumulated coke possess a very high reactivity in hydrogen. This possibility is supported by the prominence of the first maximum in the toxic coke profiles for the cycle in which accumulation was observed - cycles 16-26, 32-51 (see Figures 17a and 17b).

Oxidizable Coke Deposition Rate.

Figure 18a and 18b are plots of oxidizable coke deposited per minute (that is between the start of deactivation to the time when the product conversion has dropped to 5% on the catalyst) versus cycle number. In other words, they are plots of the overall oxidizable coking rate versus cycle number. At that point (i.e when the conversion has dropped to 5%), it is not economic to continue the deactivation process and the catalyst must be regenerated.

Generally, from the peaks, the higher the oxidizable coking rate, the earlier the deactivation times. The rapid rate of oxidizable coke deposition led to earlier blockage of alumnina micropores leading to high oxidizable coke deposition for cycles where the peaks occured. Deactivation times were expectedly very high for those cycles with low oxidizable coking rate, particularly those beyond cycle 36 (see Figure 17a and 17b).

Comparison of Results of Cyclohexane and Methylcyclopentane Reforming on $Pt - Al_2O_3$

In the introduction to this work, it was stated that the use of multiple deactivation -regeneration scheme with the highest possible removal of toxic coke had been used to study methylcyclopentane (MCP) deactivation of $Pt - Al_2O_3$ catalyst in H_2 and N_2 atmospheres. A similar procedure was adopted here using cyclohexane. It is therefore necessary to compare the effects of the scheme on MCP and cyclohexane reforming with respect to deactivation and coking.

Conversion: The highest possible conversion of MCP to the reaction product (cy-

clohexane, benzene, hydrogenolysis products) was 0.73 on the fresh catalyst while the highest possible conversion to benzene from cyclohexane reforming was 0.929.

Oxidizable Coke: Table(6) show coke level for cyclohezane and MCP respectively. Only values for 11 cycles for MCP are available for comparison. With both reactants there was no correlation between coking levels and deactivation times. Unfortunately, literature support is contradictory in this regard. Wolf and Alfani(91), in their review, presented evidence showing the existence for and against a correlation between activity and carbon content. Toei et al.(51) showed that a correlation existed between the carbon content and reaction rate during dehydrogenation of butane on chromia-alumina, while data of Plank and Nace(92) showed no such correlation during the cracking of cumene-hydroperoxide. The discrepancies reported illustrate the the fact that the effect of coke must be due to several factors - difference in coke precursors and catalyst used, type of feed etc.

Cyclohexane cokes slowly over a long period of time. The oxidizable coke level decreased slightly from the first cycle (for the cycles in N_2- cycle 4) for MCP till cycle 11 Table(6). It showed some stability between cycles 7 and 10. The oxidizable coke level in cyclohexane similarly varied slightly for each cycle and did not show consistent decrease but showed irregular oscillations in between some stable values (see Figure 17a and 17b).

One interesting feature of these oscillations (maxima) in the amount of oxidizable coke deposited per cycle, as earlier noted, is that deactivation time for a cycle subsequent to one with a high oxidizable coke was relatively high. Apart from deblocking the micropores of coke, regeneration may lead to a better dispersion of metal crystallites. However, why the efficiency of this dispersion during regeneration suggests a dependence on the quantity of oxidizable coke accumulated is not clear. This will be elaborated later on in chapter six.

117

Toxic Coke Deposits

Reduceable Coke: Three reduceable coke types deposited on the catalyst surface and represented by maxima, were clearly identified in MCP. The first occured between 30 - 50 minites, the second between 150 - 160 minutes while the third occured at 370 minutes.

In this work, the maxima representing reduceable coke forms could not all be associated with occurence within the same time interval and besides, not all the maxima were well defined. The first maximum in this work can clearly be identified to occur between the time interval of 5-30 minutes - e.g. cycles 10, 14, 18 - the second maximum between 85 and 110 minutes e.g. (cycles 1, 7, 8). The third maximum occurs between 160 - 170 minutes (e.g. cycles 1, 4, 9, 17, 22, 23), the fourth between 240 - 260 minutes (cycles 1, 4, 9, 22, 23, 25), and the fifth maximum occured between 350-370 minutes (cycles 5, 20, 17, 22, 23, 27). Other maxima, some of them poorly developed occured between the 5 major identifiable time intervals. Below is a summary of time of occurence of maxima for cyclohexane and methlcyclopentane (MCP).

MCP	Time Interval	Cyclohexane	TimeInterval	
1st peak	30 − 50	1st peak	5 − 30	
2nd peak	150 − 160	2nd peak	85 − 110	(5.3)
3rd peak	370	3rd peak	160 − 170	
		4th peak	240 − 260	
		5th peak	350 − 370	

From the above summary, the closeness of some of the time intervals within which maxima in MCP and cyclohexane occur is noteworthy. The first, second and third maxima for MCP could be said to occur at the same time with the first, third and fifth maxima in cyclohexane. The coke types represented by the peaks can be assumed to

118

be of the same type. Hence all the coke types deposited in MCP were also found in cyclohexane. It is observed that within 370 minutes 5 coke types had been exhibited in cyclohexane as against 3 coke types in MCP.

Toxic Coke Levels. The toxic coke levels in both cyclohexane and MCP were high Table 6 and Figures 17a and 17b). The ratio of oxidizable to toxic coke in N_2 lay between $22 - 55 \times 10^3$ in MCP and $0.2 - 407 \times 10^3$ in cyclohexane. On the average, however, the oxidizable to toxic coke ratio in N_2 was 41.37×10^3 in MCP and 33.69×10^3 in cyclohexane.

• Effect of Flowrate

For demonstration of effect of flowrate, reference will be made to the results of experiments 6 and 7 with 31 and 24 runs respectively as the flowrates was the only difference in the conditions in which they were accomplished (Table 8). All the 31 and 24 runs involved were all done at a saturator temperature of $39°C$ (0.234 atm.), deactivation and regeneration (oxidation and reduction) temperature of $430°C$ and reduction time of 2 hours. However, experiment 6 was done at a reactant flowrate of 200 ml/min while 7 was done at a flowate of 100ml/min. The deactivation plots for experiment set 6 are shown in Figures 19 to 28 while those for experiment set 7 are shown in Figures 29 to 34.

The deactivation profiles for both experiments fitted with the description already given under mortality studies. A priori, it was expected that experiment set 6, with a higher flowrate would have lower deactivation times than runs for experiment set 7 with half the flowrate. In agreement to this, deactivation times for experiment 7 varied from 1360 minutes (Figure 30) at the 7th cycle to 85 minutes at the 22nd cycle (Figure 34) while deactivation times for experiment 6 varied from 105 minutes at the 16th (Figure

119

22) cycle to 990 minutes at the 5th cycle (Figure 21). At a higher flowrate the residence time of the reactant in the reactor is shorter and hence the reactant has a shorter time to diffuse into the sites located in the interior pores of the catalyst. Site utilization is less efficient and coking may involve pore mouth coking. This, of course, leads to lower deactivation time. On the other hand, it could be argued that at low flowrate the coke has sufficient time to convert to the deleterious forms and if the coke formation is occuring in parallel to the main reaction at the same sites, the deactivation time for the runs at lower flowrate should be shorter. This logical explanation in support of a contrary trend is probably also responsible for the non existence of clear-cut correlations between variables resulting from deactivation experiments and the strange observation that, most profiles in experiment set 7, despite low flowrate, had profiles that fell more steeply than in experiment set 6. Figures 31, 32 and 33 typify this observation.

● **Effect of Catalyst Weight**

To examine the effect of catalyst weight, reference will be made to profiles of experiment set 1 (52 runs) and 11 (12 runs) which were exact replicates except with the use of 10 gms as against 5 gms of catalyst used. The only major observation which could be attributed to catalyst weight is that the deactivation times for experiment set 1 (e.g Figures 5,6 and 7) did not fall in the range of thousands of minutes as observed in experiment set 6 and 7 (Figure 30) and the others. The coke levels with cycle number exhibited the oscillations explained before (Figures 35 and 36) although they were absent in experiments set 11 (Figure 36) which was just for 12 cycles.

5.1.3   Oxidizable Coke Structure Determination

During coke oxidation the product gases were connected via the TCD before absorption in the $Ba(OH)_2$ solution to ascertain the composition of the gas mixture. The gases identified included air, CO_2 and H_2O. CO was absent. The absence of CO indicated the completion of the combustion reaction at all times.

The profile of interest was that of CO_2 since it mirrored, in a way, the occurence and nature of oxidizable coke. The fraction of CO_2 in the combustion gases versus time was plotted in Figure 37. The profiles consist of sharp peaks typical of peaks from a temperature programmable oxidation run. As the experiment was done at constant temperature, the sharp and irregularly occuring peaks reflect the fact that oxidizable coke consists of a variety of randomly deposited molecular hydrocarbon species, unlike toxic coke found to be deposited in layers(9). The numerous sharp peaks, in addition, indicate the preponderance of the highly hydrogenated species since peaks indicate higher reactivity with oxygen.

5.1.4   Titration Experimental Results

Two sets of titration experiments were performed. The first, experiments set 9, was intended to determine the residual activity for use in the multilayer coking model, while the second titration experiment, set 11, was done cycle by cycle to profile the changes in surface characteristics of the Pt metal.

• Titration Results for the Residual Activity Determination

The summary of results of directly measured values and computationally estimated parameters for surface platinum metal atoms are displayed in Table 8 and 9. The table is self explanatory. However, some clarifications are necessary for easier interpretation

of the values. 'Conversions' refer to the conversion at the point of stoppage of the run. The uptake is the amount of gas chemisorbed, calculated from the difference in pulse size between the reference peak and the peak at any pulse. Several pulses were injected for a single titration experiment. Typically, about 6 to 8 pulses were injected for each determination. The average uptake was used for computation. Sample calculations are found in Appendix A. The interrelationship between the variables are studied from the plots.

Figure 38 is a plot of coke content versus dispersion for 6 runs carried out in N_2 with cyclohexane and 4 runs carried out in H_2 atmosphere with methylcyclopentane. For both reactants, the coke content is found to increase with increase in dispersion. However, the coke in MCP is found to be lower than in cyclohexane. Though the catalyst is platinum-alumina, the alumina support is inert to cyclohexane dehydrogenation to benzene. Hence all the carbon deposits would be expected to be on the platinum. On the other hand, MCP utilizes both the Pt and alumina sites hence coke will be distributed between the metal and support. Therefore the number of exposed platinum sites is expected to be higher when MCP is used leading to an almost constant increase in dispersion at the same coke level as shown in Figure 38.

The hydrogen uptake versus pulse number remained averagely constant (Figures 39 and 40). Some of the runs (3, 5 and 6), however, showed some oscillations, while runs 1, 2 and 3 were constant as expected. After deactivation, the numerous active sites are diminished by coke coverage. The first pulse of hydrogen easily titrates away O_2 attached to the exposed Pt atoms. As such exposed sites are few; adsorbed gas easily attains monolayer coverage and since the titrations are done at the same pressure (same pulse size) no more gas can be adsorbed and hence the eluting amount of hydrogen gas will rapidly be constant and equal to the amount injected. The occurrence of oscillations, on

the other hand, may suggest the occurence of some accompanying reaction or difference in states of adsorption of gases. These and other possibilities and the attendant arguments will be developed in the discussion of results.

The plot of fractional activity versus coke content (Fig 41) is what was used for the determination of the multilayer coking model on real surface parameters. Another set of 12 experimental runs (experiment set 10) was carried out at a flowrate of 200ml/min and at a partial pressure of 0.118 atm. Oxidation and reduction were carried out at $430°C$ and reduction was carried out for two hours. At the 11th cycle a titration experiment was carried out before oxidation and at the 12th cycle the titration experiment was carried out after oxidation and after reduction. The dispersion before oxidation at the 11th cycle was 0.4734 while the dispersion after oxidation in the 12th cycle was 0.533 and 0.4426 after reduction. The conversion and toxic coke removal profiles for experiment set 10 are shown in Figures 42 to 47. They showed trends similar to those observed in the mortality studies although the deactivation times were unusually very long particularly for cycles 1 and 2 (Figure 42) and cycles 9, 10 and 11(Figure 44).

- **Results of the Determination of the Stability of the Metal Surface During Successive Reaction-Oxidation and Reduction**

Titration experiments, cycle by cycle, as earlier mentioned in the introduction, were done to profile the stability of the catalyst Pt metal surface as the dehydrogenation of cyclohexane to benzene uses just the metal component of the $Pt - Al_2O_3$. The performance of this experiment was informed by the need to explain some observations in the previous experiments. Oxidation and reduceable coke data showed showed irregular oscillations which were a clear indication of the existence of reversible surface change (Figures 17a, 17b and 35). A total of 12 runs were made on fresh and deactivated catalyst

at a reaction temperature of 430°C and cyclohexane partial partial pressure of 0.1052 atm. at N_2 flowrate of 100ml/min. Titration was carried out after oxidation of coke at 430°C and after prolonged reduction (above 5 hours) at 500°C. These experimental conditions were an exact replica of the conditions under which the first set of experiments (52 runs) were carried out. This was the mortality studies in which the oscillations were first observed. The conversion profiles are shown in Figures 48 to 50 and the profiles for toxic coke removals of in Figures 51 to 55.

Table 11 is a summary of the results of the directly measured values and the computationally estimated parameters. Figure 56 is a plot of the variation of the metal dispersion with cycle number after oxidation and after reduction for the 12 runs. Figure 57 is a plot of the ratio of the dispersion at any cycle, D, to the dispersion on the fresh catalyst, D/D_o. From Figure 56 and 57 it is clear that reduction at 500$C°C$ under the stated conditions led to a lowering of dispersion from the fresh catalyst down to the 12th run. The plot also showed the dispersion after oxidation to be higher than the dispersion after reduction. Both dispersion after oxidation and reduction rose sharply from $D/D_o = 1$ but while the dispersion after reduction declined only after 2 runs showing regular oscillations, the dispersion after oxidation was stable for about 5 cycles before declining and oscillating.

Results of the sintering at different temperatures by Sieghard Wanke(92,93) on different catalysts, showed, in agreement to the results obtained here, that the dispersion after oxygen treatment is markedly higher than after hydrogen treatment at all the temperatures from 500$_oC$ to 700°C. In conflict to this result, however, his results showed the D/D_o to be constant after O_2 and H_2 treatment for more than 50 hours. The difference may be explained by the inclusion of a reforming reaction in our scheme. This possibility will be further examined in chapter 6.

124

Literature data on the effect of reduction on dispersion is not free of conflict. Turkevich et al.(95) carried out dispersion measurement from hydrogen chemisorption at different temperatures on a variety of of catalysts and showed that for Pt on platlike Baymol alumina catalysts, the dispersion remained constant at 27% up to $250^\circ C$ before declining markedly to about 16% while for the Engelhardt commercial Pt on alumina, the dispersion remained constant up to $450^\circ C$. Turkevich et al.(95) also showed the occurence of redispersion on oxidation in line with the observation here. They(95) did not, however, quantify the increase in redispersion.

The turn over number(TON), which is the rate of product per site varied from $383.6hr^{-1}$ at a dispersion of 0.36244 to $2137.9hr^{-1}$ at a dispersion of 0.2483 for cyclohexane deactivation runs in N_2, (Table 10). The oxidizable coke and the dispersion, however, showed the frequently observed trend i.e. increase in the coke content with dispersion as determined after oxidation and after reduction (Figure 44). Figure 59 is a plot of the reduceable coke and the oxidizable versus cycle number. As in the mortality studies (52 cycles), the reduceable coke decline as the oxidizable coke declined up to about the 5th cycle before irregularity (Figure 59). Unlike in the mortality studies, which this experiment is a duplicate of, the oscillations in oxidizable coke with cycle number were not as pronounced. They remained relatively stable. The interesting observation here is that the dispersion too after oxidation as shown in Figure 56, could be said to have remained stable up to the 8th run after the initial increase to the 2nd cycle. Hence dispersion after oxidation seems to be more sensitive to the amount of reduceable coke.

A probable link between oxidizable coke and dispersion after oxidation during multiple deactivation regeneration was first suspected in the mortality runs. It was observed during those runs that the deactivation times on cycle following those with a high oxidizable coke were generally high. It was explained, at that point, that better dispersion

125

was associated with large deposit of oxidizable coke. Explanations will be discussed in the next chapter on the basis of these results and previous works.

Unlike the oxidizable coke level that stayed averagely constant, the reduceable coke with cycle number showed oscillations (Figure 59). The peaks seemed to be closely related to the deactvation times. High at cycle 1 and 2 with deactivation times of 320 and 360 minutes and with a major peak at the 10th cycle with a deactivation time of 895 minutes - the longest in the set of experiments. This apparent existence of correlation between the reduceable coke and deactivation time seem to suggest the reduceable coke could be much more related to the activity of the catalyst than oxidizable coke, or a greater determinant of the activity. This view is supported by the Figure 60 which shows clearly that the dispersion rapidly passes through a maximum and then declines gradually with increase in the reduceable coke removal. The point of significance to note here is that it is in the region of low dispersion that the high deactivation times occured (Figure 56 and 60). If dispersion is a measure or determinant of activity, then this is conflicting. Three things can however be inferred from this occurence viz,

1. that though hydrogen treatment leads to a reduction in dispersion, this does not affect the quality of the catalyst.

2. that the deactivation reaction being examined may not be very structure sentitive with particular reference to dispersion, or if it is, as Somorjai(19,20) says, then it can be assumed that it is only sensitive to the specific surface factors he mentioned i.e. the existence of steps on the surface of the catalyst.

3. that the higher removal of toxic coke left a much more cleaner catalyst surface (free of coke). Hence clean catalyst surface may not be synonimous with better dispersion.

126

5.2 MODELLING RESULTS

5.2.1 Multilayer Coking on real Surface

A summary of the results of residual activity determination from hydrogen chemisorption experiments are shown in Table 13. A plot of fractional residual activity versus coke content was made and is shown in Figure 41. The range of values was increased by extrapolating several other values from the plot. The plot showed a decaying curve with little scatter.

From the plot, data form the model equation were extrapolated. The model equation for the multilayer coking on real surface was plotted for the evaluation of the model parameters.

$$\frac{1-A}{C_c} = \frac{1}{2Q} + \frac{\beta' A}{2Q(1-A)} \tag{5.4}$$

From the model equation we have:

$$slope = \frac{\beta'}{2Q} \tag{5.5}$$

$$\text{and the intercept} = \frac{1}{2Q}$$

$$\text{The slope} = \frac{\beta'}{2Q} = 21/0.25 = 84.0 \tag{5.6}$$

and

$$\beta' = 84 \times 2(0.025) = 4.2 \tag{5.7}$$

From Figure 61, Q, the monolayer coke coverage can be calculated from the value of the intercept:

$$\text{intercept} = 20 \ units \tag{5.8}$$

and

$$Q = 0.025 \tag{5.9}$$

127.

Figure 62 is the plot of the model equation which is Klingman and Lee(41) multilayer coking model (Ideal surface) for the comparison of catalytic activity determined by multilayer technique and the experimental. From the model equation for the Klingman and Lee multilayer coking,

$$\frac{C_c}{1-A} = \frac{1}{Q} + \frac{Q}{K_p}\left(\frac{1-A}{A}\right) \tag{5.10}$$

$$Intercept = Q = 0.0128 \tag{5.11}$$

$$and\ slope\frac{Q}{\overline{K_p}} = 0.004/(2.25 - 1.0) \tag{5.12}$$

$$0.004/1.25 = 0.0032 \tag{5.13}$$

$$i.e\frac{Q}{\overline{K_p}} = 0.0032 \tag{5.14}$$

Hence

$$\overline{K_p} = 0.0128/0.0032 = 4 \tag{5.15}$$

Figure 61 also compares multilayer coking on real surface and ideal surface(Klingman and Lee). From the plot of model 5.10, (Klingman and Lee) the infinite layer results i.e $N = \infty$, for which the model equation is derived predicts the experimental coke content throughout the entire range of activity investigated, under the conditions of the experiments.

From Figure 61 it is observed that the multilayer coking results developed for real surface predicts a higher coke content than the experimental. This is expected because there must be a finite number of layers. It is therefore apparent that the finite layer results is needed to describe the relationship in the entire range of interest. Hence, the distribution factor for the finite layer on real surface has to be rederived. From equation 3.41

$$\frac{k_{p_c}C_t}{k_{p_1}C_{p.s}}\frac{1-\gamma}{(1+G)^n} + \frac{k_{p_2}}{k_{p_1}} - 1 = f \tag{5.16}$$

128

From equation 3.39

$$\frac{C_t}{C_{p.s}} = \frac{(1-f^n)}{\gamma(1-f)} \tag{5.17}$$

$$\frac{k_{p_c}}{\gamma k_{p_1}}\left(\frac{1-f^n}{1-f}\right)\left(\frac{1-\gamma}{1+G^n}\right) + \frac{k_{p_c}}{k_{p_1}} - 1 = f \tag{5.18}$$

$$\frac{\beta}{\gamma}\left(\frac{1-f^n}{1-f}\right)\frac{1-\gamma}{1+G^n} + \alpha - 1 = f \tag{5.19}$$

$$4.2\left(\frac{1-f^n}{1-f}\right)\frac{A}{(1-A)} + \alpha - 1 = f \tag{5.20}$$

Recall that $\gamma = 1 - A$. Choosing a value of $\alpha = 2$ say.

To use the finite layer result, the number of layers, N, has to be determined first. We determine N for the largest γ of interest. This will give accurate results for the entire range of activity not predicted by the model.

Now using the value of Q and β' determined from Figure 61 for multilayer coking, the maximum number of layers can be determined from equation 5.20 and the equation below.

$$\frac{C_c}{Q} = \gamma\left[\frac{1}{1-f} - \frac{Nf^N}{1-f^N}\right] \tag{5.21}$$

The largest value of γ is that corresponding to $A = 0.20$ i.e $\gamma = 0.80$. The activity, A, corresponds to a coke value of 0.0225 g carbon. Hence we have:

$$C_c = 0.0225 = (0.025)(0.80)\left[\frac{1}{1-f} - \frac{Nf^N}{1-f^N}\right] \tag{5.22}$$

$$C_c = 1.125\left[\frac{1}{1-f} - \frac{Nf^N}{1-f^N}\right] \tag{5.23}$$

and substituting $A = 0.20$, equation 5.20 becomes

$$2 = f - 1.05\left(\frac{1-f^N}{1-f}\right) \tag{5.24}$$

Equations 5.23 and 5.24 are solved simultaneously to determine the value of N and f. For a given A, and a selected α, 5.24 is solved for f and then used to determine coke content from 5.23. The obtained values would then give a better prediction.

129

From equation 3.39

$$\frac{C_t}{C_{p.s}} = \frac{(1-f^n)}{\gamma(1-f)} \qquad (5.17)$$

$$\frac{k_{p_c}}{\gamma k_{p_1}} \left(\frac{1-f^n}{1-f}\right) \left(\frac{1-\gamma}{1+G^n}\right) + \frac{k_{p_c}}{k_{p_1}} - 1 = f \qquad (5.18)$$

$$\frac{\beta}{\gamma} \left(\frac{1-f^n}{1-f}\right) \frac{1-\gamma}{1+G^n} + \alpha - 1 = f \qquad (5.19)$$

$$4.2 \left(\frac{1-f^n}{1-f}\right) \frac{A}{(1-A)} + \alpha - 1 = f \qquad (5.20)$$

Recall that $\gamma = 1 - A$. Choosing a value of $\alpha = 2$ say.

To use the finite layer result, the number of layers, N, has to be determined first. We determine N for the largest γ of interest. This will give accurate results for the entire range of activity not predicted by the model.

Now using the value of Q and β' determined from Figure 61 for multilayer coking, the maximum number of layers can be determined from equation 5.20 and the equation below.

$$\frac{C_c}{Q} = \gamma \left[\frac{1}{1-f} - \frac{Nf^N}{1-f^N}\right] \qquad (5.21)$$

The largest value of γ is that corresponding to $A = 0.20$ i.e $\gamma = 0.80$. The activity, A, corresponds to a coke value of 0.0225 g carbon. Hence we have;

$$C_c = 0.0225 = (0.025)(0.80) \left[\frac{1}{1-f} - \frac{Nf^N}{1-f^N}\right] \qquad (5.22)$$

$$C_c = 1.125 \left[\frac{1}{1-f} - \frac{Nf^N}{1-f^N}\right] \qquad (5.23)$$

and substituting $A = 0.20$, equation 5.20 becomes

$$2 = f - 1.05 \left(\frac{1-f^N}{1-f}\right) \qquad (5.24)$$

Equations 5.23 and 5.24 are solved simultaneously to determine the value of N and f. For a given A, and a selected α, 5.24 is solved for f and then used to determine coke content from 5.23. The obtained values would then give a better prediction.

The monolayer coke weight on real surface, Q, was found to be higher than that when a homogenous surface is considered given the condition under which it is evaluated. However, the deactivation parameters β' and $\overline{K_p}$ for real surface and ideal surface respectively, were almost the same (4.2 and 4).

The larger values of the parameters for real surface is a reflection of the energies associated with interparticle interractions and non uniformity of the surface sites which assumptions in the development of the homogenous model ignores. This will be elaborated in the discussion.

5.2.2 Catalyst Regeneration Modelling Results

The model was developed for the regeneration of a homogenously coked spherical catalyst pellet with diffusional gradients. The model is intended to compute the gas and coke profiles within the catalyst pellet at any time in the regeneration process and assess the importance of diffusional resistances during the process. Hence the profiles were computed at different dimensionless times, θ and at different modified modified Biot numbers-recalling that the modified Biot number is the ratio of the bulk mass transfer to the diffusivity. The following modified Biot numbers were used: 10, 0.5 and 0.05.

The coke profiles are generally seen to increase from the external surface of the particle towards the interior (Figures 63 to 65). The gas profiles are presented in Figures 66 to 69. At small dimensionless times, i.e, when the regenerating gas has just contacted the coke, the profiles are almost horizontal i.e. dimensionless coke = 1 and reduce to about 0.82 at dimensionless time $\theta = 3$. The increase of the profiles towards the interior with dimensionless reflects non uniform coke consumption along the radial positions. This is due to a combination of mass transfer diffusion resistance at the external surface of the particle and the intraparticle diffusional resistances encountered by the regenerating

130

gas due to counter diffusion of the product gas and that due to the porous ash layer which it diffuses through to get to the reaction interface. Hence, the reduction in gas diffusing towards the center. With higher diffusional resistance i.e. at low modified Biot number (Figure 65), even less gas gets through and henceless coke is consumed. The coke profiles are seen to change from a dimensionless coke value at 0.82 at the external surface in Figures 63 and 64 which have a modified Biot number of 10 and 0.5 respectively to 0.88 in Figure 65 with a modified Biot number of 0.05. The reverse situation is true for gas profiles. The gas profiles are seen to decrease towards the center of the particles with dimensionless times for reasons given above. At higher diffusional resistance the gas profile has reduced from about 0.73 (Figure 66) at the external surface (at modifiedBiot number = 10) to about 6.8 at modified Biot number = 0.05 (Figure 68). The general increase of the coke profiles towards the center clearly shows the existence and significance of intraparticle diffusional resistance in the regeneration process. Though this numerical change was not very significant for about a 200 fold increase in diffusional resistance (modified Biot number from 10 to 0.05), the S-shape of the profiles instead of the horizontal lines reported by Weisz and Goodwin(55) and Wen(63), was a clear indication of the importance of external mass transfer. For highly exothermic reactions (most regeneration reactions are), and for surface reaction controlling, the reaction rate which is fast, increases towards the center of the particle where the concentration of the solid reactant is higher. It is clear that for the model developed, and for the parameters selected, the increase in the total resistance due to the inclusion of bulk mass transfer resistance is not sufficient to offset the rapid reaction rate. This is obvious from the low numerical change in coke values at the external surface for the very high variation in modified Biot number.

Panchenkov and Golovanov(97) using pelleted silica alumina granules have demon-

strated qualitatively the existence of operating conditions where external diffusional effects will not modify reaction behaviour. Carberry and Gorring(96) carried out an extensive study of the combustion of metal ores and presented curves showing how the fraction of carbon reacted varied with time for various degrees for bulk mass transfer limitation, and for three degrees of approach to the shell-type model, the latter represented by Damkohler number, $N_{Da} = \frac{k_s R}{D_{eff}}$. Here k_s is the first order reaction-rate constant(cm/sec). The implications of the results of the results presented here will be examined further in the discussion together with other existing results in the literature.

5.2.3 Reaction-Deactivation Kinetic Modelling Results

The general procedure in kinetic data procurement is to obtain conversion on a fresh catalyst at different flowrates at times when coking is not important. Modelling equations are then tested with the data and the appropriate model model parameters are obtained from model equations selected among others on the basis of goodness of fit and the positivity of the parameters. The parameters are then used in the main reaction which is coupled to a coking reaction to give a complete description of the decline in activity or rate.

The deactivation kinetic model derived in chapter three for the dehydrogenation of cyclohexane to benzene is a dynamic one and as such requires use of deactivation run data with time. A procedure was used as explained in chapter three which did not require decoupling of the main equation from the coking equation. From physical reasoning, the model parameters were constrained to be greater than zero and the modified method of Nelder and Mead (Flexible Polyhedron Simplex method) (86)for non-linear parameter estimation routine was used to estimate the parameters. Below are the results of the simulations. In the absence of deactivation data on the fresh catalyst for a wide range

132

of flowrates, the deactivation data on fresh catalyst at cyclohexane partial pressures of 0.234 atm., 0.10526 atm. and 0.118atm. at the same flowrate of 200ml/min at a constant temperature of $430^{\circ}C$ were used for the modelling.

The Computer program for the modelling is labelled Flexty.for in the Appendix C. The final estimates of the deactivation parameters are listed below. The final values of the parameters are: For $h = 1$

$$k_r = 12.799 \tag{5.25}$$

$$K_A = 241.66 \tag{5.26}$$

$$C_t = 6.725 \tag{5.27}$$

$$f = 0.918 \tag{5.28}$$

$$k_d = 31.6099 \tag{5.29}$$

and for $h \neq 1$

$$k_r = 22.5 \tag{5.30}$$

$$K_A = 131.38 \tag{5.31}$$

$$C_t = 8.239 \tag{5.32}$$

$$f = 0.948 \tag{5.33}$$

$$k_d = 49.182 \tag{5.34}$$

Hence from the above estimated values the rate prediction model equations can be fully written as: For $h = 1$

$$r_{A_1} = \frac{20793.966 C_A}{(1 + 241.66 C_A)} \left[1 - 0.917 \left(1 - exp\left(-\int_0^t \frac{7638.87 C_A^2}{(1 + 241.66 C_A)} dt\right)\right)\right]^m$$

133

and for $h \neq 1$

$$r_{A_2} = \frac{24356.749 C_A}{(1 + 131.39)}$$
$$\left[1 - 0.948 \left(1 - \left[-\frac{h(1-h)}{8.239} \int_0^t \frac{(49.189)(131.399)^h C_A^{(1+h)}}{(1 + 131.39 C_A)} dt + 1 \right] \right) \right]^m.$$

The above rate models were confronted with experimental data to compute the decline in rate with time.

Rates from raw data were calculated from

$$r_A = \frac{C_{Ao} v X}{w} \tag{5.35}$$

where X is the conversion. The computed declines in rates were confronted with the experimental data viz: Figure 69, Figure 70, Figure 71.

Statistical anlysis of fit shows model $1 (h = 1)$ to have an average standard deviation of 12.83% and 10% for model 2 $(h \neq 1)$

$$\sigma(r_{A_1}) = 12.83\% \tag{5.36}$$

$$\sigma(r_{A_2}) = 10\% \tag{5.37}$$

Non of the models was observed to be superior to the other but on purely statistical grounds the model with $h = 1$ gave a better prediction of the data than $h \neq 1$, and hence will be prefered. Preference for model 1 is even enhanced by its simplicity.

Table 5
Summary of Experiments Performed: Objectives,Conditions,Remarks

| OBJECTIVE | DEACTIVATION RUNS CONDITIONS | | | REDUCTION RUNS TOXIC COKE MONITOR CONDITION | | Reduction Times | REMARKS | EXPERIMENT |
	Temp.	Flowrate ml/min	Vap.Pres. atm.	Temp.	Flowrate	hours		NUMBER
Achieving Catalyst Mortality and quantifying Coke	430	100	0.10526	500	40	>5	Mortality not achieved. Oxidizable and Toxic Coke	1
Same as above	430	100	0.10526	500	40	>5	Catalyst discharged due to unexpectedly long deactivation	2
Same as above	430	100	0.10526	500	40	>5	Catalyst removed due to long deactivation time	3
Segmented Runs after 6 Runs to check for reproducibility	430	100	0.10526	500	40	>5	After 6 runs prolonged reduction was carried out. Combustion gas monito|	4
Segmented Runs to ascertain reproducibility in coke	430	100	0.10526	500	40	>5	Done again due to to unconvincing results.	5
Replication of work of Omoleye	430	200	0.234	430	40	>2	No similarity with Omoleye's	6
Effect of Flowrate on Deactivation	430	100	0.234	430	40	>2	Not exact duplicate of Omoleye's work	7
Titration Experiments for determination of surface coverage	430	100	0.10526	430	40	>2	Catalyst Surface characterization for residual activity|	8
Titration experiments with MCP reactant	430	100	0.10526	430	40	>2	Same as above. Testing Variation with Reactant.	9
Effect of Change in reactant vapour pressure	430	200	0.118	430	40	>2	Fresh Catalyst	10
Effect of flowrate and the change in surface characteristics with cycle number	430	100	0.10526	500	40	>5	Unexpectedly, the deactivation times were far shorter than the previous though both i.e. previous and this	11

134b

Table 6
Comparison of Coking in CH and MCP

Primary Coke(MCP) Deposits	Ratio of Primary Coke in CH to MCP	Secondary Coke Deposits X10^(6) MCP	Ratio of Coke in CH to MCP X10^(6)
2.130	35.000	1.160	1.350
2.330	38.000	1.410	1.320
3.140	20.000	0.210	2.220
4.420	15.000	0.083	13.550
4.390	13.550	0.079	11.000
4.200	32.000	0.064	147.600
4.310	26.000	0.096	4.164
4.310	9.000	0.108	17.926
3.300	14.000	0.127	15.450
3.300	9.000	0.152	8.059
2.210	15.000	0.092	10.020

CH(Cyclohexane), MCP(Methylcyclopent

135

Table 7. Mechanism and model of deactivation by Corella and Asua

	Deactivation function, $\psi(P_1,T)$	
Mechanism	Controlling step: 2nd	Controlling step: 3rd

d-1 $\quad nM_{(g)} + hM1 \rightarrow P_1 1_h$

$$\frac{mhL^{h-1}k_d K_m^h P_m^{n+h}}{(1+k_A P_A + K_R P_R + (m-1)K_S P_S)^h} \quad \ldots\ldots\ldots(1)$$

d-1 $\quad \rightleftharpoons P_2 1_h \rightleftharpoons P_3 1_h \rightleftharpoons$

for h=1

$$\frac{mk_d K^{*'}_m P_m^{n+1}}{1+K_A P_A + K_R P_R + (m-1)K_S P_S + k^{\prime\prime}_m P_m^{n+1}} \quad \ldots\ldots\ldots(4)$$

d-2 $\quad nM_{(g)} + hM^*1 \longrightarrow P_1 1_h$

$$\frac{mhL^{h-1}k_d K^{*h}_m P_m^{n+h}}{(1+K_A P_A + K_R P_R + (m-1)K_S P_S + K^*_m P_m)^h} \quad \ldots\ldots\ldots(2)$$

d-2 $\quad \rightleftharpoons P_n 1_h \rightleftharpoons P_3 1_h \rightleftharpoons$

for h=1

$$\frac{mk_d K^{*'}_m P_m^{n+1}}{1+K_A P_A + K_R P_R + (m-1)K_S P_S + K^*_m P_m + K^{*''}_m P_m^{n+1}} \quad \ldots\ldots\ldots\ldots\ldots(5)$$

d-3 $\quad nM_{(g)} + hM1 \rightarrow P_1 1_h$

(same as equation (1))

d-3 $\quad P_1 1_n \overset{+M}{\underset{(g)}{\rightleftharpoons}} P'_2 1_h \xrightarrow{+M(g)} P_3 1_h$

for h=1

$$\frac{mk_d K_m P_m^{n+3}}{1+K_A P_A + K_R P_R + (m-1)K_S P_S + K_1 K_m P_m^{n+1} + K_1 k_2 K_m P_m^{n+2}} \quad \ldots\ldots\ldots(6)$$

d-4 $\quad nM_{(g)}^+ + hM^*1 \longrightarrow P_1 1_h$

(same as equation (2))

d-4 $\quad P_1 1_h \overset{+M(g)}{\underset{}{\rightleftharpoons}} P_2 1_h \xrightarrow{+M(g)} P_3 1_h$

for h=1

$$\frac{mk_d K^{*'}_m P_m^{n+3}}{1+K_A P_A + K_R P_R + (m-1)K_S P_S + K^*_m P_m + K_1 K^*_m P_m^{n+1} + K_1 K_2 K^*_m P_m^{n+2}} \quad \ldots\ldots\ldots\ldots(7)$$

Table 8

Summary of Titration Results:Uptakes with Pulse Number

Run 1 X=0.7 Pulse Number	Hydrogen Uptake cm^(3)	Run 2 X=0.43 Pulse Number	Hydrogen Uptake cm^(3)	Run 3 X=0.58 Pulse Number	Hydrogen Uptake cm(3)	Run 4 X=0.42 Pulse Number	Hydrogen Uptake cm^(3)	Run 5 Pulse Number	Hydrogen Uptake cm^(3)
1.000	0.734	1.000	0.689	1.000	0.575	1.000	0.431	1.000	0.320
2.000	0.723	2.000	0.681	2.000	0.408	2.000	0.592	2.000	0.235
3.000	0.734	3.000	0.674	3.000	0.378	3.000	0.581	3.000	0.257
4.000	0.734	4.000	0.666	4.000	0.439	4.000	0.632	4.000	0.227
5.000	0.734	5.000	0.658	5.000	0.469	5.000	0.632	5.000	0.242
		6.000	0.666	6.000	0.439	6.000	0.632	6.000	0.227
		7.000	0.651	7.000	0.424	7.000	0.592	7.000	0.235
		8.000	0.651	8.000	0.431	8.000	0.592	8.000	0.235
		9.000	0.651	9.000	0.469			9.000	0.250

3.77	0.41	4.14	20.26
2.85	0.31	3.14	26.74
1.32	0.14	1.45	57.92
1.13	0.12	1.24	67.43
2.59	0.28	2.84	29.50
2.55	0.28	2.81	29.87
0.51	0.05	0.56	149.80

Table 9

Summary of Titration Results (Continued):Uptakes with Pulse Number

Run 6 X=0.05 Pulse Number	Hydrogen Uptake cm^(3)	Run 7 X=0.185 Pulse Number	Hydrogen Uptake cm^(3)	Run 8 X=0.0175 Pulse Number	Hydrogen Uptake cm^(3)	Run 9 X=0.0175 Pulse Number	Hydrogen Uptake cm^(3)	Run 10 X=0.0175 Pulse Number	Hydrogen Uptake cm^(3)
1.000	0.439	1.000	0.469	1.000	0.719	1.000	0.530	1.000	0.643
2.000	0.386	2.000	0.439	2.000	0.704	2.000	0.540	2.000	0.643
3.000	0.378	3.000	0.439	3.000	0.689	3.000	0.550	3.000	0.643
4.000	0.416	4.000	0.439	4.000	0.681	4.000	0.550	4.000	0.643
5.000	0.431	5.000	0.454	5.000	0.681	5.000	0.568	5.000	0.636
6.000	0.416	6.000	0.446	6.000	0.674	6.000	0.550	6.000	0.643
7.000	0.431	7.000	0.446	7.000	0.659	7.000	0.570	7.000	
8.000	0.431	8.000	0.454	8.000	0.674	8.000	0.590	8.000	
				9.000	0.689	9.000			

137

138

Table 10
Summary of Titration Parameters: Determined Parameters

Run Number	Deactiv. Times minutes	Convers. X	Oxidiz. Coke g carbon	Average Hydrogen Uptake cm^(3)	Platinum Metal Dispers.	Metal Area cm^(2) X10^(3)	Cluster Diameter Angstr. Units	Turn Over Number hr^(-1)	Platinum Metal Sites X10^(18)	Fract. Residual Activity A
1.000	30.000	0.510	0.004	0.732	0.638	6.506	12.898	1010.760	5.915	0.986
2.000	60.000	0.560	0.002	0.668	0.582	5.940	14.120	1215.600	5.400	0.900
3.000	90.000	0.590	0.011	0.435	0.379	3.866	21.700	1961.000	3.515	0.586
4.000	120.000	0.420	0.010	0.585	0.510	5.204	16.120	1040.670	4.731	0.414
5.000	525.000	0.370	0.019	0.248	0.248	2.533	33.127	2137.940	2.303	0.211
6.000	550.000	0.110	0.044	0.416	0.362	3.697	22.690	383.600	3.361	0.616
7.000	100.000	0.184	0.003	0.448	0.398	3.982	21.070	873.500	3.620	
8.000	180.000	0.018	0.004	0.678	0.590	6.026	13.920	54.890	5.478	
9.000	380.000	0.018	0.004	0.554	0.480	4.932	17.010	67.060	4.484	
10.000	10.000	0.018	0.005	0.642	0.560	5.706	14.700	57.970	5.187	

Table 11
Summary of Titration Parameters:Determined Parameters(Cycle by Cycle Titrations)

Run Number	Deactiv. Time mins	Oxidiz. Coke g Carbon	Secondary Coke X10^(-5)	Uptake cm^(3)	Pt Atoms X10(18)	Dispers.	Metal Area cm cm^(2) X10^(18)	Cluster Diameter Angstrong units	Uptake cm(3)
1.000	320.000	0.046	10.540	0.671	5.42	0.58	5.96	14.07	0.64
2.000	360.000	0.033	9.280	0.671	5.42	0.58	5.96	14.07	0.68
3.000	80.000	0.030	5.280	0.742	6.00	0.65	6.60	12.72	0.70
4.000	125.000	0.030	5.220	0.742	6.00	0.65	6.60	12.72	0.36
5.000	90.000	0.030	4.800	0.742	6.00	0.65	6.60	12.72	0.46
6.000	120.000	0.030	7.840	0.742	6.00	0.65	6.60	12.72	0.47
7.000	145.000	0.025	4.024	0.684	5.53	0.60	6.08	13.80	0.35
8.000	125.000	0.024	5.768	0.729	5.89	0.64	6.48	12.90	0.16
9.000	820.000	0.028	3.920	0.474	3.38	0.41	4.21	19.92	0.14
10.000	510.000	0.022	3.560	0.606	4.90	0.53	5.39	15.57	0.32
11.000	895.000	0.021	14.430	0.427	3.45	0.37	3.80	22.11	0.32
12.000	360.000	0.021	12.620	0.448	3.62	0.39	3.98	21.07	0.06
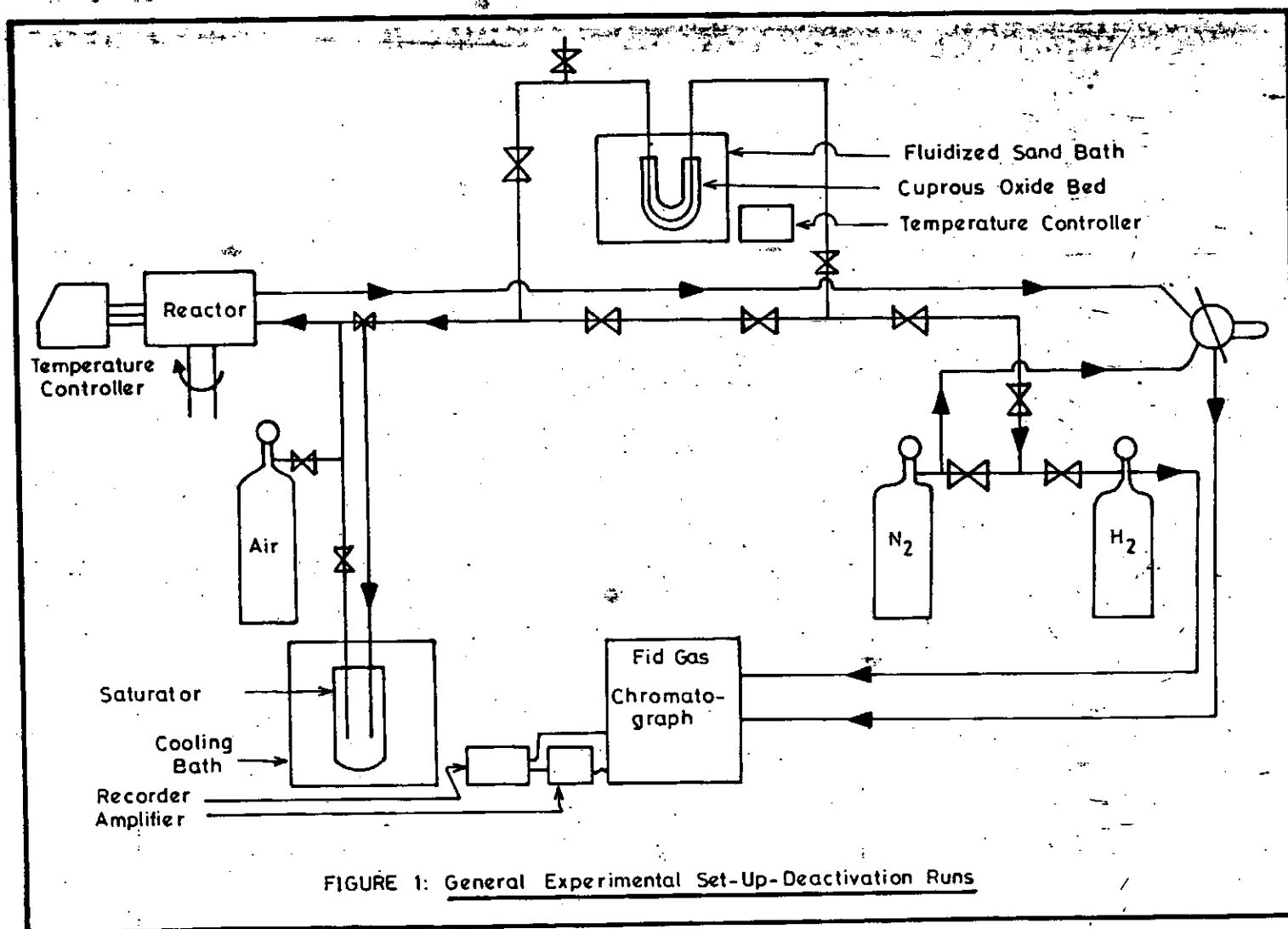
FIGURE 1: General Experimental Set-Up-Deactivation Runs

Fluidized Sand Bath
Cuprous Oxide Bed
Temperature Controller

Reactor

Temperature Controller

Air

N_2

H_2

Fid Gas Chromatograph

Saturator

Cooling Bath

Recorder Amplifier
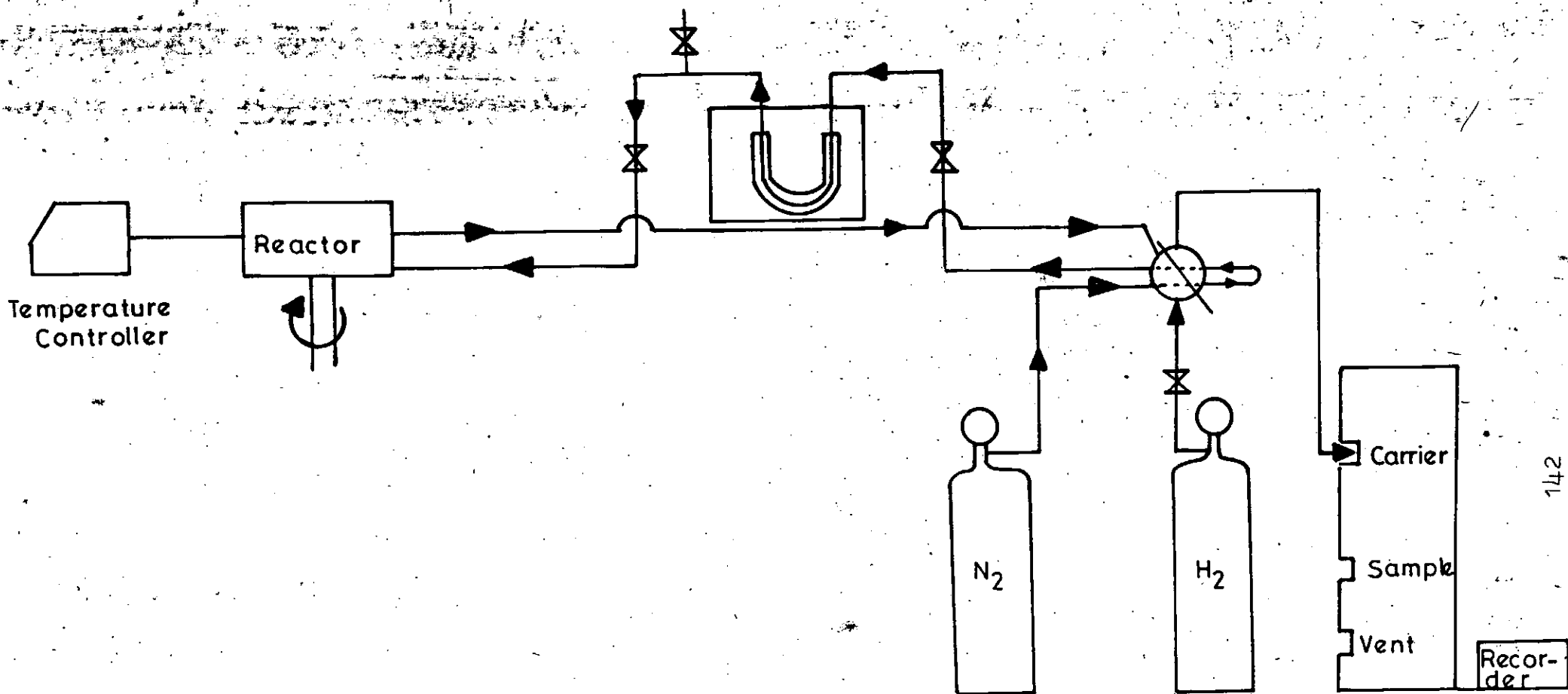
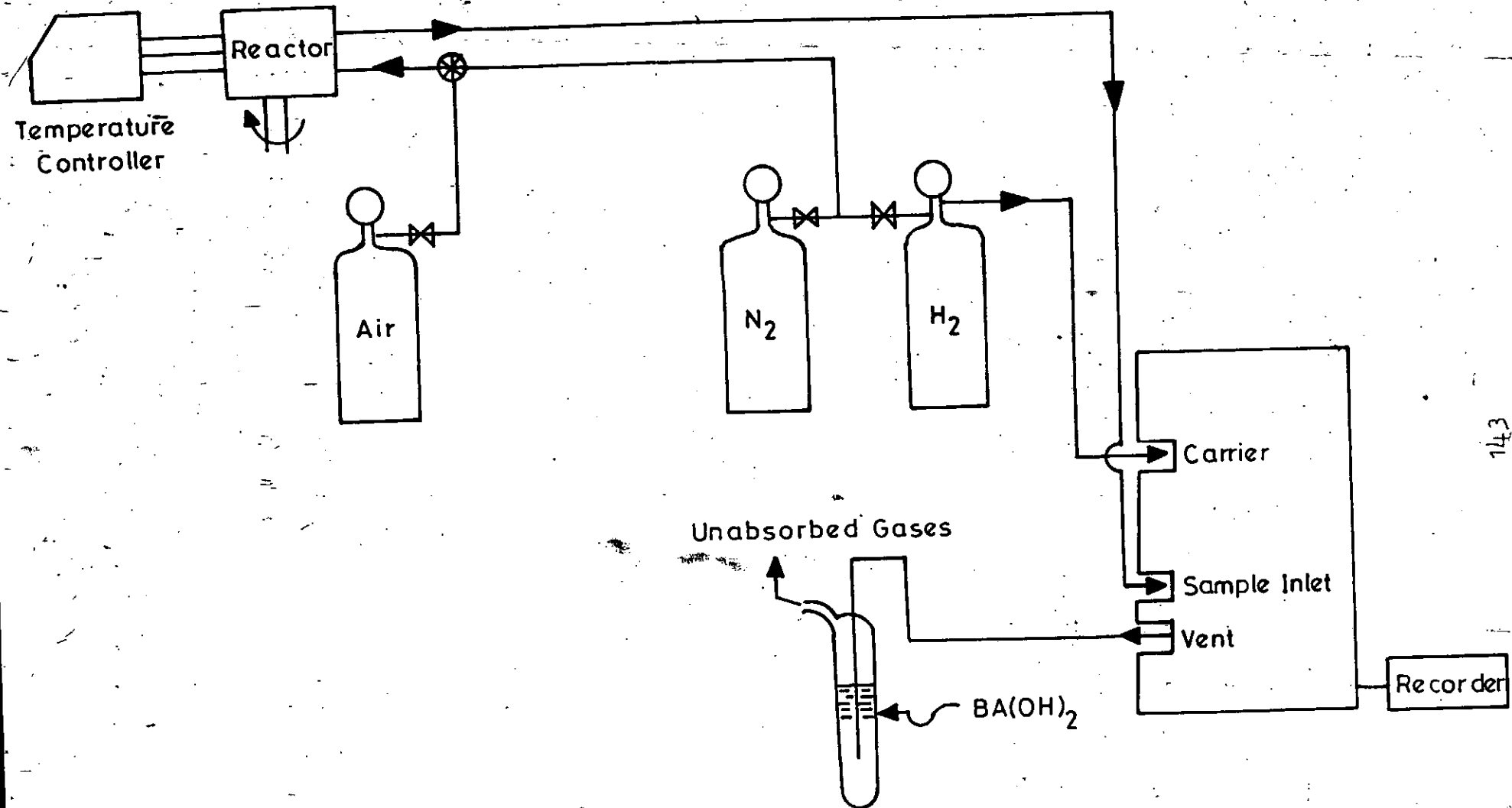FIGURE 2: Experimental Set-Up For Titration And
Mixing Experiments

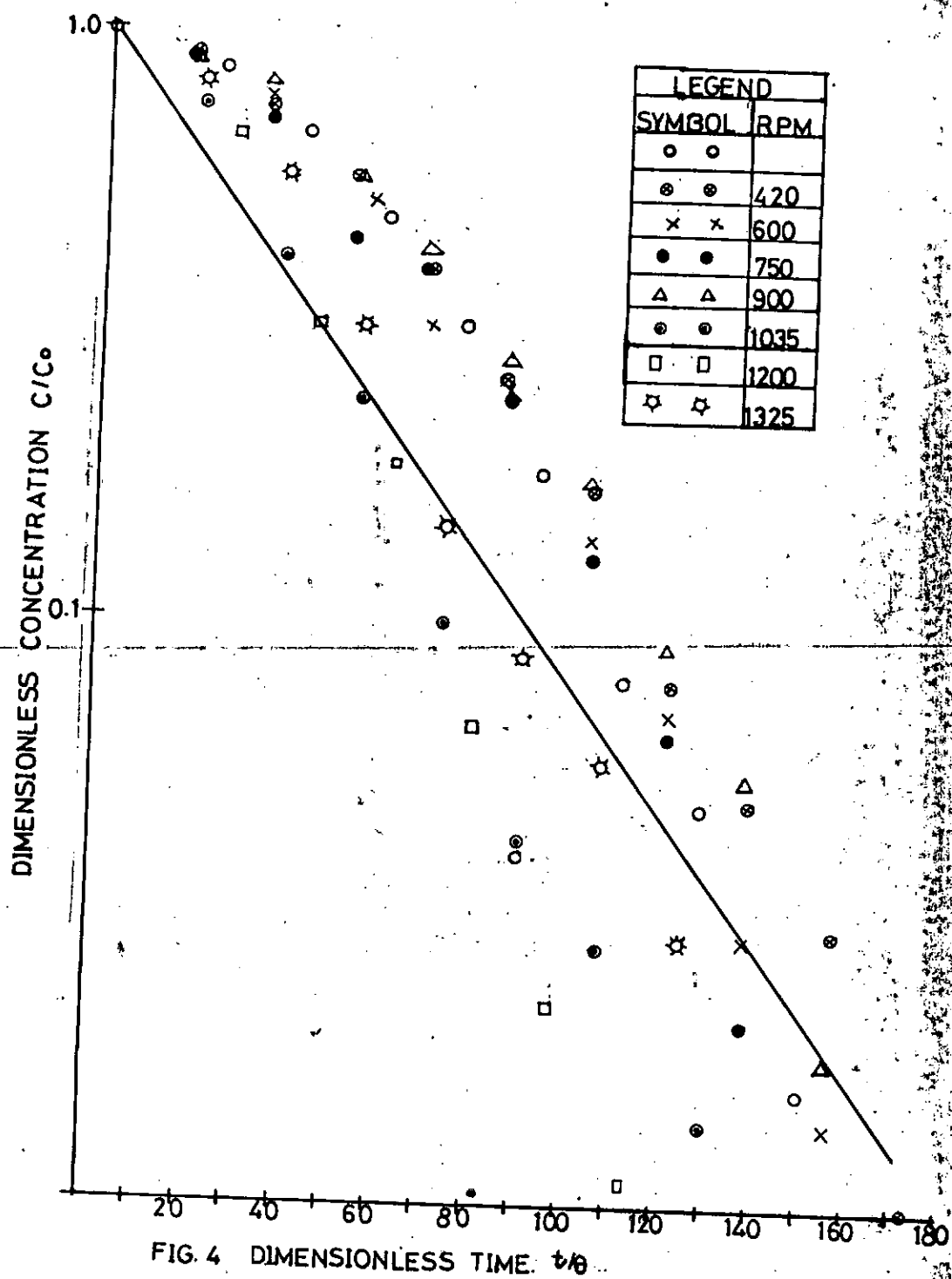FIGURE 3: Experimental Set-Up For Oxidizable Coke Structure
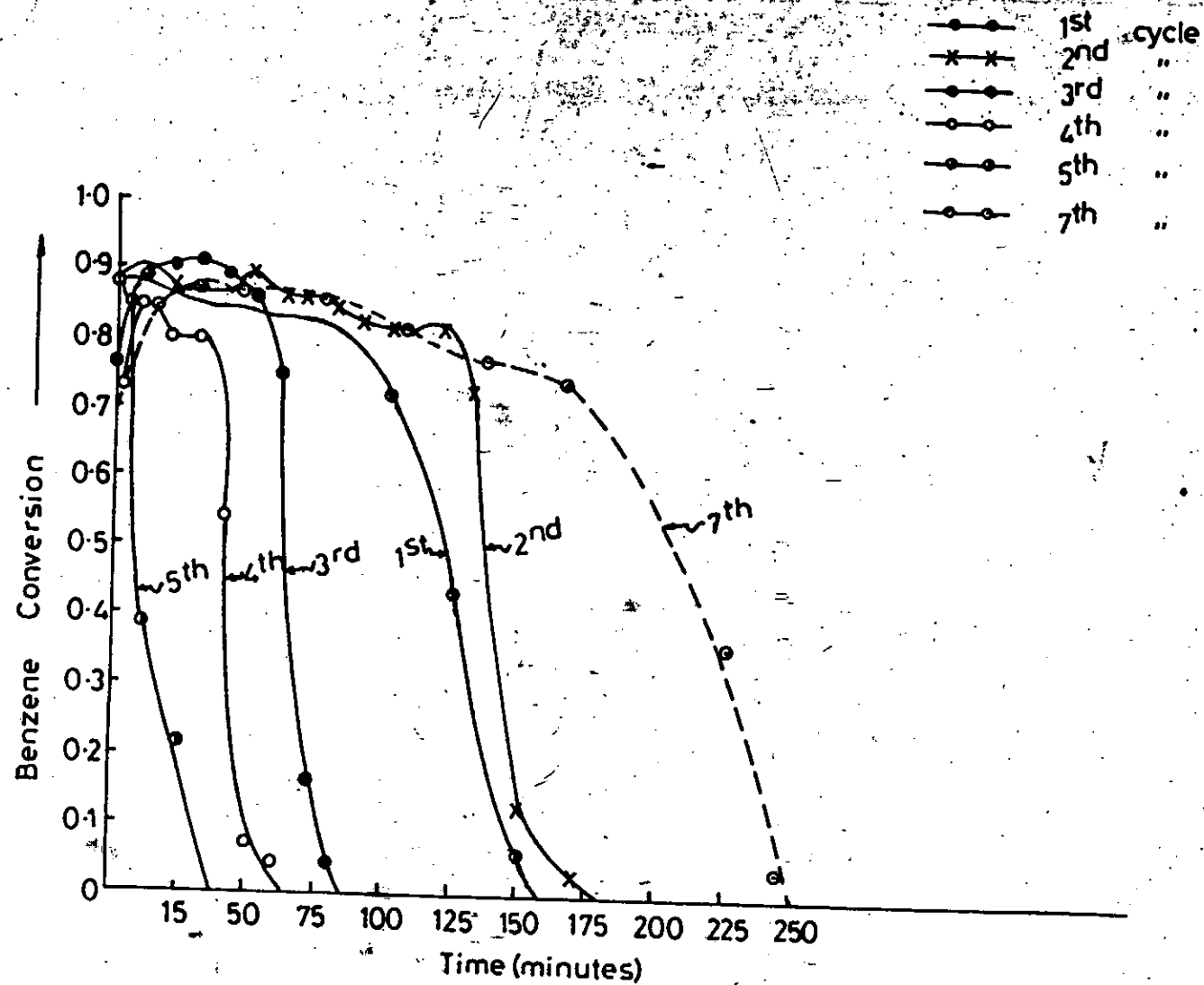Determination(Coke Burn-Off)

143

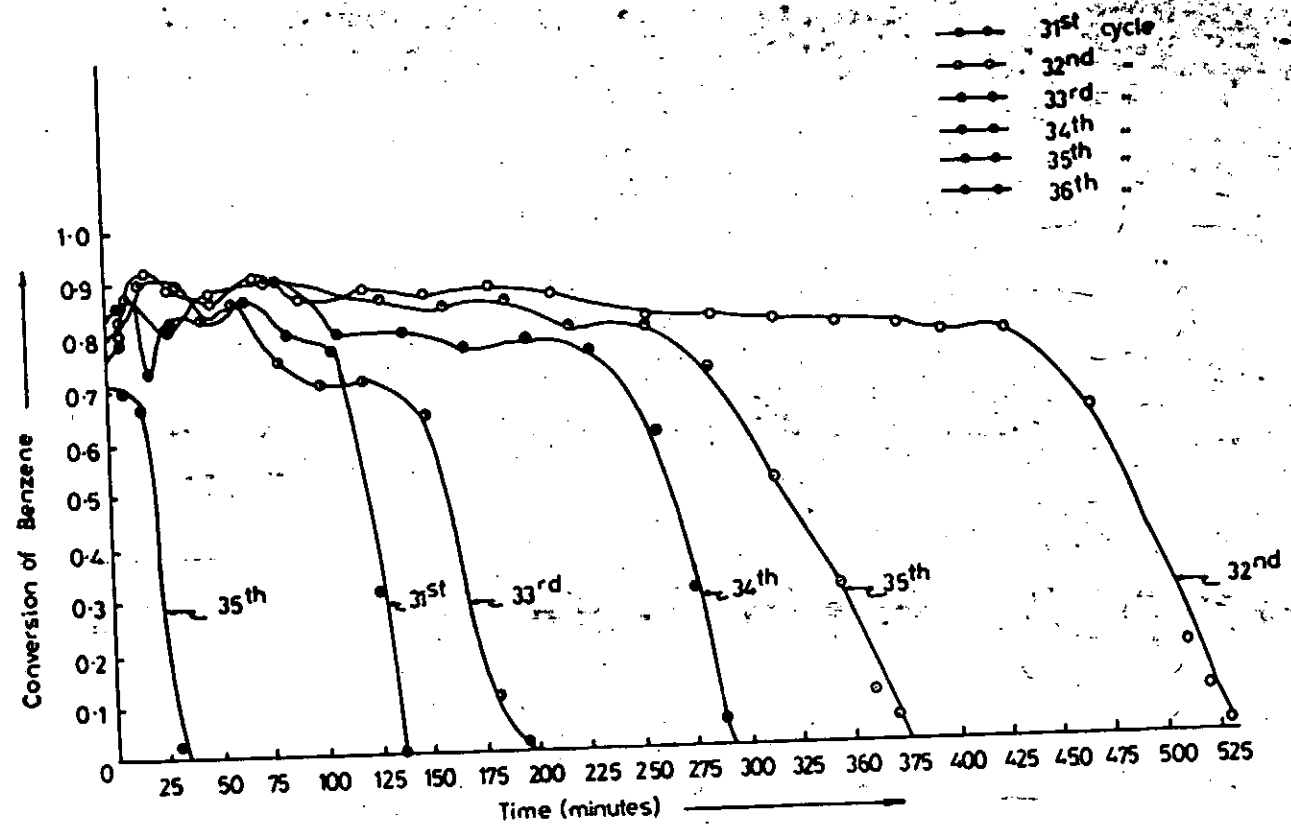FIG. 4 DIMENSIONLESS TIME. t/θ

FIG.5   PLOT OF CONVERSION VS TIME.

FIG. 6   PLOT   OF   BENZENE   CONVERSION   VS   TIME

146
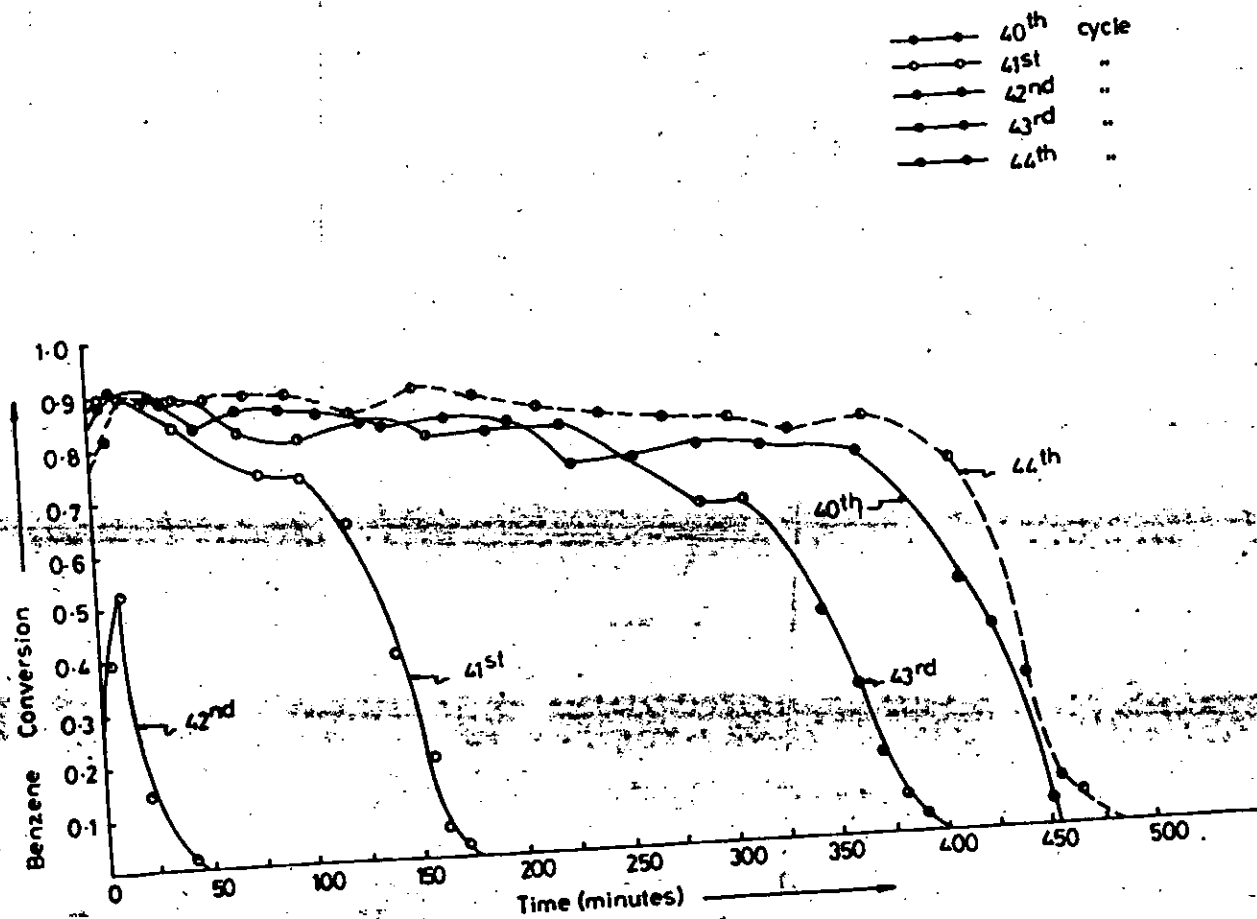
FIG. 7   PLOT OF BENZENE CONVERSION VS TIME
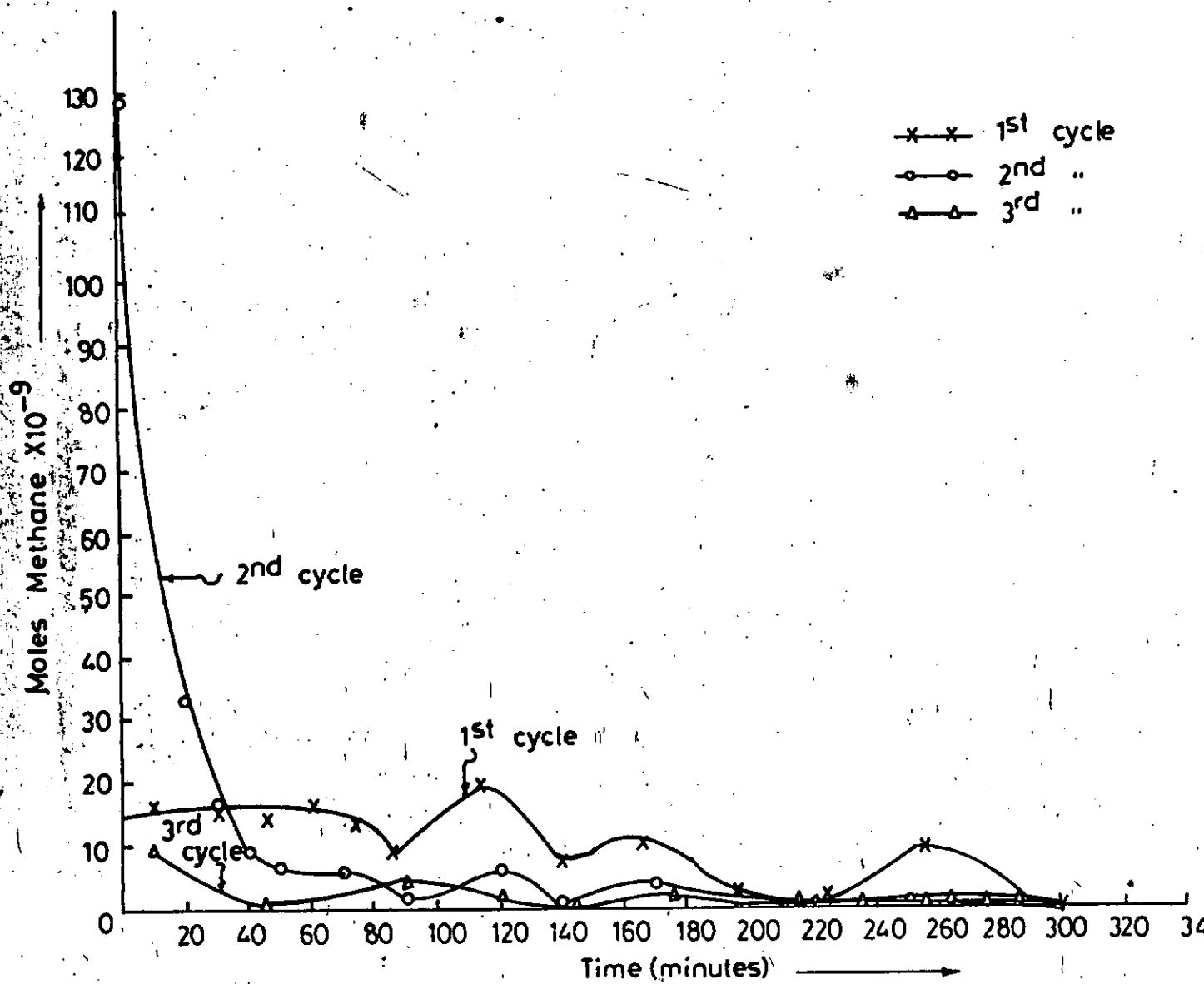
FIG. 8 PLOT OF METHANE REMOVAL VS TIME
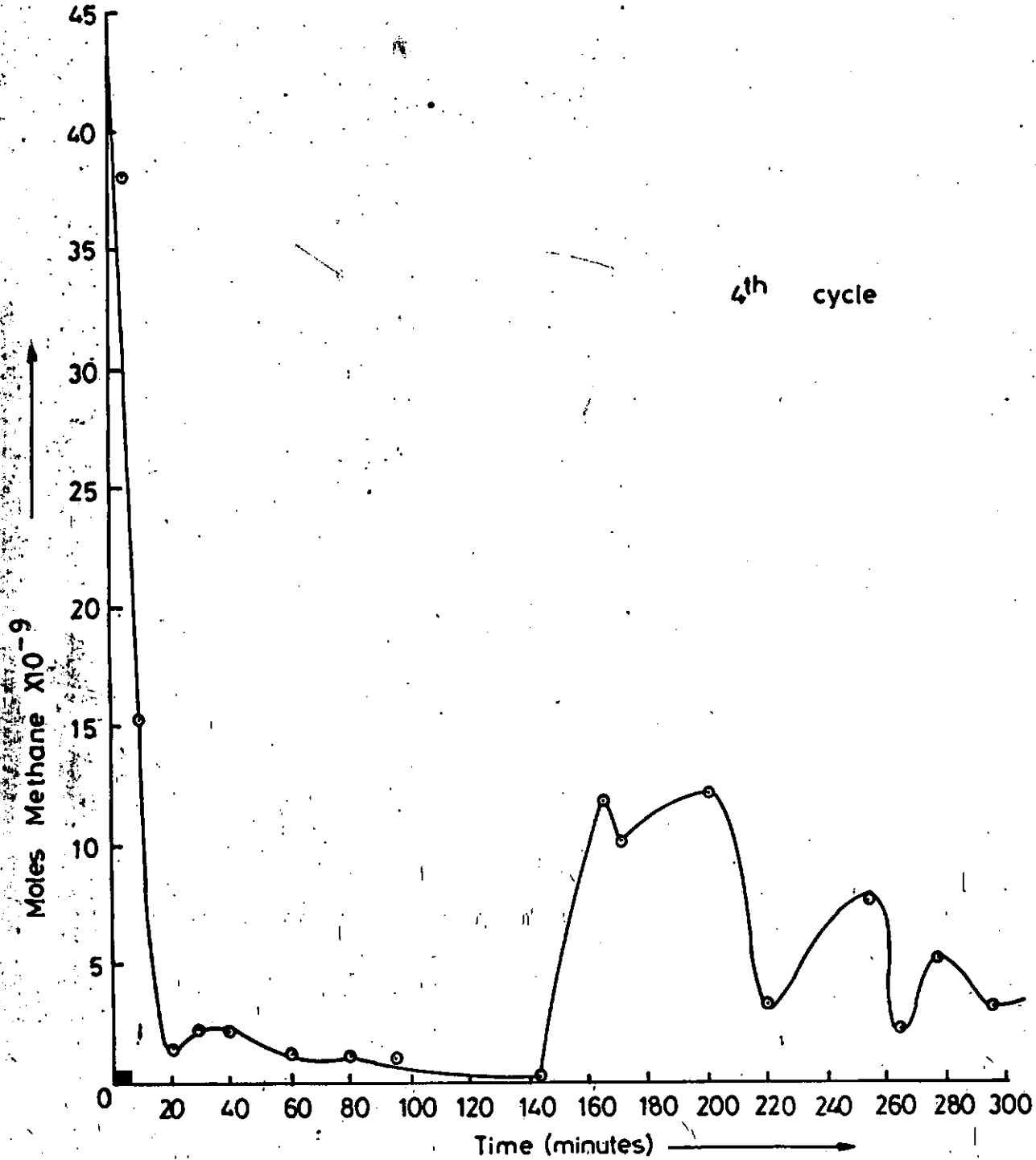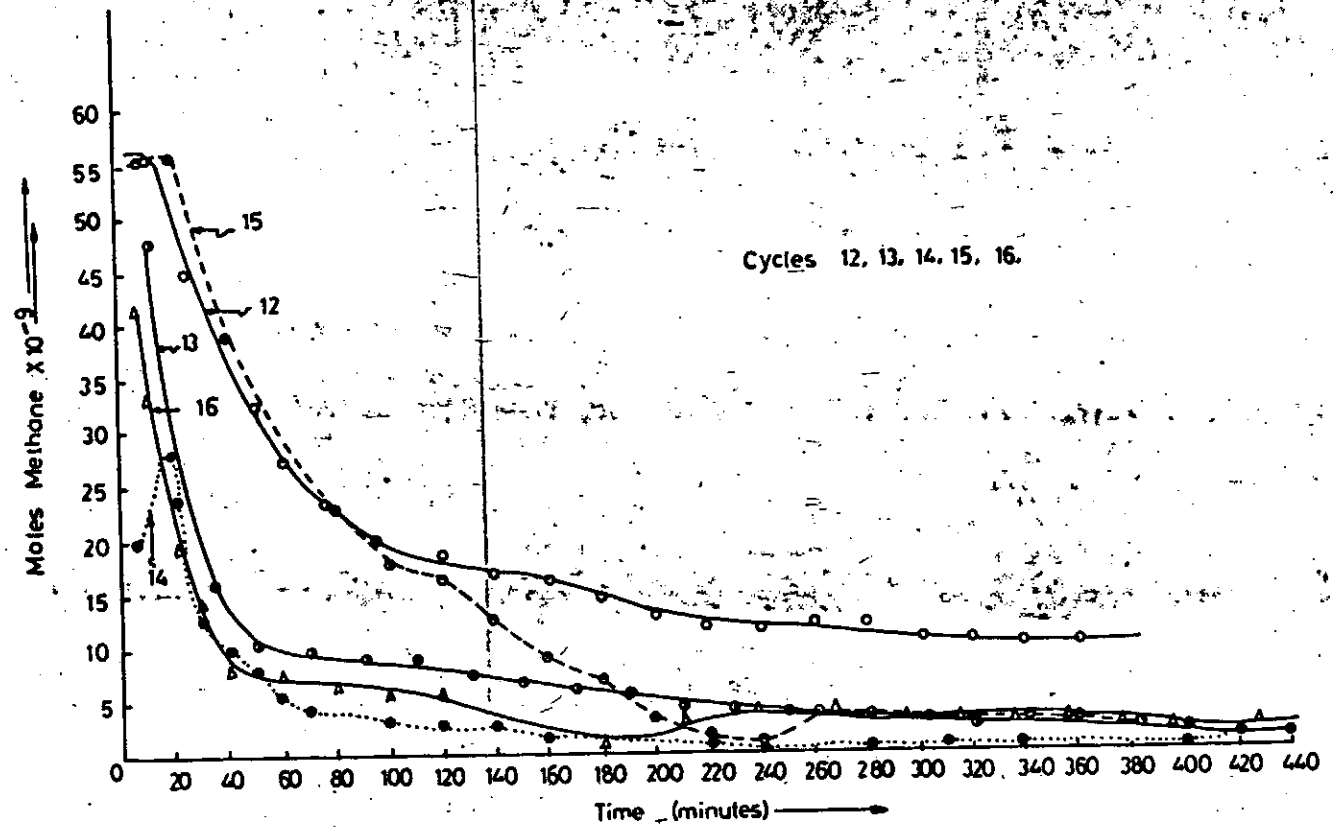
148

FIG. 9   PLOT OF TOXIC COKE   REMOVAL WITH TIME

The y-axis is labelled "Moles Methane $\times 10^{-9}$" and the x-axis is labelled "Time (minutes)". The plot is annotated "4th cycle".

149

FIG. 10   PLOT OF TOXIC COKE REMOVAL WITH TIME   TEMP = 500°C

Cycles   12, 13, 14, 15, 16.

150
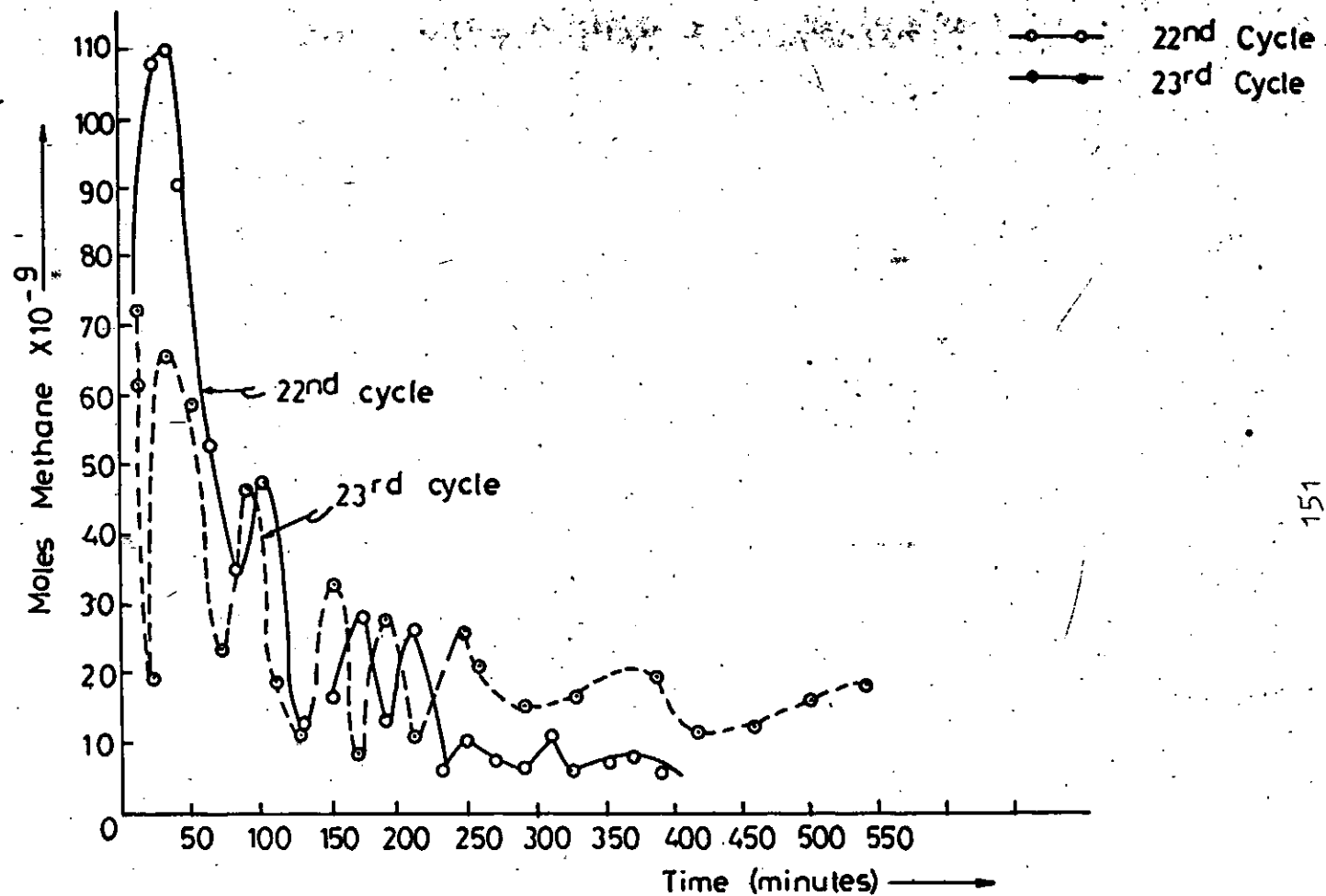
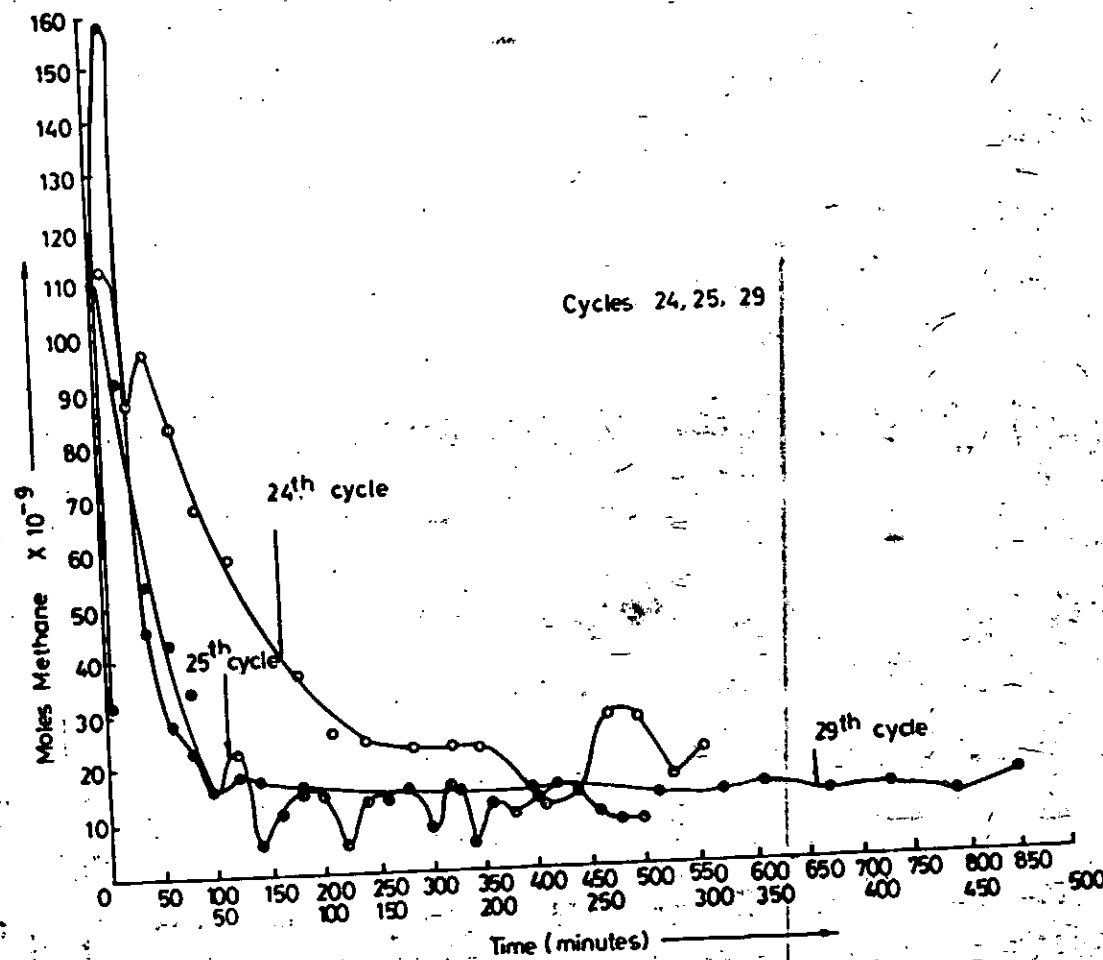FIG. 11 PLOT OF TOXIC COKE   REMOVAL WITH TIME TEMPERATURE = 500°C

151

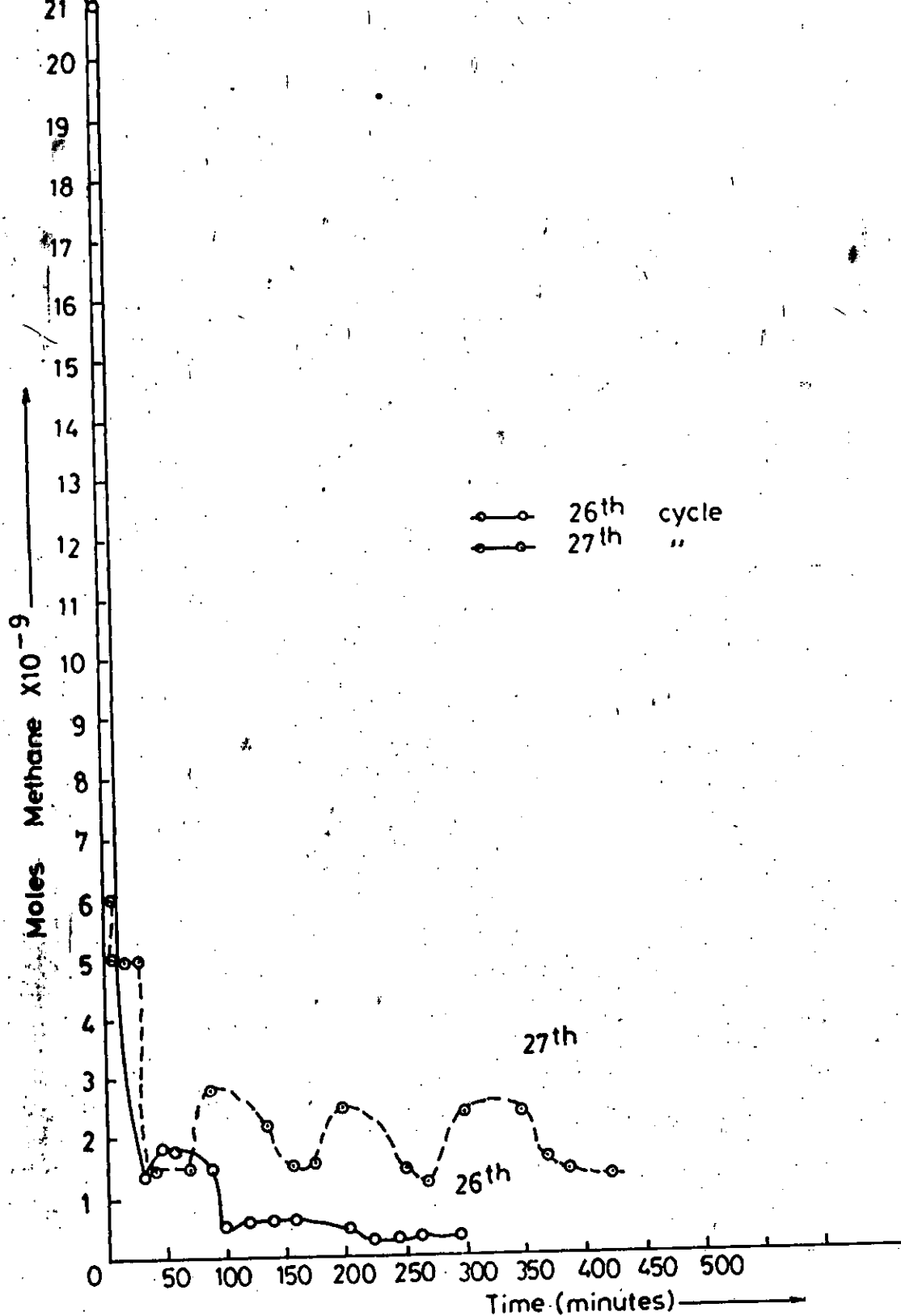FIG. 12   PLOT OF TOXIC COKE REMOVAL WITH TIME TEMPERATURE = 500°C

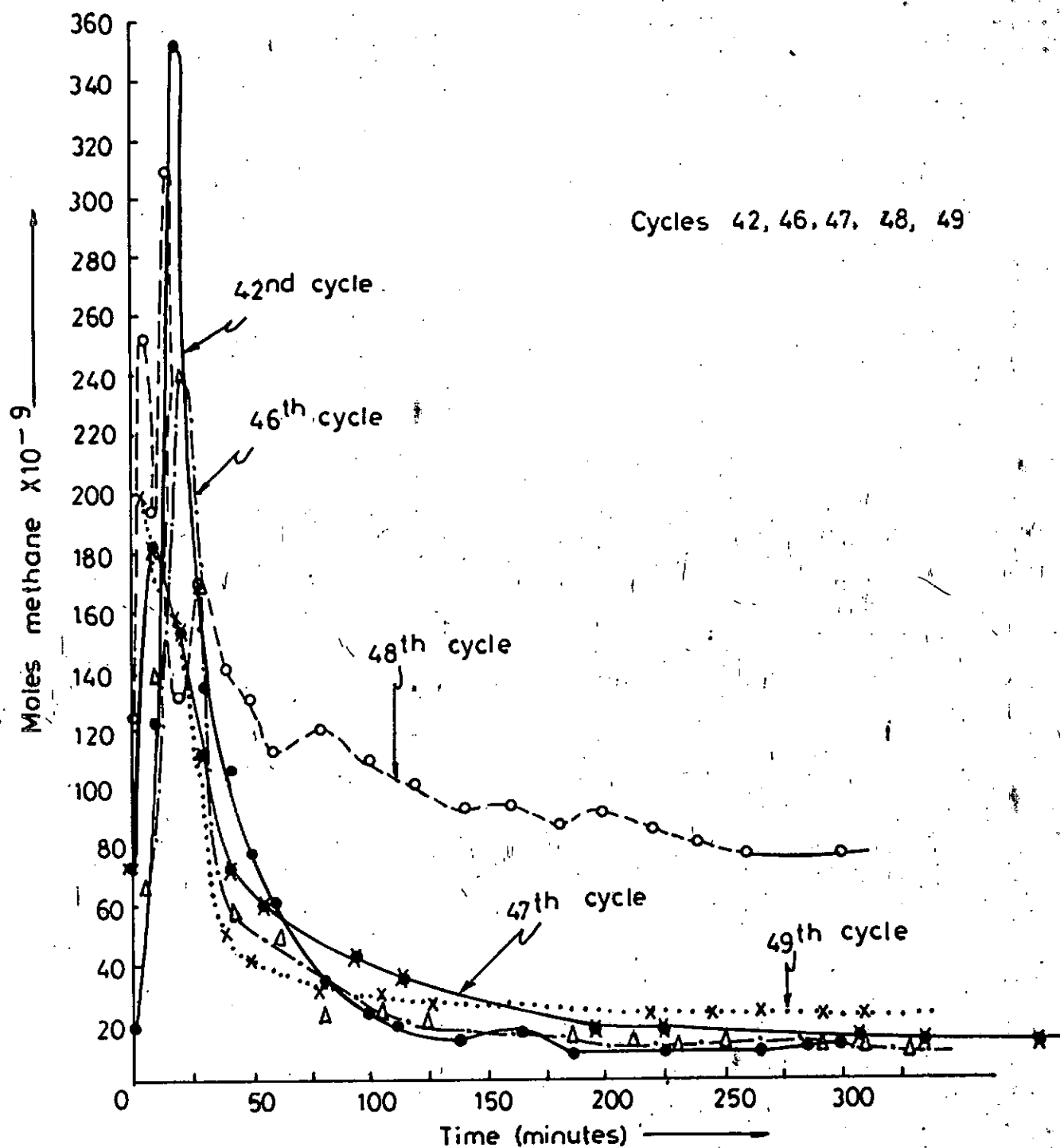FIG. 13 PLOT OF TOXIC COKE REMOVAL WITH TIME TEMPERATURE = 500°C
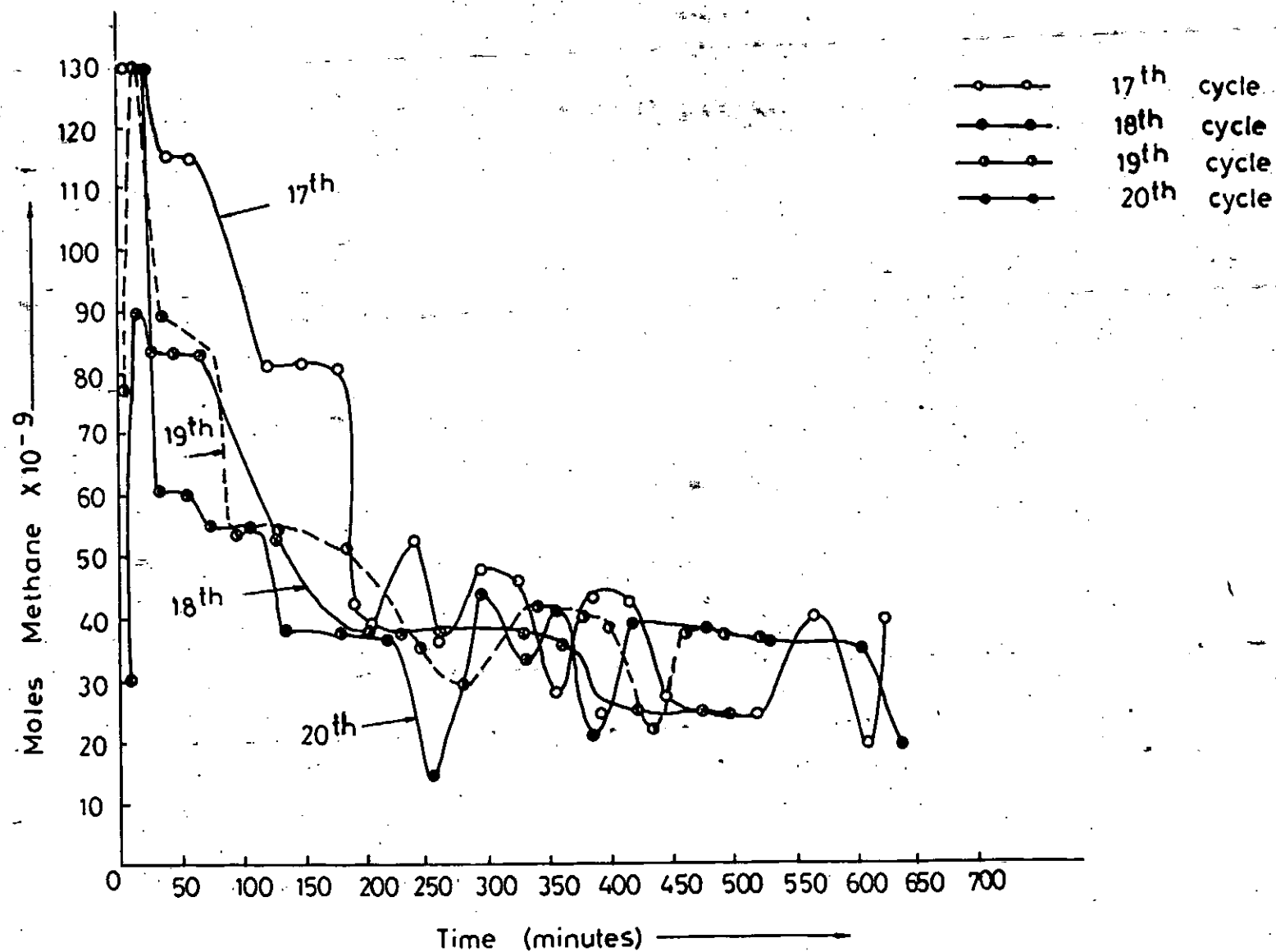
153

FIG. 14   PLOT OF TOXIC COKE REMOVAL VS TIME

154

FIG. 15 PLOT OF TOXIC COKE REMOVAL WITH TEMPERATURE = 500° C

Legend:
- 17th cycle
- 18th cycle
- 19th cycle
- 20th cycle

X-axis: Time (minutes)
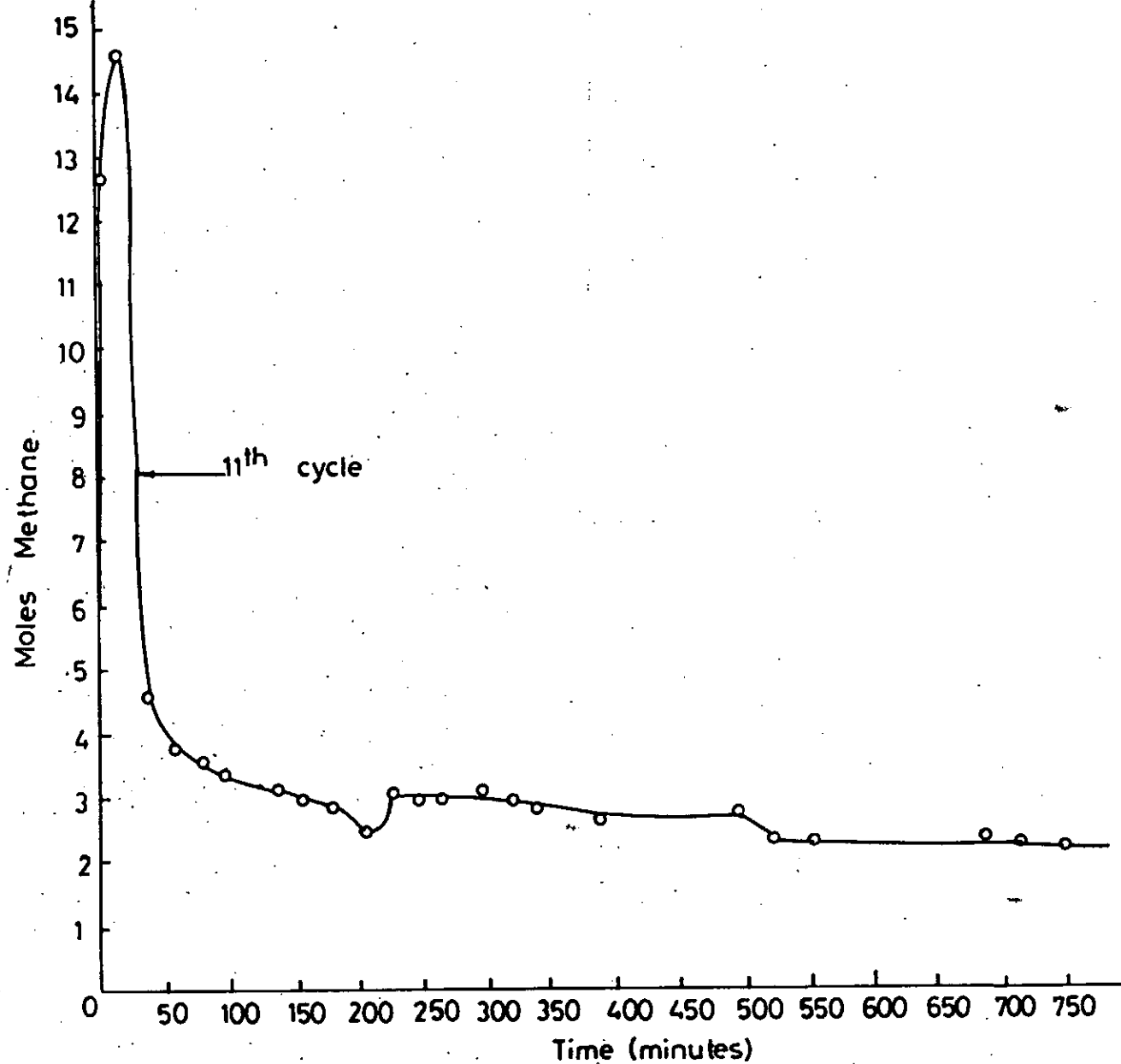Y-axis: Moles Methane $\times 10^{-9}$

155

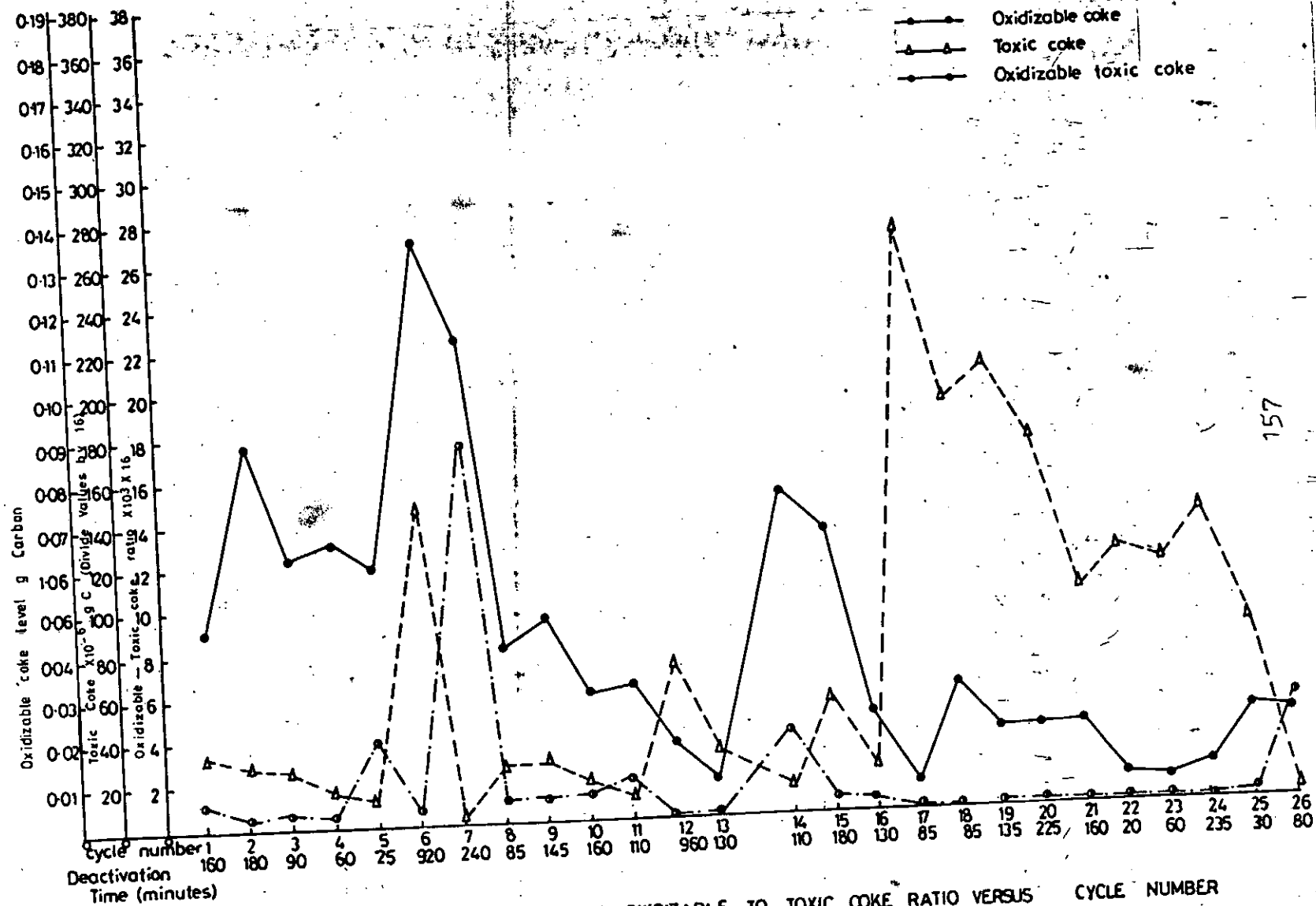FIG. 16   PLOT OF TOXIC COKE REMOVAL WITH TIME

156

FIG. 17a PLOTS OF OXIDIZABLE COKE, TOXIC COKE, OXIDIZABLE TO TOXIC COKE RATIO VERSUS CYCLE NUMBER

FIG. 17^b

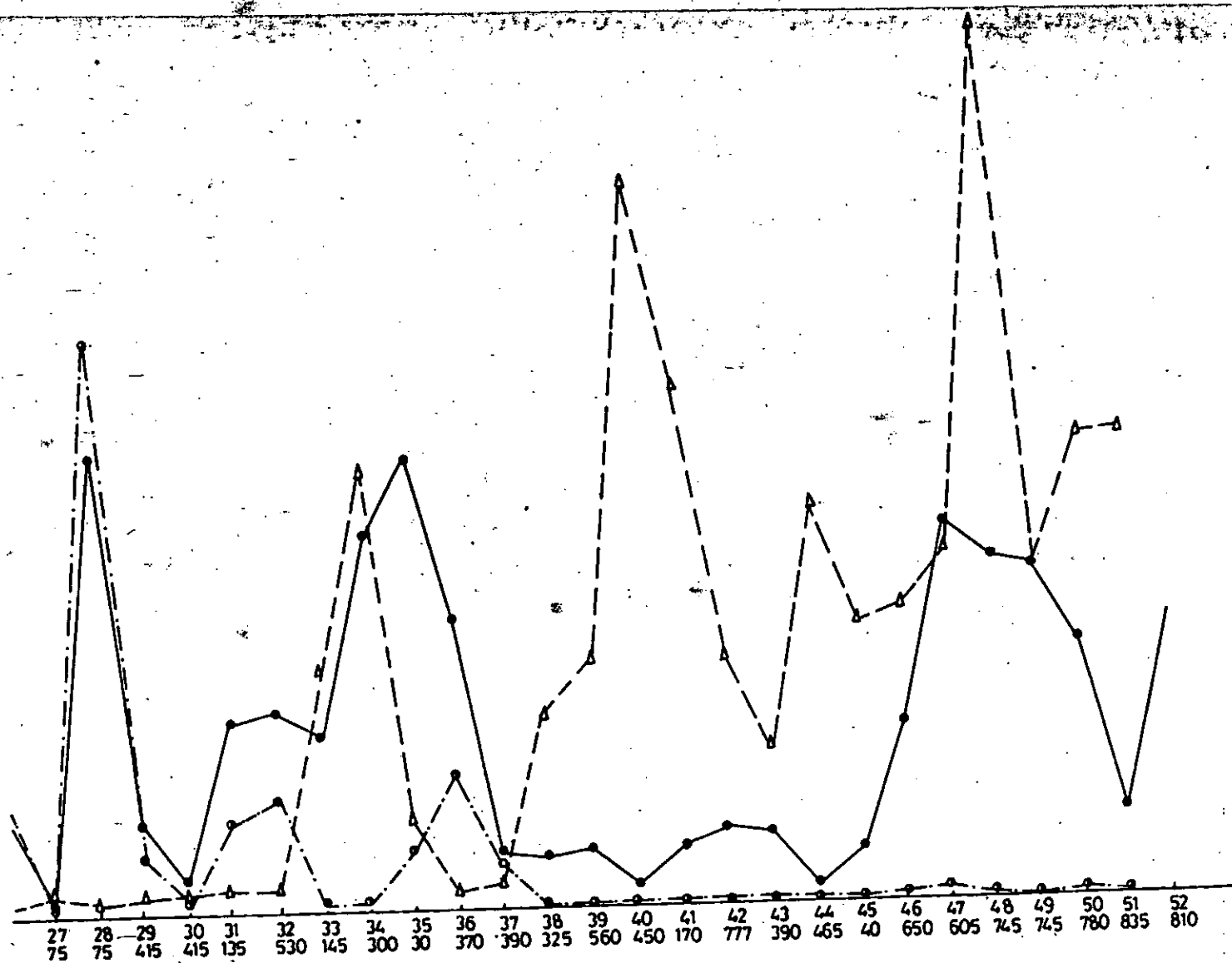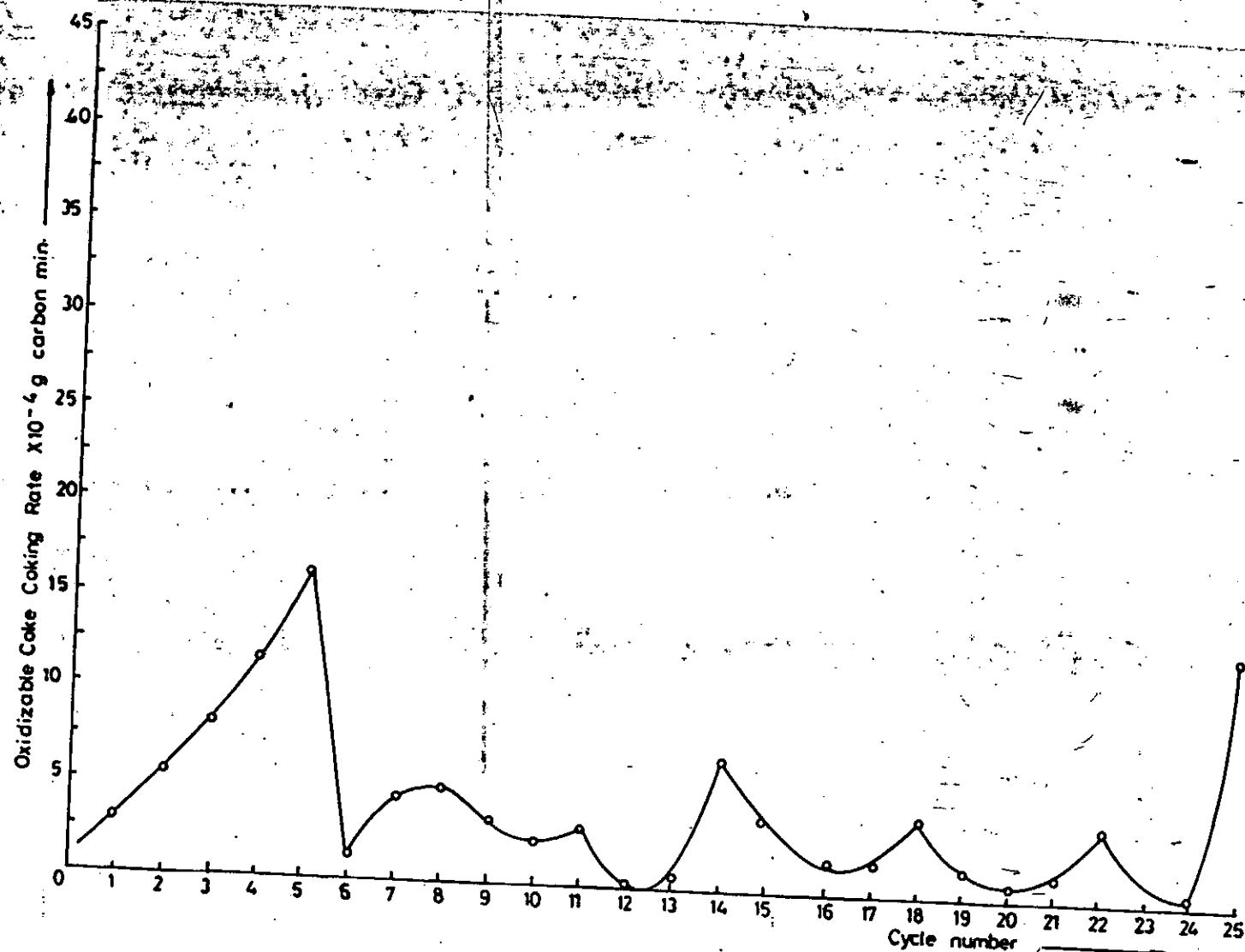FIG. 18a   PLOT OF COKING RATE VS CYCLE NUMBER
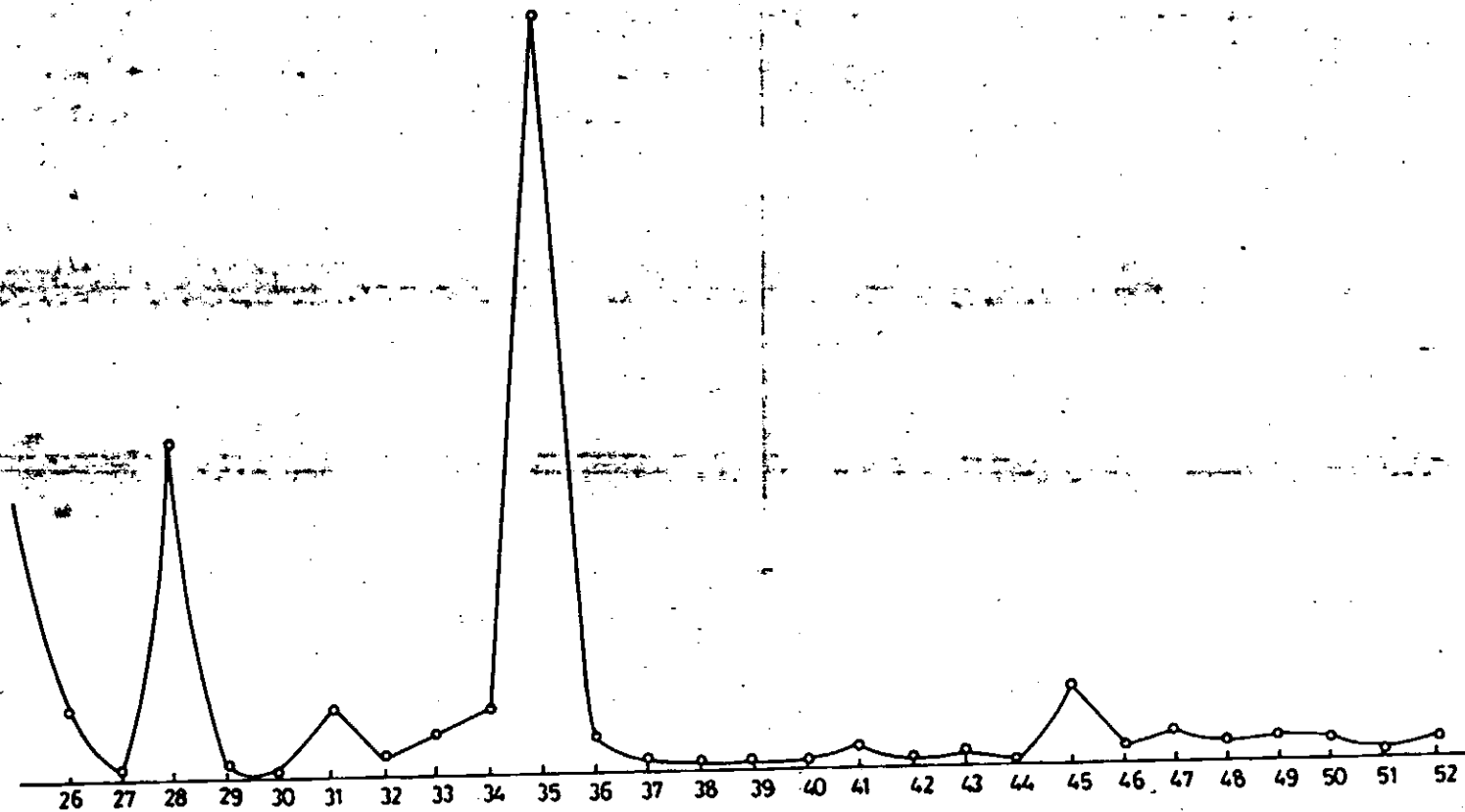
FIG. 18^b

For 31 Cycles

Run	Deactivation Time
1	620
2	420

Flow Rate : 200ml/min
5g Pt /Al$_2$O$_3$, Saturation Temp· 39°C
Temperature 430°C
Gas N$_2$

2nd Cycle

1st Cycle

Conversion

Time (min)
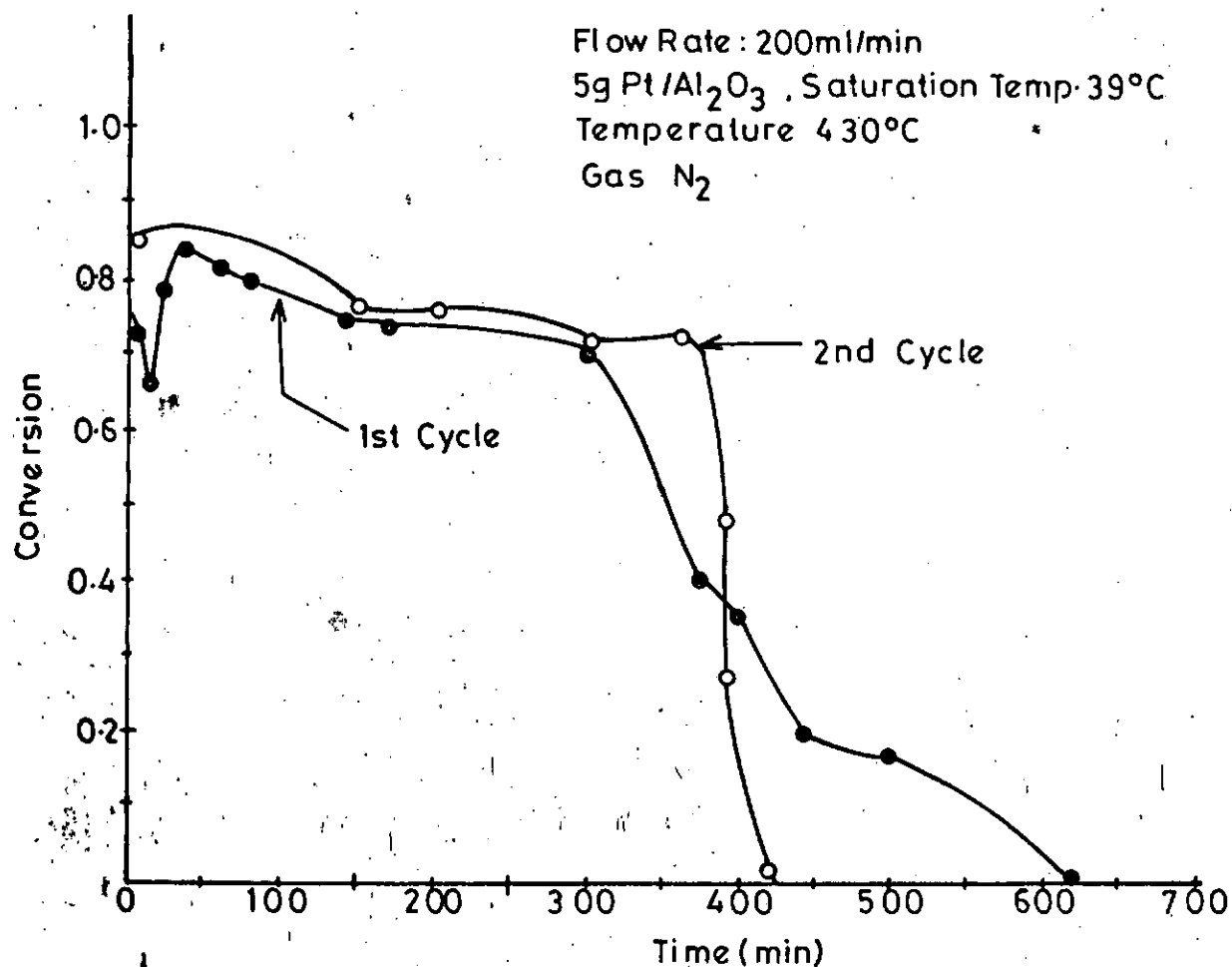
Benzene Conversion Profiles
Fig:19 (Dilution Of Regenerating Gas With N$_2$
For All 31 Runs)

161

Benzene Conversion Profiles
Fig:20 (Dilution Of Regenerating Gas With N₂)

162

Run	Deactivation Time
5	390
6	660
9	810
15	550

Fig:21 Benzene Conversion Profiles

Fig:22 Benzene Conversion Profiles
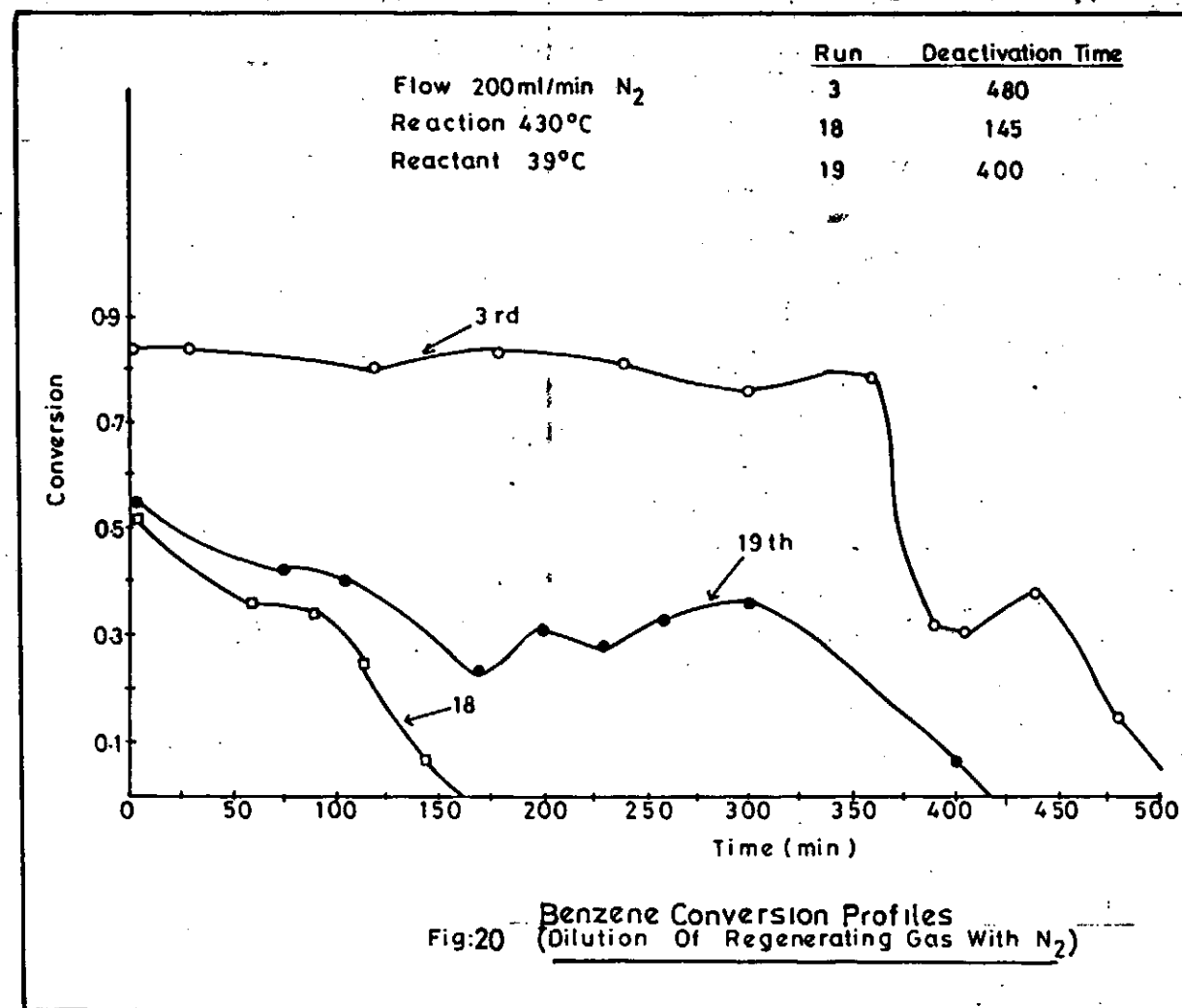
Fig:23 Benzene Conversion Profiles

Fig:24 Benzene Conversion Profiles

Run	Deactivation Time
11	400
12	480
13	365
14	320

11th Cycle

12th Cycle

14th Cycle

13th Cycle

Conversion

Time (min)

166
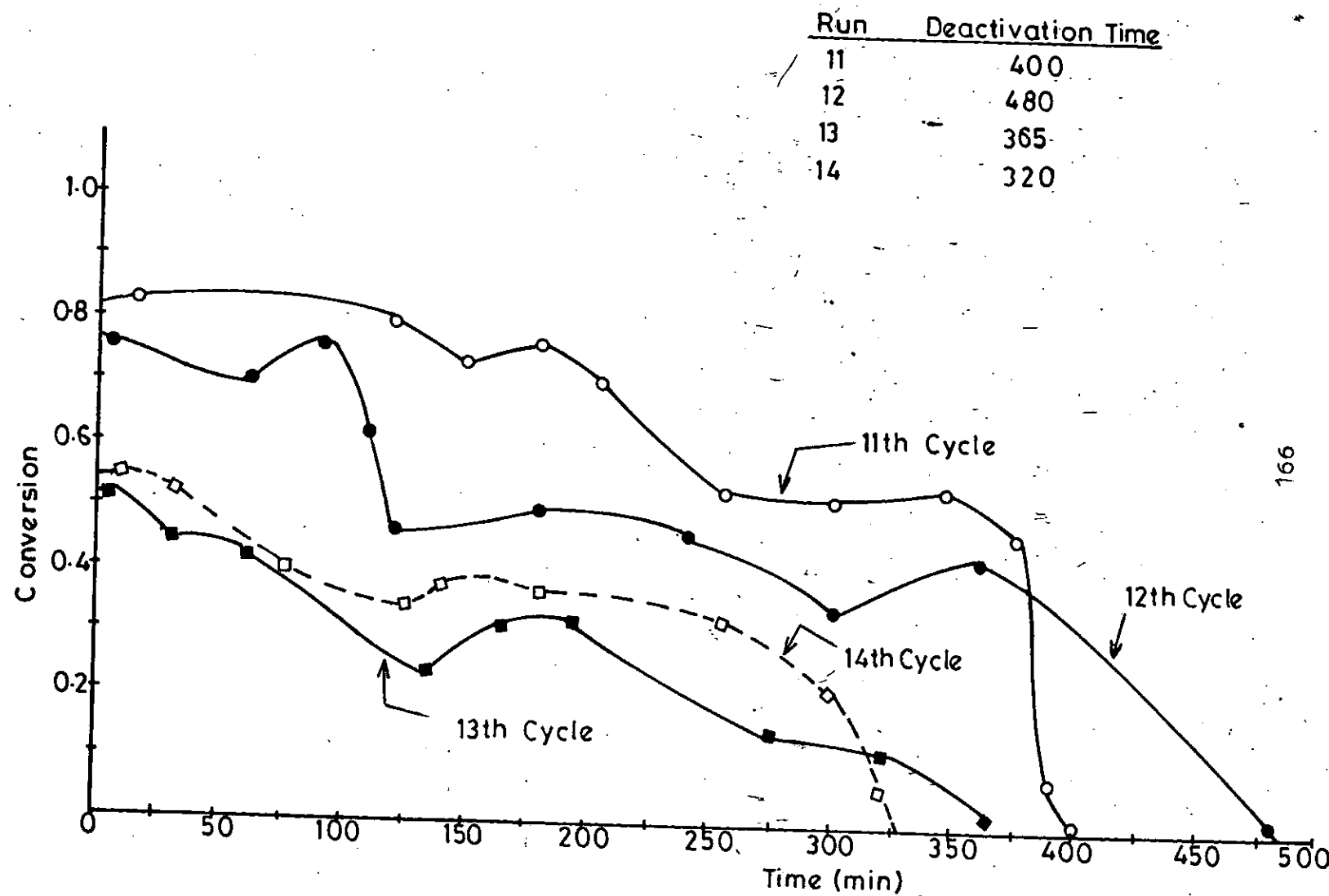
Fig:25 Benzene Conversion Profiles

Fig:26 Benzene Conversion Profiles

Run	Deactivation Time
23	120
24	160
25	130

168

Fig:27 Benzene Conversion Profiles

Run	Deactivation Time
26	120
27	235
28	100

27th Cycle
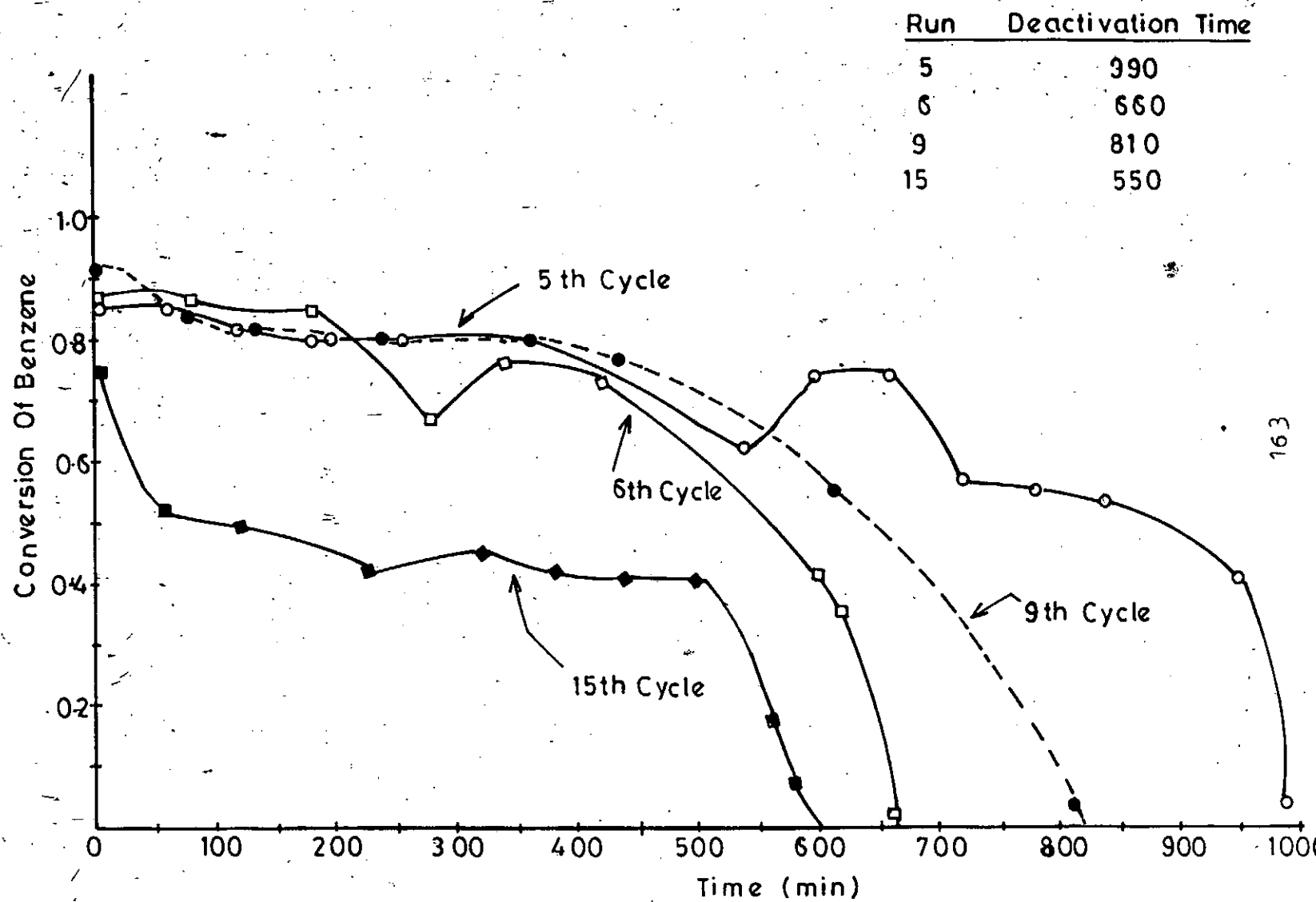
28th Cycle
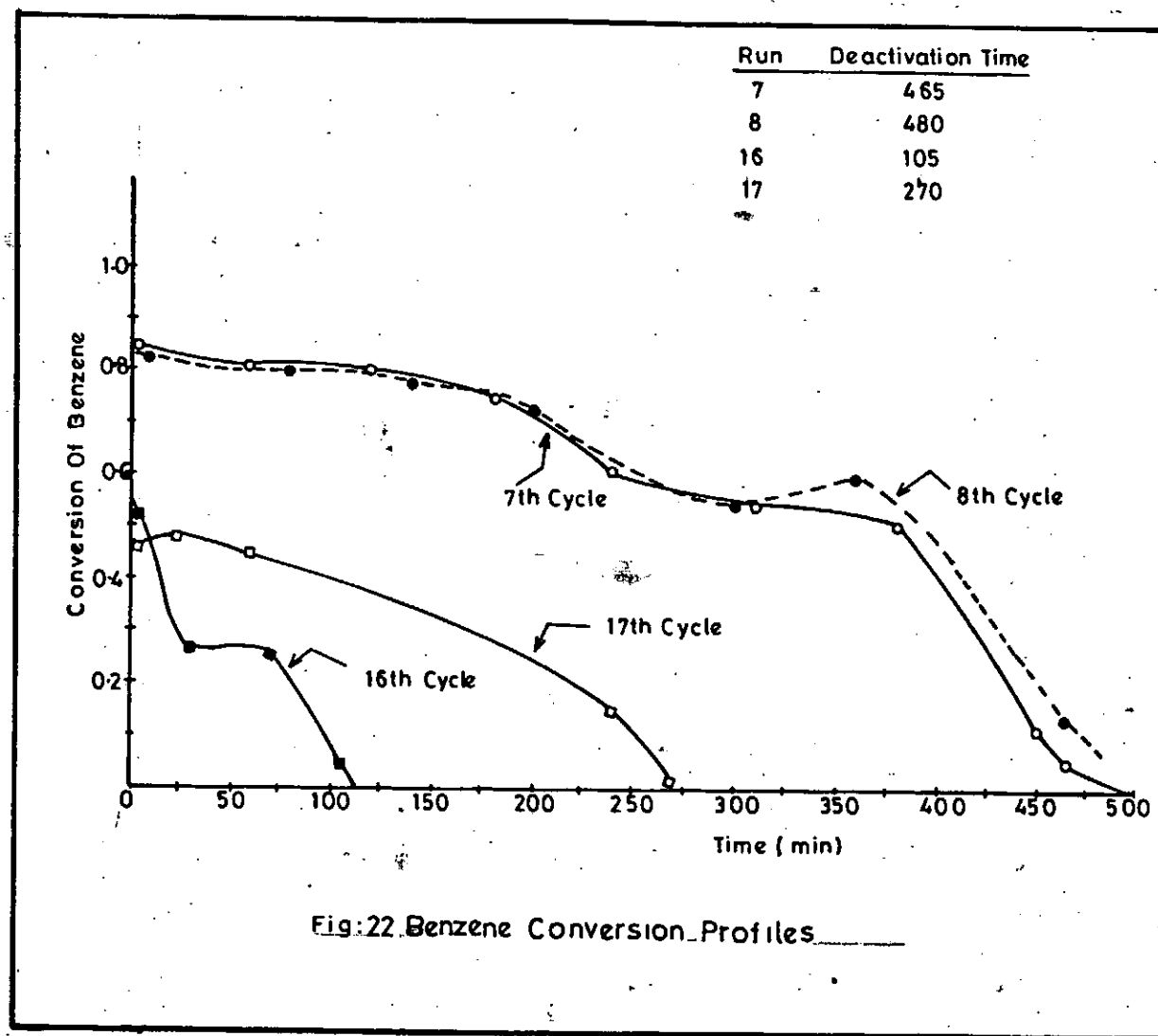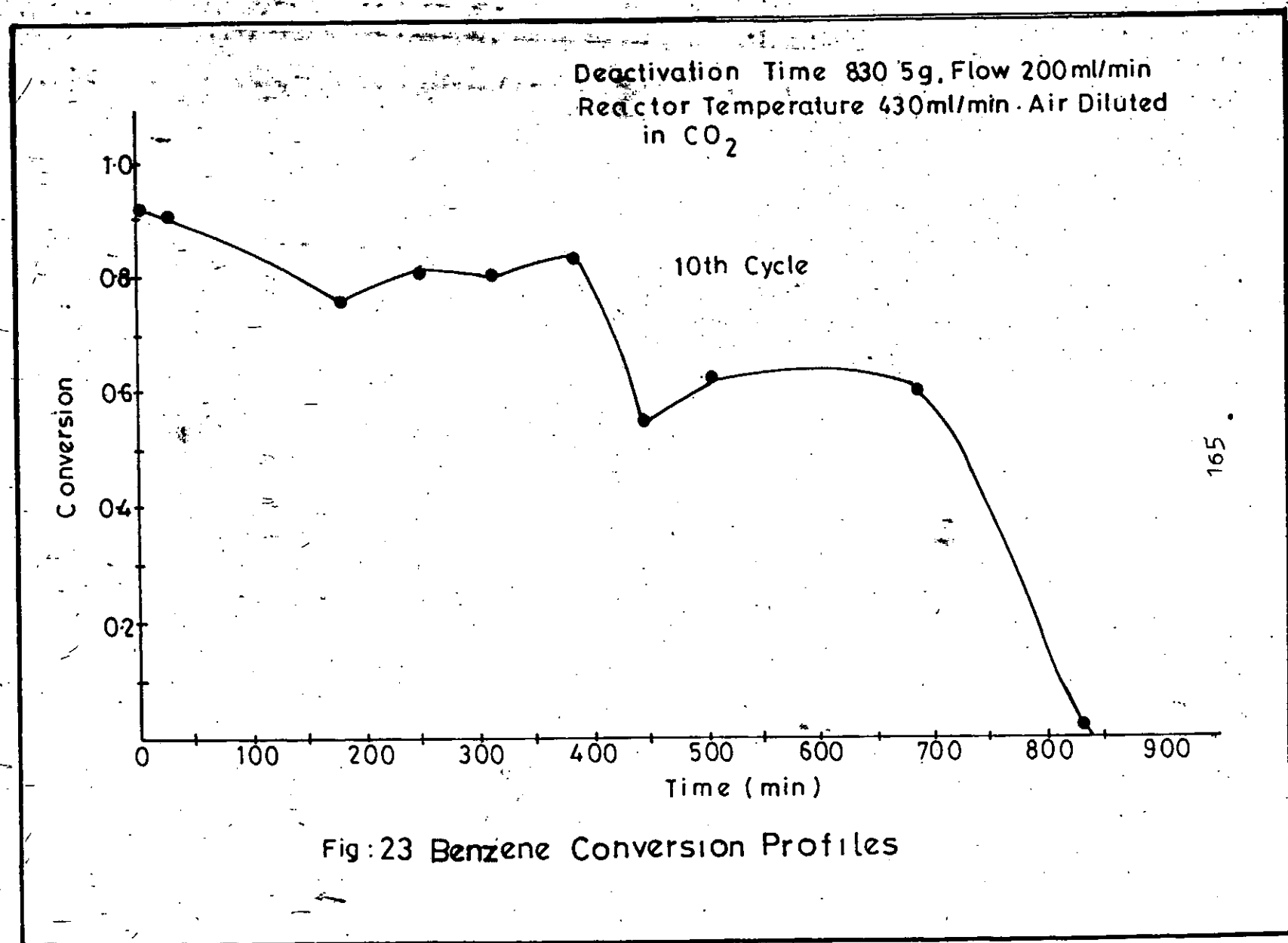
26th Cycle

Conversion Of Benzene

Time (min)

169

Fig:28 Benzene Conversion Profiles

Fig.29 Benzene Conversion Profiles
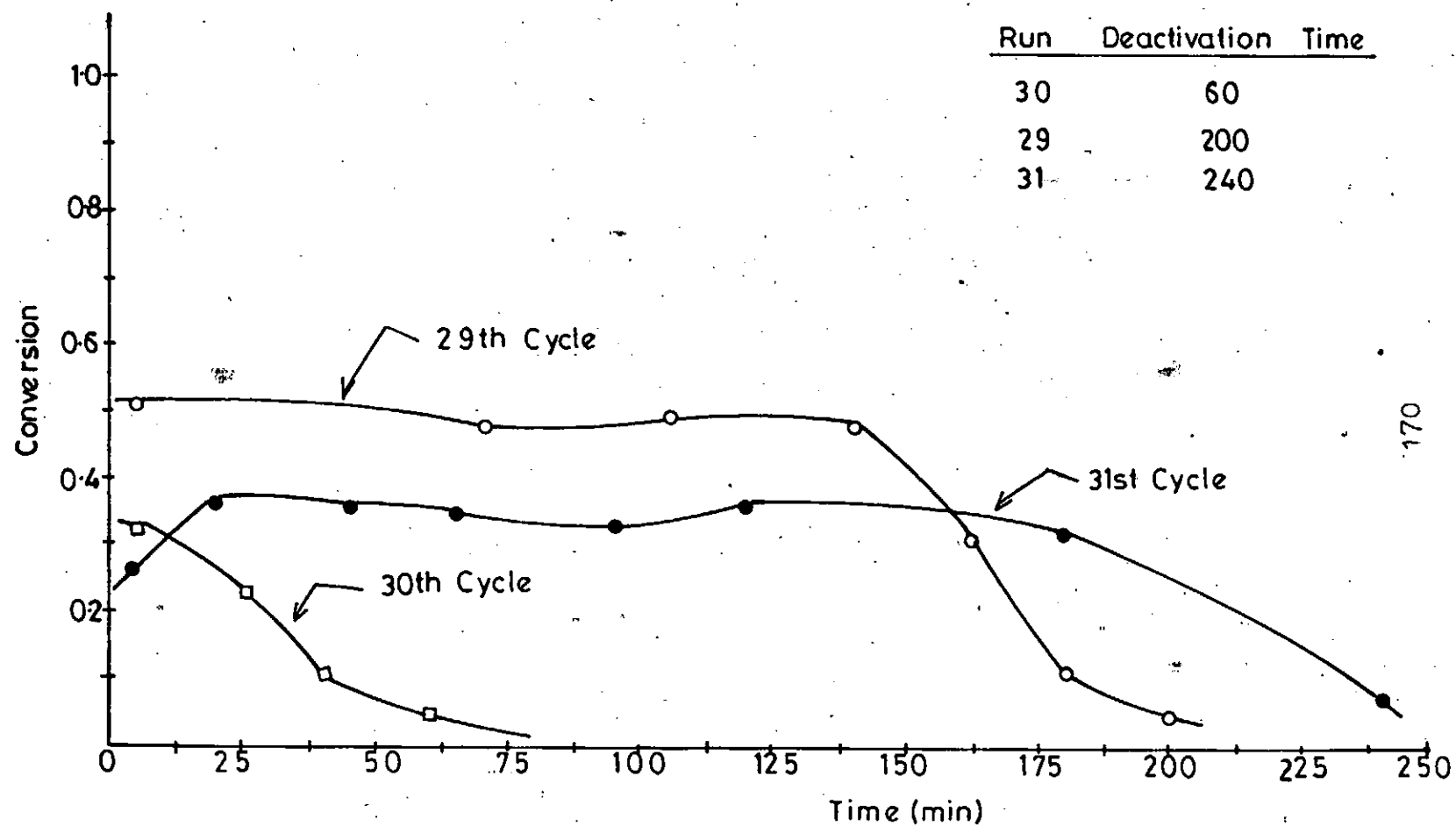
Fig:30 Benzene Conversion Profiles
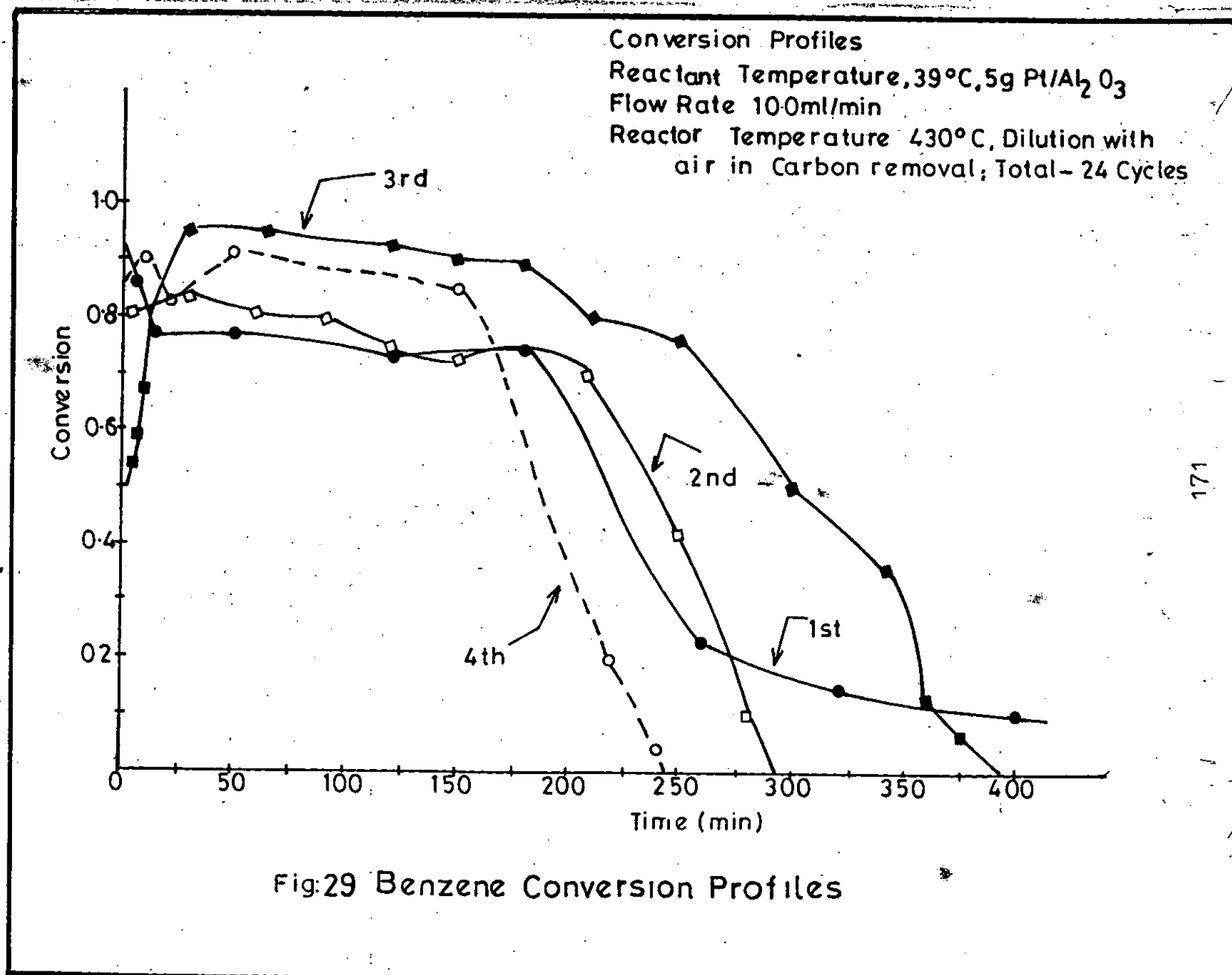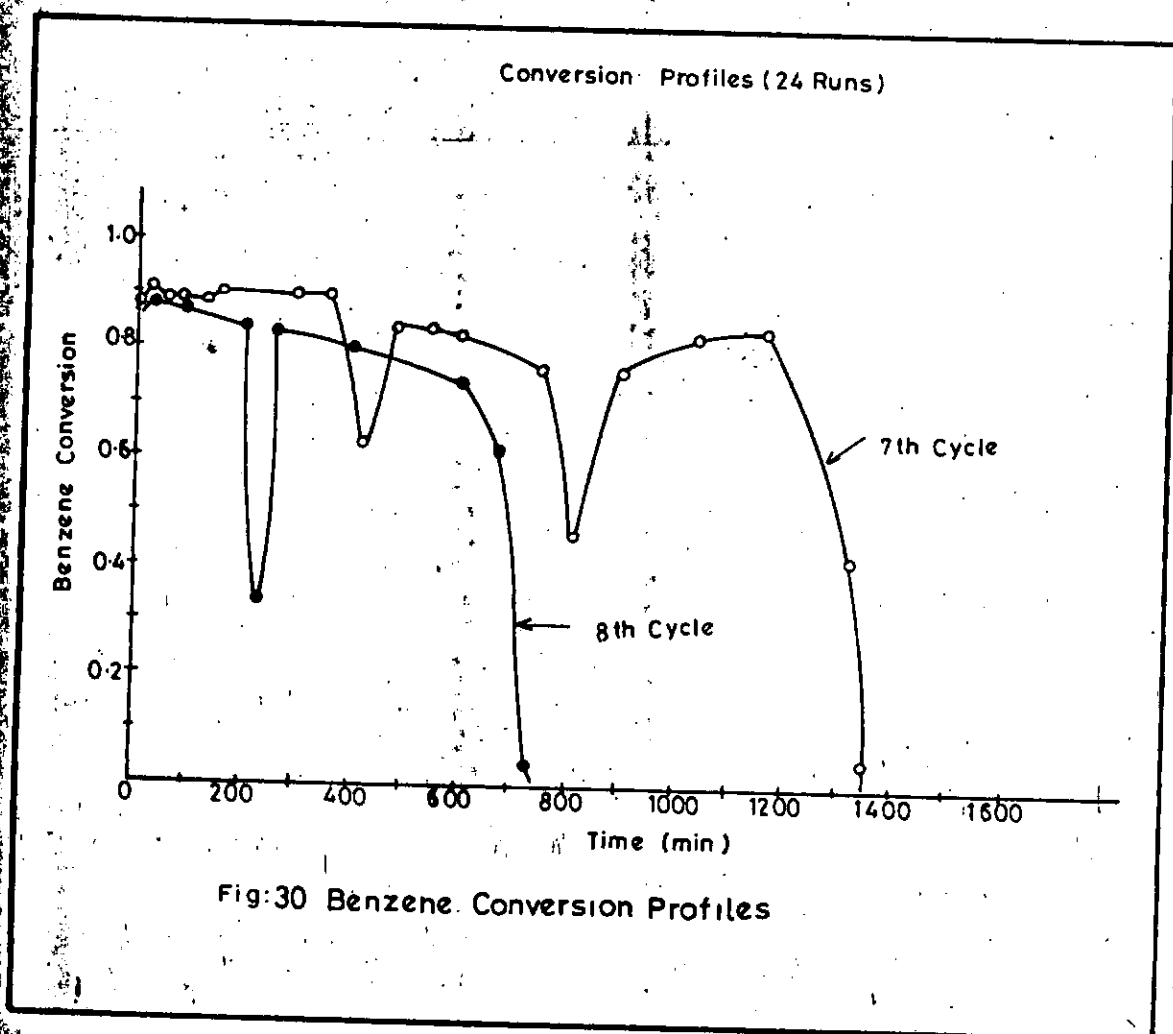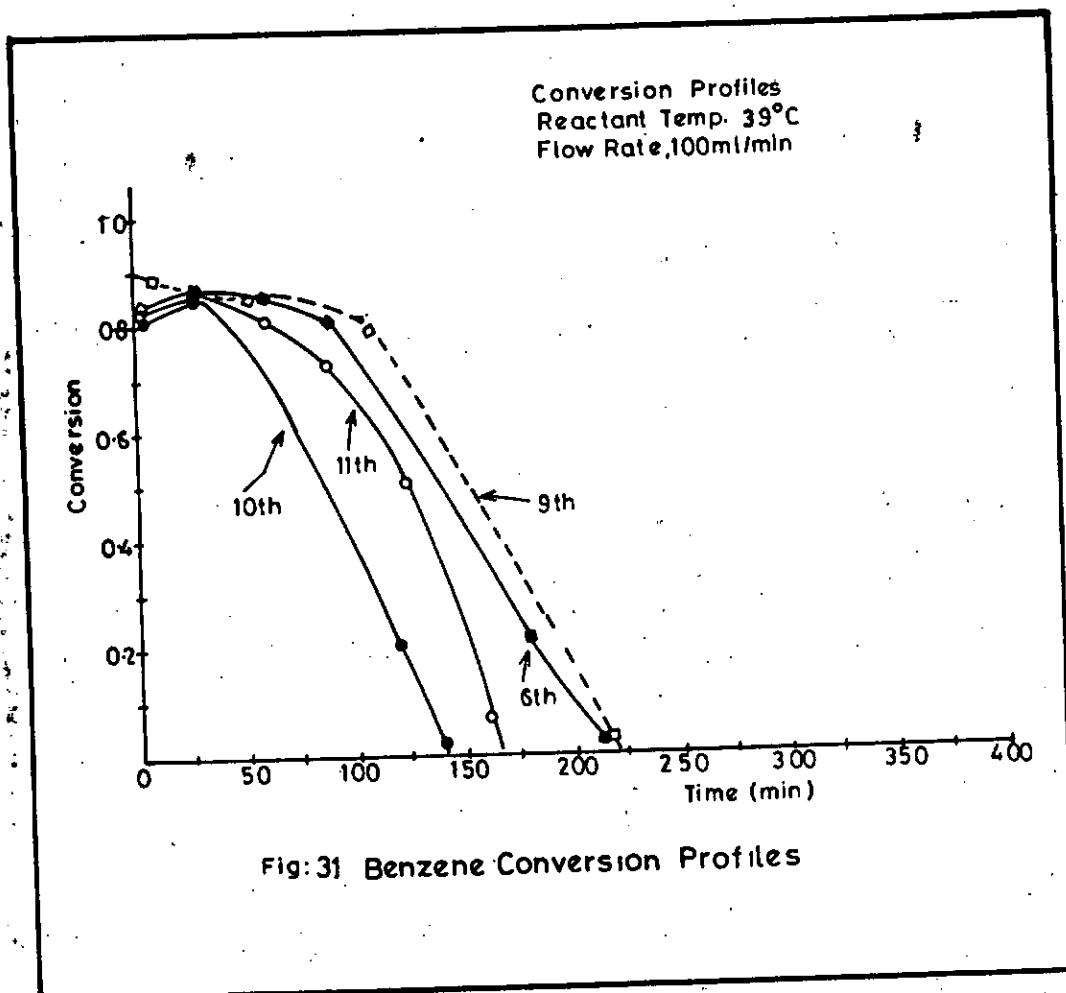
Conversion Profiles
Reactant Temp. 39°C
Flow Rate,100ml/min

Fig:31 Benzene Conversion Profiles

173

Fig:32 Benzene Conversion Profiles

174

Conversion Profiles
Reactant Temperature 39 °C , Reactor Temp. 430°C
Flow Rate 100ml/min

Fig:33 Benzene Conversion Profiles

175
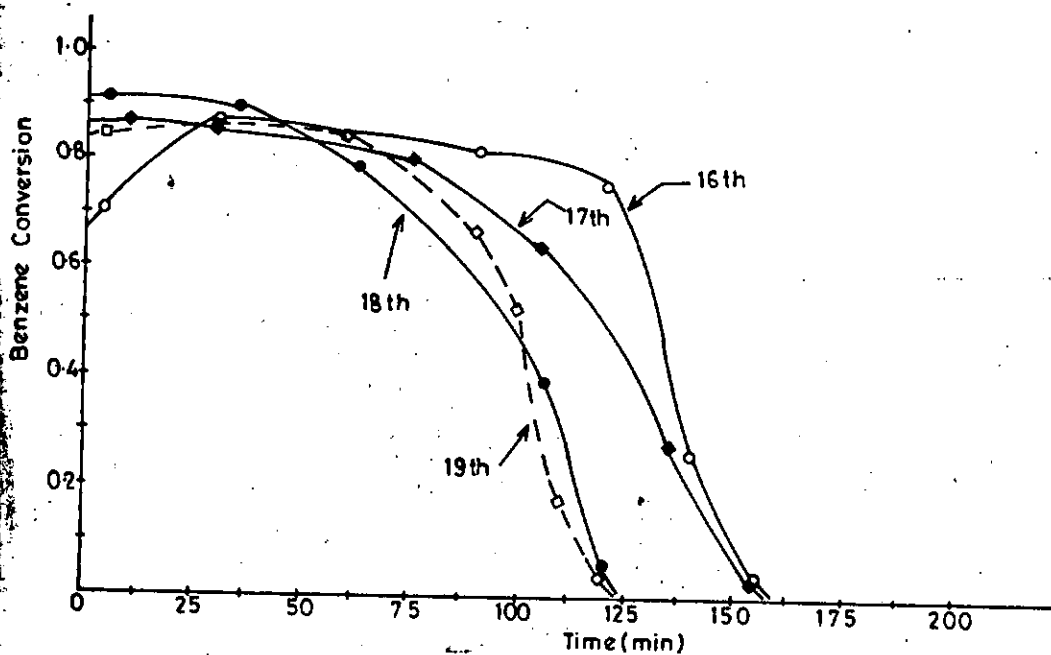
Fig:34 Benzene Conversion Profiles
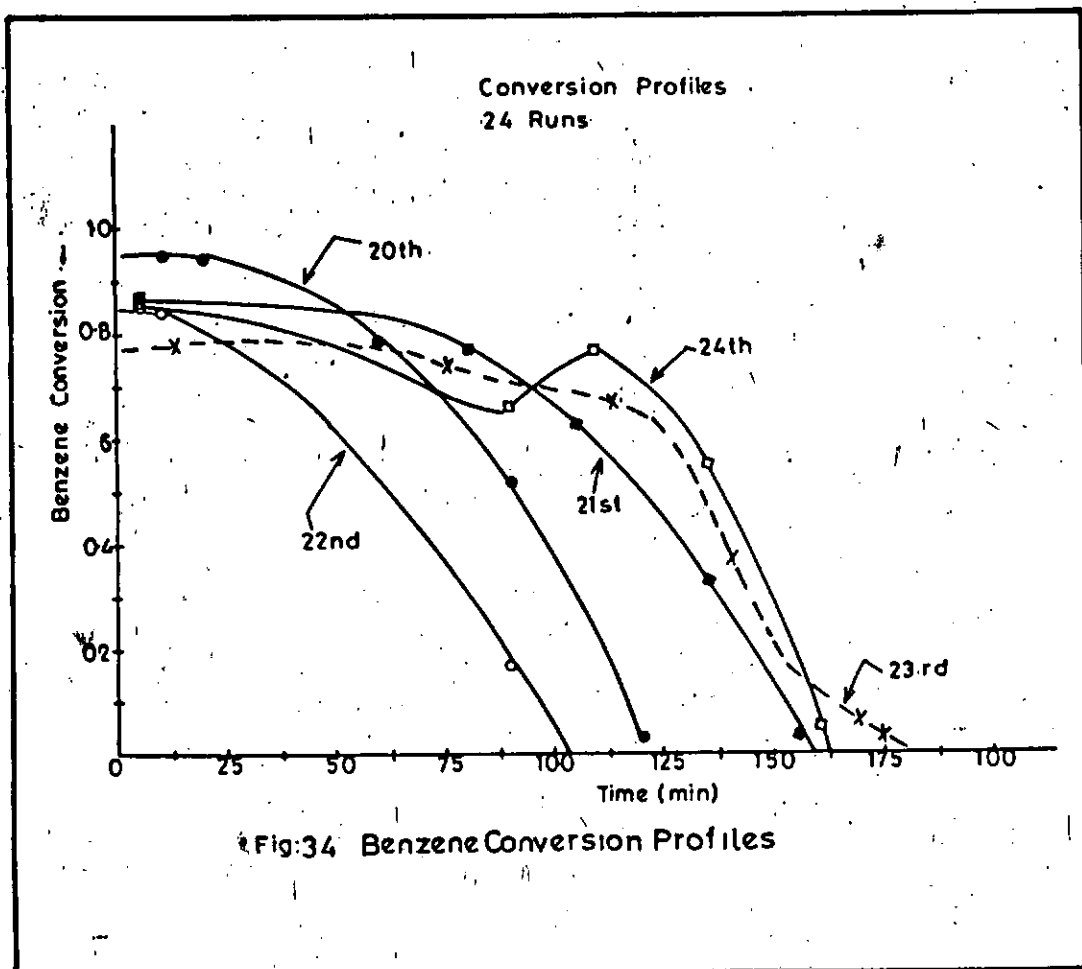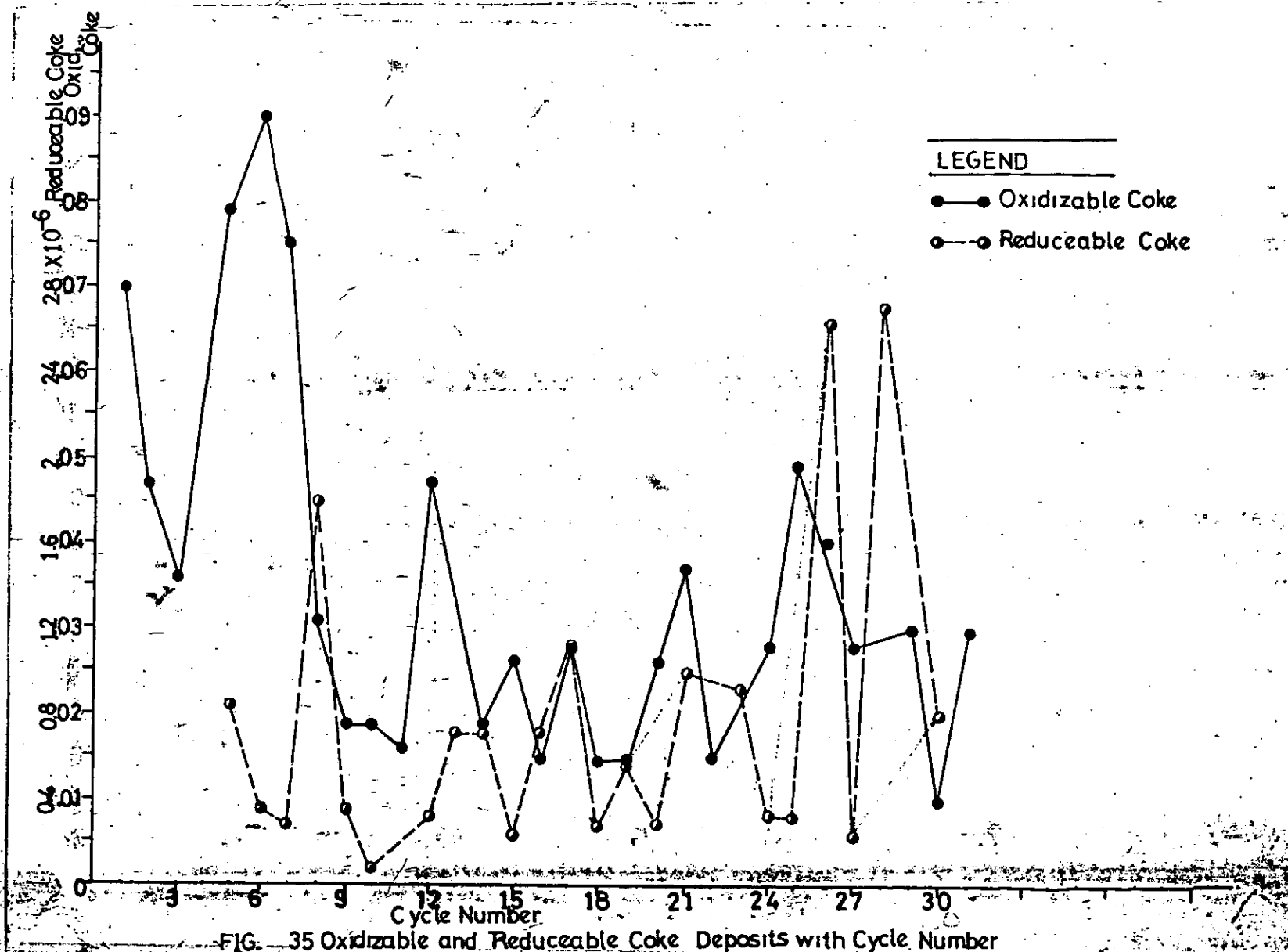
FIG. 35 Oxidizable and Reduceable Coke Deposits with Cycle Number

LEGEND
●——● Oxidizable Coke
o——o Reduceable Coke

Fig:36 Oxidizable Coke Deposits with cycle number

179
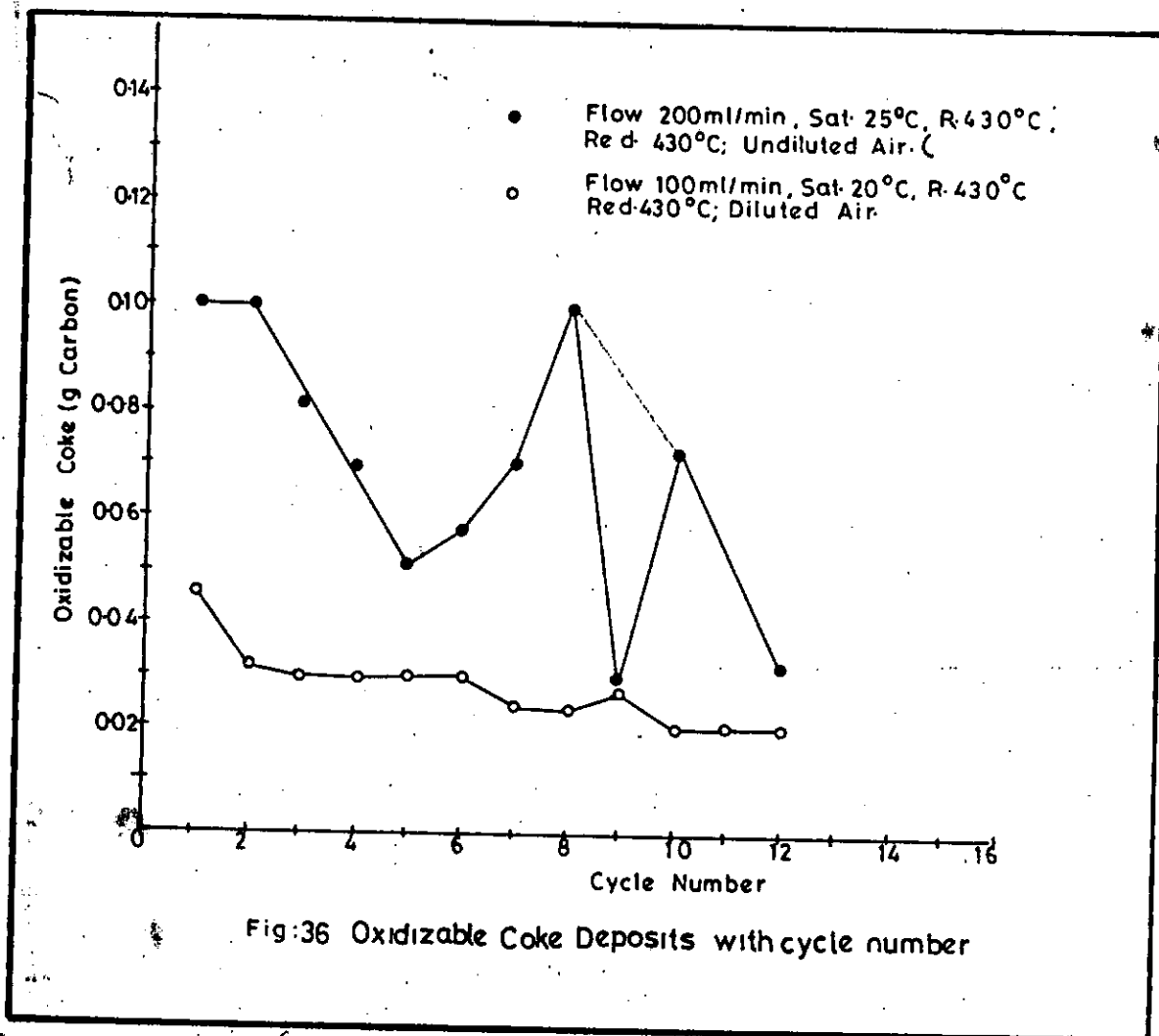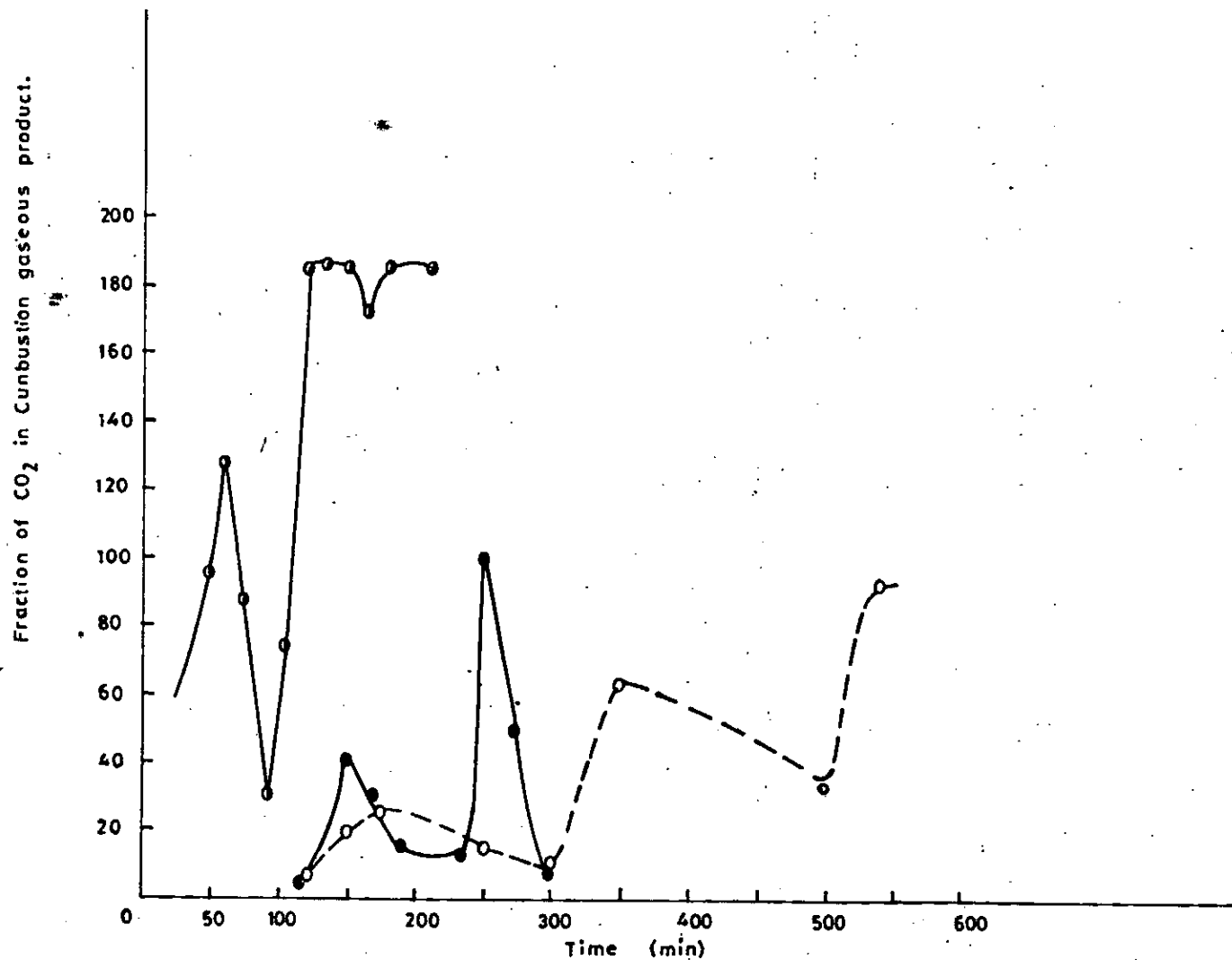
Fig.37 Oxidizable Coke structure CO$_2$ Profile during oxidation at 430°C flowrate Combustion mixture
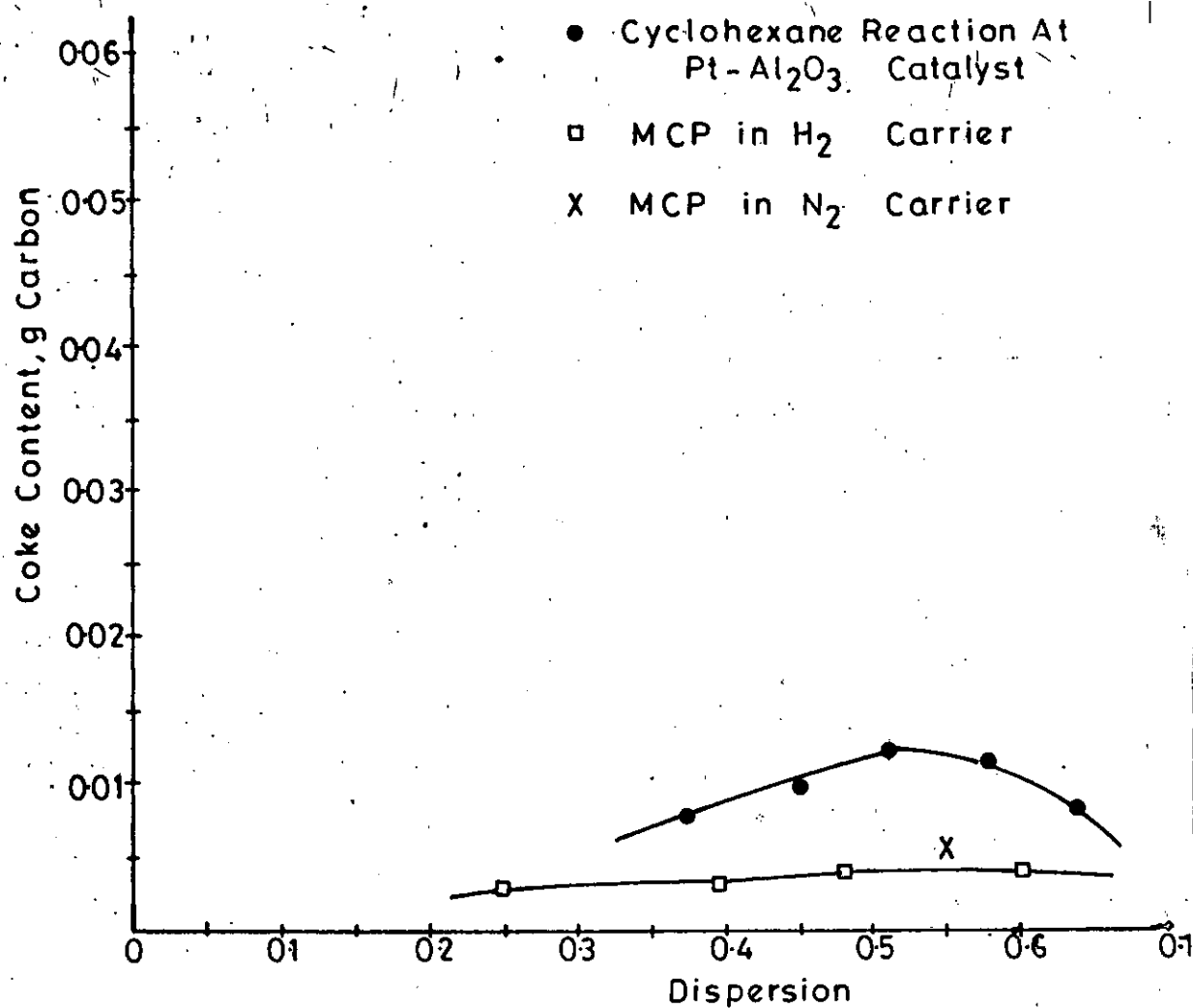
Fig: 38 Coke Content Versus Pt. Metal Dispersion
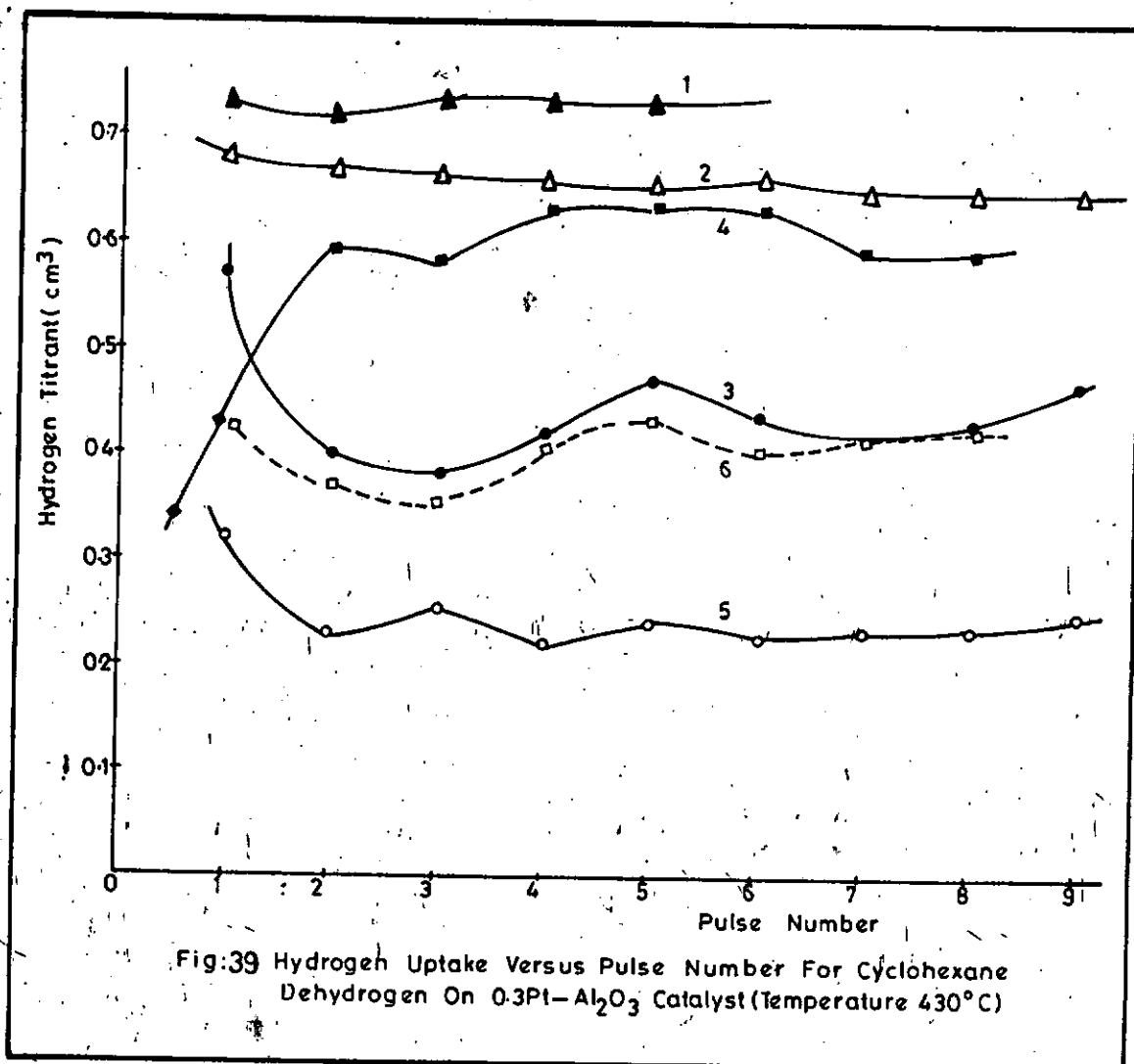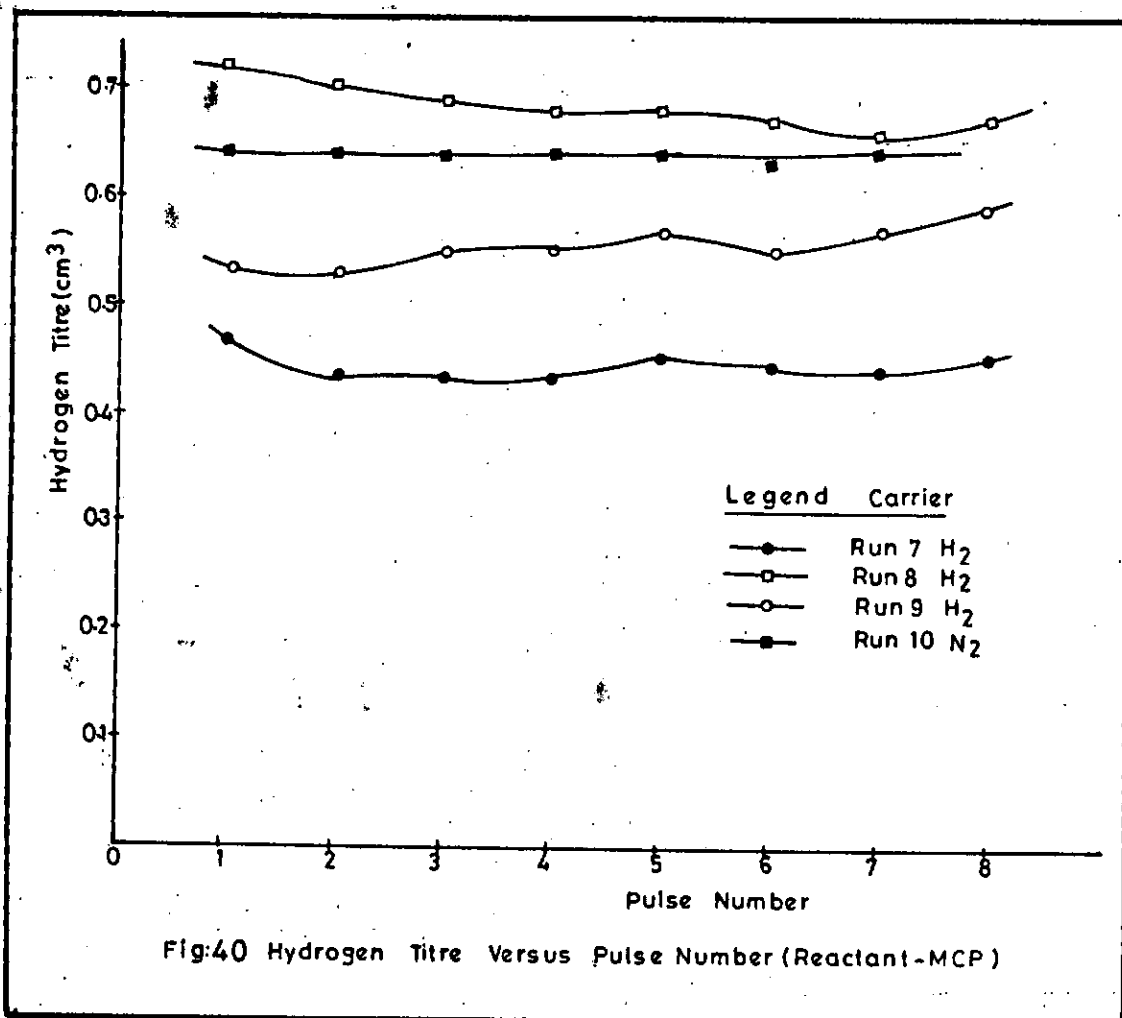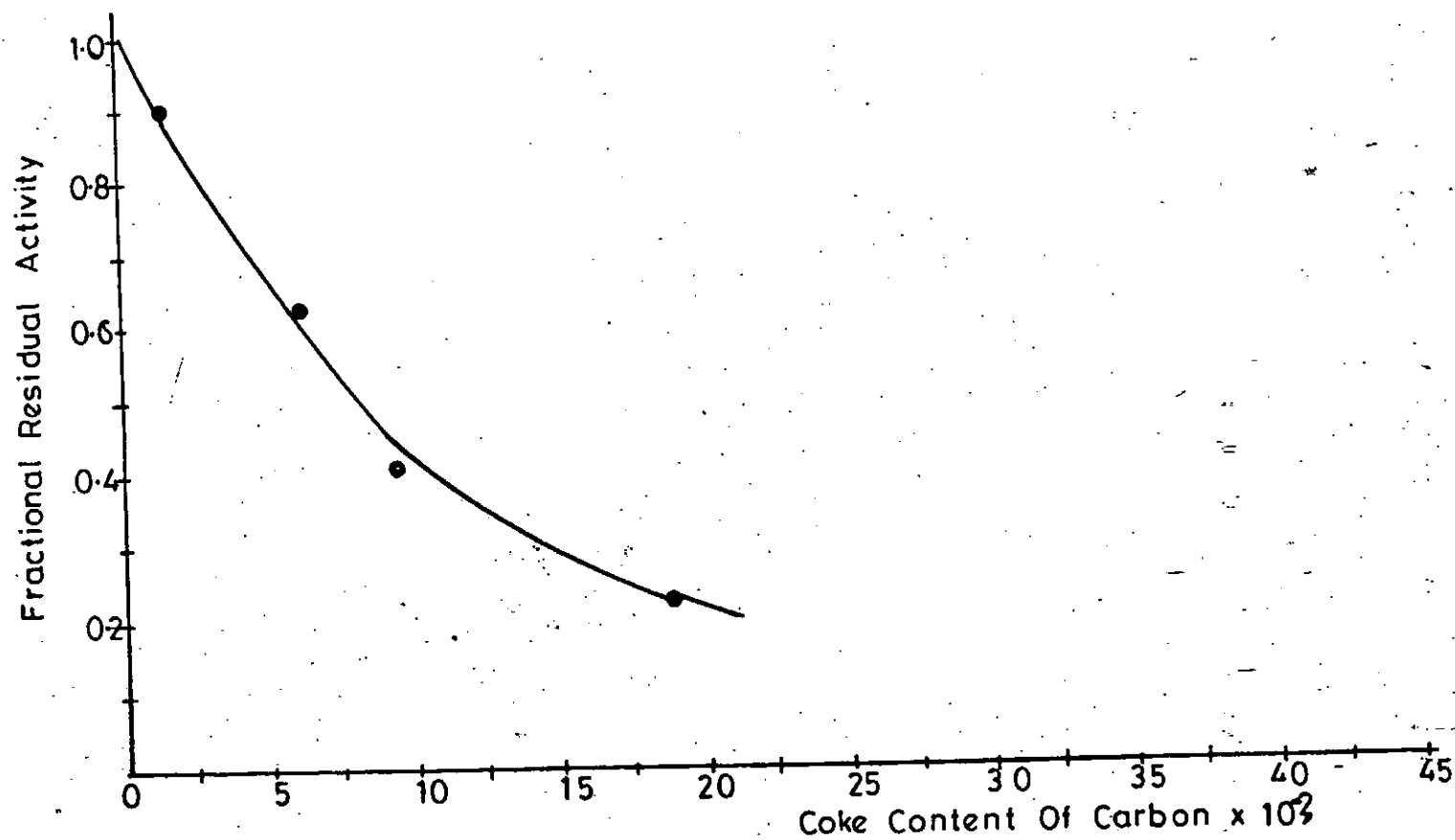
180

Fig:39 Hydrogen Uptake Versus Pulse Number For Cyclohexane Dehydrogen On $0.3Pt-Al_2O_3$ Catalyst (Temperature $430°C$)

181

Fig.40 Hydrogen Titre Versus Pulse Number (Reactant-MCP)

Fig:41 Fractional Residual activity versus Coke Content

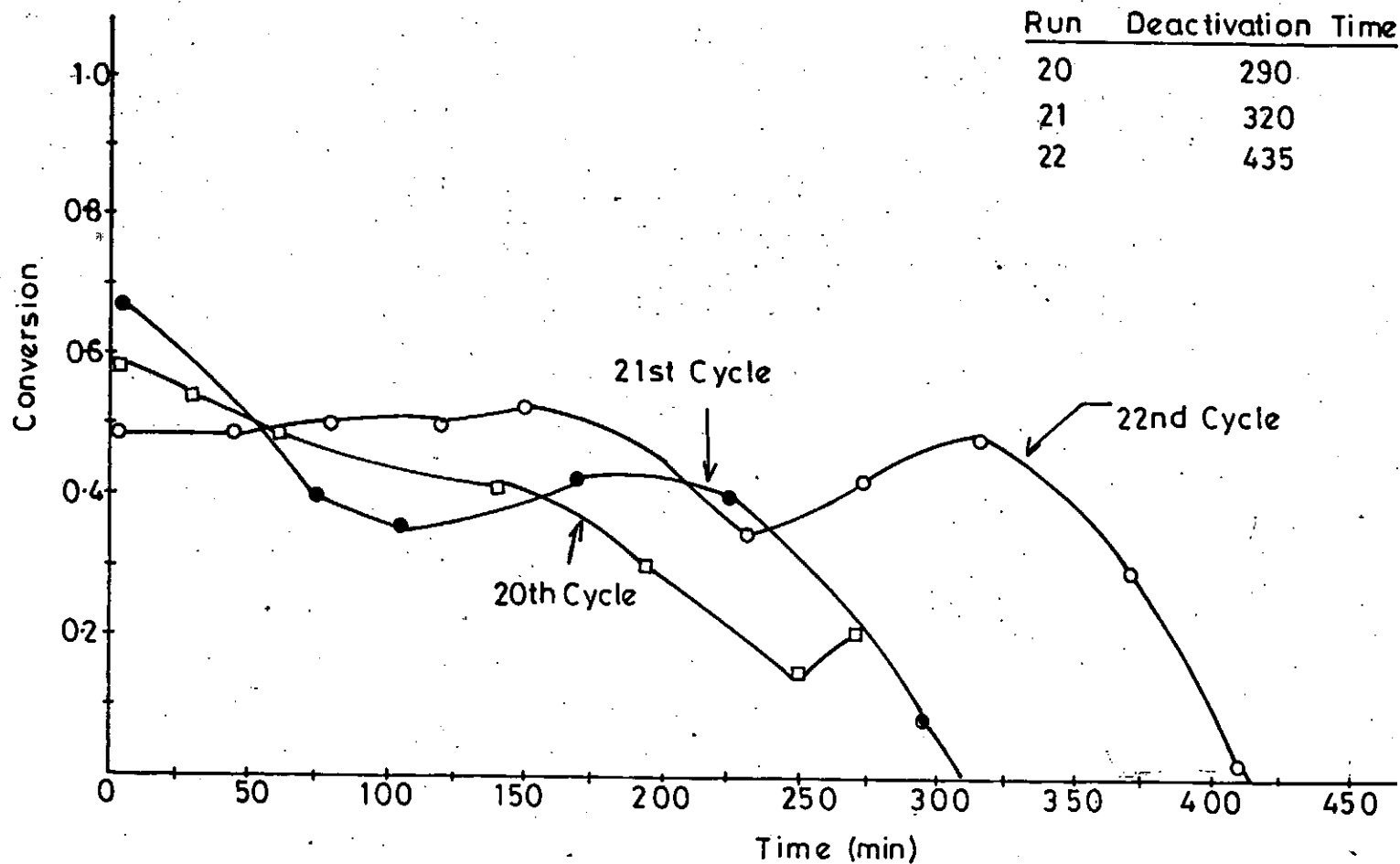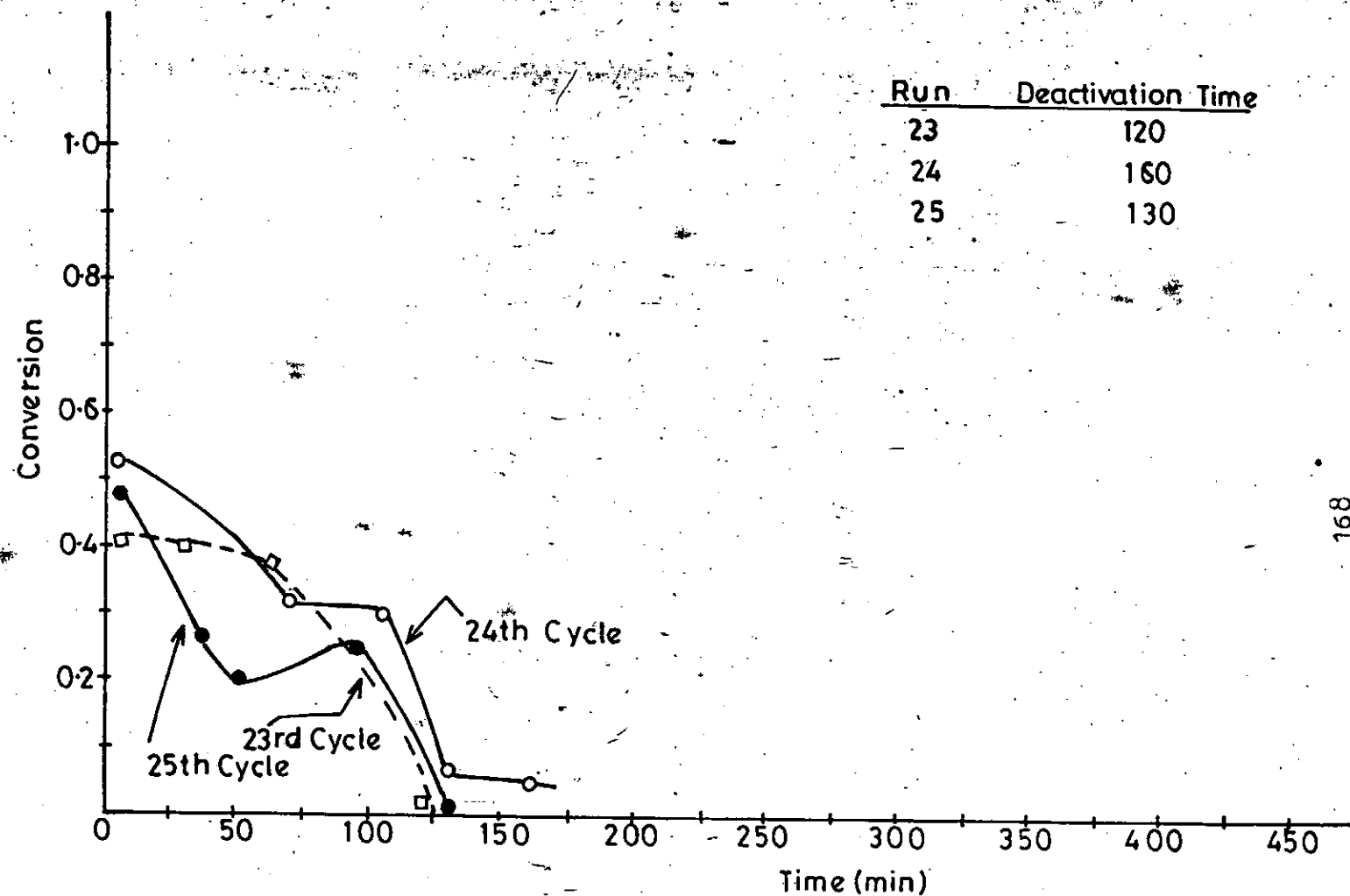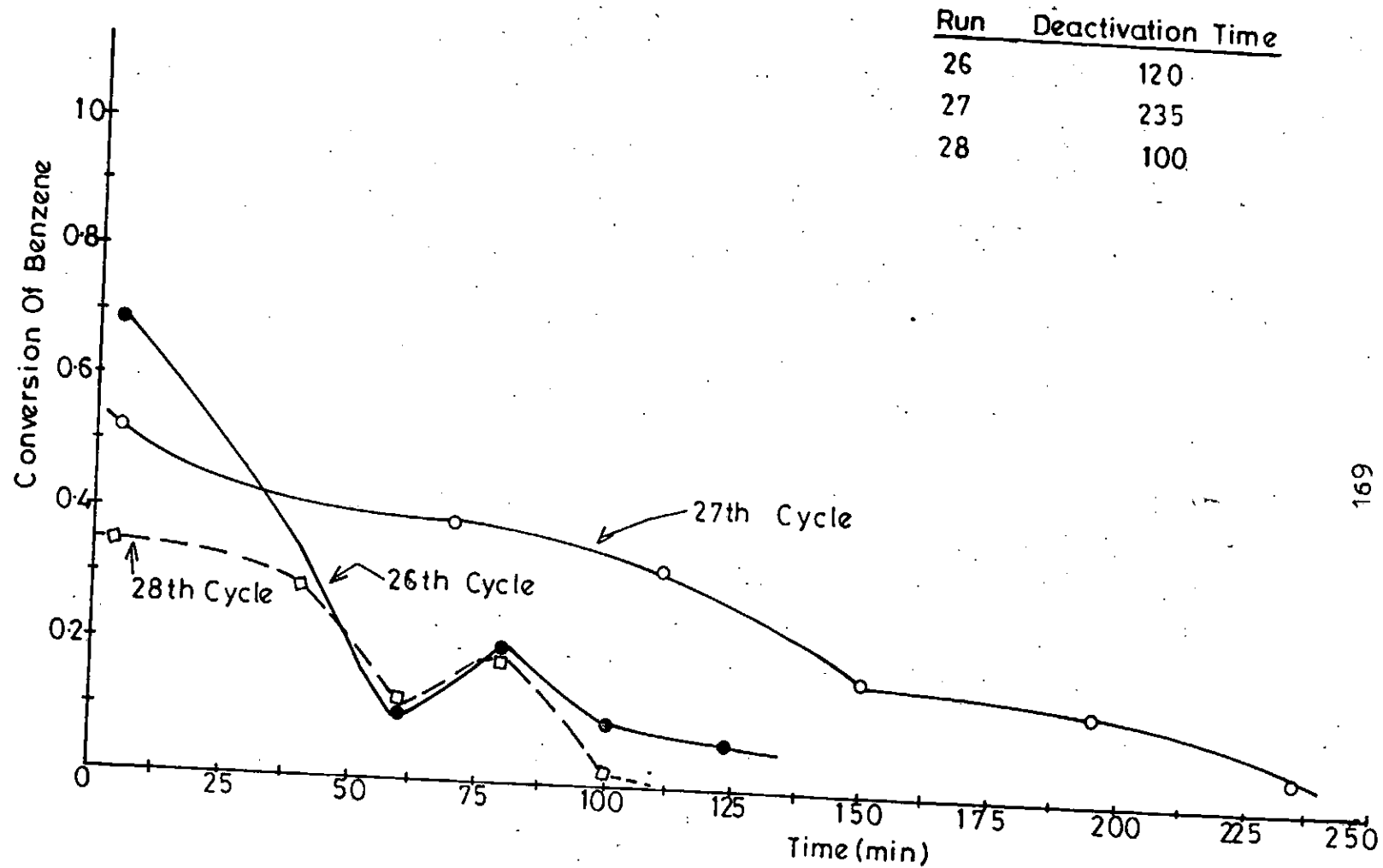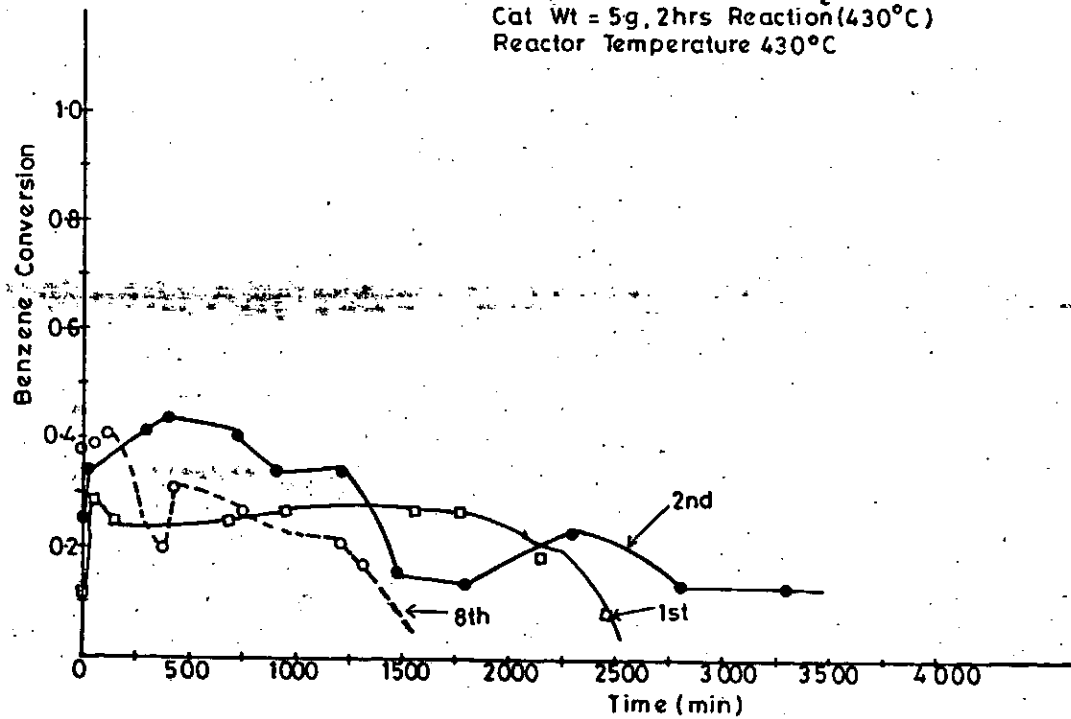Fig:42 Benzene Conversion Profiles

Fig:43 Benzene Conversion Profiles

185

LEGEND

●—●	7th	cycle
○—○	9th	,,
⊙--⊙	10th	,,
▲—▲	11th	,,
✕--✕	12th	,,
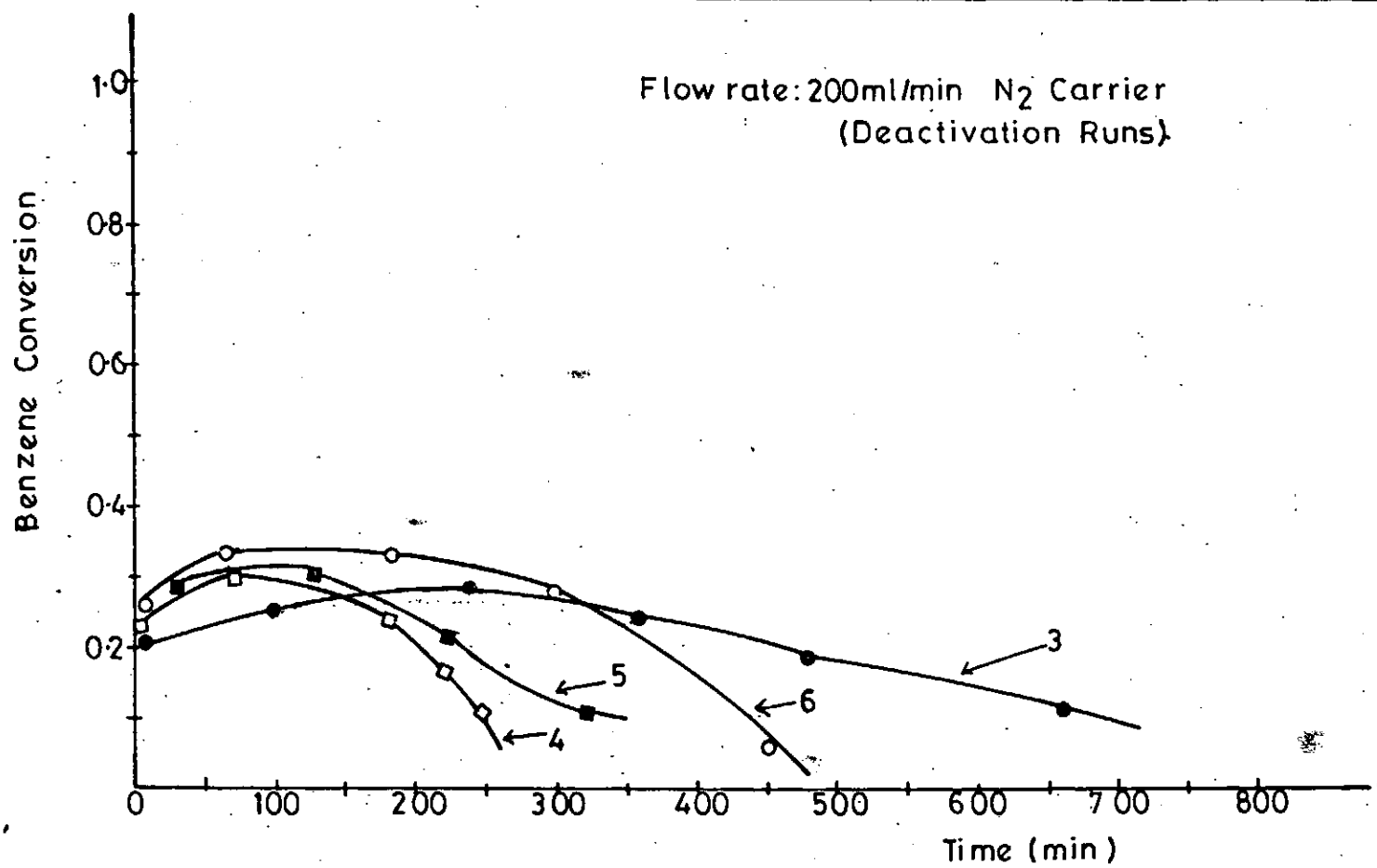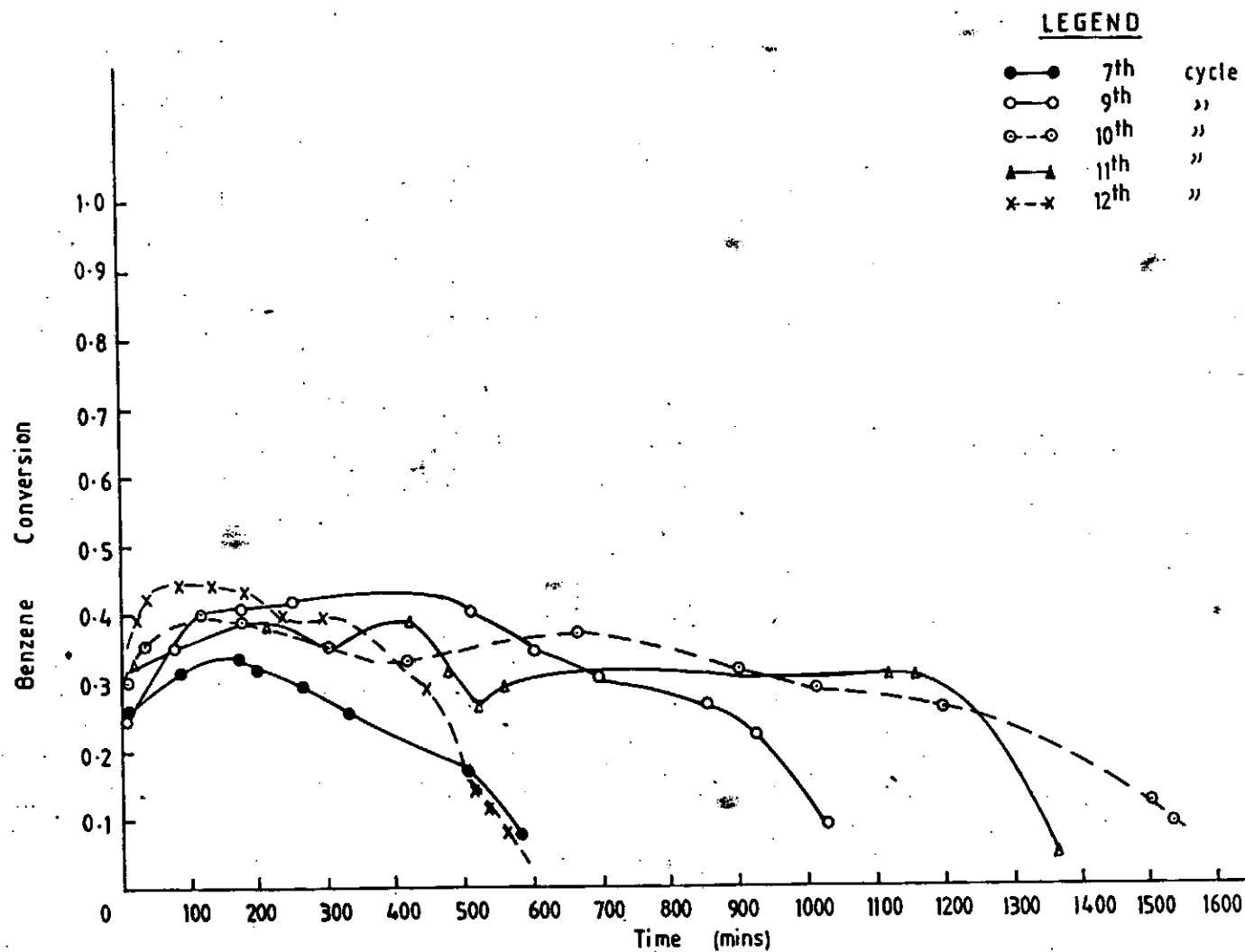
Fig.44   Benzene Conversion profiles of 0·3% pt/Al₂O₃   w/c = 430°C
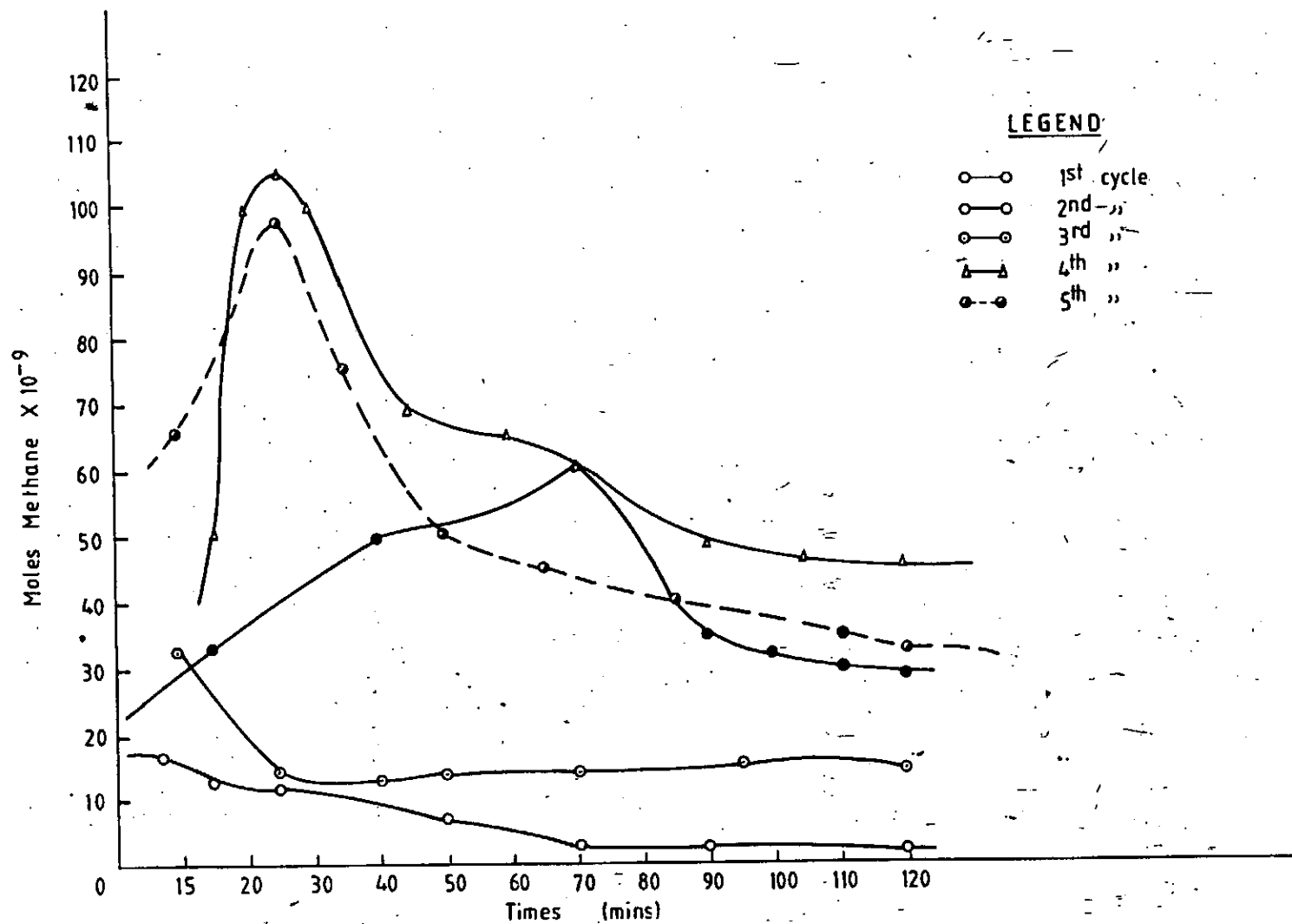
Fig:45   Toxic Coke Removal, Removal for   2 hours at 430°C
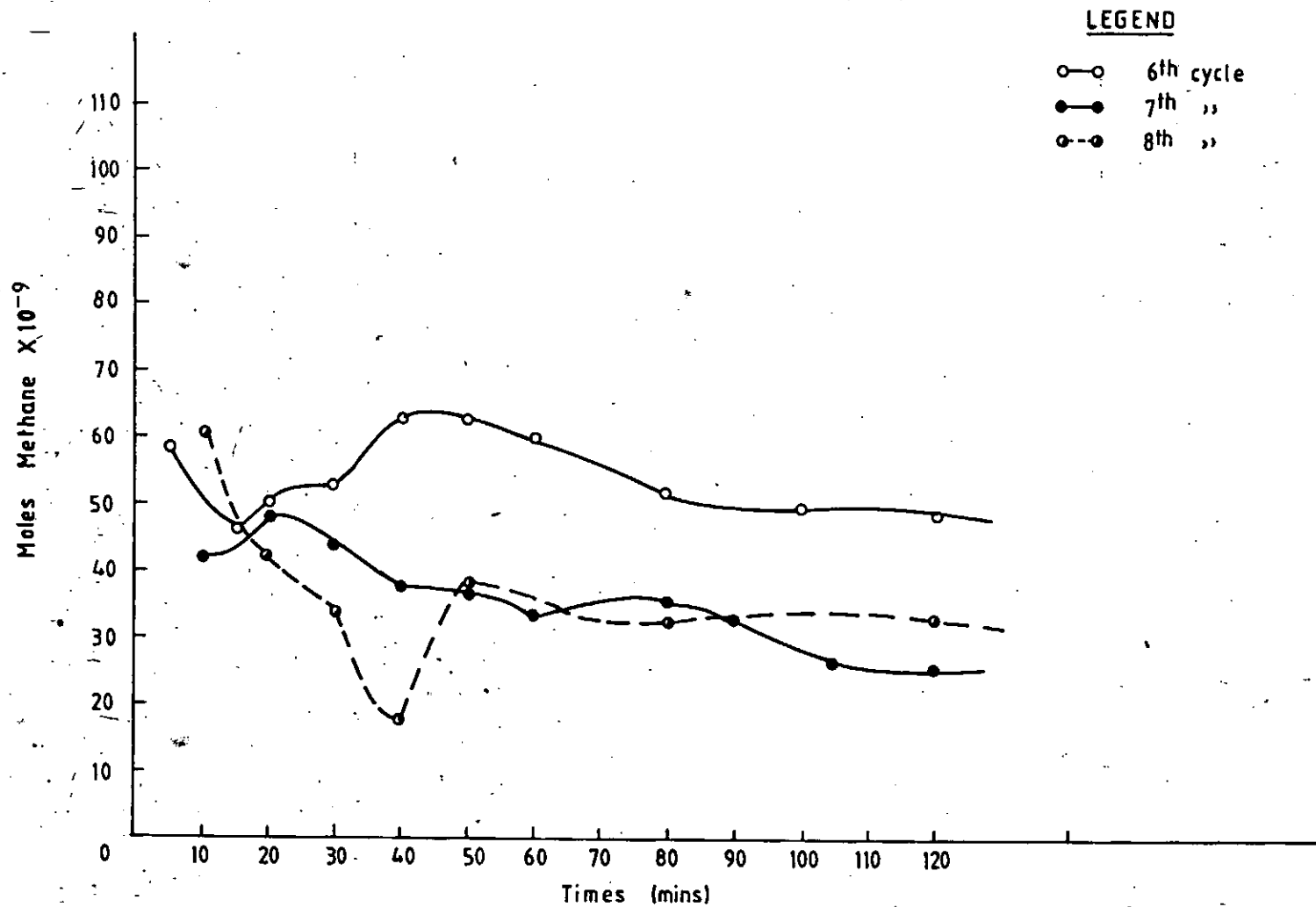
Fig:46   Toxic Coke Removal profiles, Removal for 2 hours at   430°C
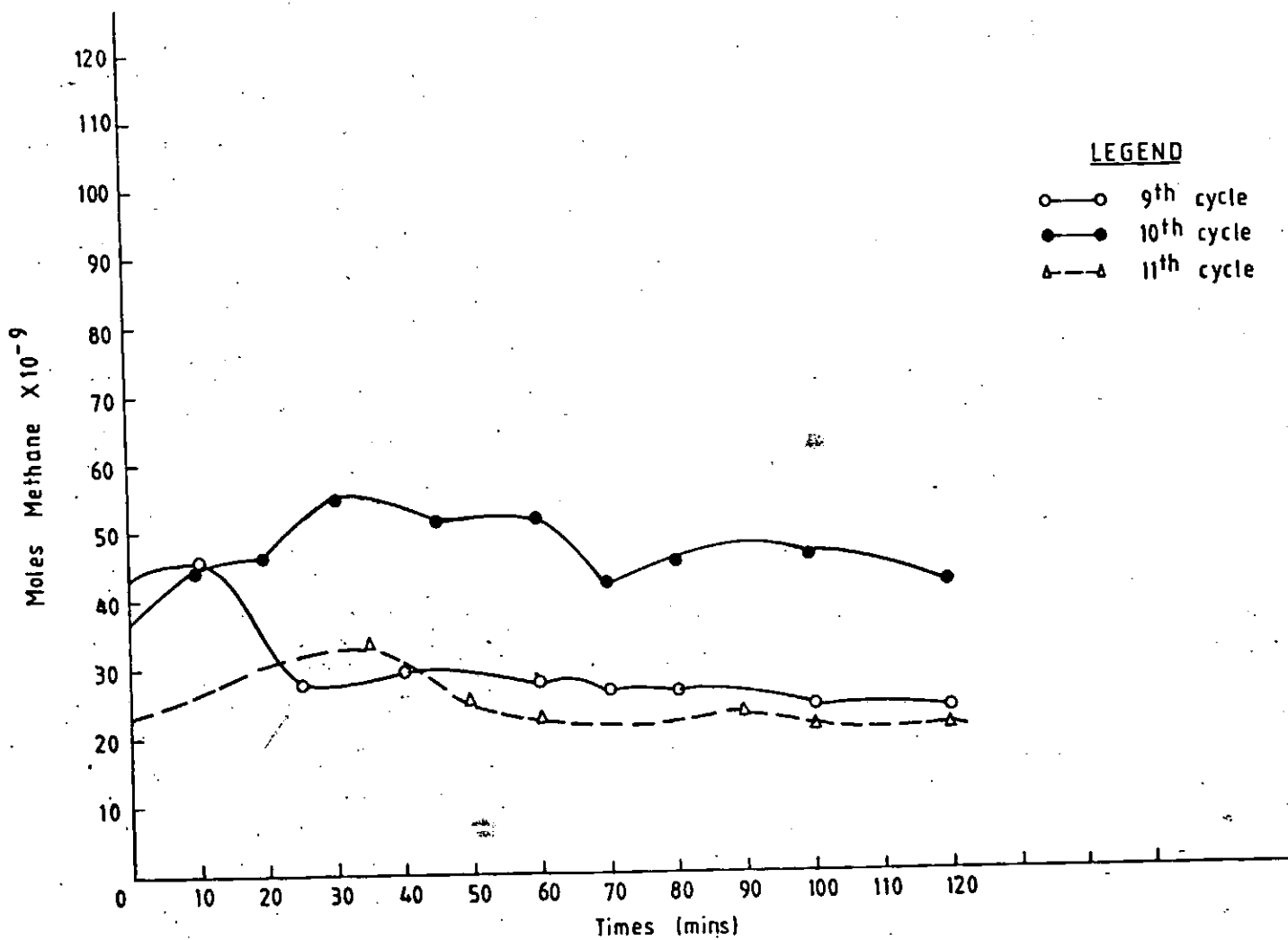
Fig. 47 Toxic Coke Removal profiles, Removal for 2 hours at 430°C

189
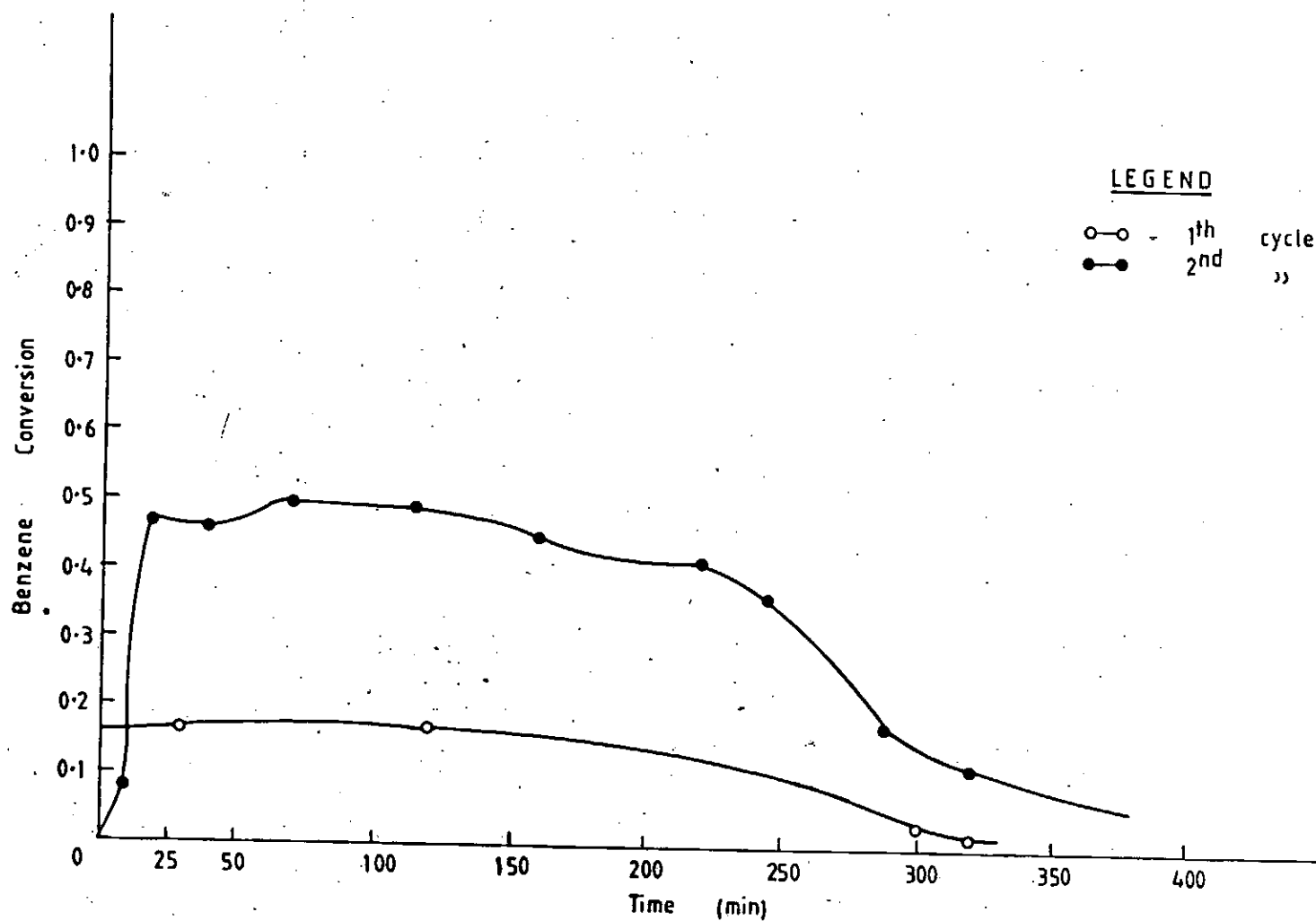
Fig. 48   Cyclohexane reactivation of 0·3% pt/ Al_2O_3 W/F= Benzene Conversion profiles – Reactor 430°C
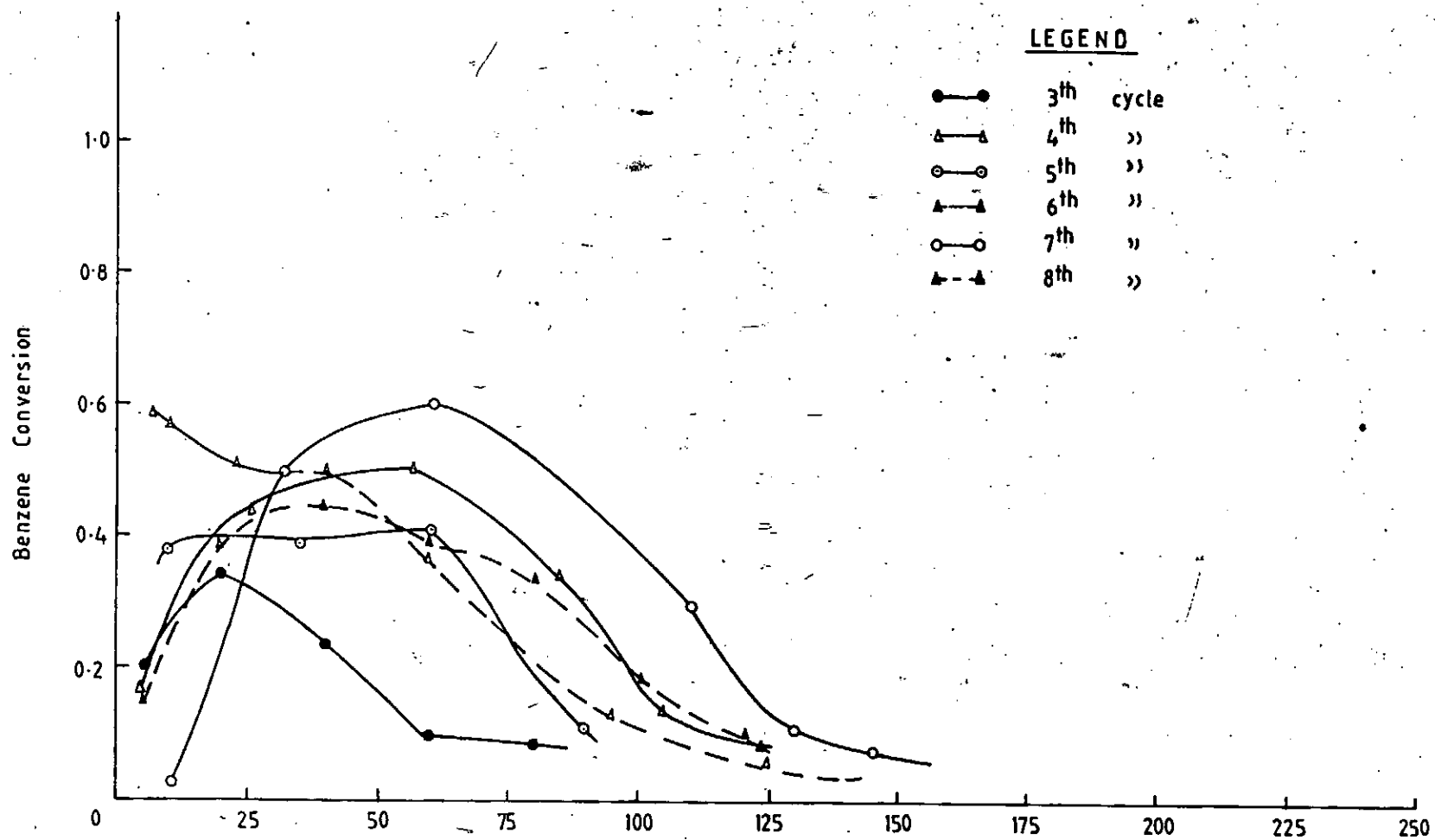
Fig. 49 Cyclohexane reactivation of   0·3 % pt/Al₂O₃ W/ꜰ = Benzene   Conversion profiles.
Reactor   430°C
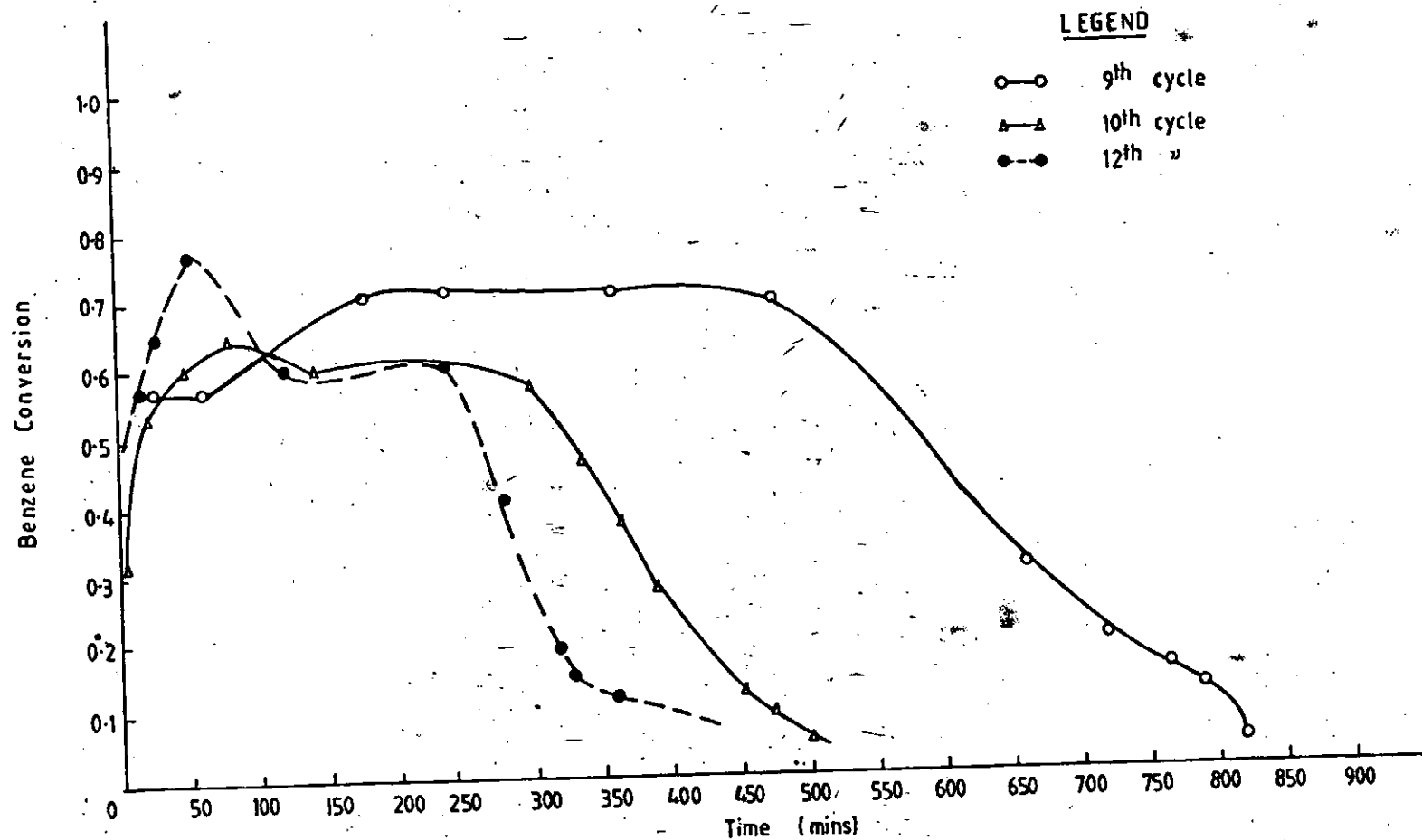
Fig.50 Cyclohexane reactivation of 0·3% pt/Al₂O₃ W F = Benzene Conversion profiles - Reactor 430°C
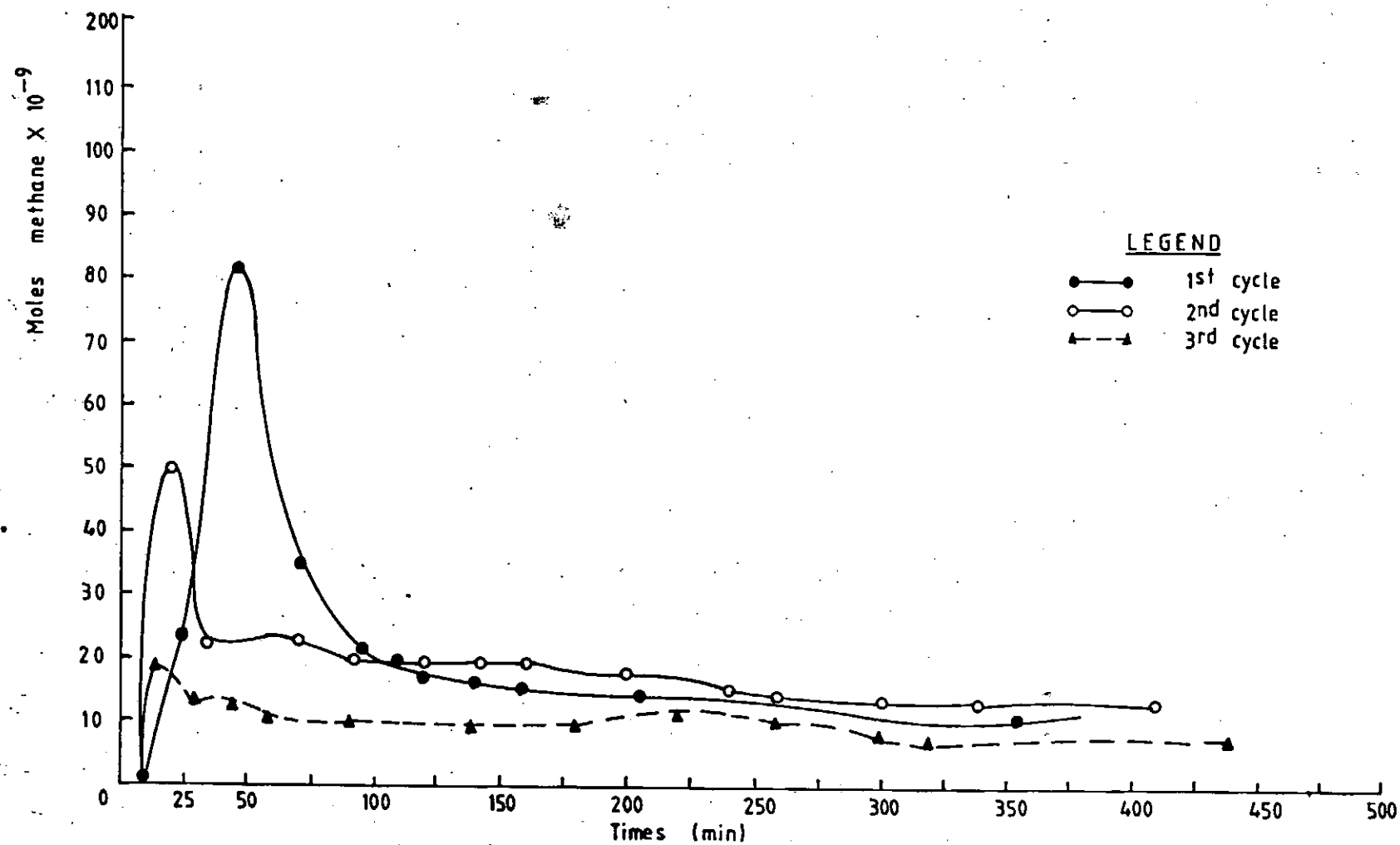
Fig. 51   Toxic Coke Removal profiles, prolonged Removal at 500°C

193
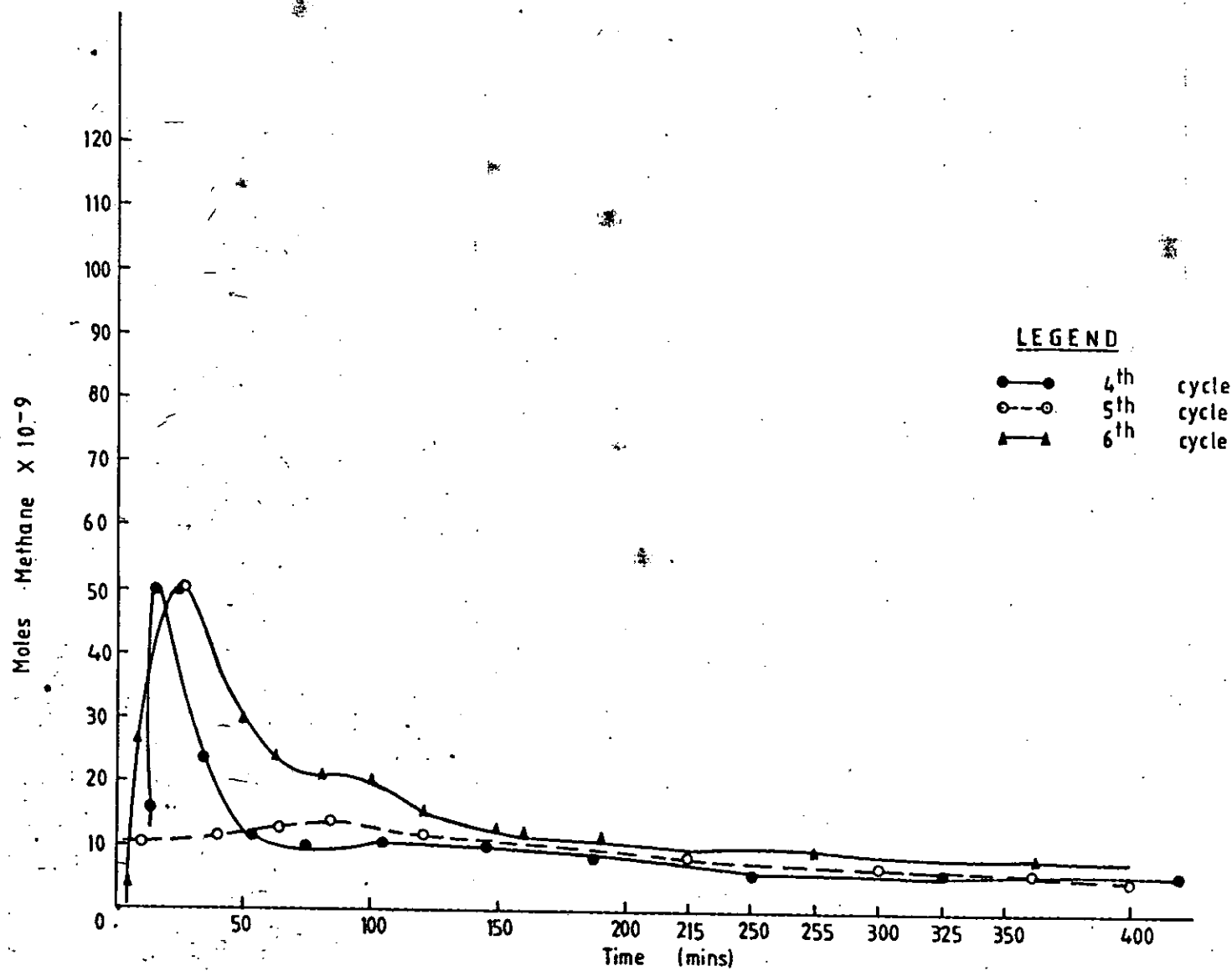
Fig. 52 Toxic Coke Removal profiles, prolonged Removal at 500°C
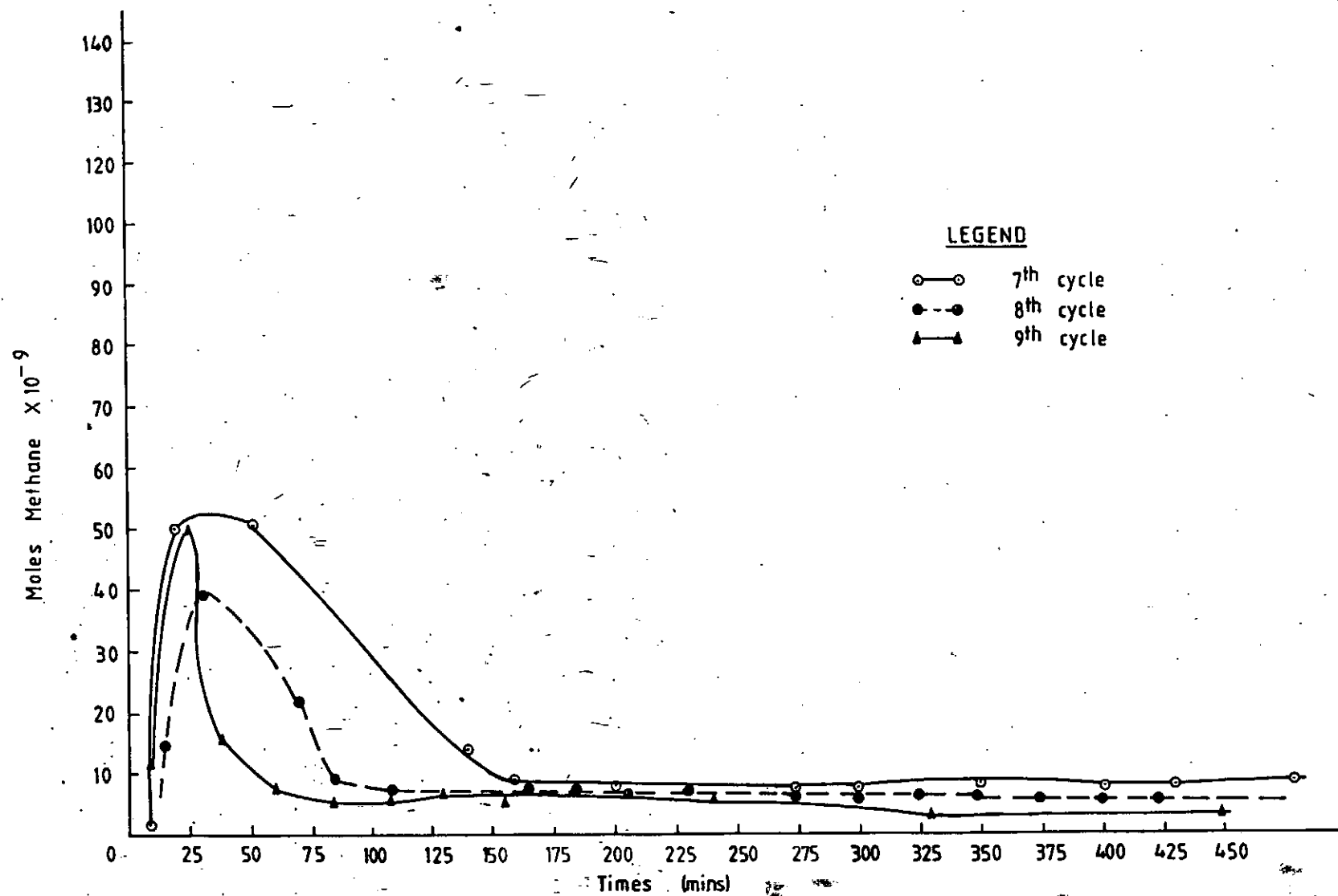
Fig. 53 Toxic Coke Removal profiles, Prolonged Removal at 500°C
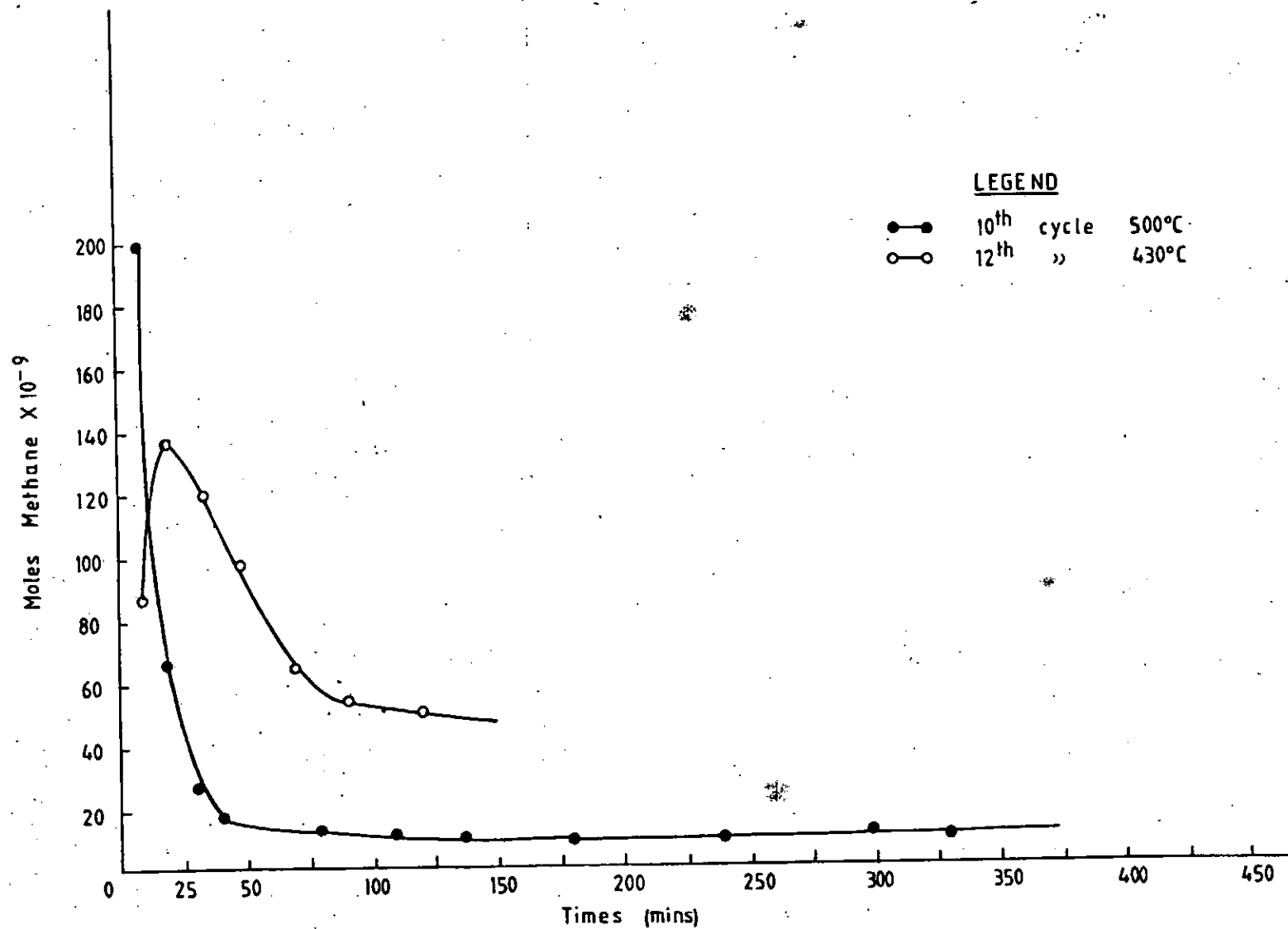
Fig. 54 Toxic Coke Removal profiles, Prolonged Removal at 500°C
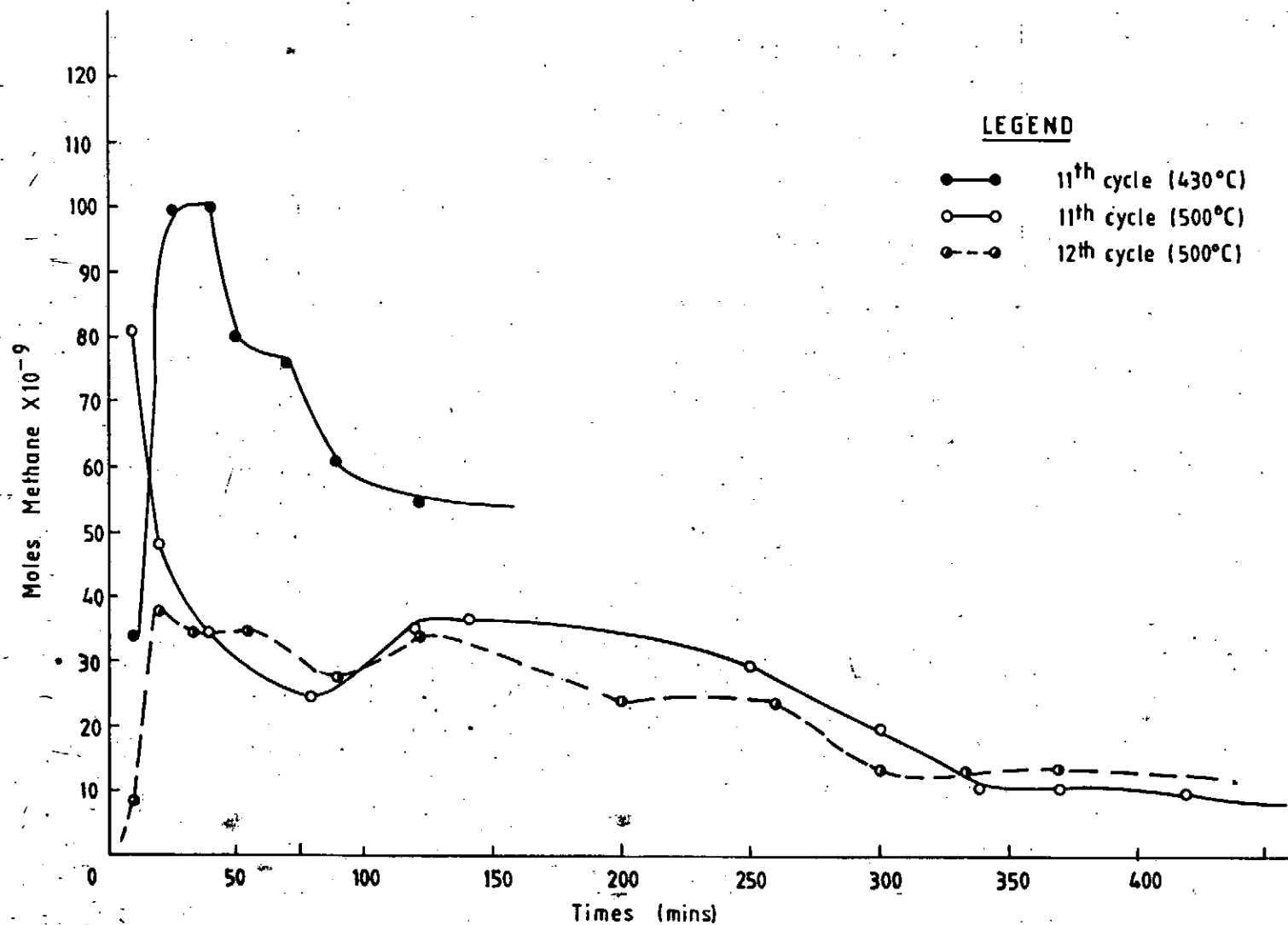
Fig. 55 Toxic Coke Removal profiles, Prolonged Removal at 500°C
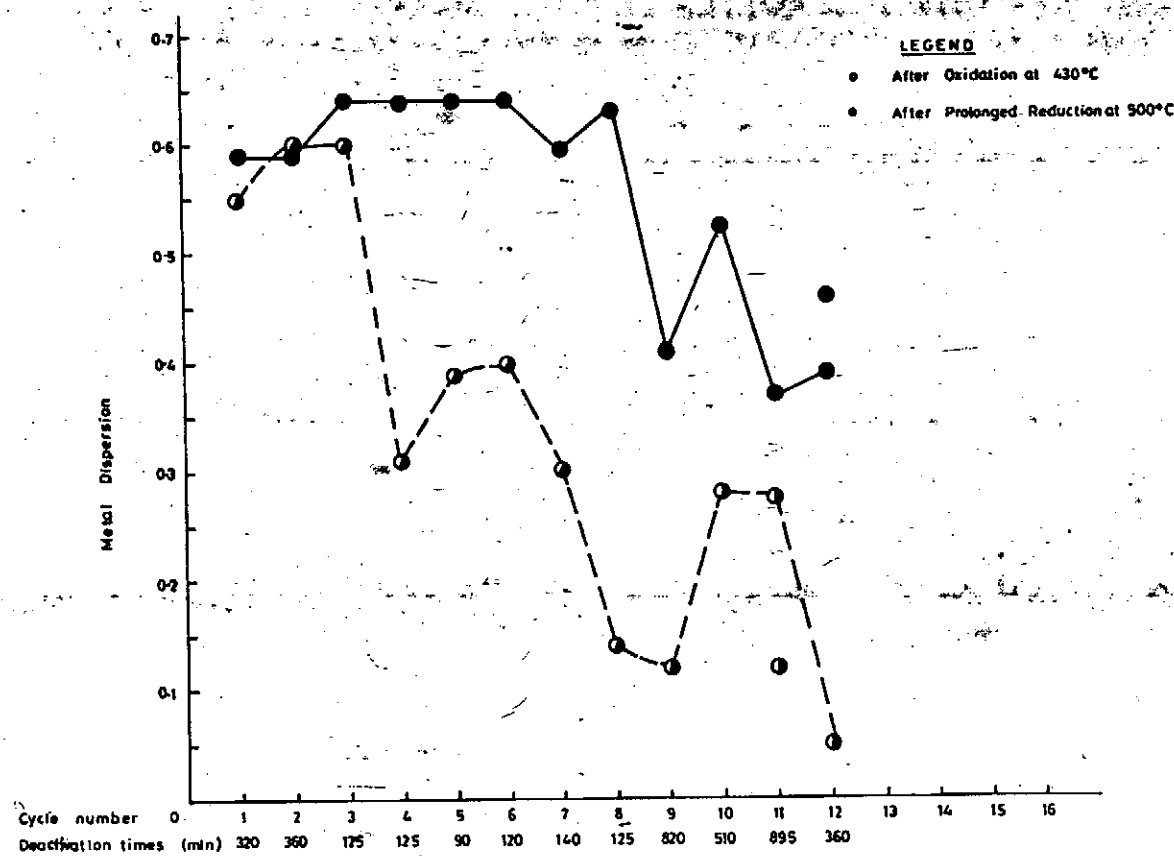
Fig. 56 Variation of Metal Dispersion with Cycle Number after Oxidation and after Reduction
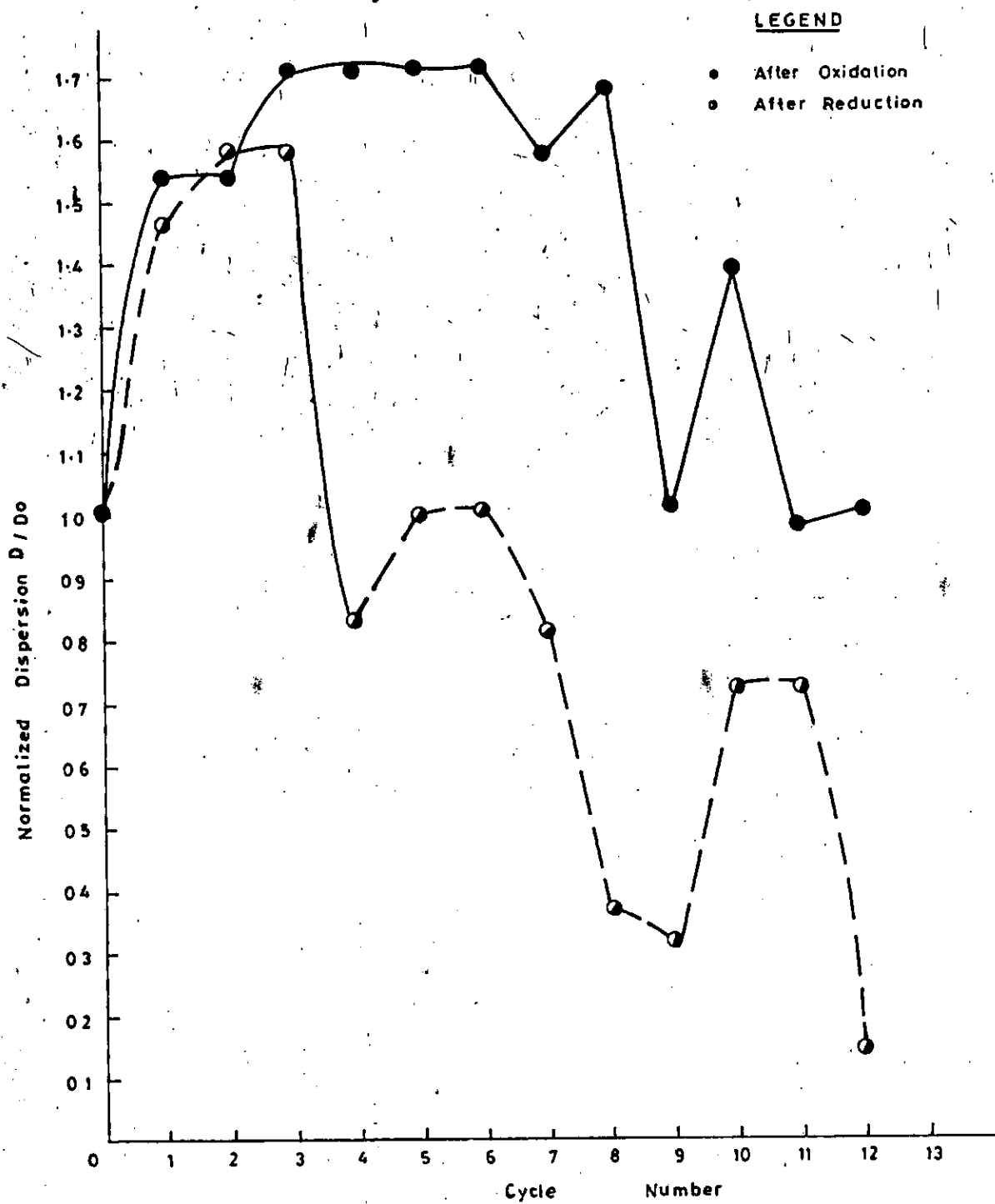
Fig. 57 Variation of normalized dispersion with cycle number

199
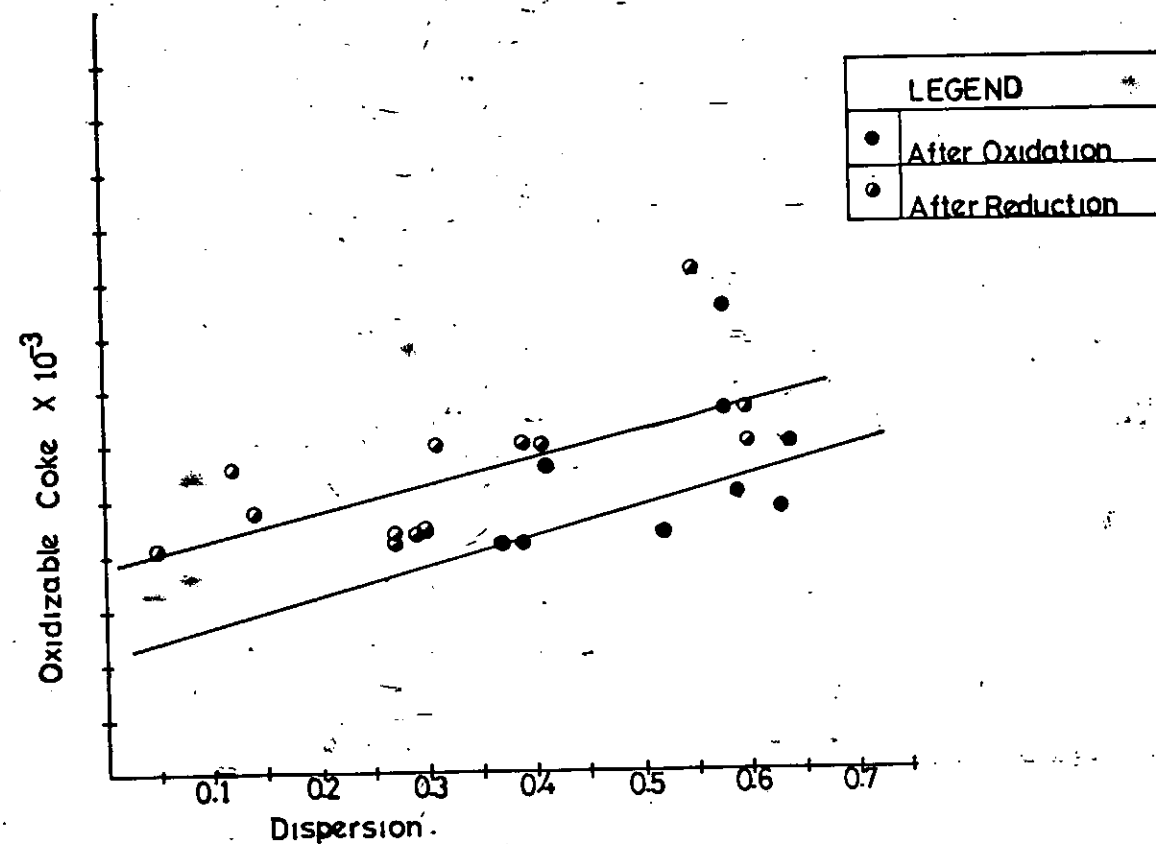
FIG 58 Comparison of Dispersion vs Oxidizable Coke after
Oxidation and after Reduction
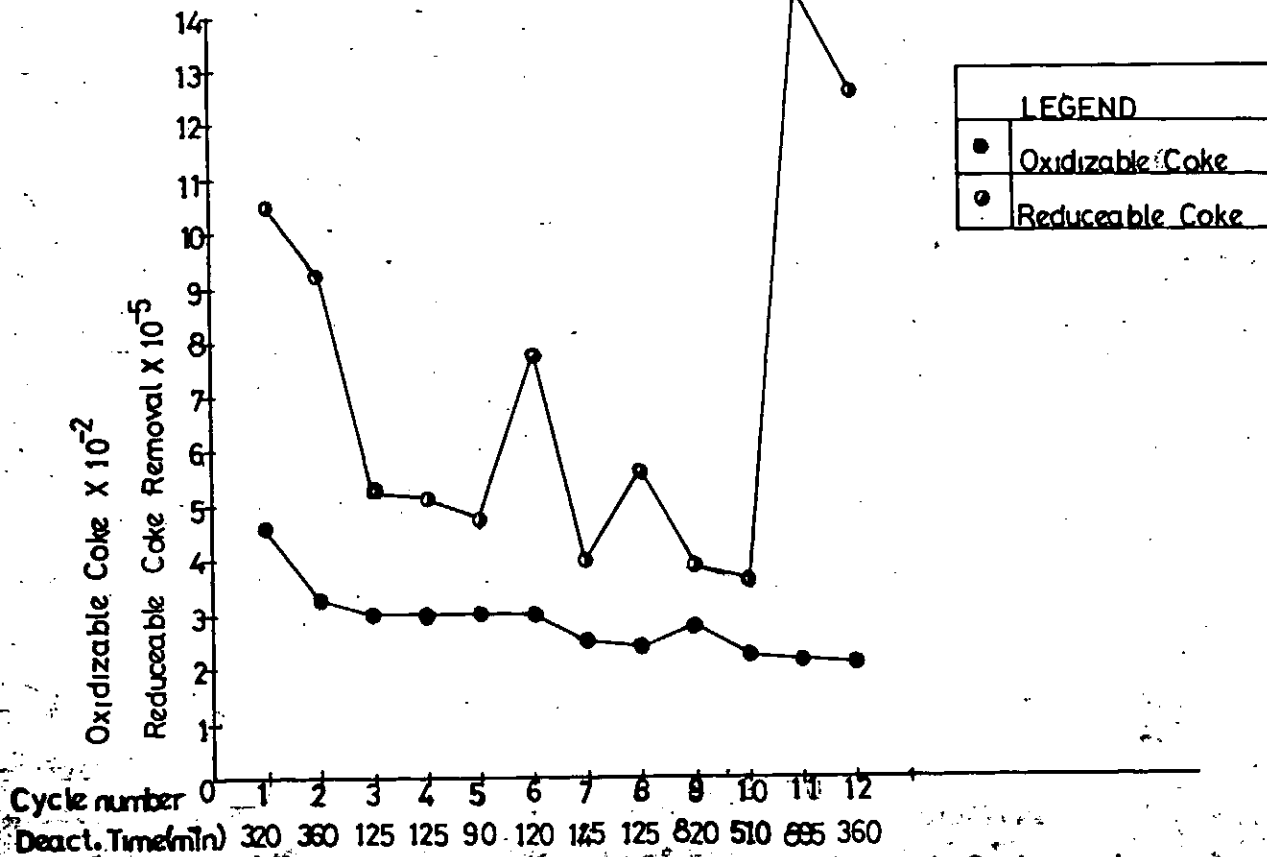
FIG 59 — Reduceable and Oxidizable Coke Deposits with Cycle number
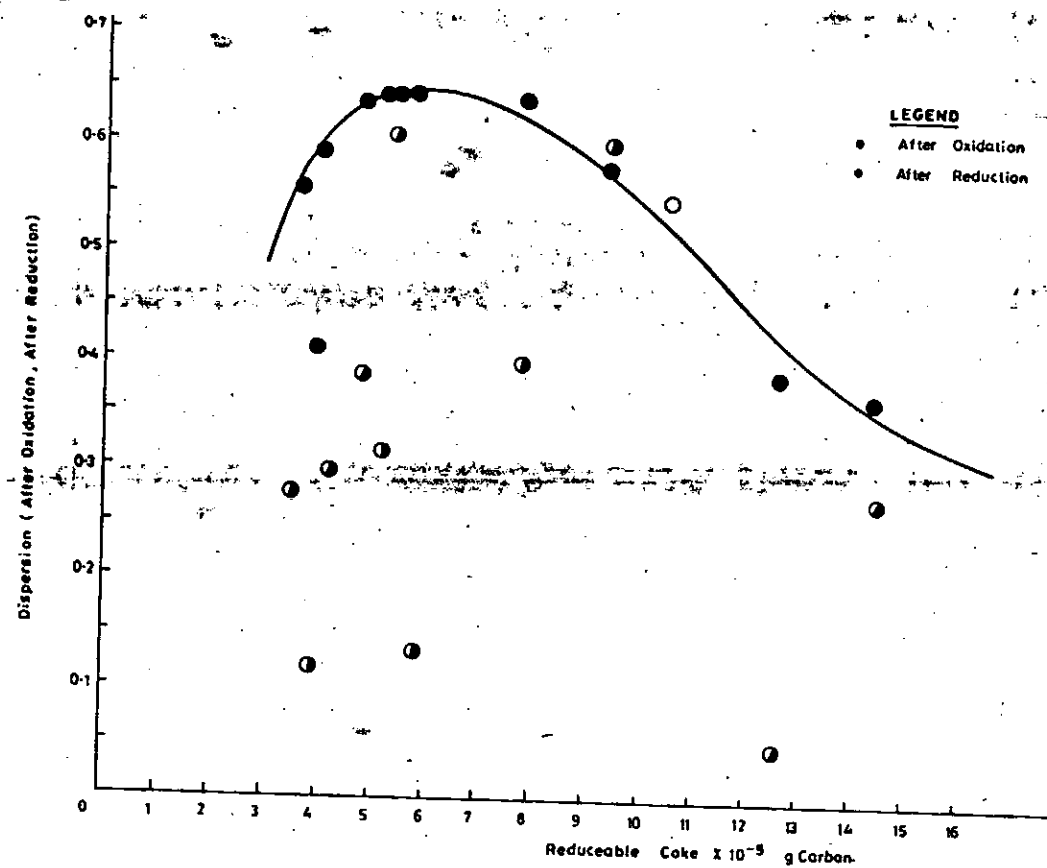
Fig. 60   Dispersion after Oxidation and after Reduction versus Reduceable Coke

LEGEND
● After Oxidation
◐ After Reduction

Dispersion (After Oxidation, After Reduction)

Reduceable Coke X 10⁻⁵ g Carbon.

202

61 Comparison of Real Surface and Klingman Models
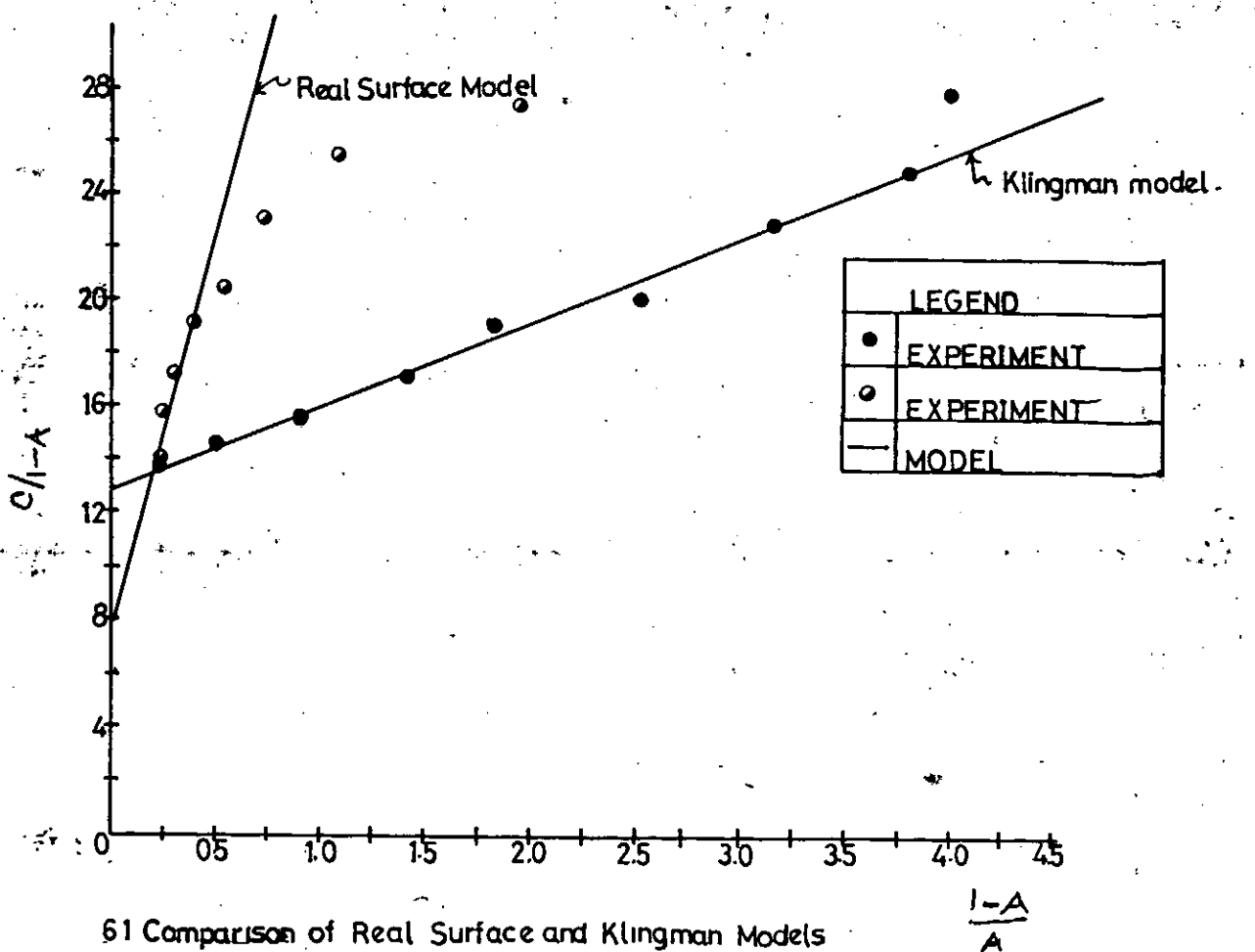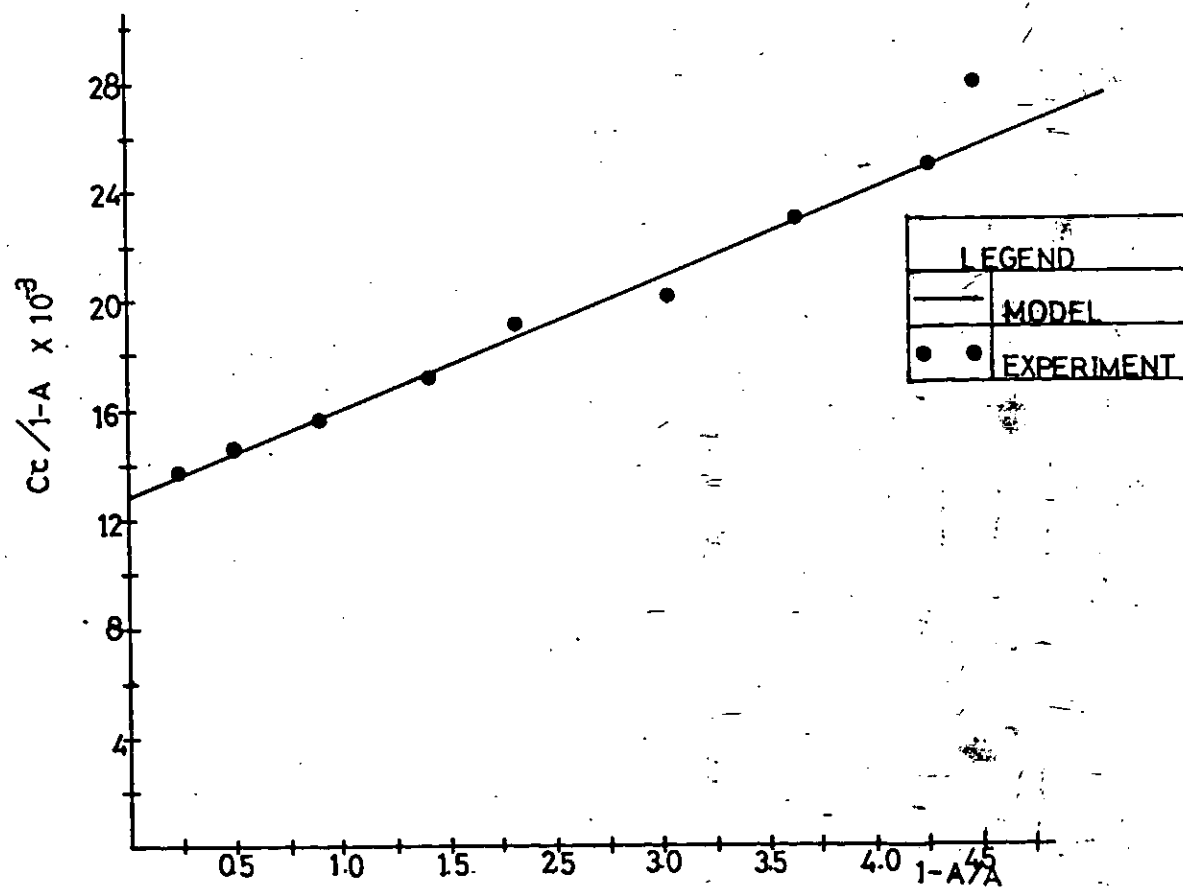
FIG. 62 Multilayer Coking–Comparison of Catalytic activity
determined by Multilayer Technique and experimental
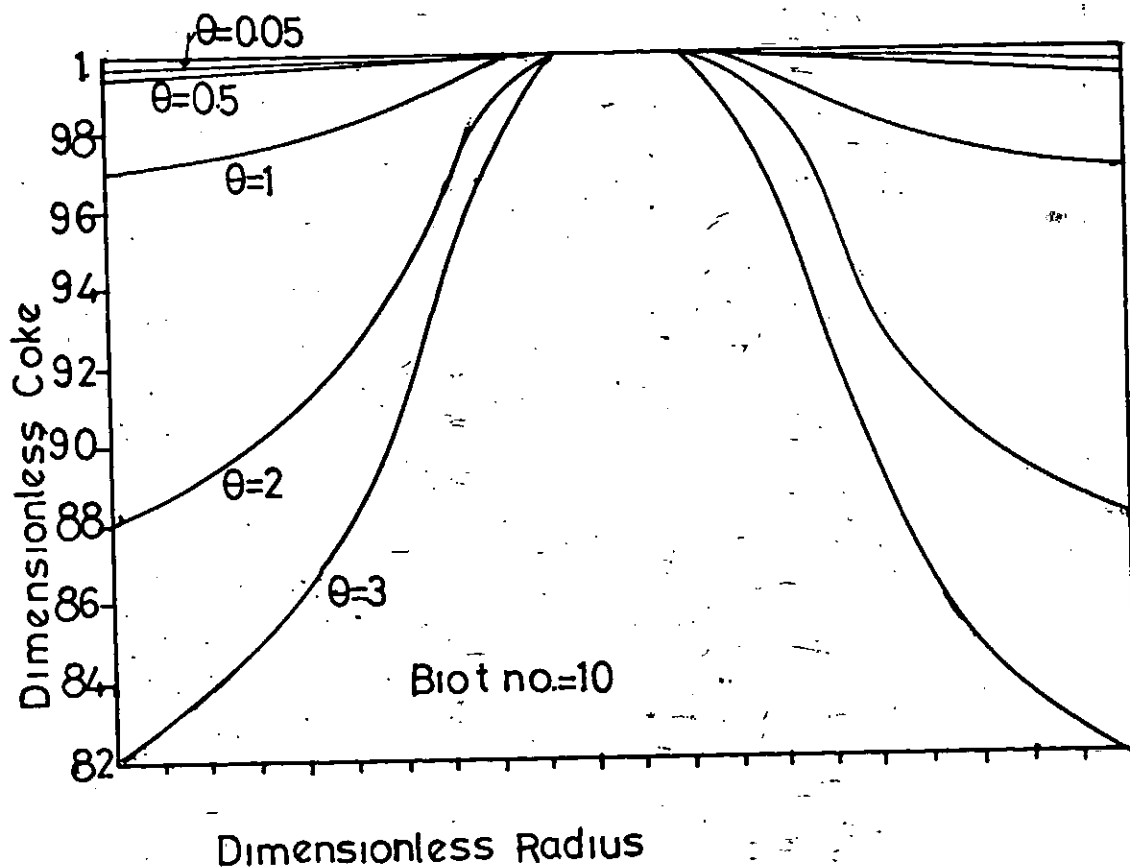
FIG. 63   Simulated Coke Consumption Profiles
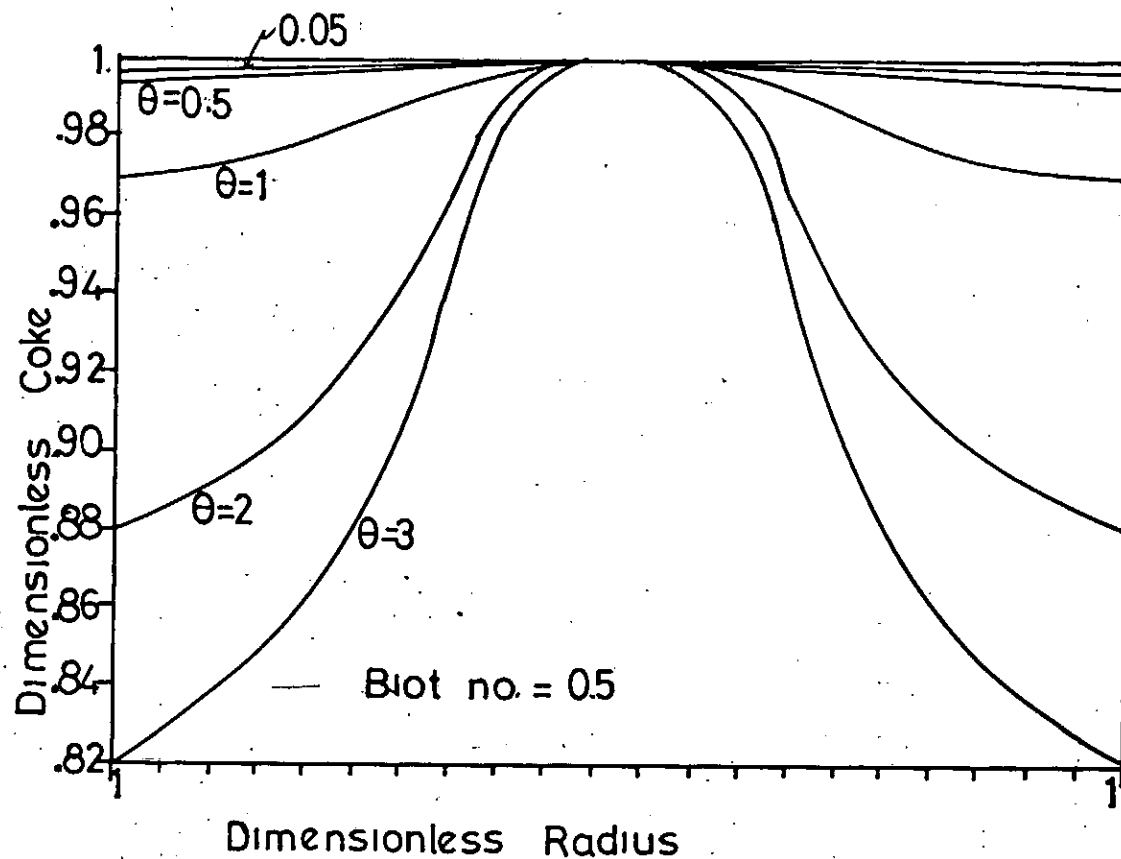
FIG. 64   Simulated Coke Consumption Profiles
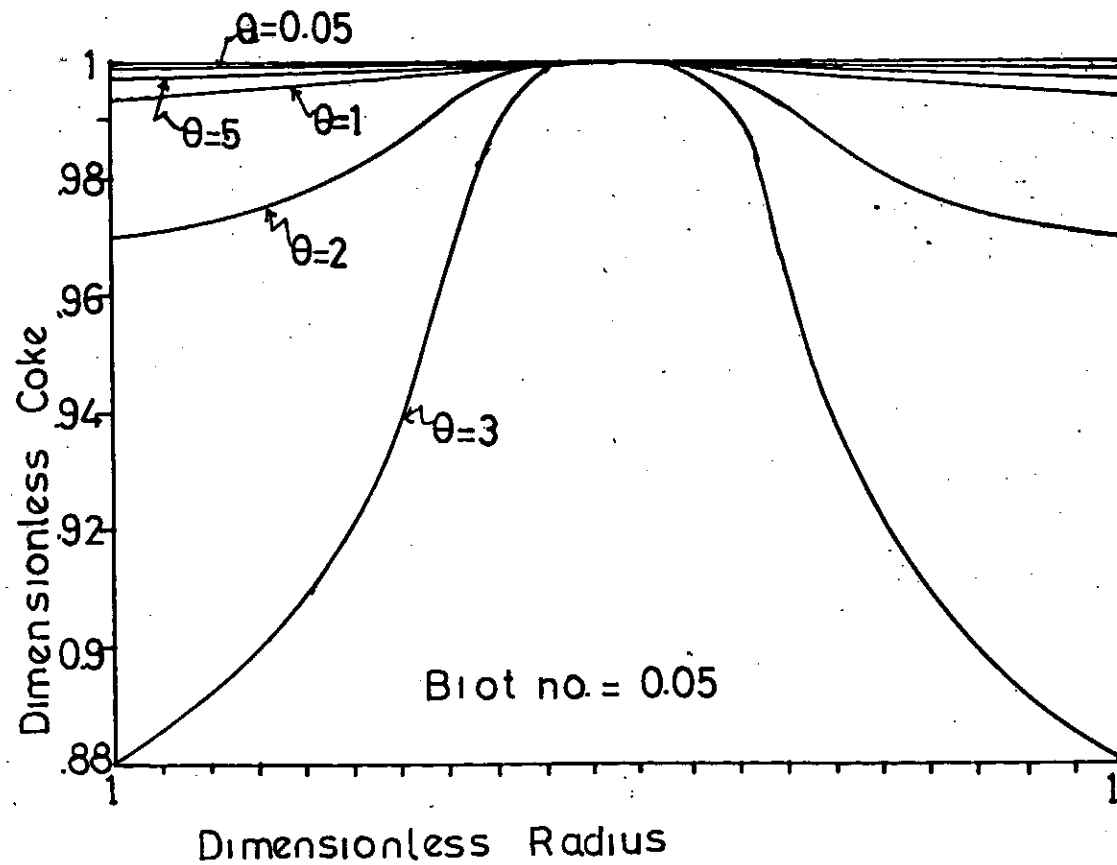
FIG. 65 Coke Consumption Profiles
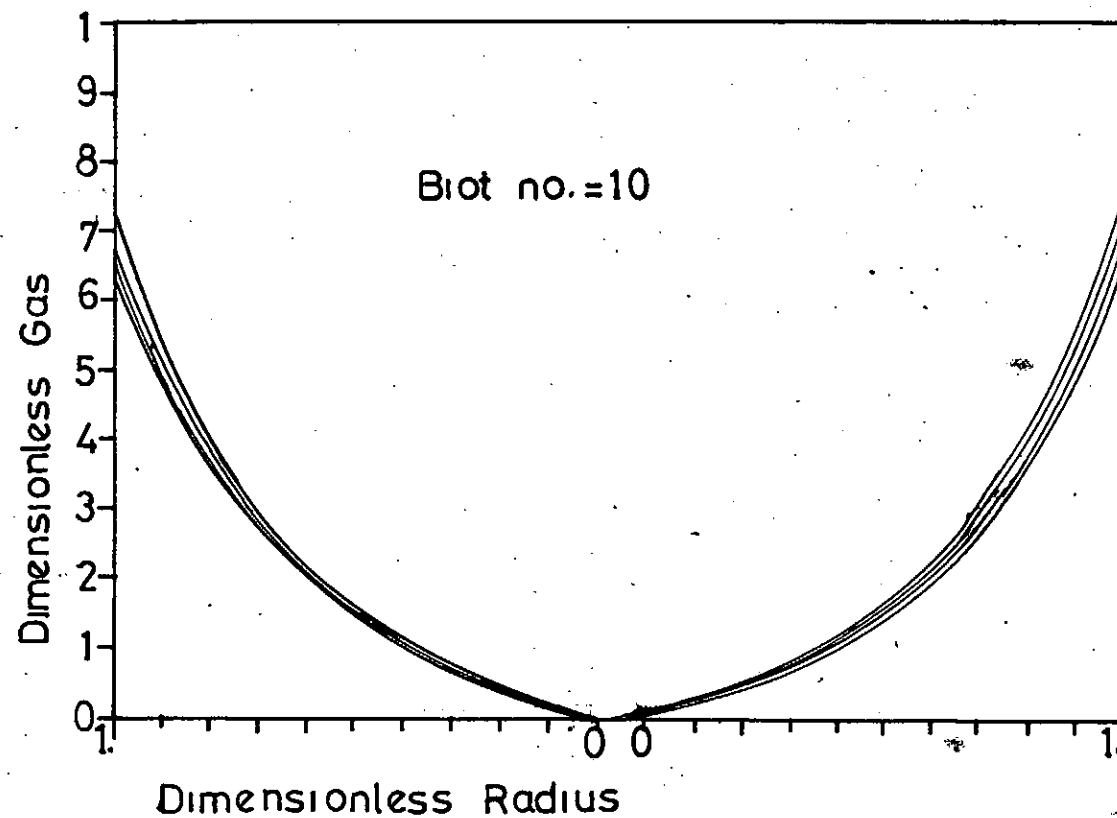
FIG. 66 Simulated Gas Consumption Profiles
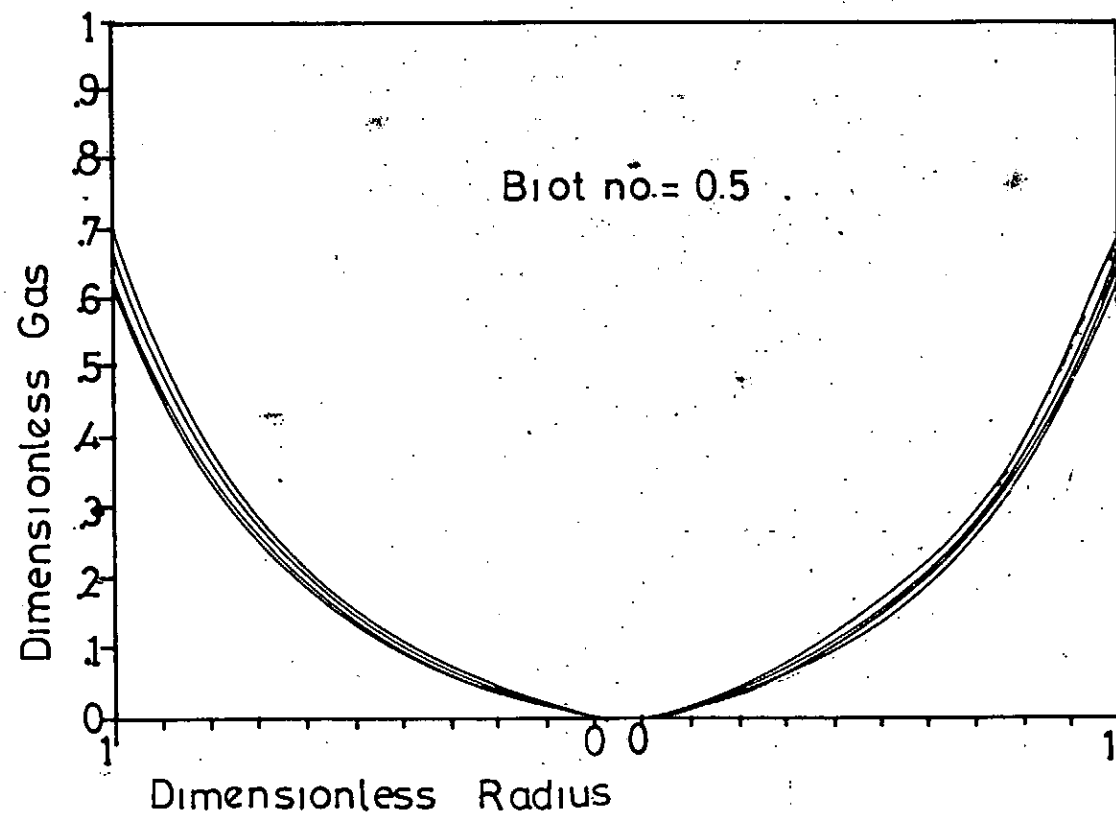
FIG. 67 Simulated Gas Consumption Profiles
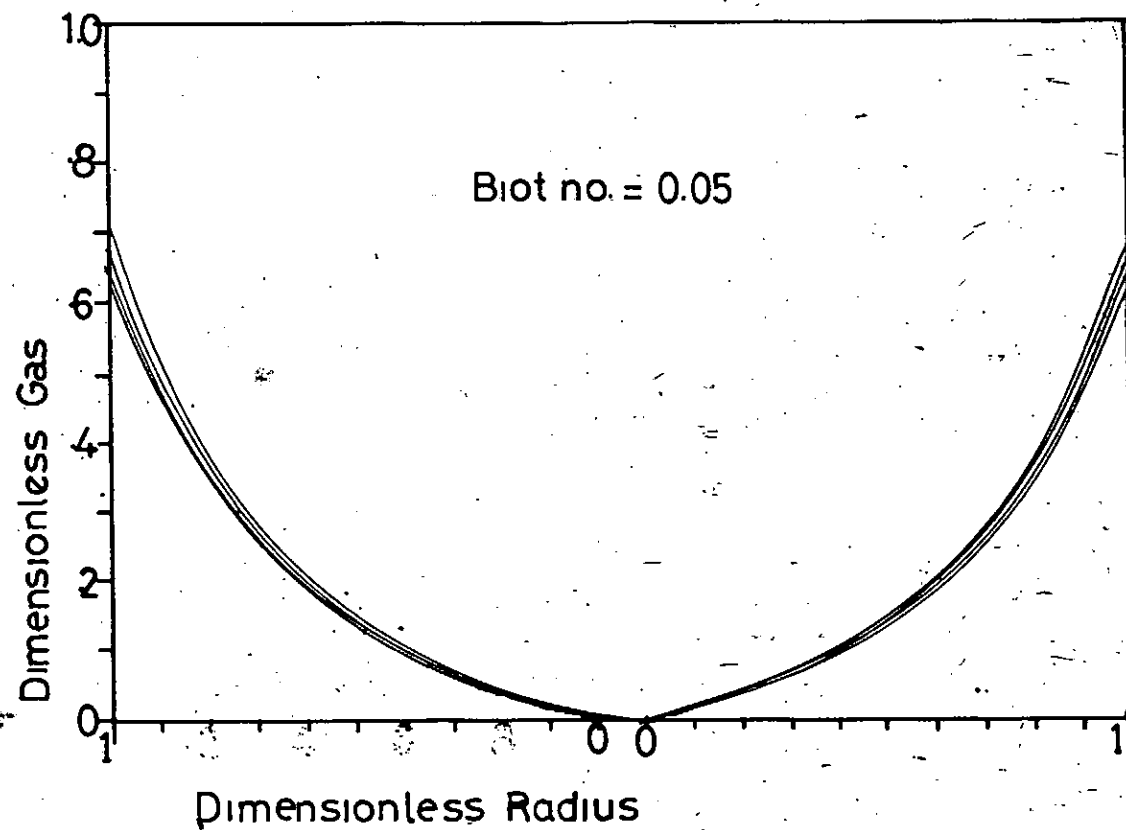
FIG. 68 Simulated Gas Consumption Profiles

210
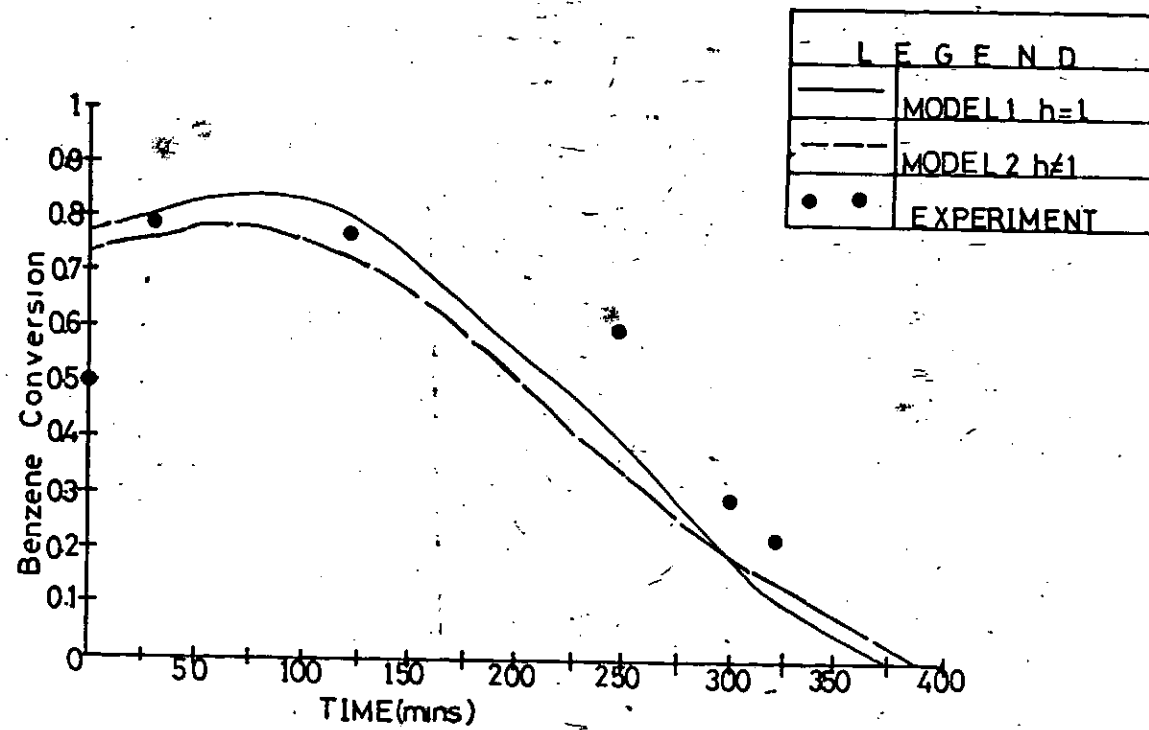
FIG 69 Model Prediction of Conversion
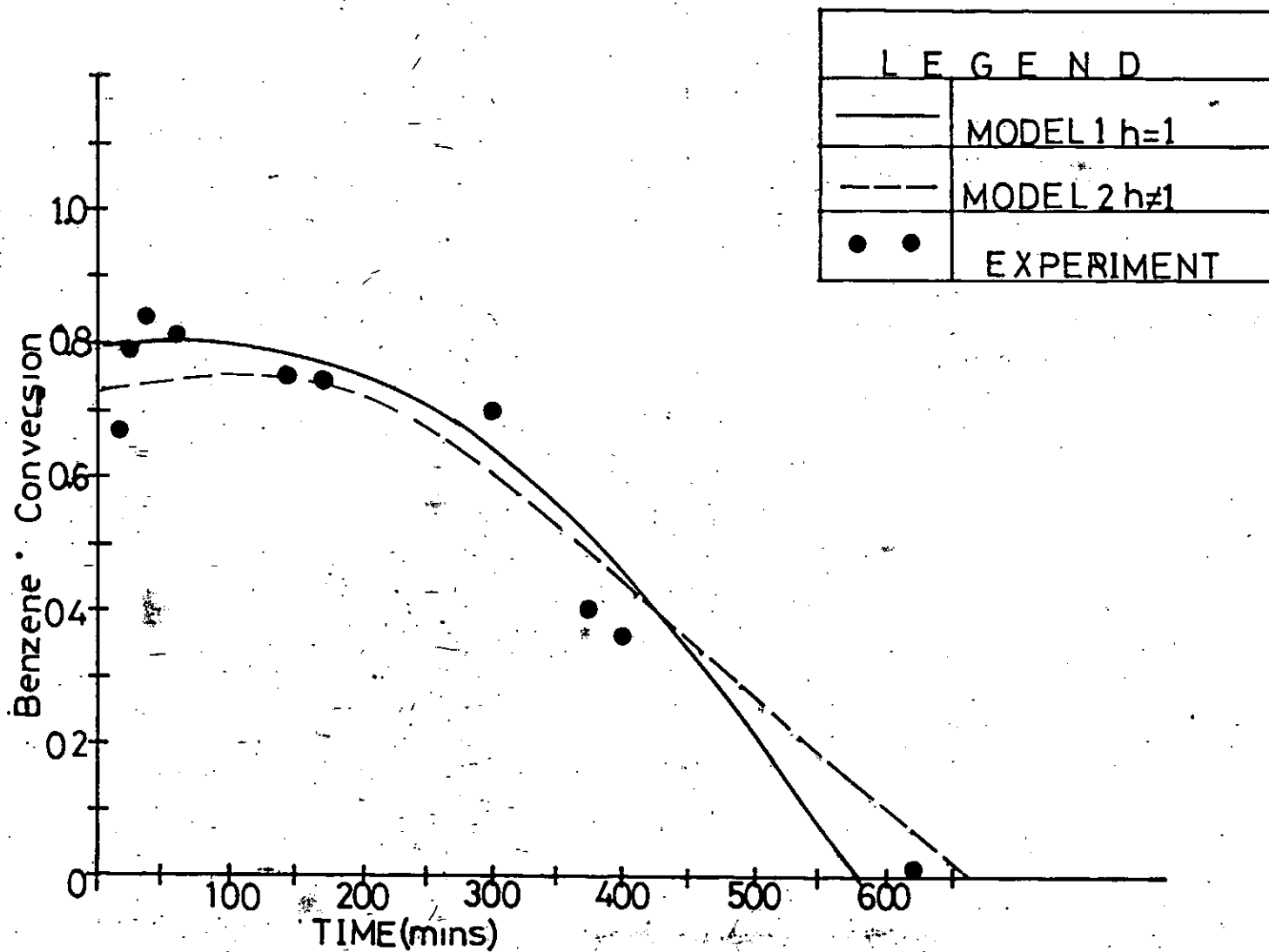
FIG. 70 Model Prediction of Conversion
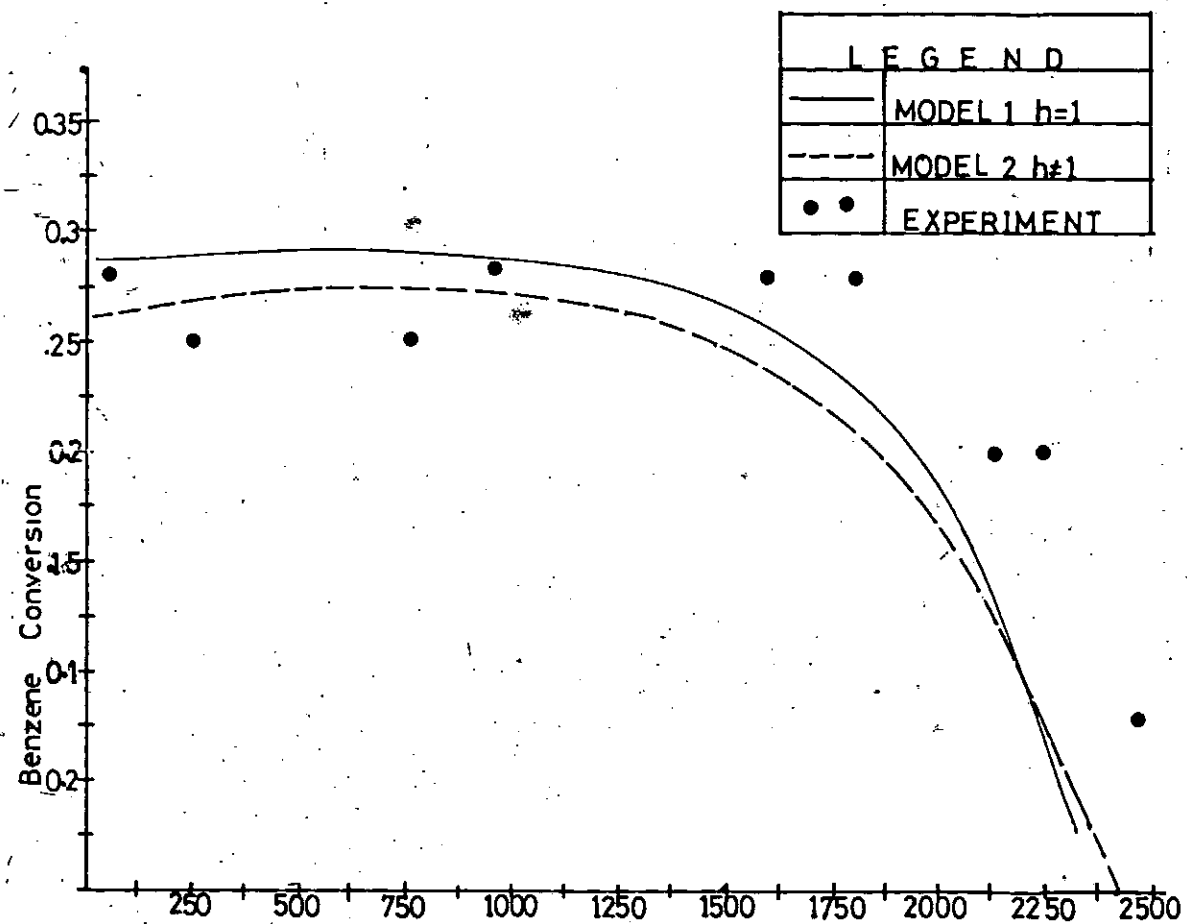
FIG. 71 Model Prediction of Conversion

213
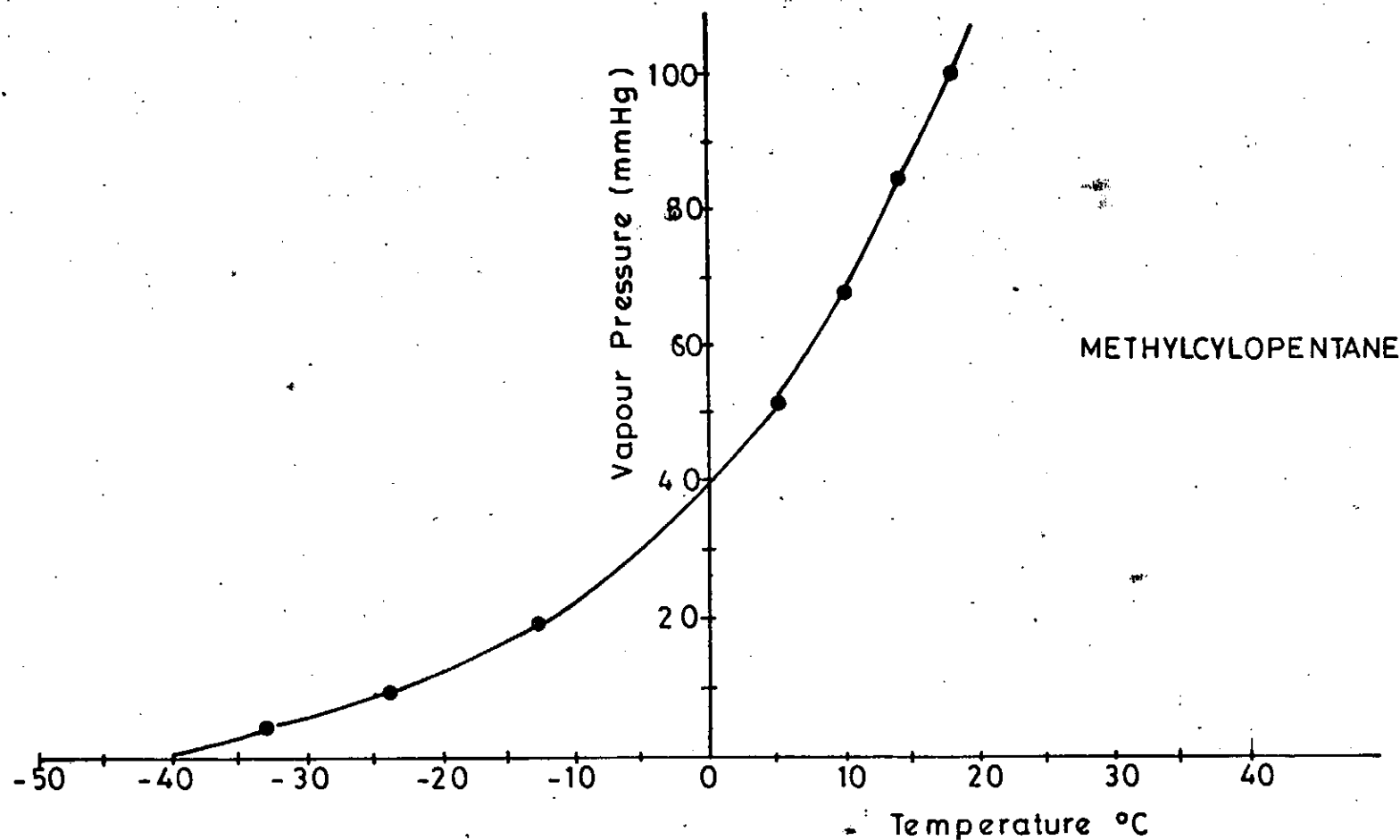
Fig: 72 Methylcyclopentane–Variation of Vapour Pressure with temperature
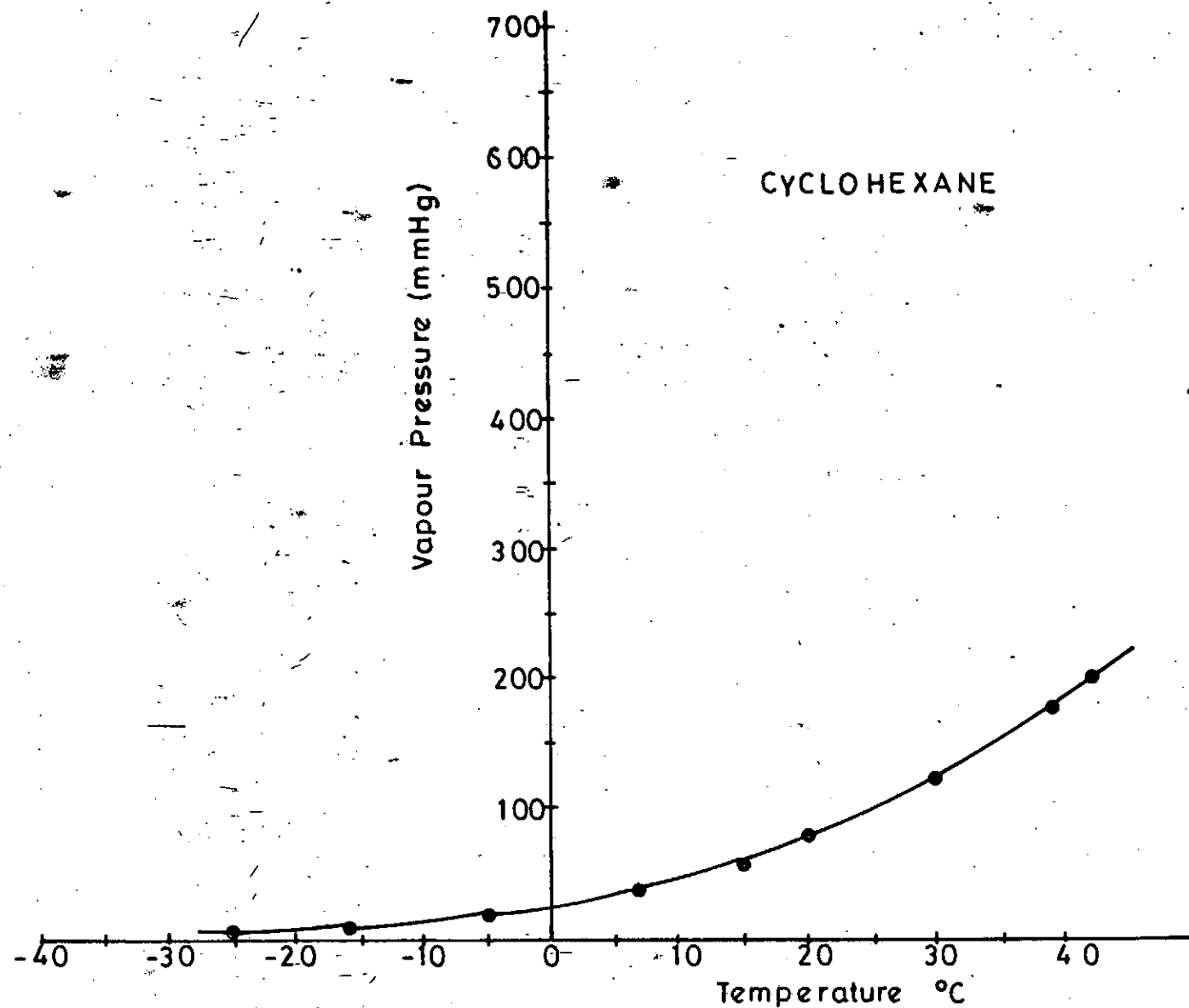
Fig 73 : Cyclohexane-Variation of Vapour
Pressure with temperature

Chapter 6

DISCUSSION OF RESULTS

Introduction

The results from the sequence of experiments as presented in Chapter 5 showed some discernible trends. While some results were expected, others were, to varying degrees, at variance with reported ones. The body of results will be discussed and explanations attempted with supportive evidence from literature.

The discussion will be carried out under the following headings:

1. Multiple deactivation - regeneration and mortality studies

2. Titration experiments for catalyst characterization.

3. Catalyst regeneration

4. Multilayer coking

5. Modelling of reaction-deactivation kinetics of cyclohexane.

214

6.1 EXPERIMENTAL RESULTS

6.1.1 Multiple Deactivation-Regeneration and Mortality Studies

At the 52nd cycle when the mortality runs were terminated, the catalyst was still very active. In this study, the reduction with hydrogen in the regeneration process was prolonged and was only stopped when the moles of methane removal with time at $500^\circ C$ was stable. In a previous experiment in this laboratory, the mortal state of monometalic $Pt - Al_2O_3$ catalyst had been reportedly achieved after only 22 cycles(6). In that work, the catalyst reduction was done at $430^\circ C$ for only 2 hours. The continuous removal of toxic coke in this work ensured that the surface of the catalyst was clean after each deactivation, to support the consistently high activity with cycle number as observed with time.

The methane reduction profiles also showed that the toxic coke is deposited in layers as revealed by the maxima exhibited in the profiles before the stabilization of the level of toxic coke (Figures 11, 13, 14, 16). The decline in the maxima before stability also reveals the decline in the reactivity of the various coke layers with the least reactive lying closest to the catalyst-coke interface.

The fact that not all the toxic coke deposits could be removed after long reduction times means that at least 3 coke forms exist on $Pt - Al_2O_3$ surface, the first is oxidizable (primary) coke. The second is reduceable (secondary) coke with at least 5 types with decreasing reactivity in H_2. The third type (tertiary coke) is neither oxidizable nor reduceable and must be graphitic in form. Previous workers had studied the toxic coke deposition from methylcyclopentane reforming on $0.3\%Pt - Al_2O_3$ (9). They reported

the same layered structure for toxic coke. Hence this work confirmed their results.

From the toxic coke profiles it took more than 4 hours for the profiles to stabilize. It therefore seems that reduction for two hours, as was done by previous workers (6,7) was not sufficient to guarantee a clean catalyst surface - leading to the mortality of the catalyst after just 22 cycles. Hence, the application of prolonged reduction clearly leads to a cleaner catalyst surface after coke coverage. The results also confirm the toxicity of reduceable coke to catalyst life. The irremovable type (tertiary coke), which sticks to the surface of the catalyst and not responsive to both oxidation and reduction was suggested to be graphitic in form. J. Biswas(16) had identified and reported the existence of two coke types after oxidation deposited on long term reformer operation. One, easily removed by hydrogen and a less readily removable type which he suggested must be graphitic in structure. X-ray analysis of unextractable coke by J. Barbier (17) showed that such deposits are composed of pseudo graphitic phases with crystallographic characteristics very close to pure graphite. Graphite is less hydrogenated and according to Bernal (98) is composed of layer planes formed by carbon atoms ordered in regular hexagons, similar to those in the rings of aromatic organic compounds.

The results of oxidizable coke structure determined in this work (Figure 37) suggested that oxidizable coke, which is first to be deposited, consists of disosrdered deposits of hydrogenated coke. Hence, it seems like coke formation starts with the rapid irreversible adsorption of dehydrogenated hydrocarbon species on the metal. The metal sites are easily covered by these dehydrogenated species. J. Biswas (16) and J. Barbier (17) had separately reported that coke deposition in short term reformer operation was on the metal support. On covering the metal sites, these dehydrogenated species now spread to the support. This spread is aided by their mobility which is due to their poorly developed crystallite structure and weak cross-linking between the atoms in the crystallites (98).

216

With time on stream, and with further loss of hydrogen, the carbon atoms move to the corners of a regular hexagon which is a more stable configuration. With time, the hexagonal carbon structures build up into a tightly held crystalline structure with strong interatomic bonding. The crystalline growth is assisted by high temperatures. The bonding strength of the inter layers make the graphite structure very unreactive with hydrogen. It is probably at the setting of the formation of the graphitic structure that the stability of the methane removal profile starts setting in.

From the above discussion, the following sequence can be postulated for coke formation:

$$Coke\ precursors \rightarrow oxidazable\ coke \rightarrow Secondary coke \rightarrow Tertiary coke$$

This sequence is in agreement with the postulation of Osaheni and Susu(9) and could be implied from the discussion of J. Biswas (16). The sequence suggests that all the coke types are formed at the same coke location. This is in conflict with the finding of Barbier et al. (17) and N. S. Figoli (99). Barbier(17) carried out a Temperature Programmable Oxidation(TPO) of coke $Pt - Al_2O_3$ catalyst and found two oxidation states, one at $300°C$ and the other at about $450°C$. Barbier concluded that the lower temperature oxidation was due to coke deposited on the metallic phase while the higher temperature oxidation at $450°C$ was due to coke on the alumina support. He explained the difference by assuming that either platinum catalyzes the oxidation of carbon or that coke deposited on the metal is different from that on the support. Barbier also found that the location of coke deposition was influenced by experimental conditions. Increasing coking pressure induced a decrease of the low temperature combustion peak, giving a clear indication of a change of coke location with coking pressure. At high pressure, coke was in preference deposited on the support than on the metal. N. S. Figoli et al. (99) carried out a TPO of coke deposited during naptha reforming over $Pt - Al_2O_3$ and

217

like Barbier (17) reported two combustion zones. The first between $123 - 369°C$ and the second between $369°C$ and $555°C$. N. S. Figoli et al.(99) reported that the coke due to low temperature combustion had a lower C/H ratio than the coke due to high temperature combustion zone consistent with the finding of Barbier (17).

In a later work, Barbier and co-workers(100) reported that the mechanism of coke formation during cyclopentane reforming on $Pt - Al_2O_3$ involved as a first step, the dehydrogenation of cyclopentane to cyclopentadienne catalyzed at the Pt sites before the spreading of the unsaturated hydrocarbon to the support where they are converted to coke by a sequence of reaction catalyzed by the acidic sites on the alumina. Of signifance was their finding that the coke formed on the Pt or alumina sites was essentially amorphous carbon although they qualified the one on the alumina support to be more dehydrogenated. Amorphous carbon is disordered form of carbon, frequently referred to in this thesis as oxidizable coke. Since the coke on the support was reported to be more dehydrogenated, this confirmed the TPO measurements by Barbier(17) and N. S. Figoli et al.(99) showing that mild oxidation treatments at about $300°C$ could eliminate the coke on the Pt, while that on the support required severe oxidation treatments at $450°C$ and above. Osaheni and Susu(9) provided further evidence of the formation of different types of coke on the support and metal sites on comparison of the amount and nature of coke deposited in H_2 and N_2 atmospheres. They(9) suggested that oxidizable coke may be forming on the weak acid sites, which are isolated hydroxyl ions attached to Al atoms. These sites are known for deposition of coke with low C/H while toxic coke or coke with high C/H could be forming in Lewis acid sites.

Even though there may be more than one site for coke formation, this experiment does not provide any evidence to invalidate the proposed coking sequence. The starting point of coke formation is coke precursors to oxidizable coke since the frequently used

218

parameter for differentiating the coke is the level of dehydrogenation. The two extremes of coke structure are the amorphous and graphitic types. In between, the level of dehydrogenation is used in coke description and there are no assigned values to the level of C/H which universally define oxidizable or toxic coke. This author ascribes the differences in the coke on the metal and support to the fact that the Brønsted and Lewis acid sites in the alumina support may only be enhancing or retarding the dehydrogenation of coke such that on either site, the concentration of coke with predominantly the same level of C/H will be different.

Since coke formation on alumina depends on the level of acidity on the alumina sites, it seems reasonable to assume that the chlorine content of the catalyst should affect coking. More so since the active sites for coking on the alumina are either the Lewis and/or the Brønsted sites. Therefore, the chlorine content is an important coking parameter. However, it has been shown that the chlorine content of a reforming catalyst could remain unchanged for prolonged periods under reaction for up to 24 hours(30). The dependence of activity on the chlorine content had been investigated by Nora Figoli et al.(30) and Parmaliana et al.(32). Nora Figoli et al. (30) carried out n-heptane reforming on $Pt - Al_2O_3$ catalysts of varying acidity (varying Cl^-) content and at temperatures between 485 and 515°C with WHSV between 6 and 18. In all cases n-heptane was used as liquid feed, with a H_2:hydrocarbon molar ratio of 8 to accelerate the deactivation. They showed that after 24 hours of continuous operation or about 1000ml of n-heptane processed, the initial value of chlorine content did not change and hence it was not necessary to add chlorine to maintain its concentration in the catalyst. Nora Figoli also showed that catalyst with Cl^- content between 0.8-0.9 was most stable under the conditions of their investigation.

The deactivation-reduction cycles reported here were performed without a conscious

effort at maintaining the chlorine level constant. The total period of reaction for the 52 cycles is 264 hours. The total duration of other runs reported here were 187 hours and 107 hours for experiment set 6 and set 7 respectively. Therefore, the chlorine content could have changed, given the very long periods of continuous operations. However, two experimental evidence support the fact that the chlorine content could not have affected the coking results: the coking profiles were either found constant with time or behaved in a manner that was far from being progressively lower with time. If significant reduction of the chlorine content occurred, it will be expected that the coke deposited on the catalyst surface would progressively decrease with time on stream.

6.1.2 Titration Experiments for Catalyst Characterization

Titration experiments, done after each cycle, served to probe the changes on the catalyst surface. The characterization of the catalyst was done by hydrogen chemisorption on the catalyst surface. The occurrence of oscillations in the amount of uptake with pulse number was unexpected (Figures 39 and 40). The oscillations could be due to accompanying reactions. Theoretically, pulsed hydrogen could react with the available oxygen held to the Pt metal or with carbon. If it reacted with carbon it would yield methane by the following reaction,

$$C + 2H_2 \rightarrow CH_4$$
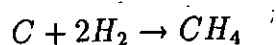
. The methane producing reaction must have been significant enough to have produced the oscillations observed during the pulse experiment. And in fact the oscillations were so similar to the oscillations ascribed to the layered structure of toxic coke typified by Figures 8, 11, 12 and 13.

From the residual activity determination, the Turn Over Number (TON), which

is the rate of product per site, varied from $383.6 hr^{-1}$ at a dispersion of 0.36244 to $2137.9 hr^{-1}$ at a dispersion of 0.2483 for cyclohexane deactivation runs in N_2, Table 10. The TON is useful in defining structure sensitivity and insensitivity in heterogenous catalysis. Boudart(23) proposed that, for structure sensitivity, TON's should differ by more than a factor of 5-10 when the dispersion is varied sufficiently. He did not specify what ~~constituted~~ constituted a sufficient variation. It could then be assumed, from the Boudarts' criterion that the dehydrogenation of cyclohexane to benzene may be structure sensitive.

The results of the titration experiments reveal that during the multiple deactivation and regeneration scheme, sintering and redispersion occur during the prolonged reduction process and during the oxidation process (Figures 56 and 57). It is also clear that the dispersion after oxidation following deactivation is higher than the dispersion after reduction. In other words, the catalyst sinters during the reduction process. The average decline in dispersion, per cycle, from oxidation to reduction is 39.25%. Turkevich et al. (95) showed that redispersion after H_2 treatment can be induced by reoxidation for all catalyst he experimented with. Sienghard Wanke(93,94) carried out sintering studies on fresh samples of Pt, Ir and different mixtures of Pt and Ir at temperatures of 300, 400, 500, 600, 700 and $800°C$ and measured the dispersions in $situ$ at room temperature. He observed, as in this work, that the dispersions on O_2 treatment was higher than the dispersion after treatment in H_2 at different or at constant temperatures. While the dispersion during O_2 treatment remained constant for upward of 50 hours, the dispersion in H_2 declined at temperatures above $500°C$ according to Sienghard Wanke's study(93).

The temperature of occurrence of sintering has been a subject of controversy. Keith(101) reported redispersion of platinum crystallites on a commercial Pt on alumina catalyst heated in dry air around $510°C$ or in 11 atmosphere around $580°C$. According to his

221

studies, temperatures higher than $580°C$ caused sintering. It is the belief of Keith(101) that below a critical temperature a Pt-alumina complex existing in an oxidized state is stable and responsible for redispersion. Turkerich et al. (95) also showed that the Engelhardt commercial Pt on alumina maintained a constant dispersion up to $450°C$. The dispersion beyond $450°C$ was not investigated.

The dispersion of the catalyst in this work, as measured after oxidation, was found to be constant for about 6 runs before redispersion started occuring during oxidation (Figure 56). This finding is analogous to the results of Ruckestein and Chu(102) who observed that it took several cycles of alternating heat treatment at $750°C$ in O_2 and H_2 atmospheres of $Pt - Al_2O_3$ before Pt redisperse during the oxidation step and that thereafter redispersion or sintering could be reproduced periodically by changing the atmosphere from an oxidizing to a reducing one. The conclusion of Ruckestein and Chu(102) were hence clear, and in line with the results obtained here - the crystallites redisperse during the oxidizing step and sinter during reduction. The reasons proferred to explain redispersion by various authors have been as varied as the temperatures at which redispersions are believed to occur. A few will be reviewed here. Ruckestein and Chu's explanation will be reviewed in greater detail here owing to the very close similarity of their results with the one obtained here.

Ruckestein and Chu(102) proposed two mechanisms to explain redispersion:

1. fracture of crystallites.

2. spreading of Pt oxide formed in the oxidizing atmospheres over the surface of the support.

Ruckestein and Chu explained the fracture of crystallites mechanism by the stability theory of Ruckestein and Dunn(103). This theory ascribes the fracture of crystallites as

222

a response to pertubation in the film existing between the support and the crystallites. Accordingly, oxidation of platinum to platinum oxide generates an internal stress and decreases the film-gas surface tension. Fracture occurs when the internal stress is larger than a critical stress. Rapid cooling is also known to generate internal stress because of differences in the internal thermal expansion coefficients of the metal and support and thus can induce fracture.

In explaining spreading, the first point to note according to the theorists (Ruckestein and Dunn(103)) is that the surface tension of metal oxides is lower than that for the metal. The prerequisites for spreading is the enhancement of the oxidation of the small crystallites due to the probable generation of some porosity in the crystallites during the first five or six cycles of heating in O_2 and H_2 atmospheres. This also produces some surface reconstruction. Redispersion then occurs in the oxidizing atmosphere by the mobility of the Pt oxide over the surface of the support. Spreading occurs either because no wetting angle can exists between the oxidized crystallites and support or most probably because a two dimensional fluid of Pt oxide can exist with the crystallites.

In this work, unlike in the studies of Ruckestein and Chu(102), the temperature at which oxidation was carried out was different from that at which H_2 treatment was carried out. Oxidation was done at $430°C$ after reaction at the same temperature and hydrogen reduction was carried out at $500°C$. In view of the alternating temperatures, a thermodynamic element is introduced to explain this result. A thin film is known to exist between the metal crystallites and the support (101,103). Reduction at a higher temperature $500°C$ does two things to the oxide film. It reduces the volume of the film and then increases the surface tension. Since the cohesive forces between the crystallites is greater than the adhesive forces between the crystallites and the support, the crystallites will be pulled together during the drying up process rather than remain at their

223

respective locations. While this results into an effective increase in the cluster radius of the metal crystallites and hence sintering, it results into a cleaner catalyst surface. On reducing the temperature to $430^{\circ}C$ at which the titration experiments were carried out, the reverse effect takes place. The sudden cooling leads to a rapid volumetric contraction resulting in the developments of lines of weakness in the interatomic boundaries in the crystallites which are aggravated during the reaction and deposition of oxidizable coke leading to fracture and redispersion of the crystallites. Whatever interactions may be proposed to be occuring between the metal and support, the overall effect as a result of alternating oxidation and reduction at markedly different temperatures of 430 and $500^{\circ}C$, ($70^{\circ}C$ difference) will certainly be to impart to the $Pt - Al_2O_3$ specimen a behaviour associated with elastic bodies. Hence failure of the dispersion after oxidation to stay constant after 6 runs may be due to the gradual setting in of such 'elastic' behaviour as a result of some reversible structural defects.

If the dispersion is higher with higher coke content as suggested by the results of the mortality studies then, it may seem that the oxidizable coke must be catalyzing its own deposition. Therefore, at the end of the deactivation the metal crystallites, though covered with coke, have been spread apart from each other owing to the increase in the metal suport film thickness. This brings to question, the actual commencement of dispersion as measured after the oxidation process. When does the redispersion start? Is it during the reaction or during the oxidation? Results of titration experiments done before and after oxidation at $430^{\circ}C$ and after reduction at same temperature, showed that the dispersion after deactivation before oxidation was 0.4734 and after oxidation was 0.533 while that after reduction was 0.4426 ($12^{th}cycle$ of experiment set 10). This could mean that redispersion as observed after oxidation may effectively commence during

224

reaction. Hence it follows that redispersion

$$after\ oxidation > after\ deactivation > after\ reduction$$

. The result of this experiment is not conclusive because it was only done in the 12th cycle in experiment set 10 which had a total of 12 cycles. Formation of coke with catalytic activity as suggested above has been reported by R. Fiedrow et al.(104) during oxidative dehydrogenation of ethyl benzene. During the oxidative dehydrogenation reaction, it was observed that the catalytic activity of $\gamma - alumina$ initially increased with a rise in coke coverage and then stabilize to what they(104) termed quasi stationary activity. The latter term reflected their view that the chemical composition of this oxygen-rich coke was also a factor in the activity exhibited.

If dispersion is the index of catalyst life-time, it is surprising that sintering that occurs during hydrogen treatment did not lead to a correspondingly decreased catalyst life time thereafter. In fact the highest deactivation times occured during the runs with low dispersion (Figures 56). Several explanations can be attempted. It may be that at the temperature of $500°C$ that the hydrogen chemisorption is carried out, the Pt atoms have adopted a configuration that allows them catalyze a reaction but lack the ability to chemisorb hydrogen.

Alternatively, the occurrence of the high deactivation times at low dispersions may be due to the fact that dehydrogenation of cyclohexane on $Pt - Al_2O_3$ is structure insensitive despite evidence from Boudart's Turn Over Number(TON) criterion(23) earlier on discussed, or if it is structure sensitive, it may be with respect to specific character-istics like the existence of steps and kinks as reported by Somorjai(19,20). According to Boudart et al.(105), coke tends to mask structural changes on the catalyst surface. Hence it may account for the structure insentivity observed here.

225

Evidence abound in literature that the lowering of dispersion as observed during hydrogen treatment in may not be the true representation of the state of the catalyst surface. As part of a broad report on the effects of hydrogen-metal interactions, Paàl and Menon(106) reviewed the results of H_2 chemisorption experiments by various workers in which sintering was reported to have occured while analytical techniques revealed otherwise. Of particular relevance were the works of Dautzenberg et al. (107), Tauster et al.(108) and Turkevich et al.(95).

First of all, hydrogen-metal interactions are responsible for the dependence of stoichiometric ratio of chemisorbed H_2 to chemisorbed O_2 to H_2 on duration of reduction (Freel,(68)), on temperature of gas titration (Wilson and Hall(79)), and on hydrogen pressure. Dautzenberg and co-workers(107,109) found that during the heat treatment of $Pt - Al_2O_3$ catalysts in H_2, above 770K, a certain fraction of the surface Pt atoms becomes 'inaccessible', and causes a decrease in H/Pt ratio, sometimes interpreted as sintering of Pt. The extent of Pt (% by weight) rendered inaccessible to H_2 at 950K for 10 hours, for example, was found to be 60%. On examination by electron microscopy, there was no indication of any appreciable change in particle size during pretreatments with H_2. Dan Otter and Dautzenberg(109) suggested that the inaccessible part of Pt might have been due to a reversible surface combination between reduced Pt and reduced Al to form some sort of superficial alloy; a mild oxidation at 670k to 770k could restore the catalyst back to its original state with all the surface Pt atoms once again accessible for chemisorption of H_2.

Turkevich et al.(95) observed this decrease in Pt dispersion as measured by H_2 chemisorption, on exposure of $Pt - Al_2O_3$, $Pt - SiO_2$ and $Pt - NaY$ Zeolite catalysts to H_2 at 570K to 720k and the restoration of the original dispersion on oxidation at 570k and reduction at 270k. They ascribed this loss of dispersion and loss of a number

of catalytic centers to a decomposition of Pt particles or clusters into molecular forms involving Pt diads on silica.

Tauster et al. (108) found that reduction of noble metals supported on TiO_2 at 470K produced well dispersed metals while reduction of the same materials at 770k decreased H_2 and CO chemisorption to near zero in all cases. Strangely enough, Election Microscopy and X-ray diffraction showed that the loss of chemisorption capacity was not due to any sintering or agglomeration of the metal particles in the TiO_2 surface. From these results Tauster et al.(108) concluded that a Strong Metal Support Interaction (SMSI) was occuring on exposure of the $Pt - TiO_2$ and other catalysts to H_2 at higher temperatures.

The results of Dautzenberg(107) were contested by Graham and Wanke (110). These authors studied the thermal stability of supported metal catalysts. They measured the hydrogen uptakes on fresh samples of Pt and Ir supported on alumina after which the catalysts were treated in flowing hydrogen or oxygen at elevated temperatures above $300°C$. Thermal treatment times of 1 hour and 16 hours were used. The temperature range for treatment in O_2 was $300°C$ to $600°C$ and sintering in H_2 was done at $650°C$ and $800°C$. Graham and Wanke(110) never observed decreases in the H/Pt ratios of the magnitude reported by Dautzenberg and co-workers for treatment of $Pt - Al_2O_3$ catalyst in hydrogen at temperatures of $\leq 600°C$. On the basis of their observation, Graham and Wanke(110) reported that the anomalous results reported by Dautzenberg and co-workers may be due to the low temperatures at which they (Dauzenberg and co-workers) measured H_2 uptakes, $(-78°C$ and $0°C)$ and/or the relatively low evacuation temperature $(400°C)$ Graham and Wanke reasoned that evacuation at $400°C$ may be sufficient to remove adsorbed hydrogen from catalyst that have not been treated in H_2 at elevated temperatures, but according to Menon and Froment (111) desorption of H_2

227

becomes more difficult after $Pt - Al_2O_3$ catalyst have been exposed to high temperatures. Menon and Froment(111) also even found that the changes in H_2 desorption behaviour are not due to metal support interactions.

If the observations in this work regarding the occurence of sintering are real with no occurrence of anomalies as reported by Dautzenberg(107,109) and co-workers and Tauster et al.(108) then this author is inclined to ascribe the long deactivation times during the runs with low dispersion (Figure 56) to the cleaner catalyst surface since high toxic coke removal characterised those runs. Dispersion seems to be a different concept from clean catalyst surface. This fact is also supported by Sinfelt and Yates (112). They investigated the specific activity of rhodium for ethane hydrogenolysis as a function of state of dispersion of rhodium and reported that effects on catalytic properties only became important when extreme conditions were considered. Similarly, Boudart and co-workers (23) concluded that the specific activity of platinum for the hydrogenation of cyclopropane was effectively independent of the degree of dispersion of the platinum over a very broad range of activities.

Hence, from the preceding discussions we can conclude that generally no corelations exists between dispersion and activity. The constancy of the activity, despite the low dispersion, means that the dehydrogenation of cyclohexane to benzene, despite evidence suggesting the contrary, may fall within the group of reactions termed facile reactions. Boudart(23) defines facile reaction as those that fail to sense the non uniformity of solid surfaces. These are the reactions which are commonly referred to as structure insensitive reactions. Hence, while there could be no correlation between dispersion and activity, such lack of correlation should be limited to facile reactions or structure insensitive reactions. This author therefore concludes that for structure insensitive or facile reactions, a clean catalyst surface is a more crucial factor than dispersion in determining catalyst

activity and life time.

More significantly, this author can conclude, in the absence of any means of validating the possible occurence of Dautzenbergs anomalies, that the prolongation of catalyst lifetime from 22 cycles in a previous work to 52 cycles in this investigation as seen in our mortality studies derives from the maintenance of a cleaner catalyst surface through prolonged secondary coke removal which leads to sintering. Unfortunately, this improvement in catalyst lifetime by this procedure may be limited to facile reaction.

On the whole, this experiment has shown that the catalyst surface is very unstable and changes with cycle without affecting the activity for facile reactions.

6.2 MODELLING RESULTS

6.2.1 Catalyst Regeneration

Most commonly used industrial reforming catalysts are entirely precious metals or are precious metals on an inert or active support. Their high cost provides sufficient justification for the need to regenerate them and to study the limitations of the regeneration process. This is with a view to restoring the maximum possible activity. This is particularly so when it is realised that regeneration is never completely achieved as not all of the coke is removed. While it is possible to detect, via thermocouple networks, the existence of gross temperature gradients within a fixed bed, such measurements are really averages. J. J. Carberry(87) notes that the direct measurements of temperature and concentration is impossible. At present, the only alternative is computation based on existing relations obtained from experiments with either non reactive systems or those derived from theory.

As catalyst regeneration is generally considered to be a non-catalytic gas-solid re-

229

action, most workers have modelled catalyst regeneration by use of power law kinetics usually first order to the concentration of the solid reactant and first order to the concentration of the gaseous reactant: Weisz and Goodwin(55,56), Haggerbaumer and Lee(57), Sohn and Szekely(61). One of the most studied limitations of the regeneration reaction is the intraparticle diffusion of the regenerating gas through the porous catalyst. Surprisingly, most of the studies have not taken into account the effect of external mass transfer limitations though the effect of mass transfer limitations on gas-solid reactions are generally known(59). Secondly, despite evidence of catalytic oxidation of coke, few attempts have been made at modelling regeneration of coked catalyst by assuming the regeneration reaction to follow Langmuir-Hinshelwood kinetics. A pioneering attempt at modelling coke gasification by Langmuir-Hinshelwood kinetics was that of Effron and Hoelscher(60). They(60) studied the low temperature oxidation of graphite. They assumed the regeneration reaction to proceed by the formation, on the surface, of an oxygen-surface complex before reaction of the gas with carbon.

Hence, the regeneration model whose results are discussed here is deemed to give a complete desciption of the regeneration process as it took into account the external mass transfer limitations in addition to intraparticle diffusion and with the assumption of Langmuir-Hinshelwood kinetics. The model was solved numerically by the finite difference approximations to yield coke removal and reactant consumption profiles with time. The model assumed the regeneration of a uniformly coked spherical pellet.

Though developed for a spherical catalyst, the model is general as to accommodate particles of any known geometry, undergoing regeneration and with gas and solid products. As expected, coke consumption profiles were horizontal at small dimensionless times (Figures 63 to 64). At small dimensionless times $\theta = 0.05$, the regenerating gas has just contacted the catalyst and combustion is just at its initial stage, hence the coke

230

consumption profiles are horizontal lines as the coke consumption profiles are above 0.97. However, the coke consumption profiles reduce to about 0.82 at dimensionless time of $\theta = 3$. The gradual departure from the horizontal lines to S-shape at high dimensionless time reflects non uniform coke consumption caused by retardation of gas flow to the reaction interface due to intraparticle diffusional resistances encountered by the regenerating gas. As combustion proceeds and more of product is produced, the limitation to the flow of reactant gas due to the counter diffusion of the product gas becomes significant, leading to the flattening of the profiles towards the center, for the coke consumption profiles.

Wen (63) intergrated the general model with the assumption of only intraparticle diffusion and no bulk mass transfer limitation for a rate equation which was n^{th} order to the concentration of the gas and m^{th} order to the concentration of the solid concentration. A further assumption in Wen's model was equal access of the reactant gas at all radial possitions. Hence, for all values of dimensionless concentrations, he obtained straight horizontal lines as a result of the assumptions. Wen's variation of dimensionless time between the minimum and maxinim was just 5 fold whereas the variation of dimensionless time in this work, from 0.05 to 3 was 60 fold.

Weisz and Goodwin(55) showed that parallel coke profiles are obtained during the regeneration process in agreement with the results of Wen(63) and this work at low dimensionless times. On changing modified Biot number in this work, the bulk mass transfer, the change of the dimensionless coke from 0.82 at a modified Biot number of 10 to 0.88 at a modified Biot number of 0.05, for a modified Biot number change of 200 fold, was not an appreciable numerical change. For the highly exothermic reaction (most regeneration reactions are), and for surface reaction controlling, the reaction rate increases towards the zone of higher concentration of the solid reactant. If the process

231

were not limited by diffusion of the gas towards the reaction surface, then the profile would have been entirely straight lines towards the center of the pellet as Wen observed.

It is clear that for the model developed here, and for the parameters selected, the increase in interfacial resistance is not sufficient to offset the rapid reaction rate. Hence, for this model, the controlling parameter seems to be a combination of surface reaction and diffusion.

The similarity of the profiles developed in this work with well known established profiles such as those of Wen(63) for the general model and Weisz and Goodwin(55) for the shell progressive model shows that the regeneration process is also adequately modelled by assumptions of Langmuir-Hinshelwood kinetics. This similarity may indicate a very weak surface adsorption of the reactant gas and hence confirms the validity of the assumption of Effron and Hoelscher(60) who approximated their reaction scheme to a power law as a result of the assumption of weak adsorption of surface-oxygen complex in their analysis of the oxidation of graphite.

6.2.2 Multilayer Coking Model On Real Surface

The multilayer coking model on real surface was developed by the introduction of suitable modifications of the Klingman's multilayer coking model to reflect the energy variation due to the non uniformity of the real surface. The multilayer coking model ralates the coke content as a function of activity. The parameters in the multilayer coking model on real surface were successfully lumped and estimated with experimental data of residual activity after coking of $Pt - Al_2O_3$ in a CSTR, (Table 10). This is the very first time, known to this author, that the multilayer coke parameters would be estimated for the specific case of $Pt - Al_2O_3$ data in a CSTR.

A comparison of the metal prediction showed that the monolayer coverages for the real

surfce was 0.025g carbon while that on ideal surface was 0.0128g carbon. To appreciate the implications of this result, it is pertinent to recall first of all the considerations and assumptions leading to the development of Klingman and Lee's multilayer coking model. It should be recalled that the model takes root from the gas adsorption on multilayers as presented by Branauer, Emmet and Teller(BET)(64), the BET development itself being an extension of the Langmuir adsorption isotherm. The Langmuir isotherm relates the uptake of gas with increase in pressure up to the adsorption of a monolayer. On adsorption of a monolayer of gas, a much lower energy barrier is presented against further adsorption of a second layer. However, BET theory further extends this Langmuir theory to the case for the adsorption of subsequent layers. The BET theory explained the non linear region in the Langmuirs isotherm as due to multilayer adsorption of gas. Analogous to the multilayer gas adsorption, the deactivation of a reactive surface by the uptake of coke in multilayers was presented by Klingman and Lee. The major assumption, at variance with the reality of a reactive surface, is the uniformity of the surface. Evidence abound that the surface is not uniform(16,19,20). By assuming surface uniformity, Klingman and Lee's(41) multilayer coking model by extension, assumed that the energies of adsorption of subsequent gas molecules and layers were the same. The multilayer coking model on real surface, however, by eliminating that assumption is a much more realistic model.

It is with the above background that the differences in the parameters between the multilayer coking on real surface and ideal surface are easily explained. Simply, the higher monolayer coke coverage Q, in the multilayer coke on real surface means it requires much more coke to provide complete monolayer coverage. Somorjai's surface model(19) shows that reactive surfaces are generaly characterized by corners, kinks, and spaces which coke species have to fill to attain monolayer. From the data of the coke

233

deposition on $Pt - Al_2O_3$ in a CSTR, the multilayer coke model on real surface was seen to predict the experimental coke profile although the model predicted a higher coke than the experimental at higher activities (Figure 61). It then required the application of the finite layer assumption to predict the coke in the entire range of activities. The lumped parameter, β', deactivation parameter for coking on real surface was estimated to be 4.2 while $\overline{K_p}$ was 4.0 on ideal surface. From chapter 3

$$\beta' = \frac{k_{p_c}}{k_{p_1}} \cdot \frac{1}{(1+G)^n}$$

and the equivalent for ideal surface coking (Klingmans and Lee's model) is

$$\overline{K_p} = \frac{K_p}{(1+G)^n}$$

The values 4.2 and 4.0 can be said to be the same. This is probably due to the much lower energy required to deposit the second and subsequent layers of coke. From the theory of coking, once deposited, the coke acts as centers for further deposition(104) particularly for this analysis where it is assumed that the main and coking reactions take place on the same sites. Hence the deactivation parameters could not have been expected to be much different.

6.2.3 Modelling Of Reaction-Deactivation Kinetics Of Cyclohexane

Parameter estimation of the reaction deactivation kinetic model for $h = 1$ and $h \neq 1$ was carried out by the non-linear regression routine the modifed Nelder and Mead non-linear regression routine(Flexible Polyhedron). The models were dynamic models and used deactivation run data on fresh catalyst. The parameter estimation was carried out by a method that did not require decoupling of the main reaction from the coking reaction.

234

On confronting the data with the models, they were found to give a good fit for the entire period of the run. h is the number of active sites participating in the coking reaction. The standard derivation for the model with $h = l$, is 10% while that for $h \neq 1$ is 12%. None of the models is superior to the other. For having a lower standard deviation, however, the model with $h = 1$ is prefered to that with $h \neq 1$.

Deactivation parameters estimated without decoupling the model are found to be accurate and hence constitute an alternative method of estimating paramaters accurately and doing so with a lower number of runs. The model formulation has also been able to compute an estimate of the level of residual activity after catalyst deactivation. A high value of the partial deactivation constant, f, as was obtained in the analysis 0.948 and 0.917, indicates low residual activity i.e (1-0.948) (1-0.917) respectively. This of course implies a very efficient utilization of the active sites and good control of the operating conditions during deactivation runs.

Estimation of reaction-deactivation kinetic model parameters by a similar computational procedure are rare in literature. The only one known to this author is that of Forzatti and Ferraris(42). Forzatti and Ferraris studied the reaction-deactivation kinetics of methanol oxidation over a silica supported $Fe_2O_3 - MoO_3$ catalyst in a plug flow reactor. They described the reaction- deactivation kinetics of $Fe_2O_3 - MoO_3$ with two models. The models were derived by a consideration of two deactivation mechanisms based on the chemical investigation of the deactivation of the fresh and deactivated $Fe_2O_3 - MoO_3$ catalyst by Carbucicchio et al.(84). The parameters of the model were simulated with the same procedure used here. Both models gave good predictions and the mean percentage error for the models were 15.97% and 13.48%.

This work has proved that the methodology for the straight-forward simultaneous determination of both reaction kinetics and decay rates, without decoupling the main

235

reaction from the decay, used by Forzatti and Ferraris for an intergral reactor data is also applicable for the system examined here with success. This success has demonstrated the reliability of the reaction deactivation model developed. Both models were found to adequately represent the deactivation data.

Chapter 7

CONCLUSIONS

The following conclusions have been drawn from the results of the investigation.

(1). Comparing the mortality studies results in this work and that of Omoleye and Susu(6), toxic coke removal in the highest possible quantity is responsible for the prolongation by more than two fold (22 cycles in a previous work to 52 cycles here) of the life of the catalyst. Hence a balance is necessary between the savings from the added life time of the catalyst and the cost of hydrogen. A more than two fold increase in catalyst life time is evidently in favour of more investment in hydrogen especially since hydrogen is generated during the reforming process.

(2). The secondary coke is confirmed to be deposited in layers on the catalyst surface and consists of several types with varying reactivity in H_2. Five types were clearly distinguishable here. Three of them were similar to the three deposited on $Pt - Al_2O_3$ catalyst during MCP reforming (9). All five layers deposited here occured within the same time as the three deposited in MCP(9). Therefore the number of reduceable cokes formed may be dependent on the coking propensity of the reactant while the type of reduceable coke formed is not.

237

(3). After prolonged removal, not all the coke could be removed confirming the existence of three types of coke deposited on the catalyst surface. The first, oxidizable coke, removed by oxidation in air. The second, reduceable coke, removed by reduction to methane and the third, tertiary coke, is resistant to both oxidation and reduction and hence suggested to be graphitic in nature. The tertiary coke is found to lie closest to the catalyst-coke interface.

(4). Omoleye and Susu found that three stability states occured in the oxidizable coke level per cycle. In this investigation, however, the level of oxidizable and toxic coke per cycle is characterised by oscillations in between some fairly stable intervals. Characterization of the catalyst surface with each cycle in this work has revealed the occurence of redispersion which indicates the instability of the catalyst surface and the probable cause of the oscillations in oxidizable and toxic coke with cycle number.

(5). This work confirms the postulated coking sequence of Osaheni and Susu

$$Coke\ precursor \rightarrow oxidizable\ coke \rightarrow toxic\ coke \rightarrow tertiary\ coke.$$

Coke formation, in whatever location it occurs, follows the above sequence. Consequently, coke of a particular level of C/H at a given location is due to the properties of the location (Brønsted or Lewis acid sites).

(6). No clear cut correlations between catalyst parameters exist. Where correlations exist, they are dependent on too many conditions. Even the location of coke, as concisely shown by J. Barbier(17) changes with process conditions - pressure, temperature, reactant flowrate etc. Hence the results from a reactive surface is an interplay of a lot of factors many of which may not be easily understood.

(7). No correlation exists between activity and dispersion. The deactivation times were found to be highest in the cycles characterized by the lowest dispersion and highest

toxic coke removal. Hence highest toxic coke removal was responsible for high activity and hence determining the catalyst life-time. This confirms the conclusions reached in this work and by others before (6,7,9,16,34) that toxic coke is responsible for the catalyst mortality. Toxic coke is therefore more crucial in determining catalyst life-time than the level of dispersion. The relationship between dispersion and activity has generated so much controversy. The conclusion from this work is clear - no correlation is found to exist between activity and dispersion.

(8). During multiple deactivation-regeneration cycles, the catalyst sinters during reduction and redisperses during oxidation. Using our scheme and conditions it takes about 6 cycles to produce redispersion during oxidation.

(9). The multilayer coking model on real surface adequately describes the data of residual activity and coke content. From the model, the monolayer coke coverage has been evaluated to be 0.025g coke as against 0.0128g coke for the ideal surface. The difference between the values have been explained.

(10). The computational technique in reaction-deactivation kinetic modelling which gives a straight forward prediction of decline in rates, without decoupling the coking reaction from the main reaction has been successfully applied. The technique was first used by Forzatti and Ferrari for models developed from a chemical investigation of the deactivation of $Fe_2O_3 - MoO_3$. In this work it was used on models developed from a mechanistic investigation of the deactivation of $Pt - Al_2O_3$ catalyst. None of the models developed here is better than the other, though on statistical grounds, the model with the number of active sites in the coking reaction, $h = 1$, is better. It may be appropriate to propose that deactivation by coking in this work occured preferably by a single site mechanism of the rate controlling step of the coking reaction.

Chapter 8

REFERENCES

1. J.M. Smith,"Chemical Engineering Kinetics", Mcgraw-Hill, Inc., Third Edition, (306)1981.

2. G.C. Bond,"Principles of Catalysis", *The Chemical Society, London(1972).*

3. H.A.C.M. Hendrickx, "Adsorption and Reactions of Simple Gases on Pd and I.R.Study", Conference Proceedings, University of Leinden, Leinden, Holland, January(1988).

4. M.J.P. Botman,"Pt and Pt/Re Catalysis in Hydrocarbon Reactions: The Influence of the State of Pt and Re", Conference Proceedings, University Of Leinden, Leinden, Holland, June(1987).

5. S.J. Thomson and G. Webb,"Heterogenous Catalysis",University Chemical Texts, T.L.Cottrell(ed.),Oliver and Boyd LTD, Edinburg and London(1968).

6. Omoleye, J.A. and Susu, A.A.,"Effect of Coking Levels on Reforming Catalyst Mortality, $Pt - Al_2O_3$ Catalyst", *(Submitted for Publication).*

7. James Omoleye,"Ph.D Thesis",University of Lagos,1986

8. E.Broekhaven and V. Ponec,"Mechanisms of Skeletal Reactions of Hydrocarbons on Metals",*Progress in Surface Science, Vol. 19(4)(1985)*.

9. Osaheni, J.A; Onukwuli, D.O; Susu, A.A,"Estimation of Toxic Coke Deposits on Fresh and Regenerated $Pt - Al_2O_3$ Catalyst from MCP Reforming in H_2 and N_2 Atmospheres", Proceedings of Conference on Chemical and Process Engineering for Development held at the University of Dares Salaam, 17-21,September 1990, Pp 209-217.

10. A.I.M. Keulemans and G.C.A. Schuit,"The Mechanisms of Heterogenous Catalysis",*J.H. de Boer (ed.), Elsevier, Amsterdam(1960)*.

11. G.A. Mills; H. Heinemann; T.H. Milliken and A.G. Oblad, *Ind.Eng.Chem. 45,134(1953)*.

12. J.R.Anderson, Nature(London)187,937(1960).

13. Z. Paalm *J.Catalysis 3,129(1964)*.

14. M.J. Sterba and V. Haensel,*Ind. Eng. Chem. Prod. Res. Dev., 15,2(1976)*

15. A.D van Langefieveld, F.C.M.J.M.van Delft and V.Ponec, *Surface Sci., 135, 93(1983)*.

16. J.Biswas, G.M. Bickle; P.G.Gray and D.D. Do,"The Role of Crystallite Structure on Mechanisms of Coke and Sulphur Poisoning in Catalytic Reforming",*(Submitted for Publication)*.

17. J.Barbier, "Coke of Reforming Catalysts",Catalyst Deactivation, B. Delmon and F.Froment (eds) Elsevier, Amsterdam(1987).

18. J. Barbier; P. Marercot; N. Martin; L. Elassal; and R. Maurel, "Selective Poisoning by Coke Formation on $Pt - Al_2O_3$," Catalyst Deactivation, B.Delmon and F.Froment(eds.),Elservier,Amsterdam,93(1980)

19. G.A. Somorjai, "Atomic and Molecular Processes at Solid Surfaces", *J.of Colloidal and Interface Sci., Vol.58,No 1(1977).*

20. G.A. Somorjai, "Correlations between the Structure and Reactivity at Solid Liquid Interfaces," Reviews and News, *J. Electrochem. Soc. 154,205(1977).*

21. P.P Lankhoerst; H.C.de Jongste and V. Ponec, "Particle Size and Carbon Deposition Effects in the Hexane Reforming Reactions" Catalyst Deactivation, B.Delmon, G. Froment(eds) Elservier, Amsterdam(1980).

22. A. Sarkany, "Carbon Poisoning of $Pt - SiO_2$ Catalysts", Presented at the 4th International Symposium on Catalyst Deactivation, 29th Sept. 1 Oct.(1987), Antwerp(Belgium).

23. M. Boudart; A. Aldag; J. Benson; A. Dougharty; C. Girvin, "On the Specific Activity of Platinum Catalysts", J. Catal. 6, 92(1966).

24. Agwaral P.K; Fitzharris W.D; Katzer J.R.; Catalyst Deactivation, B. Delmon and F. Froment (eds)Elsevier, Amsterdam,179-199(1980).

25. Voorhie A. Jr. "Carbon Formation in Catalytic Cracking" *Ind. Eng. Chem. 37, 318-322 (1945).*

26. Wojciechowski, B.W.,*Can. J.Chem.Eng.46,48(1968).*

27. J.Barbier; P. Marecott; N. Martin; L. Elassal; Maurel R.; Catalyst Deactivation B.Delmon and F.Froment (eds), Elsevier, Amsterdam,53-62(1980).

28. F.Froment and Bischoff *Chem. Eng. Sci. 16, 189(1961)*.

29. Dumez and Froment *Ind. Eng. Chem. Proc. Des. Dev.,15,291(1976)*.

30. Nora Figoli; Marrio Sad; Jorge Beltramini and Estanislo Jablonski, Jose Perara, "Influence of the Chlorine Content on the Behaviour of Catalyst for n-Hexane Reforming".,*Ind. Eng. Chem. Fund. 551,19(1980)*.

31. Svajgl, O., *Intern. Chem. Eng., 12,55(1972)*

32. Parmaliana, Frusteri, Nesterov, Paukshtis, Giordano, "Effects of Chlorine content on coking and Catalyst Self-Regeneration" *Submitted for Publication*

33. Cooper B.J., Trimm D.L., "Coking in $Pt - Al_2O_3$ Reforming Catalyst", Catalyst Deactivation, B. Delmon and F. Froment (eds) Elsevier, Amsterdam, 63-71(1980).

34. Szepe S. and Levenspiel O. "Proceedings, Fourth European Symposium", Brussels (1968), Pergamon Press, London, 1971.

35. Levenspiel, O."Experimental Search for a Simple Rate Equation to Describe Deactivating Porous Catalysts", *J. Catal. 25, 265(1972)*.

36. Eduardo E. Wolf and Eugene E. Peterson.,"On the Kinetics of Self-Poisoning Catalystic Reactions" *J. Catal. 47, 28(1977)*.

37. Corella, J and Asua, M.,"Kinetic Equations of Mechanistic Type with Non-separable Variables For Catalysts Deactivation by Coke. Models and Data Analysis Methods". *Ind.Eng.Chem.Proc.Des.Dev.,21,55-61,(1982)*.

38. Susu, A.A.; Enow, F.E. and Ogunye A.F. "Cyclohexane Dehydrogenation Kinetics on a Platinum-Rhenium/Aluminium Oxide Catalyst with Hydrogen and Inert Diluents" *J. Chem. Tech. Biotech., 30,(735-747)(1980)*.

39. Eciyoga E. and Toyota K., *Kogaku Kogaku, 32, 1005(1968)*.

40. Blackeley, D.W.; Somorjai, G.A., *J.Catal. 43,181(1976)*.

41. Klingman and Lee, "Catalyst Deactivation by Multilayer Coking: A Kinetic Model", *A.I.Ch.E. Vol.32, 2(1986)*.

42. Pio Forzatti and Buzzi Ferraris, "Reaction-Deactivation Kinetics of Methanol Oxidation over a Silica-Supported $Fe_2O_3 - MoO_3$ Catalysts", *Ind. Eng. Chem. Proc. 21,67-73(1982)*.

43. Butt, J., "Catalyst Deactivation", *Adv.Chem.Ser. 109,259(1972)*.

44. Eberly P.E.; Kimberlin, C.N.; Miller W.H. and Drushel H.V., "Coke Formation on Silica Alumina" *Ind. Eng. Chem. Proc. Des. Dev., 5, 2(1966)*.

45. Wheeler, A. and Robell A.J. "Performance of Fixed Bed Catalytic Reactors with Poison in the Feed" *J. Catal. 13, 299 (1969)*

46. Bohart and Adams "Adsorptive Properties of Synthetic Resins" *J. Soc. Chem. Ind., (1935),541T*

47. Carberry, J.J "Chemical and Catalytic Engineering", McGraw-Hill, New York, 356 (1976)

48. M. Masai; K. Noma; Miyamoto M.; H. Kaibara; S. Tsuruya, "Effect of Coke on the Dehydrogenation Activity of Pd-Sn-Silica"., *Applied Catalysis 4, (1982)83-86*.

49. S. Uchida; S. Osuda and M. Shindo, "On the Dehydrogenation Reaction of n-Butane with the Deactivation of Alumina-Chromia Catalyst, "*Can. J. Chem. Eng. 53, 666 (1975)*.

50. Otake T. and Morita Y., *Advances in Catalysis 68,58(1965)*.

51. R.Toei, *Symposium of Soc. of Chem.Eng.Japan (1963)*.

52. Charles L. Thomas,"Catalytic Proceses and Proven Catalysts", Academic Press Inc., New York and London(1970).

53. E. W. Thiele "Relations between Catalytic Activity and Size of Particle" *Ind. Eng. Chem. 31, 916(1936)*

54. Alborn Wheeler "Reaction Rates and Selectivity in Catalytic Pores" *Advances in Catalysis III, 249(1951)*

55. Weisz P.B. and Goodwin R.D.,"Combustion of Carbonaeceous Deposits within Porous Catalysts Particles

(I) Diffusion-Controlled Kinetics.", *J. of Catal. 2,397-404(1963)*.

56. Weisz P.B. and Goodwin R.D.,"Combustion of Carbonaeceous Deposits within Porous Catalyst Particles

(II) Intrinsic Burning Rate" *J. Catal. 6,227(1966)*

57. Haggerbaumer, W.A. and Lee R., *Oil and Gas J. 45,76,(1947)*

58. Pansing, W.F., *A.I.Ch.E J. 2,71 (1956)*

59. Charles N. Satterfield "Mass Transfer in Heterogenous Catalysis" The Massachusette Institute of Technology (1970)

60. Edward Effron and H.E Hoelscher,"Graphite Oxidation at Low Temperature." *A. I. Ch. E. J. (10), 388(1964)*

61. H.Y. Sohn and J. Szekely,"A Structural Model for Gas-Solid Reactions with a Moving Boundary

    (III) A general Dimensionless Representation of the Irreversible Reaction between a Porous Solid and a Reactant Gas." *Chem. Eng. Sci.*, *27,763(1972)*

62. Froment F. Gilbert and Kenneth Bischoff B.,"Chemical Reactor Analysis and Design",John Wiley, New York,(1979)

63. Wen C.Y., "Non Catalytic Heterogenous Solid Fluid Reaction Model" *Ind. Eng. Chem. 60, 934(1968).*

64. S. Brunauer; P. H. Emmet and E. Teller, "Adsorption of Gases in Multi Molecular Layers", *J. Amer. Chem. Soc., 60,1309(1938).*

65. T.E. Whyte,*J. Catalysis Review.8(1)117-134(1973).*

66. Hans L. Gruber,"Chemisorption Studies on Supported Platinum", *J. Phys. Chem. 66,48(1962).*

67. John E. Benson and Michel Boudart, "Hydrogen-Oxygen Titration Method for the Measurement of Supported Platinum Surfaces Areas" *J. Cat. 4,704(1965).*

68. John Freel, "Chemisorption On Supported Platinum"

    I. Evaluation of a Pulse Method" *J. Catal. 25,139(1972).*

69. John Freel, "Chemisorption On Supported Platinum

    II. Stoichiometry for Hydrogen, Oxygen and Carbon Monoxide." *J. Catal. 25, 149(1972)*

70. Hans Gruber *Anal. Chem. 34, 1828 (1962)*

71. Roca F. de Moorgetes, and Tambouze, Y. *J. Gas Chrom. 6,161,(1968)*

72. H.A Beneresi, L.T Atkins and R.B Mosely "Rapid Measurement of Hydrogen Chemisorption", *J. Catal. 23,211(1971).*

73. L. Spenadel and M. Boudart J. Physical Chem. 41,103(1969)

74. Amenomiya,Y., "Adsorption of Hydrogen and $H_2 - D_2$ Exchange Reaction on Alumina" *J. Catal.22,169 (1971).*

75. Stephen F. Adler and James Keaveny *J. Phys.Chem.64,208(1960).*

76. D.Bianchi, M. Lacroix, G. Pajonk, S.J. Teichner"Catalytic and infrared Demonstration of the Effect of Hydrogen Spill over on a Gel of Silica." *J. Catal. 59,467(1979).*

77. R. Kramer and Andre "Adsorption of atomic Hydrogen on Alumina by Hydrogen Spill Over" *J.Catalysis. 58,287(1979).*

78. D.E. Mears and R.C. Hansford "The Stoichiometry for Hydrogen Titration of Oxygen on Supported Platinum", J. Catal. 9, 125(1967)

79. Geoffrey R. Wilson and Keith Hall, "Studies of the Hydrogen Held by Solids XVII Hydrogen and Oxygen Chemisorption on Alumina and Zeolites and Zeolite-Supported Platinum." *J. Catal. 17, 190(1967).*

80. Masayoshi Kobayashi; Yasunobi Inoue; Nobuo Takahashi; Robert L.; Burwell Jr; John B. Butt and Jerome B. Cohen;

"$Pt - Al_2O_3$

1.Percentage Exposed and its Effects Upon the Reactivity of Adsorbed Oxygen". *J. Catal. 64,74-83(1980)*

81. Robert J. Farrauto "Determination and Applications of Catalytic Surface Area Measurements". Proceedings of the A.I.Ch.E. National Meeting 77th June (1974).

82. T. Akehata; S. Namkong;H. Kubota and M. Shindo,"Effect of Intraparticle Temperature Distribution on the catalytic Effectiveness Factor of a Porous Catalyst" *Can. J. Chem. Eng. 127(1961)*

83. Prata and Lago "The Kinetics of Cracking of Cumene by Silica Alumina" *Advances in Catalysis VIII, 293(1951)*

84. Carbucicchio, M.; Cairati L.,; Ruggeri, O.; Trifiro, F., *Surf. Sci. Catal. 1979, 3,279*

85. David M. Himmelblau "Process Analysis by Statistical Methods" John Wiley and Sons Inc. 1970.

86. David M. Himmelblau "Applied Non Linear Programming" McGraw Hill, Inc. New York, Pp190-217,(1982)

87. J.J Carberry "Designing Laboratory Catalytic Reactors" *Ind. Chem. and Fundamentals. Vol 56, no 11(1964)(39-46)*

88. Octave Levenspiel "Chemical Reaction Engineering" John Wiley and Sons Inc. (1972) Second Edition.

89. Levenspiel O. *Ind. and Engineering Fund. Vol. 5,2(1966) 171*

90. C.O. Bennette, M.B Cutlip and Yara." Gradientless Reactors and Transient Methods" *Chem. Eng. Sci. 27,2255(1972)*

91. E.E. Wolf and F. Alfani, "Catalyst Deactivation by Coking" *Catalytic Review Sci., Eng. 24(3),329-371(1982)*

92. C.J. Plank and D.M. Nace, "Coke Formation and its Relationship to Cumene Cracking" *Ind. Eng. Chem., 47, 2374(1955)*

93. Sieghard E. Wanke "Sintering of Commercial Supported Pt Group Metal Catalyts" Progress in Catalysts Deactivation, Jose Luis Figueiredo(ed), Nato Advanced Study Institutes Series, Martnus Nijhoff Publishers, The Hague (1982)

94. Ryszard M.J Fredorow and Sieghard E. Wanke "The Sintering of Supported Metal Catalysts".

    1. Redispersion of Supported Pt in O_2 *J. Catal. 43,34(1976)*

95. L. Gonzalez-Tejuka, K. Alkai, S. Namba, and John Turkevich "Poisoning Titration Technique for Determining the Number of Active Centers in a Supported Platinum Catalyst" *J. Phys. Chem. 81,14,1399 (1977)*

96. J.J Carberry and Gorring, "Time-Dependent Pore-Mouth Poisoning of Catalyst" *J. Catal. 5, 529 (1966)*

97. Panchenkov and Golonov *Soviet Catalytic Reviews, 15(1957)*

98. J.D Bernal Proceedings of the Royal Society(Lond.), A106 (1924)749

99. N.S Figoli, J.N. Beltramini, E.E Martinelli, M.R. Sad and J.M. Perera "Operating Conditions and Coke Formation on $Pt - Al_2O_3$ Reforming Catalyst" Catalyst Deactivation, Delmon B., Froment (eds) Elsevier Publishing Company (1982).

100. P.Gallezot, C. Leclercq, J. Barbier, P. Marecot "Location and Structure of Coke Deposits on Alumina-Supported Platinum Catalysis by EELS Associated with Electron Microscopy", *J. Catal. 116,164-170(1989)*

101. Marvin F.L Johnson and Carl O. Keith "The State of Platinum in Reforming Catalysts" *J. Catal. 67(200)1963*

102. E. Ruckenstein and Y.F. Chu;"Redispersion of Platinum Crystallites Supported on Alumina- Role of Wetting",*J. Catal. 59,109(1979)*

103. E. Ruckenstein and Dunn C., *Thin Solid Films 51,43(1978)*

104. R. Fiedorow; W. Przystajko; M. Sopa and I.G. Dalla "The Nature and Catalyst Influence of Coke Formed on Alumina: Oxidative Dehydrogenation of Ethylbenzene *J. Catal. 68,33-54(1981)*

105. M. Boudart, G. Djega-Mariadassou; "Kinetics of Heterogenous Catalytic Reactions", Princeton University Press(1984)

106. Z. Paal and P.G. Menon, "Hydrogen Effects in Metal Catalysts" *Catalytic Rev-Sci. Eng., 25(2), 229-324(1983)*

107. F. M. Dauzenberg and H.B.M. Wolters."State of Dispersion Platinum Supported Catalysts" *J. Catal. 51,26(1978)*

108. S.J. Tauster, S.C. Fung, and R. L. Garten,"Strong Metal-Support Intractions. Group 8 Noble Metals Support on TiO_2" *J. Amer. Chem. Soc. 100,170(1978)*

109. G.J. Den Otter and F.M. Dauzenberg.,"Metal Support Interactions in $Pt-Al_2O_3$" Catalysts.*J. Catal. 53,116(1978)*

110. Andrew G. Graham and Sieghard E. Wanke "The Sintering of Support Metal Catalysts.

   III The Thermal Stability of Bimetallic Pt-Ir Catalyts Supported on Alumina" *J. Catal. 68, 1-8(1981)*

250

111. G.F. Froment and P.G. Menon, "Modification of the Properties of $Pt - Al_2O_3$ Catalyst by Hydrogen at High Temperatures" *J. Catal. 59, 138(1979)*

112. D. J. C.Yates and J.H. Sinfelt,"The Catalytic Activity of Rhodium in Relation to its State of Dispersion" *J. Catal. 8,348(1967)*.

Chapter 9

APPENDICES

Appendix A

Determination of metal Area, Metal Dispersion and average particle diameter by hydrogen Chemisorption Technique.

The metal area dispersion and particle diameter were calculated from the experimental data according to the stoichiometry proposed by Benson and Bourdart hydrogen chemisorption on oxidized platinum below.

$$Pt - O + 3/2H_2 \rightarrow Pt - H + H_2O$$
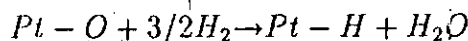
Dimension of sampling valve

$$Length = 42cm$$

$$Diameter = 1.5mm$$

$$Volume = \pi \frac{(0.15)^2}{4} \times 42 = 0.742cm^3$$

253

Assume Ideality

$$n = \frac{PV}{RT}$$

Operating Conditions:

$$P = 1 \ atmosphere$$

$$T = 30°C$$

$$R = 82.06 \frac{cm^3.atm.}{gm - mol.K}$$

- Reactor temperature $430°C$

- Saturator Temperature $14°C$

- Deactivation runs in $N_2, H_2, 100ml/min$

- Reactants-cyclohexane, methylcyclopentane

- Reduction temperature $500°C - 2 \ hours$

- TCD Temperature $70°C$

- Attenuation 1

- Catalyst weight 5 gms

The number of moles

$$n = \frac{PV}{RT} = \frac{1 \times V}{82.06 \times 303}$$

$$n = 4.02 \times 10^{-5} \times V$$

The number of particle $n = 4.02 \times 10^{-5} \times V \times$ Avogadros number

$$= 4.02 \times 10^{-5} \times 6.03 \times 10^{23}$$

Sample Calculation

For Run 1

$$\text{Average Hydrogen titre} = 0.7318cm^3$$

Hence the number of H atoms:

$$= 4.02 \times 10^{-5} \times 0.732 \times 10^{23}$$

$$= 1.774412 \times 10^{19}$$

- **Calculation of the Surface Pt atoms**

The chemisorption equation

$$Pt - O + (3/2)H_2 \rightarrow Pt - H + H_2O$$
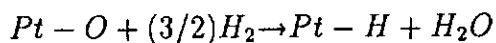
assumes that 1 atom of Pt is on the surface and interacts with one atom of oxygen or hydrogen.

From the stoichiometry:

$$(3/2)H_2 = 1.774412 \times 10^{19} \text{atoms H}$$

1 H atom from stoichiometry is equivalent to

$$\frac{1.774412}{3} \times 10^{19} \text{atoms H adsorbed}$$

Hence

$$1H \ atom = 5.914706 \times 10^{18} \text{atoms H}$$

Hence Pt surface atoms is $= 5.914706 \times 10^{18}$

$$\text{Number of moles of Pt } n = \frac{5.914706 \times 10^{18}}{6.03 \times 10^{23}} = 9.808799 \times 10^{-6}$$

- **Calculation of dispersion of Pt atoms or Support (Alumina)**

255

At weight

$$Pt = 195.05$$

and for $0.3Pt - Al_2O_3$

$$\text{Moles Pt} = \frac{0.003}{195.05}$$

$$= 1.538 \times 10^{-5}$$

$$\text{Dispersion} = \frac{\text{moles Pt surface}}{\text{Pt total moles}}$$

$$= \frac{9.808799 \times 10^{-6}}{1.538 \times 10^{-5}}$$

$$\text{Dispersion} = 0.637763$$

- **Metal Area Calculation**

Metal area occupied by hydrogen on Pt has been reported to be 11 Anstrong units. Area H on $Pt = 11 \times 10^{20} m^2$ Hence total area due to Pt

$$= 5.914706 \times 10^{18} \times 11 \times 10^{20} m^2$$

$$= 0.650617 m^2$$

$$= 6.50617 \times 10^3 cm^3$$

- **Average Cluster Diameter, d**

The average diameter is given by:

$$\overline{d_s} = \frac{6V}{A}$$

where V is the volume of metal and A the metal area. For monomettallic cluster of Pt atoms

$$V = \frac{m}{\rho}$$

where:

$$m_{Pt} = 0.003g$$

$$\rho_{Pt} = 21.45\frac{g}{cm^3}$$

$$A_{Pt} = 6.50617 \times 10^3 cm^2$$

Hence:

$$d_{Pt} = \frac{6(0.003/21.45)}{6.50617 \times 10^3}$$

$$= 1.28982 \times 10^{-7} cm$$

$$= 12.8982\mathring{A}$$

- **Calculation of Turn Over Number(TON)**

Turn Over number = Moles product per hour exposed mole of metals

$$TON = \frac{F'\overline{C_{Ao}}X}{nW}$$

$whereF' = flowrate\ (l/hr)$

$\overline{C_{Ao}} = $ Average Concentration

$X = $ Conversion

$n = $ number of moles exposed metal on 1 gm catalyst (moles/g)

$w = 5g$

- **Sample Calculation**

Turn Over Number for Run 1

$$C_{Ao} = 0.00324 mole/l$$

$$F = 6l/hr$$

$$n = 9.808799 \times 10^{-6} mole$$

$$TON = \frac{6 \times 0.00324 \times 0.51}{(\frac{9.808799 \times 10^6}{5} \times 5)} \frac{l}{hr} \frac{mol}{l} \frac{1}{mol}$$

$$= 1010.76 hr^{-1}$$

Appendix B

CALALYST REGENERATION

From the boundary condition, at $i = 10$ equation 47 we have, after rearranging

$$-(N_B' + 20 + P_1\phi_{c(10,j)}\xi)\phi_{A(10,j)} + 200\phi_{A(9,j)} = N_B' + \phi_{c(10,j)}\xi[P - P_2]$$

This equation is combined with the other equations generated from the main equation at $i = 9$, to $i = 0$, to give a set of 11 linear simultaneous equations: Writing the equations, we have,

$$-(N_B' + 20 + P_1\phi_{c(10,j)}\xi)\phi_{A(10,j)} + 200\phi_{A(9,j)} =$$

$$N_B' + \phi_{c(10,j)}\xi[P - P_2]$$

$$1000\phi_{A(10,j)} - (1800 + P_1 9\phi_{c(9,j)}\xi)\phi_{A(9,j)} + 800\phi_{A(8,j)} = 9\phi_{c(9,j)}[P - P_2]$$

$$900\phi_{A(9,j)} - (1600 + P_1 8\phi_{c(8,j)})\xi)\phi_{A(8,j)} + 700\phi_{A(7,j)} = 8\phi_{c(8,j)}\xi[P - P_2]$$

$$800\phi_{A(8,j)} - (1400 + P_1 7\phi_{c(7,j)}\xi) + 600\phi_{A(6,j)} = 7\phi_{c(7,j)}\xi[P - P_2]$$

$$700\phi_{A(7,j)} - (1200 + P_1 6\phi_{c(6,j)}\xi)\phi_{A(6,j)} + 500\phi_{A(5,j)} 6\phi_{c(6,j)}\xi[P - P_2]$$

$$600\phi_{A(6,j)} - (1000 + P_1 5\phi_{c(5,j)}\xi)\phi_{A(5,j)} + 400\phi_{A(4,j)} = 5\phi_{c(5,j)}\xi[P - P_2]$$

$$500\phi_{A(5,j)} - (800 + P_1 4\phi_{c(4,j)}\xi)\phi_{A(4,j)} + 300\phi_{A(3,j)} = 4\phi_{c(4,j)}\xi[P - P_2]$$

$$400\phi_{A(4,j)} - (600 + P_1 3\phi_{c(3,j)}\xi)\phi_{A(3,j)} + 200\phi_{A(2,j)} = 3\phi_{c(3,j)}\xi[P - P_2]$$

$$300\phi_{A(3,j)} - (400 + P_1\phi_{c(2,j)}\xi)\phi_{A(2,j)} + 100\phi_{A(1,j)} = 2\phi_{c(2,j)}\xi[P - P_2]$$

$$200\phi_{A(2,j)} - (200 + P_1\phi_{c(1,j)}\xi)\phi_{A(1,j)} = \phi_{c(1,j)}\xi[P - P_2]$$

$$600\phi_{A(1,j)} - (\xi\phi_{c(0,j)}P_1 + 1)\phi_{A(0,j)} = \xi\phi_{c(0,j)}[P - P_2]$$

and from equation 3.107 Generally

$$\phi_{c(1,j)} = 1 - \theta_{(i,j+1)}[P + \phi_{A(i,j)}P_1 - P_2]_{av} \qquad (B.1)$$

Writting from $i = 10$, to $i = 0$ 11 equations will be generated

$$\phi_{c(10,j)} = 1 - \theta_{(10,j+1)}[P + \phi_{A(10,j)}P_1 - P_2]_{av}$$

$$\phi_{c(9,j)} = 1 - \theta_{(9,j+1)}[P + \phi_{(9,j)}P_1 - P_2]_{av}$$

$$\phi_{c(8,j)} = 1 - \theta_{(8,j+1)}[P + \phi_{A(8,j)}P_1 - P_2]_{av}$$

$$\phi_{c(7,j)} = 1 - \theta_{(7,j+1)}[P + \phi_{A(7,j)}P_1 - P_2]_{av}$$

$$\phi_{c(6,j)} = 1 - \theta_{(6,j+1)}[P + \phi_{A(6,j)}P_1 - P_2]_{av}$$

$$\phi_{c(5,j)} = 1 - \theta_{(5,j+1)}[P + \phi_{A(5,j)}P_1 - P_2]_{av}$$

$$\phi_{c(4,j)} = 1 - \theta_{(4,j+1)}[P + \phi_{A(4,j)}P_1 - P_2]_{av}$$

$$\phi_{c(3,j)} = 1 - \theta_{(3,j+1)}[P + \phi_{A(3,j)}P_1 - P_2]_{av}$$

$$\phi_{c(2,j)} = 1 - \theta_{(2,j+1)}[P + \phi_{A(2,j)}P_1 - P_2]_{av}$$

$$\phi_{c(1,j)} = 1 - \theta_{(1,j+1)}[P + \phi_{A(1,j)}P_1 - P_2]_{av}$$

$$\phi_{c(0,j)} = 1 - \theta_{(0,j+1)}[P + \phi_{A(0,j)}P_1 - P_2]_{av}$$

Procedure

At $\theta_{(i,j+1)}$ (dimensionless time), the $\phi_{A(i,j)}$ profile is guessed and $\phi_{c(i,j)}$ is computed from the set of above. Now the calculated set of $\phi_{c(i,j)}$ are then substituted into the first set of linear simultanous equations to calculate $\phi_{A(i,j)}$. These calculated $\phi_{A(i,j)}$ are

260

now used as the new guesses in the second set of simultanous linear equations. This procedure continues till convergence is achieved.

Appendix C

COMPUTER PROGRAMS

```
C$NOEXT
C        PROGRAM TO COMPUTE THE GAS CONSUMPTION AND COKE
C        DEPLETION PROFILE FOR VARIOUS DIMENSIONLESS
C        TIMES-USE OF FINITE DIFFERENCE APPROXIMATION.
C        BOUNDARY CONDITION AT THE
C        EXTERNAL SURFACE OF THE PARTICLE DISCRETIZED BY CENTRAL
C        DIFFERENCE. THE ENTIRE SOLUTION PROCEDURE IS AS
C        FOLLOWS. THE GAS CONSUMPTION
C        PROFILE IS FIRST GUESSED AND THE COKE CONSUMTION PROFILE
C        COMPUTED FROM THE EQUATION IN THE MAIN PROGRAM. THEN
C        THIS COKE DEPLETION PROFILE IS THEN USED TO COMPUTE NEW
C        VALUES FOR THE GAS CONSUMPTION PROFILE. THIS COMPUTED
C        GAS CONSUMPTION PROFILE NOW REPLACES THE GUESSED VALUES
C        IN THE MAIN EQUATION. EFFECT OF DIFFUSION ON PROFILES
C        IS OBSERVED BY CHANGING BIOT NUMBER, NB, AND SIGMA.
         IMPLICIT REAL*8 (A-H,O-Z)
         DIMENSION A(20,20),COKE(20),AV(20),GAS(20)
         DIMENSION TH(20)
         OPEN(1,FILE='MODEL1.INP')
         OPEN(2,FILE='MODEL2.INP')
         OPEN(3,FILE='MODEL3.INP')
         OPEN(4,FILE='MODEL4.OUT')
         READ(1,*) TA,GAO,B,N,SIGMA
         PP=0.0
         BT=0.0
          T=0.0
         NN=N-1
         NZ=N-2
         NT=N-3
         PT=TA*GAO
         DT=1+TA*GAO
         DS=(1+TA*GAO)**2.0
         P=PT/DT
         P1=TA/DT
         P2=PT/DS
C        READ_IN GUESSES OF INITIAL GAS PROFILE HERE AND VALUES OF
C        THETA(DIMENSIONLESS TIME), J'S, AT WHICH THE COMPUTATIONS
C        WILL BE DONE.
         READ(2,*) (GAS(I), I=1,N)
         READ(3,*) (TH(LL), LL=1,5)
         LL=1
  125    CONTINUE
         DO 50 I=1,N
       . AV(I)=(P+GAS(I)*P1-P2)/(4.0)
         COKE(I)=1-TH(LL)*AV(I)
   50    CONTINUE
         A(1,2)=200.0
         DO 75 I=2,NZ
         LS=I+1
         A(I,LS)=800.-T
         T=T+100.0
   75    CONTINUE
         A(11,10)=200.0
         DO 15 LS=1,NZ
         I=LS+1
```

1

```fortran
      A(I,LS)=1000.0-BT
      BT=BT+100
   15 CONTINUE
      DO 29 I=1,NT
      DO 29 LS=I+2,N
      A(I,LS)=0.0
      A(9,11)=0.0
      A(10,11)=0.0
   29 CONTINUE
      A(3,1)=0.0
      DO 32 I=4,N
      DO 32 LS=1,I-2
      A(I,LS)=0.0
   32 CONTINUE
      DO 10 I=2,NN
      A(1,1)=-(B+20+COKE(1)*SIGMA)
      A(N,N)=-(SIGMA*COKE(11)*P1+1)
      A(I,I)=-(1800-PP)+P1*(N-I)*COKE(I)*SIGMA
      PP=PP+200.0
   10 CONTINUE
      DO 18 I=2,NN
      A(1,N+1)=B+COKE(1)*SIGMA*(P-P2)
      A(N,N+1)=SIGMA*COKE(N)*(P-P2)
      A(I,N+1)=((NN-I)+1)*COKE(I)*SIGMA*(P-P2)
   18 CONTINUE
      CALL GAUSL(20,20,N,1,A)
      DO 37 I=1,N
      TOL=A(I,N+1)-GAS(I)
      IF(ABS(TOL).GE.0.0001) THEN
      DO 370 K=1,N
      CALL INTCHG(A(K,N+1),GAS(K))
  370 CONTINUE
      GO TO 125
      ENDIF
   37 CONTINUE
      WRITE(4,*) ' '
      WRITE(4,*) ' '
      WRITE(4,*) 'GAS VALUES, G(I)      COKE VALUES, COKE(I)'
      WRITE(4,*) '****************      ********************'
      DO 128 I=1,N
      WRITE(4,319) ABS(A(I,N+1)),COKE(I)
  319 FORMAT(/2X,F8.3,8X,F8.3)
  128 CONTINUE
      LL=LL+1
      IF(LL.GT.5) GO TO 91
      GO TO 125
   91 CLOSE(4)
      STOP
      END
      SUBROUTINE INTCHG(A,G)
      IMPLICIT REAL*8(A-H,O-Z)
      DIMENSION COKE(20),AV(20),GAS(20),TH(20)
      T=A
      A=G
      G=T
```

2

```
      RETURN
      END


C     THIS IS THE GAUSEAN ELIMINATION SUBROUTINE.
C     GAUSL SOLVES  A*X=B, WHERE A IS NXN AND B IS NXNS,
C     GAUSSIAN ELIMINATION WITH PARTIAL PIVOTING. THE MATRIX
C     (OR VECTOR) B IS PLACED ADJACENT TO A IN COLUMNS N+1  TO
C     N+NS .
C     A IS DESTROYED, AND THE RESULTING MATRIX X REPLACES B.
C.................................................................
      SUBROUTINE GAUSL(ND,NCOL,N,NS,A)
      IMPLICIT REAL*8(A-H,O-Z)
      DIMENSION A(ND,NCOL)
      N1 = N + 1
      NT =N + NS
      IF (N .EQ. 1) GO TO 50
C     START ELIMINATION
C........ ........................................................
      DO 10 I=2,N
      IP = I - 1
      I1 = IP
      X = DABS(A(I1,I1))
      DO 11 J = I,N
      IF (DABS(A(J,I1)) .LT. X) GO TO 11
      X = DABS(A(J,I1))
      IP =J
   11 CONTINUE
      IF (IP .EQ. I1) GO TO 13
C
C     ROW INTERCHANGE
C....................................................
      DO 12 J = I1,NT
      X = A(I1,J)
      A(I1,J) = A(IP,J)
   12 A(IP,J) = X
   13 DO 10 J = I,N
      X = A(J,I1)/A(I1,I1)
      DO 10 K = I,NT
   10 A(J,K) = A(J,K) - X*A(I1,K)
C
C
C     ELIMINATION FINISHED, NOW BACK SUBSTITUTION.
C.................................................................
   50 DO 20 IP = 1,N
      I = N1 - IP
      DO 20 K = N1,NT
      A(I,K) = A(I,K)/A(I,I)
      IF (I .EQ. 1) GO TO 20
      I1 = I - 1
      DO 25 J = 1, I1
   25 A(J,K) = A(J,K) - A(I,K)*A(J,I)
   20 CONTINUE
      RETURN
      END
```

```
C   NX      TOTAL NUMBER OF INDEPENDENT VARIABLES
C   NC      TOTAL NUMBER OF EQUALITY CONSTRAINTS
C   NIC     TOTAL NUMBER OF INEQUALITY CONSTRAINTS
C   SIZE    EDGE LENGTH OF THE INITIAL POLYHEDRON
C   CONVER  CONVERGENCE CRITERION FOR TERMINATION OF THE SEARCH
C   ALFA    THE REFLECTION COEFFICIENT
C   BETA    THE CONTRACTION COEFFICIENT
C   GAMA    THE EXPANSION COEFFICIENT
C   X(I)    THE ASSUMED VECTOR TO INITIATE THE SEARCH
C   FDIFER  THE TOLERANCE CRITERION FOR CONSTRAINT VIOLATION
C   ICONT   A COUNTER TO RECORD STAGE COMPUTATIONS


C       ESTIMATION OF THE PARAMETERS OF A DEACTIVATION KINETIC MODEL
C       TO BE USED IN THE PREDICTION OF DEACTIVATION PROFILES
C       THIS IS THE FLEXIBLE POLYHEDRON SEARCH TECHNIQUE KNOWN AS
C       THE BOX METHOD FOR NON LINEAR PARAMETER ESTIMATION.
        DIMENSION RT(50)
        DIMENSION X(50),X1(50,50),X2(50,50),R(100),SUM(50),F(50),SR(50)
        DIMENSION ROLD(100),H(50),CA(50),XA(50),XAREA(50),CONC(50),RX(50)
        COMMON/A/NX,NC,NIC,STEP,ALFA,BETA,GAMA,IN,INF,FDIFER,SEQL,K1,K2
        COMMON/B/K3,K4,K5,K6,K7,K8,K9,X,X1,X2,R,SUM,F,SR,ROLD,SCALE,FOLD
        COMMON/C/LFEAS,L5,L6,L7,L8,L9,R1A,R2A,R3A,CONC,XAREA,XA,RX,RT,CA
        OPEN(1,FILE='FLEXTY.INP')
        OPEN(2,FILE='FLEXTY2.INP')
        OPEN(3,FILE='FLEXTY.OUT')
        READ(1,*) NX,NC,NIC,SIZE,CONVER
        ALFA=1.0
        BETA=.5
        GAMA=2.
        STEP=SIZE
C  .THE ASSUMED INITIAL VECTOR IS READ IN AFTER THIS CARD
        READ(1,*) (X(I), I=1,NX)
        READ(2,*) (XA(MN), MN=1,14)
   11   K1=NX+1
        K2=NX+2
        K3=NX+3
        K4=NX+4
        K5=NX+5
        K6=NC+NIC
        K7=NC+1
        K8=NC+NIC
        K9=K8+1
        N=NX-NC
        N1=N+1
        IF(N1.GE.3) GO TO 50
        N1=3
        N=2
   50   N2=N+2
        N3=N+3
        N4=N+4
        N5=N+5
        N6=N+6
        N7=N+7
        N8=N+8
        XN=N
```

1

```
            XNX=NX
            XN1=N1
            R1A=.5*(SQRT(5.)-1.)
            R2A=R1A*R1A
            R3A=R2A*R1A
            L5=NX+5
            L6=NX+6
            L7=NX+7
            L8=NX+8
            L9=NX+9
            ICONT=1
            NCONT=1
            WRITE(3,*) (X(J), J=1,NX)
            FDIFER=2.*(NC+1)*STEP
            FOLD=FDIFER
            IN=N1
            CALL SUMR
            SR(N1)=SQRT(SEQL)
            IF(SR(N1).LT.FDIFER) GO TO 341
            CALL WRITEX
            WRITE(3,*) 'THESE INITIAL VECTORS UNSATISFIE',CRITER
            INF=N1
            STEP=0.05*FDIFER
            CALL FEASBL
            WRITE(3,*) 'THESE VECTORS SATISFY CRITERION',CSATIS
            IF(FOLD.LT.1.0E-09) GO TO 80
      341   WRITE(3,*) 'STAGE CALCULATION NUMBER',ICONT,FDIFER
            CALL WRITEX
            FTER=R(K9)
            WRITE(3,*) 'THIS ARSEVEN IS',FTER
C  COMPUTE CENTROID OF ALL VERTICES OF INITIAL POLYHEDRON
      237   STEP1= STEP*(SQRT(XNX+1.)+XNX-1.)/(XNX*SQRT(2.))
            STEP2=STEP*(SQRT(XNX+1.)-1.)/(XNX*SQRT(2.))
            ETA=(STEP1+(XNX-1.)*STEP2)/(XNX+1.)
            DO 4 J=1,NX
            X(J)=X(J)-ETA
        4   CONTINUE
            CALL START
            DO 9 I=1,N1
            DO 9 J=1,NX
            X2(I,J)=X1(I,J)
        9   CONTINUE
            DO 5 I=1,N1
           .IN=I
            DO 6 J=1,NX
        6   X(J)=X2(I,J)
            CALL SUMR
            SR(I)=SQRT(SEQL)
            IF(SR(I).LT.FDIFER) GO TO 8
            CALL FEASBL
            IF(FOLD.LT.1.0E-09) GO TO 80
        8   CALL PROTWO
            F(I)=R(K9)
        5   CONTINUE
     1000   STEP =0.05*FDIFER
```

2

```
                 ICONT=ICONT+1
      C          SELECT LARGEST VALUE OF OBJECTIVE FUNCTION FROM POLYHEDRON VERTICES
                 FH=F(1)
                 LHIGH=1
                 DO 16 I=2,N1
                 IF(F(I).LT.FH) GO TO 16
                 FH=F(I)
                 LHIGH=I
          16     CONTINUE
      C   SELECT MINIMUM VALUE OF OBJECTIVE FUNCTION FROM POLYHEDRON VERTICES
          41     FL=F(1)
                 LOW=1
                 DO 17 I=2,N1
                 IF(FL.LT.F(I)) GO TO 17
                 FL=F(I)
                 LOW=I
          17     CONTINUE
                 DO 86 J=1,NX
          86     X(J)=X2(LOW,J)
                 IN=LOW
                 CALL SUMR
                 SR(LOW)=SQRT(SEQL)
                 IF(SR(LOW).LT.FDIFER) GO TO 87
                 INF=LOW
                 CALL FEASBL
                 IF(FOLD.LT.1.0E-09) GO TO 80
                 CALL PROTWO
                 F(LOW)=R(K9)
                 GO TO 41
          87     CONTINUE
      C.         FIND CENTROID OF POINTS WITH I DIFFERENT THAN LHIGH
                 DO 19 J=1,NX
                 SUM2=0.
                 DO 20 I=1,N1
          20     SUM2=SUM2+X2(I,J)
          19     X2(N2,J)=1./XN*(SUM2-X2(LHIGH,J))
                 SUM2=0
                 DO 36 I=1,N1
                 DO 36 J=1,NX
                 SUM2=SUM2+(X2(I,J)-X2(N2,J))**2
          36     CONTINUE
                 FDIFER=(NC+1)/XN1*SQRT(SUM2)
                 IF(FDIFER.LT.FOLD) GO TO 98
               . FDIFER=FOLD
                 GO TO 198
          98     FOLD=FDIFER
         198     CONTINUE
                 FTER=F(LOW)
         137     NCONT=NCONT+1
                 IF(NCONT.LT.4*N1) GO TO 37
                 IF(ICONT.LT.1500) GO TO 337
                 FOLD=0.5*FOLD
         337     NCONT=0
                 CALL WRITEX
          37     IF(FDIFER.LT.CONVER) GO TO 81
```

3

```
C   SELECT SECOND LARGEST VALUE OF OBJECTIVE FUNCTION
        IF(LHIGH.EQ.1) GO TO 43
        FS=F(1)
        LSEC=1
        GO TO 44
    43  FS =F(2)
        LSEC=2
    44  DO 18 I=1,N1
        IF(LHIGH.EQ.I) GO TO 18
        IF(F(I).LT.FS) GO TO 18
        FS=F(I)
        LSEC=I
    18  CONTINUE
C   REFLECT HIGH POINT THROUGH CENTROID
        DO 61 J=1,NX
        X2(N3,J)=X2(N2,J)+ALFA*(X2(N2,J)-X2(LHIGH,J))
    61  X(J)=X2(N3,J)
        IN=N3
        CALL SUMR
        SR(N3)=SQRT(SEQL)
    89  IF(SR(N3).LT.FDIFER) GO TO 82
        INF=N3
        CALL FEASBL
        IF(FOLD.LT.1.0E-09) GO TO 80
    82  CONTINUE
        CALL PROTWO
        F(N3)=R(K9)
        IF(F(N3).LT.F(LOW)) GO TO 84
        IF(F(N3).LT.F(LSEC)) GO TO 92
        GO TO 60
    92  DO 93 J=1,NX
    93  X2(LHIGH,J)=X2(N3,J)
        SR(LHIGH)=SR(N3)
        F(LHIGH)=F(N3)
        GO TO 1000
C       EXPAND VECTOR SEARCH ALONG DIRECTION THROUGH CENTROID AND
C       REFLECTED VECTOR
    84  DO 23 J=1,NX
        X2(N4,J)=X2(N3,J)+GAMA*(X2(N3,J)-X2(N2,J))
    23  X(J)=X2(N4,J)
        IN=N4
        CALL SUMR
        SR(N4)=SQRT(SEQL)
        IF(SR(N4).LT.FDIFER) GO TO 25
        INF=N4
        CALL FEASBL
        IF(FOLD.LT.1.0E-09) GO TO 80
    25  CALL PROTWO
        F(N4)=R(K9)
        IF(F(LOW).LT.F(N4)) GO TO 92
        DO 26 J=1,NX
    26  X2(LHIGH,J)=X2(N4,J)
        F(LHIGH)=F(N4)
        SR(LHIGH)=SR(N4)
        GO TO 1000
```

4

```
 60   IF(F(N3).GT.F(LHIGH)) GO TO 64
      DO 65 J=1,NX
 65   X2(LHIGH,J)=X2(N3,J)
 64   DO 66 J=1,NX
      X2(N4,J)=BETA*X2(LHIGH,J)+(1.0-BETA)*X2(N2,J)
 66   X(J)=X2(N4,J)
      IN=N4
      CALL SUMR
      SR(N4)=SQRT(SEQL)
      IF(SR(N4).LT.FDIFER) GO TO 67
      INF=N4
      CALL FEASBL
      IF(FOLD.LT.1.0E-09) GO TO 80
 67   CALL PROTWO
      F(N4)=R(K9)
      IF(F(LHIGH).GT.F(N4)) GO TO 68
      DO 69 J=1,NX
      DO 69 J=1,N1
 69   X2(I,J)=0.5*(X2(I,J)+X2(LOW,J))
      DO 70 I=1,N1
      DO 71 J=1,NX
 71   X(J)=X2(I,J)
      IN=I
      CALL SUMR
      SR(I)=SQRT(SEQL)
      IF(SR(I).LT.FDIFER) GO TO 72
      INF=I
      CALL FEASBL
      IF(FOLD.LT.1.0E-09) GO TO 80
 72   CALL PROTWO
 70   F(I)=R(K9)
      GO TO 1000
 68   DO 73 J=1,NX
 73   X2(LHIGH,J)=X2(N4,J)
      SR(LHIGH)=SR(N4)
      F(LHIGH)=F(N4)
      GO TO 1000
 81   WRITE(3,*)'TOTAL NUMBER OF STAGE CALCULATIONS ARE',ICONT,FDIFER
      CALL WRITEX
 80   WRITE(3,*)'TOTAL NUMBER OF STAGES CALCULATIONS ARE',ICONT,FDIFER
9999  STOP
      END
      SUBROUTINE FEASBL
      DIMENSION X(50),X1(50,50),X2(50,50),R(100),SUM(50),F(50),SR(50)
      DIMENSION ROLD(100),R2(100),R3(100),FLG(10),H(50),CA(50)
      DIMENSION R1(100),XA(50),XAREA(50),CONC(50),RX(50),RT(50)
      COMMON/A/NX,NC,NIC,STEP,DUM1,DUM2,DUM3,IN,INF,FDIFER,SEQL,K1,K2
      COMMON/B/K3,K4,K5,K6,K7,K8,K9,X,X1,X2,R,SUM,F,SR,ROLD,SCALE,FOLD
      COMMON/C/LFEAS,L5,L6,L7,L8,L9,R1A,R2A,R3A,CONC,XAREA,XA,RX,RT,CA
      ALFA=1.
      BETA=0.5
      GAMA=2.
      XNX=NX
      ICONT=0
      LCHEK=0
```

5

```
   60   IF(F(N3).GT.F(LHIGH)) GO TO 64
        DO 65 J=1,NX
   65   X2(LHIGH,J)=X2(N3,J)
   64   DO 66 J=1,NX
        X2(N4,J)=BETA*X2(LHIGH,J)+(1.0-BETA)*X2(N2,J)
   66   X(J)=X2(N4,J)
        IN=N4
        CALL SUMR
        SR(N4)=SQRT(SEQL)
        IF(SR(N4).LT.FDIFER) GO TO 67
        INF=N4
        CALL FEASBL
        IF(FOLD.LT.1.0E-09) GO TO 80
   67   CALL PROTWO
        F(N4)=R(K9)
        IF(F(LHIGH).GT.F(N4)) GO TO 68
        DO 69 J=1,NX
        DO 69 I=1,N1
   69   X2(I,J)=0.5*(X2(I,J)+X2(LOW,J))
        DO 70 I=1,N1
        DO 71 J=1,NX
   71   X(J)=X2(I,J)
        IN=I
        CALL SUMR
        SR(I)=SQRT(SEQL)
        IF(SR(I).LT.FDIFER) GO TO 72
        INF=I
        CALL FEASBL
        IF(FOLD.LT.1.0E-09) GO TO 80
   72   CALL PROTWO
   70   F(I)=R(K9)
        GO TO 1000
   68   DO 73 J=1,NX
   73   X2(LHIGH,J)=X2(N4,J)
        SR(LHIGH)=SR(N4)
        F(LHIGH)=F(N4)
        GO TO 1000
   81   WRITE(3,*)'TOTAL NUMBER OF STAGE CALCULATIONS ARE',ICONT,FDIFER
        CALL WRITEX
   80   WRITE(3,*)'TOTAL NUMBER OF STAGES CALCULATIONS ARE',ICONT,FDIFER
 9999   STOP
        END
        SUBROUTINE FEASBL
        DIMENSION X(50),X1(50,50),X2(50,50),R(100),SUM(50),F(50),SR(50)
        DIMENSION ROLD(100),R2(100),R3(100),FLG(10),H(50),CA(50)
        DIMENSION R1(100),XA(50),XAREA(50),CONC(50),RX(50),RT(50)
        COMMON/A/NX,NC,NIC,STEP,DUM1,DUM2,DUM3,IN,INF,FDIFER,SEQL,K1,K2
        COMMON/8/K3,K4,K5,K6,K7,K8,K9,X,X1,X2,R,SUM,F,SR,ROLD,SCALE,FOLD
        COMMON/C/LFEAS,L5,L6,L7,L8,L9,R1A,R2A,R3A,CONC,XAREA,XA,RX,RT,CA
        ALFA=1.
        BETA=0.5
        GAMA=2.
        XNX=NX
        ICONT=0
        LCHEK=0
```

```
          ICHEK=0
    25    CALL START
          DO 3 I=1,K1
          DO 4 J=1,NX
          X1(1,J)=0.
     4    X(J)=X1(I,J)
          IN=I
          CALL SUMR
     3    CONTINUE
C         SELECT LARGEST VALUE OF SUM(I) IN SIMPLEX
    28    SUMH=SUM(1)
          INDEX=1
          DO 7 I=2,K1
          IF(SUM(I).LE.SUMH) GO TO 7
          SUMH=SUM(I)
          INDEX=I
     7    CONTINUE
C         SELECT MINIMUM VALUE OF SUM(I) IN SIMPLEX
          SUML=SUM(1)
          KOUNT=1
          DO 8 I=2,K1
          IF(SUML.LE.SUM(I)) GO TO 8
          SUML=SUM(I)
          KOUNT=I
     8    CONTINUE
C         FIND CENTROID OF POINTS WITH I DIFFERENT THAN INDEX
          DO 9 J=1,NX
          SUM2=0.
          DO 10 I=1,K1
    10    SUM2=SUM2+X1(I,J)
          X1(K2,J)=1./XNX*(SUM2-X1(INDEX,J))
C         FIND REFLECTION OF HIGH POINT THROUGH CENTROID
          X1(K3,J)=2.*X1(K2,J)-X1(INDEX,J)
     9    X(J)=X1(K3,J)
          IN=K3
          CALL SUMR
          IF(SUM(K3).LT.SUML) GO TO 11
C   .SELECT SECOND LARGEST VALUE IN SIMPLEX
          IF(INDEX.EQ.1) GO TO 38
          SUMS=SUM(1)
          GO TO 39
    38    SUMS=SUM(2)
    39    DO 12 I=1,K1
          IF((INDEX-I).EQ.0) GO TO 12
          IF(SUM(I).LE.SUMS) GO TO 12
          SUMS=SUM(I)
    12    CONTINUE
          IF(SUM(K3).GT.SUMS) GO TO 13
          GO TO 14
C  FORM EXPANSION OF NEW MINIMUM IF REFLECTION HAS PRODUCED ONE MINIMUM
    11    DO 15 J=1,NX
          X1(K4,J)=X1(K2,J)+2.*(X1(K3,J)-X1(K2,J))
    15    X(J)=X1(K4,J)
          IN=K4
          CALL SUMR
```

6

```fortran
      IF(SUM(K4).LT.SUML) GO TO 16
      GO TO 14
   13 IF(SUM(K3).GT.SUMH) GO TO 17
      DO 18 J=1,NX
   18 X1(INDEX,J)=X1(K3,J)
   17 DO 19 J=1,NX
      X1(K4,J)=0.5*X1(INDEX,J) +0.5*X1(K2,J)
   19 X(J)=X1(K4,J)
      IN=K4
      CALL SUMR
      IF(SUMH.GT.SUM(K4)) GO TO 6
C     REDUCE SIMPLEX BY HALF IF REFLECTION HAPPENS TO PRODUCE A LARGER VALUE
C     THAN THE MAXIMUM
      DO 20 J=1,NX
      DO 20 I=1,K1
   20 X1(I,J)=0.5*(X1(I,J)+X1(KOUNT,J))
      DO 29 I=1,NX
      DO 30 J=1,NX
   30 X(J)=X1(I,J)
      IN=I
      CALL SUMR
   29 CONTINUE
    5 SUML=SUM(1)
      KOUNT=1
      DO 23 I=2,K1
      IF(SUML.LT.SUM(I)) GO TO 23
      SUML=SUM(I)
      KOUNT=I
   23 CONTINUE
      SR(INF)=SQRT(SUM(KOUNT))
      DO 27 J=1,NX
   27 X(J)=X1(KOUNT,J)
      GO TO 26
    6 DO 31 J=1,NX
   31 X1(INDEX,J)=X1(K4,J)
      SUM(INDEX)=SUM(K4)
      GO TO 5
   16 DO 21 J=1,NX
      X1(INDEX,J)=X1(K4,J)
   21 X(J)=X1(INDEX,J)
      SUM(INDEX)=SUM(K4)
      SR(INF)=SQRT(SUM(K4))
      GO TO 26
   14 DO 22 J=1,NX
      X1(INDEX,J)=X1(K3,J)
   22 X(J)=X1(INDEX,J)
      SUM(INDEX)=SUM(K3)
      SR(INF)=SQRT(SUM(K3))
   26 ICONT=ICONT+1
      DO 36 J=1,NX
   36 X2(INF,J)=X(J)
      IF(ICONT.LT.2*K1) GO TO 50
      ICONT=0
      DO 24 J=1,NX
   24 X(J)=X1(K2,J)
```

```
      IN=K2
      CALL-SUMR
      DIFER=0.
      DO 57 I=1,K1
   57 DIFER =DIFER +(SUM(I)-SUM(K2))**2
      DIFER =1./(K7*XNX)*SQRT(DIFER)
      IF(DIFER.GT.1.0E-14) GO TO 50
C         IF FLEXIBLE SIMPLEX METHOD FAILLED TO SATISFY THE CONSTRAINTS
C    WITHIN THE TOLERANCE CRITERION FOR THE CURRENT STAGE, THE SEARCH IS
C    PERTURBED FROM THE POSITION WHERE THE X VECTOR IS STUCK AND FEASBL IS
C REPEATED ONCE MORE FROM THE BEGINNING
   51 IN=K1
      STEP=20.*FDIFER
      CALL SUMR
      SR(INF)=SQRT(SEQL)
      DO 52 J=1,NX
   52 X1(K1,J)=X(J)
      DO 53 J=1,NX
      FACTOR =1.
      X(J)=X1(K1,J)+FACTOR*STEP
      X1(L9,J)=X(J)
      IN=L9
      CALL SUMR
      X(J)=X1(K1,J)-FACTOR*STEP
      X1(L5,J)=X(J)
      IN=L5
      CALL SUMR
   56 IF(SUM(L9).LT.SUM(K1)) GO TO 54
      IF(SUM(L5).LT.SUM(K1)) GO TO 55
      GO TO 97
   54 X1(L5,J)=X1(K1,J)
      SUM(L5)=SUM(K1)
      X1(K1,J)=X1(L9,J)
      SUM(K1)=SUM(L9)
      FACTOR=FACTOR+1.
      X(J)=X1(K1,J)+FACTOR*STEP
      IN=L9
      CALL SUMR
      GO TO 56
   55 X1(L9,J)=X1(K1,J)
      SUM(L9)=SUM(K1)
      X1(K1,J)=X1(L5,J)
      SUM(K1)=SUM(L5)
      FACTOR=FACTOR +1.
      X(J)=X1(K1,J)-FACTOR*STEP
      IN=L5
      CALL SUMR
      GO TO 56
C    ONE DIMENSIONAL SEARCH BY GOLDEN SECTION ALONG EACH COORDINATE
   97 H(J)=X1(L9,J)-X1(L5,J)
      X1(L6,J)=X1(L5,J)+H(J)*R1A
      X(J)=X1(L6,J)
      IN=L6
      CALL SUMR
      X1(L7,J)=X1(L5,J)+H(J)*R2A
```

```
         X(J)=X1(L7,J)
         IN=L7
         CALL SUMR
         IF(SUM(L6).GT.SUM(L7)) GO TO 68
         X1(L8,J)=X1(L5,J)+(1.-R3A)*H(J)
         X1(L5,J)=X1(L7,J)
         X(J)=X1(L8,J)
         IN=L8
         CALL SUMR
         IF(SUM(L8).GT.SUM(L6)) GO TO 76
         X1(L5,J)=X1(L6,J)
         SUM(L5)=SUM(L6)
         GO TO 75
  76     X1(L9,J)=X1(L8,J)
         SUM(L9)=SUM(L8)
         GO TO 75
  68     X1(L9,J)=X1(L6,J)
         X1(L8,J)=X1(L5,J)+R3A*H(J)
         X(J)=X1(L8,J)
         IN=L8
         CALL SUMR
         STEP =SIZE
         SUM(L9)=SUM(L6)
         IF(SUM(L7).GT.SUM(L8)) GO TO 71
         X1(L5,J)=X1(L8,J)
         SUM(L5)=SUM(L8)
         GO TO 75
  71     X1(L9,J)=X1(L7,J)
         SUM(L9)=SUM(L7)
  75     IF(ABS(X1(L9,J)-X1(L5,J)).GT.0.01*FDIFER) GO TO 97
         X1(K1,J)=X1(L7,J)
         X(J)=X1(L7,J)
         SUM(K1)=SUM(L5)
         SR(INF)=SQRT(SUM(K1))
         IF(SR(INF).LT.FDIFER) GO TO 760
  53     CONTINUE
         ICHEK=ICHEK+1
         STEP=FDIFER
         IF(ICHEK.LE.2) GO TO 25
         FOLD=1.0E-12
         GO TO 46
 760     DO 761 J=1,NX
         X2(INF,J)=X1(K1,J)
 761     X(J)=X1(K1,J)
  50     IF(SR(INF).GT.FDIFER) GO TO 28
C        MODIFIED LAGRANGE INTERPOLATION FOR TIGHT INEQUALITIES
         IF(SR(INF).GT.0.) GO TO 35
         CALL PROTWO
         FINT=R(K9)
         DO 139 J=1,NX
 139     X(J)=X2(INF,J)
         CALL PROONE
         DO 40 J=K7,K8
  40     R1(J)=R(J)
         DO 41 J=1,NX
```

9

```
 41   X(J)=X1(KOUNT,J)
      CALL PROONE
      DO 42 J=K7,K8
 42   R3(J)=R(J)
      DO 43 J=1,NX
      H(J)=X1(KOUNT,J)-X2(INF,J)
 43   X(J)=X2(INF,J)+0.5*H(J)
      CALL PROONE
      FLG(1)=0.
      FLG(2)=0.
      FLG(3)=0.
      DO 44 J=K7,K8
      IF(R3(J).GE.0.) GO TO 44
      FLG(1)=FLG(1)+R1(J)*R1(J)
      FLG(2)=FLG(2)+R(J)*R(J)
      FLG(3)=FLG(3)+R3(J)*R3(J)
 44   CONTINUE
      SR(INF)=SQRT(FLG(1))
      IF(SR(INF).LT.FDIFER) GO TO 35
      ALFA1=FLG(1)-2.*FLG(2)+FLG(3)
      BETA1=3.*FLG(1)-4.*FLG(2)+FLG(3)
      RATIO=BETA1/(4.*ALFA1)
      DO 45 J=1,NX
 45   X(J)=X2(INF,J)+H(J)*RATIO
      IN=INF
      CALL SUMR
      SR(INF)=SQRT(SEQL)
      IF(SR(INF).LT.FDIFER) GO TO 465
      DO 49 I=1,20
      DO 48 J=1,NX
 48   X(J)=X(J)-0.05*H(J)
      CALL SUMR
      SR(INF)=SQRT(SEQL)
      IF(SR(INF).LT.FDIFER) GO TO 465
 49   CONTINUE
 465  CALL PROTWO
      IF(FINT.GT.R(K9)) GO TO 46
      SR(INF)=0.
      GO TO 35
 46   DO 47 J=1,NX
 47   X2(INF,J)=X(J)
 35   CONTINUE
      DO 335 J=1,NX
 335  X(J)=X2(INF,J)
      RETURN
      END
      SUBROUTINE START
      DIMENSION RX(50),RT(50)
      DIMENSION X(50),X1(50,50),X2(50,50),R(100),SUM(50),F(50),SR(50)
      DIMENSION ROLD(100),A(50,50),CONC(50),XA(50),CA(50),XAREA(50)
      COMMON/A/NX,NC,NIC,STEP,ALFA,BETA,GAMA,IN,INF,FDIFER,SEQL,K1,K2
      COMMON/B/K3,K4,K5,K6,K7,K8,K9,X,X1,X2,R,SUM,F,SR,ROLD,SCALE,FOLD
      COMMON/C/LFEAS,L5,L6,L7,L8,L9,R1A,R2A,R3A,CONC,XAREA,XA,RX,RT,CA
      VN=NX
      STEP1=STEP/(VN*SQRT(2.0))*(SQRT(VN+1.)+VN-1.)
```

```
           STEP2=STEP/(VN*SQRT(2.))*(SQRT(VN+1.)-1.)
           DO 1 J=1,NX
     1     A(1,J)=0.
           DO 2 I=2,K1
           DO 4 J=1,NX
     4     A(I,J)=STEP2
           L=I-1
           A(I,L)=STEP1
     2     CONTINUE
           DO 3 I=1,K1
           DO 3 J=1,NX
     3     X1(I,J)=X(J)+A(I,J)
           RETURN
           END
           SUBROUTINE WRITEX
           DIMENSION RT(50)
           DIMENSION X(50),X1(50,50),X2(50,50),R(100),SUM(50),F(50),SR(50)
           DIMENSION ROLD(100),CA(50),XA(50),XAREA(50),CONC(50),RX(50)
           COMMON/A/NX,NC,NIC,STEP,ALFA,BETA,GAMA,IN,INF,FDIFER,SEQL,K1,K2
           COMMON/B/K3,K4,K5,K6,K7,K8,K9,X,X1,X2,R,SUM,F,SR,ROLD,SCALE,FOLD
           COMMON/C/LFEAS,L5,L6,L7,L8,L9,R1A,R2A,R3A,CONC,XAREA,XA,RX,RT,CA
           CALL PROTWO
           WRITE(3,*) 'OBJECTIVE FUNCTION VALUE IS  ',R(6)
     C     WRITE(3,*) R(6)
           WRITE(3,*) 'THE INDEPENDENT VECTORS ARE ', (X(J), J=1,NX)
     C     WRITE(3,*) (X(J), J=1,NX)
           CALL PROONE
           WRITE(3,*)'THE INEQUALITY CONSTRAINT VALUES ARE',(R(J), J=K7,K6)
     5     RETURN
           END
           SUBROUTINE SUMR
           DIMENSION RT(50)
           DIMENSION X(50),X1(50,50),X2(50,50),R(100),SUM(50),F(50),SR(50)
           DIMENSION ROLD(100),CONC(50),XA(50),CA(50),XAREA(50),RX(50)
           COMMON/A/NX,NC,NIC,STEP,ALFA,BETA,GAMA,IN,INF,FDIFER,SEQL,K1,K2
           COMMON/B/K3,K4,K5,K6,K7,K8,K9,X,X1,X2,R,SUM,F,SR,ROLD,SCALE,FOLD
           COMMON/C/LFEAS,L5,L6,L7,L8,L9,R1A,R2A,R3A,CONC,XAREA,XA,RX,RT,CA
           SUM(IN)=0.
           CALL PROONE
           SEQL=0.
           IF(NIC.EQ.0) GO TO 4
           DO 1 J=K7,K8
           IF(R(J).GE.0.) GO TO 1
           SEQL=SEQL+R(J)*R(J)
     1     CONTINUE.
     4     IF(NC.EQ.0.) GO TO 3
           CALL PROTWO
           DO 2 J=1,NC
     2     SEQL=SEQL+R(J)*R(J)
     3     SUM(IN)=SEQL
     5     RETURN
           END
           SUBROUTINE PROTWO
           DIMENSION RT(50)
           DIMENSION X(50),X1(50,50),X2(50,50),R(100),SUM(50),F(50),SR(50)
```

11

```
      DIMENSION ROLD(100),XA(50),CONC(50),CA(50),XAREA(50),RX(50)
      COMMON/A/NX,NC,NIC,STEP,ALFA,BETA,GAMA,IN,INF,FDIFER,SEQL,K1,K2
      COMMON/B/K3,K4,K5,K6,K7,K8,K9,X,X1,X2,R,SUM,F,SR,ROLD,SCALE,FOLD
      COMMON/C/LFEAS,L5,L6,L7,L8,L9,R1A,R2A,R3A,CONC,XAREA,XA,RX,RT,CA
      ZETA=0.699
      NP=15
      ITIME=225
      R(6)=0.
      AREL=0.
      CAO=0.00424
      DO 17 MN=1,14
      XT=CAO*(1-XA(MN))
      XL=1+ZETA*XA(MN)**2
      CA(MN)=XT/XL
C     NOW RAISE CONCENTRATION TO THE APPROPRIATE POWER
      CONC(MN)=(CA(MN)**2)/(1+X(2)*CA(MN))
      J=MN-1
      IF(J.EQ.0) GO TO 17
      XAREA(MN)=AREL+ITIME*(CONC(MN)+CONC(J))/(NP-1)*2
      PT=(X(3)**2)*X(1)*(X(2)*CA(MN))**2
      DT=(1+X(2)*CA(MN))**2
      RT(MN)=PT/DT
      RX(MN)=(1-X(4)*(1-EXP(-X(5)*X(2)*XAREA(MN))))**2
      AREL=XAREA(MN)
      R(6)=R(6)+(XA(MN)*5.04-RT(MN)*RX(MN))**2
17    CONTINUE
      RETURN
      END
      SUBROUTINE PROONE
      DIMENSION RT(50)
      DIMENSION X(50),X1(50,50),X2(50,50),R(100),SUM(50),F(50),SR(50)
      DIMENSION ROLD(100),XA(50),CONC(50),CA(50),XAREA(50),RX(50)
      COMMON/A/NX,NC,NIC,STEP,ALFA,BETA,GAMA,IN,INF,FDIFER,SEQL,K1,K2
      COMMON/B/K3,K4,K5,K6,K7,K8,K9,X,X1,X2,R,SUM,F,SR,ROLD,SCALE,FOLD
      COMMON/C/LFEAS,L5,L6,L7,L8,L9,R1A,R2A,R3A,CONC,XAREA,XA,RX,RT,CA
      R(1)=X(1)
      R(2)=X(2)
      R(3)=X(3)
      R(4)=X(4)
      R(5)=X(5)
      RETURN
      END
```